INNATE C–H FUNCTIONALIZATION OF CYCLIC ENAMINONES

A DISSERTATION
SUBMITTED TO THE FACULTY OF
UNIVERSITY OF MINNESOTA
BY

YIYUN YU

IN PARTIAL FULFILLMENT OF THE REQUIREMENTS
FOR THE DEGREE OF
DOCTOR OF PHILOSOPHY

ADVISOR: GUNDA I. GEORG

AUGUST 2013

Acknowledgements

"Life is like a train ride. We get on. We get off. We get back on and ride some more." As I boarded this train 6 years ago, this journey has been full of hopes, happiness, challenges, setbacks, success and goodbyes. It is bittersweet as it is my stop to get off. Looking back, I am blessed that so many great people have helped me along the way.

Dr. Gunda Georg, my mentor in graduate school, without whom all these projects would have been impossible. I am grateful for her wholehearted support of my research and the freedom to develop my projects. More importantly, her prudence, enthusiasm, and humbleness have deeply influenced my work attitude far beyond scientific research.

Dr. Micah Niphakis, who helped me make a smooth transition from a theoretical chemist to an experimental chemist at the beginning of my graduate career. His strive for greatness has always inspired me to be a better learner/researcher.

My coworkers Yong Wook Kim, Wei Li, Dr. Hajime Seki, Kwon Hong and all other ITDD members, who have been very supportive and cultured a pleasant work environment. Their expertise has always been the resource that I could count on.

Dr. Thomas Hoye and Dr. Chris Douglas, whose classes guided me into the realm of advanced organic chemistry. Their wisdom and knowledge often left me in awe.

Dr. Jane Wissinger and all my CHEM2311 students, whose complete trust in me in teaching organic labs, constantly motivated me to be a better teacher.

All my friends in Minnesota, Qianyun Xie, Lili Zhou, Danhui Ye, Qiliang Wu, Tao Yu, Bo Wang, *etc.*, whom I had the pleasure to know and whose companionship made my life in a foreign country no longer lonely. For that, I am truly grateful.

Lastly, my dear parents and extended family, who have given me unconditional love and support over the years. I am who I am because of you. I love you all.

I sometimes ask myself, will I miss it all when I get off this ride? I think I certainly will. To all my fellow travelers, I thank you for being part of my journey. I am happy that you contributed to my baggage and enriched my life, and I will be elated if I have touched yours. In this village called Earth, I look forward to seeing you again at another station or ride together some more. Until then… Bon voyage!

To my beloved parents, Guoying & Zhiyuan.

Abstract

Cyclic enaminones are versatile precursors for the synthesis of alkaloids and nitrogen-containing bioactive compounds. The development of efficient functionalization methods is vital to their synthetic utility. C–H functionalization is a tool to efficiently construct C–C bonds with high atom-economy, and to reduced waste. The work in this dissertation is directed towards the development of efficient and selective C–H functionalization methods for cyclic enaminones.

Chapter 1 serves as an introduction to cyclic enaminone chemistry. The synthesis and reactivity of cyclic enaminones, including applications in total synthesis, are summarized. In particular, our recent developments regarding enaminone chemistry are highlighted.

Chapter 2 surveys recent advances in Pd-catalyzed C–H functionalization at sp^2 carbons. The highlights and problems for C–H functionalization are discussed in detail.

Chapter 3 describes a regioselective C–H arylation of cyclic enaminones with aryl iodides. The wide availability of aryl iodides allowed rapid access to 3-arylpiperidines.

Chapter 4 expands the reaction scope of cyclic enaminones and presents a unique dehydrogenative alkenylation. This pioneering work is among the early examples of a C–H cross-coupling reaction between alkenes. A variety of cyclic enaminones and alkenes were employed. A mechanistic study of the C–H palladation is also included.

Chapter 5 focuses on the synthesis of 5-alkenyluracil scaffolds of medicinal importance. A practical, high-yielding dehydrogenative alkenylation method is presented. The generality of this new method shows a significant improvement over past syntheses.

Chapter 6 explores the synthetic utility of alkenylated cyclic enaminones. A superior dehydrogenative alkenylation reaction was discovered using a biomimetic approach. A tandem reaction was found serendipitously that led to a novel synthesis of chalcones.

Chapter 7 documents progress concerning the C–H trifluoromethylation of cyclic enaminones. Existing protocols were examined and a palladium-catalyzed protocol was pursued. Remarkably, it was discovered that a metal-free protocol was similarly effective.

Our efforts have afforded practical means to functionalize cyclic enaminones. These protocols will undoubtedly increase the synthetic value of cyclic enaminones.

Table of Contents

List of Tables

List of Figures

List of Schemes

List of Compounds

List of Abbreviations

Ac	acetyl
Ala	alanine
Alk	alkyl
Ar	aryl
atm	atmosphere
Bn	benzyl
Boc	*tert*-butoxycarbonyl
BQ	benzoquinone
br	broad
Bz	benzoyl
cat.	catalytic/catalyst
Cbz	benzyloxycarbonyl
CMD	concerted-metalation-deprotonation
Cp*	1,2,3,4,5-pentamethylcyclopentadienyl
Cy	cyclohexyl
d	doublet
dba	dibenzylideneacetone
DCE	1,2-dichloroethane
DCM	dichloromethane
dd	doublet of doublet
DDQ	2,3-dichloro-5,6-dicyano-1,4-benzoquinone
DG	directing group
DMA	dimethylacetamide
DMEDA	*N,N'*-dimethyl-1,2-ethanediamine
DMF	*N,N'*-dimethylformamide
DMOP	2,6-dimethyloxypyridine
DMSO	dimethylsulfoxide
dppb	1,4-bis(diphenylphosphino)butane

dppe	1,2-bis(diphenylphosphino)ethane
dppf	1,1′-bis(diphenylphosphino)ferrocene
dppp	1,3-bis(diphenylphosphino)propane
equiv	equivalent
ESI	electrospray ionization
Et	ethyl
ETM	electron transfer mediator
EWG	electron-withdrawing group
fppy	2-(2,4-difluorophenyl)pyridine
h	hour(s)
HCMV	human cytomegalovirus
Het	hetero
HIV	human immunodeficiency virus
HOMO	highest occupied molecular orbital
HRMS	high-resolution mass spectrometry
HSV	herpes simplex virus
ID_{50}	50% inhibitory dose
IED	inverse-electron-demand
*i*Pr	isopropyl
FTIR	Fourier-transform infrared
KIE	kinetic isotope effect
KTFA	potassium trifluoroacetate
L	ligand
LUMO	lowest unoccupied molecular orbital
M	molar
m	multiplet
MCF	Michigan Cancer Foundation
Me	methyl
MIC	minimum inhibitory concentration
min	minute(s)

MOM	methoxymethyl
MS	molecular sieve
Ms	mesyl
*n*Bu	butyl
NCI	National Cancer Institute
NED	normal-electron-demand
NMP	*N*-methyl-2-pyrrolidinone
NMR	nuclear magnetic resonance
OAc	acetate
OLED	organic light-emitting device
Ox	oxidant
Oxa	oxazolinyl
P-gp	P-glycoprotein
PEG	polyethylene glycol
Ph	phenyl
Phe	phenylalanine
phen	phenanthroline
PIDA	phenyliodine diacetate
PIFA	phenyliodine bis(trifluoroacetate)
Piv	pivaloyl
PMB	*para*-methoxybenzyl
PMP	*para*-methoxyphenyl
ppm	part per million
q	quartet
QSAR	quantitative structure–activity relationship
rt	room temperature
s	singlet
SAR	structure-activity relationship
S_E3	trimolecular electrophilic substitution
S_EAr	electrophilic aromatic substitution

S_N2	bimolecular nucleophilic substitution
t	triplet
t	time
*t*Am	*tert*-amyl
TBAB	tetrabutylammonium bromide
TBAF	tetrabutylammonium fluoride
TBHP	*tert*-butyl hydroperoxide
*t*Bu	*tert*-butyl
TEA	triethylamine
TEMPO	2,2,6,6-tetramethylpiperidine 1-oxyl
Tf	trifluoromethanesulfonyl
TFA	trifluoroacetate or trifluoroacetic acid
TFE	2,2,2-trifluoroethanol
THF	tetrahydrofuran
TIPS	triisopropylsilyl
TLC	thin layer chromatography
TMS	trimethylsilyl
Tol	tolyl
TON	turnover number
Ts	*p*-toluenesulfonyl
VZV	varicella zoster virus
X	(pseudo)halogen

Chapter 1 Cyclic Enaminones

Heterocyclic compounds are featured in the majority of natural products and pharmaceutical agents (*e.g.* alkaloids and antibiotics).[1-4] The efficient synthesis of biologically active molecules under exclusive stereo- and regioselective control still remains a challenging goal in synthetic organic chemistry.[5-8] Nitrogen-containing heterocycles, in particular, claim a distinctive position as historical pharmacophores and represent a major synthetic challenge in this field.[9-13]

1.1 Introduction to cyclic enaminones

Cyclic enaminones, also known as 2,3-dihydropyridin-4(1*H*)-ones, can be considered as β-acyl enamines or amides with an interpolated alkene (vinylogous amides). The chemical properties of cyclic enaminones are very unique. The addition of an alkene into an amide perfectly balances the reactivity and stability of enaminones between those of enamines and amides (Scheme1-1). For example, enamines are very reactive, thus unstable under hydrolytic and oxidative conditions,[14] whereas enaminones are more robust and compatible under these conditions. On the other hand, amides are the most stable among the three, while enaminones maintain a certain degree of stability but also exhibit a more diverse reactivity profile (more details in Section 1.4). In addition, enaminones also have also been seen in pharmaceutical development, serving as anticonvulsants and Pgp modulators.[15-19]

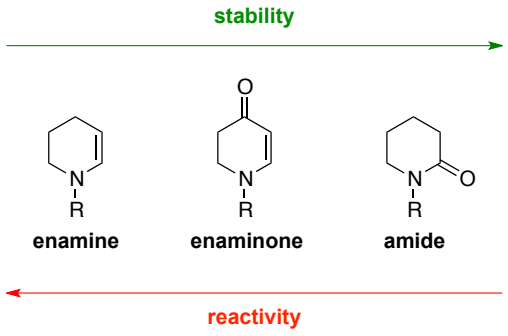

Scheme 1-1. Enamine, enaminone, and amide.

The synthetic versatility of cyclic enaminones renders them valuable building blocks for a variety of highly functionalized heterocyclic natural products, *e.g.* piperidines, quinolines, quinolizidines, and indolizidines (Scheme 1-2).[20-23] These heterocycles encompass a broad spectrum of biological and pharmacological activities.[17, 18] Due to the ubiquity of these biologically active piperidine-containing heterocycles, practical methods for constructing cyclic enaminones, particularly those with stereocenters, are of great interest.

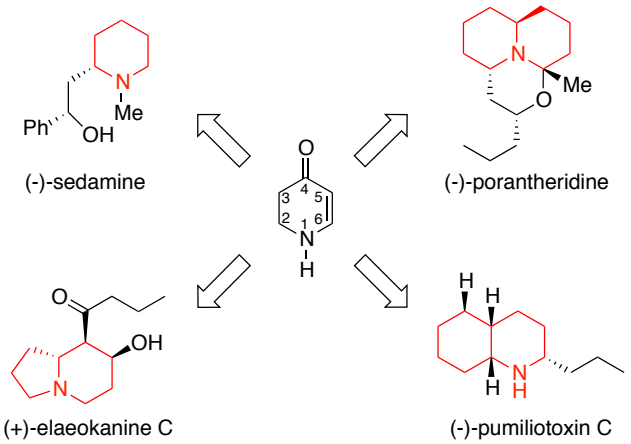

Scheme 1-2. Scaffold transformation from cyclic enaminones.

1.2 Current approaches for synthesizing cyclic enaminones

Given the importance of cyclic enaminones in total synthesis, a number of preparative protocols have been developed in the past two decades.[24-30] Only a few are capable of constructing enaminones with good stereoselectivity (Scheme 1-3). One well-established method is Comins' modification of *N*-acylpyridinium salts **1.2** with chiral auxiliaries.[31, 32] This method has been very successful in synthesizing advanced intermediates in numerous natural product syntheses. Other methodologies often use open chain precursors. For instance, the aza-Diels-Alder reaction of Danishefsky's diene **1.4** with imines is another straightforward protocol.[33] Further advances in related [4+2] cycloaddition reactions employ Lewis or Brønsted acid catalysis, such as $Yb(OTf)_3$[34] and HBF_4,[35] in organic,[36] aqueous,[37] and ionic liquids.[38] The chiral auxiliaries attached to

imines also enhance asymmetric control.[36] Combinatorial synthesis in solid[39] and liquid[40] phases supported by polymers, such as PEG, also provides efficient access to the library production of cyclic enaminone analogs via this cycloaddition pathway.[41] In a similar vein, the Rovis group developed a novel [2+2+2] cycloaddition method catalyzed by Rh complexes.[42-46] This protocol offers an efficient approach to bicyclic enaminones (*i.e.* indolizidinones **1.9**) with very good enantioselectivity. In another approach, Dallemagne and co-workers converted chiral β-aryl-β-amino acids **1.10** to δ-aryl-δ-amino-β-ketoketones **1.11** followed by intramolecular cyclization which furnishes enantiopure cyclic enaminones **1.12** in high yields.[47]

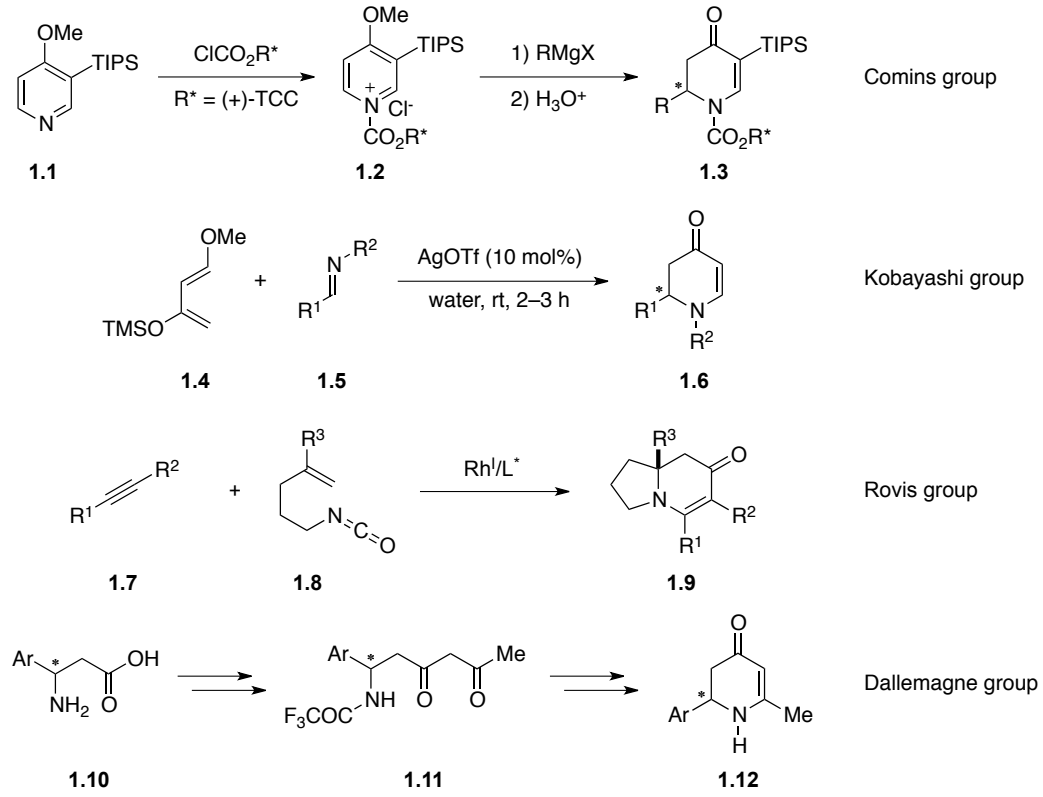

Scheme 1-3. Well-established protocols to construct nonracemic cyclic enaminones.

Recently, more flexible and novel procedures have emerged (Scheme 1-4). Svetlik's [4+1+1] strategy via cyclocondensation of methyl 3,5-dioxohexanoate (**1.13**) with aryl aldehydes **1.14** in the presence of ammonium acetate is a simple, efficient and

diastereoselective method.[48] In addition, Dong and co-workers discovered a novel [5C+1N] annulation process that combined readily available α-alkynoyl ketene-(*S*,*S*)-acetals (**1.16**) and aliphatic primary amines in one step to provide functionalized mono/bicyclic enaminones.[49] Last, but not least, our group successfully devised two remarkably concise methods to directly access asymmetric mono/bicyclic enaminones from the widely available chiral amino acid pool. Our first protocol uses β-amino acids **1.19** to afford ynones **1.20**, which undergo a *seemingly* 6-*endo*-dig cyclization to furnish enaminones in high yields.[50, 51] Our second approach applies even more readily accessible α-amino acids **1.22**.[52] A one-pot transformation yields diazoketones **1.23** and a following Wolff rearrangement quickly constructs the cyclic enaminone scaffold in excellent yields.

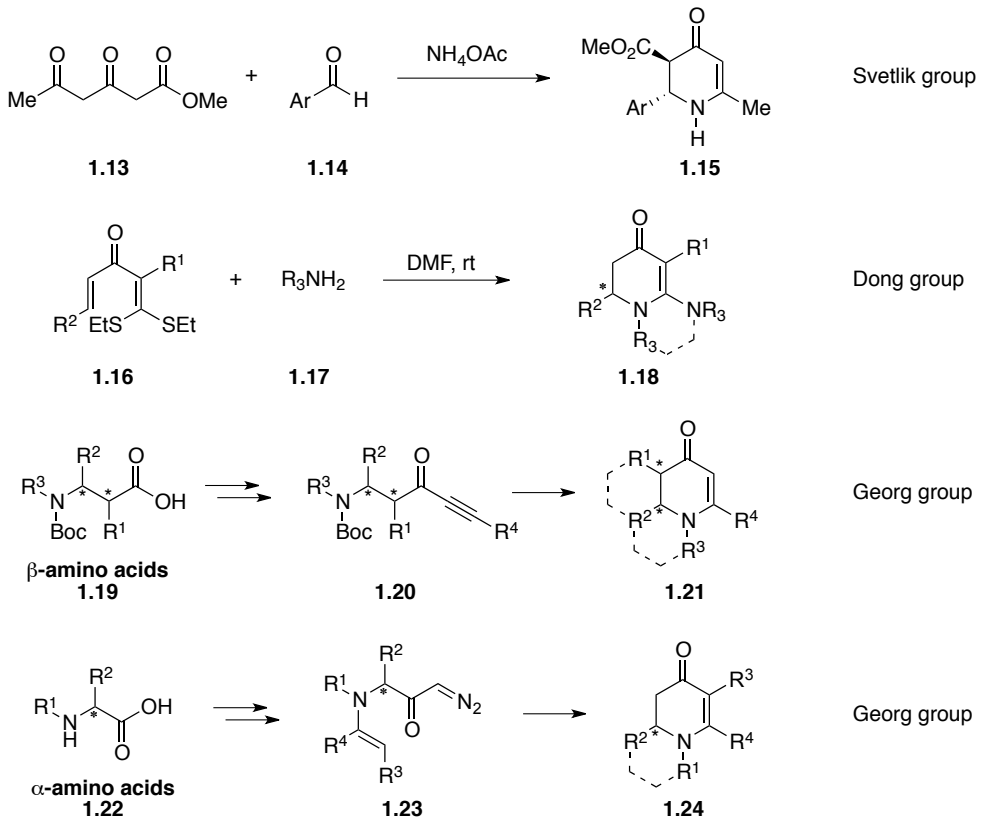

Scheme 1-4. Novel approaches to construct cyclic enaminones.

1.3 Cyclic enaminones in total synthesis

With all these preparative methods available, cyclic enaminones have been increasingly employed in total synthesis of heterocyclic natural products.[17, 53] For example, the tetracyclic tetrahydro-β-carboline framework **1.27** of the ajmaline/sarpagine alkaloids can be easily assembled using simple indole derivative **1.25** through two major steps (*i.e.* aza-Diels-Alder and intramolecular Heck cyclization) (Scheme 1-5, top).[54] More recently, Comins reported the first asymmetric synthesis of (+)-cannabisativine (**1.29**) in 19 steps with a high degree of stereocontrol (Scheme 1-5, middle).[32]

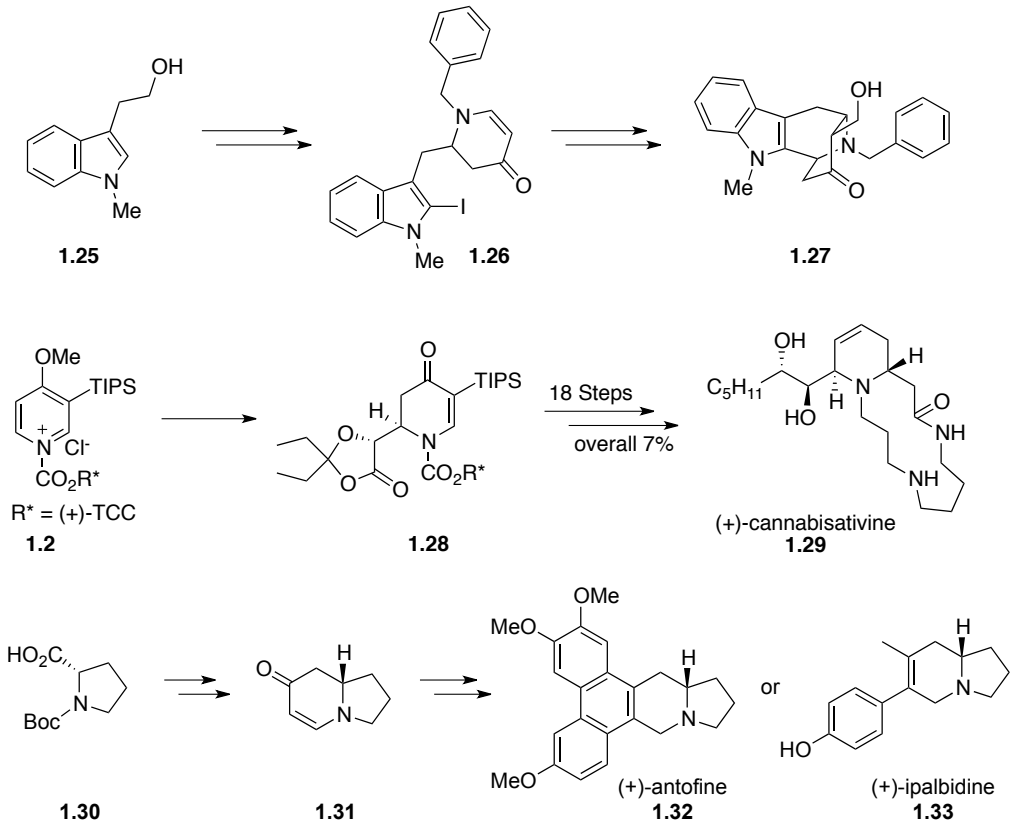

Scheme 1-5. Total synthesis examples involving cyclic enaminones.

Our group has been particularly interested in indolizidine alkaloids, which are prevalent in nature and exhibit a variety of biological properties.[55-58] Hence, their medicinal importance led us to prepare a series of phenanthropiperidine derivatives. For

example, in eight short steps, both (+)-antofine (**1.32**) and (+)-ipalbidine (**1.33**) were derived from simple Boc-L-proline (**1.30**) with up to 96% ee (Scheme 1-5, bottom).[59] Cyclic enaminone **1.31** was a key intermediate, which set the stage for subsequent C–H arylation and phenanthrene scaffold construction. Notably, (+)-antofine has shown potent antiproliferative activity on the nanomolar scale against COLO-205, MCF-7, and drug-resistant NCI/ADR-RES cell lines.[60] More alkaloids derived from cyclic enaminones in the past 5 years are summarized in Scheme 1-6, which clearly demonstrates the synthetic value of cyclic enaminones.[59, 61-66]

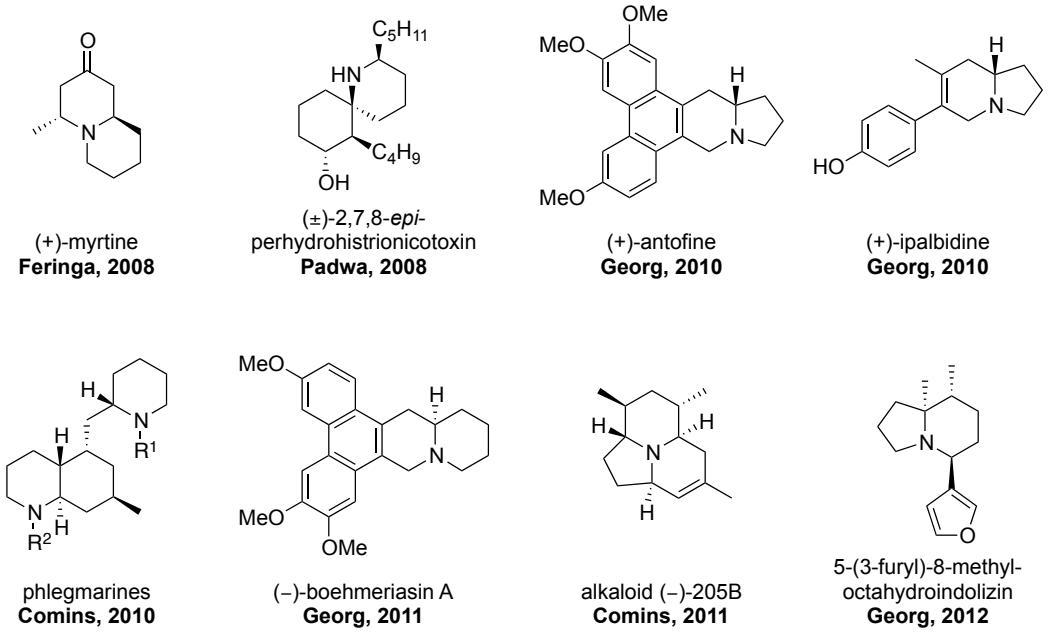

Scheme 1-6. Selected alkaloids derived from cyclic enaminones since 2008.

1.4 Versatility of cyclic enaminones

The wide applicability of cyclic enaminones in alkaloid synthesis is derived from their versatile reactivity in addition to the broad scope of their preparative methods. Indeed, the scaffold of cyclic enaminones is a functionality-dense six-membered ring, where amine, enamine, enone, and alkene moieties are all embedded. The combination of

enamine's nucleophilicity and enone's electrophilicity as a result permits a plethora of transformations of considerable value (Figure 1-1).[67, 68]

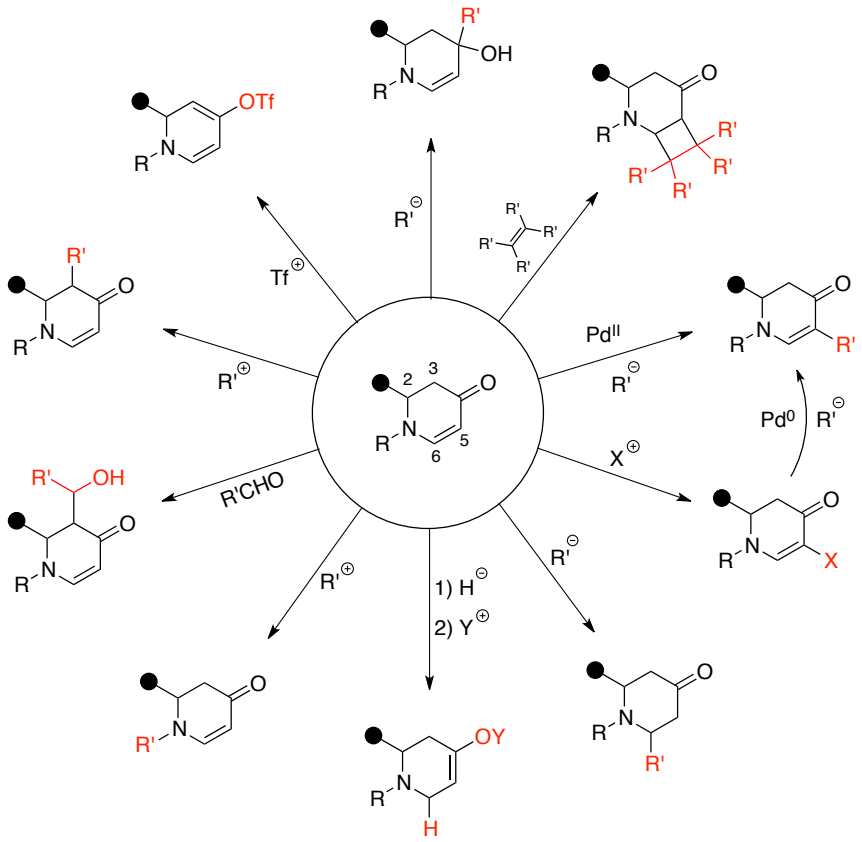

Figure 1-1. The chemical versatility of cyclic enaminones.

As an electrophile, due to the enone character, conventional 1,2-additions at the C4 position[41] and 1,4-additions at the C6 position[32] are both tolerated, which potentially serves as a means for annulation.[69, 70] As an nucleophile, enolate chemistry can be accomplished at the C3 position.[71] *N*- and *O*-functionalization are feasible as well.[72] A new functionalizing method developed in Comins' group involves the tandem C6,C5-directed lithiation, which allows the attachment of various substituents to both the C5 and C6 positions sequentially.[73] In addition, cycloaddition was also achieved on cyclic enaminones. An intramolecular [2+2] process generates a tricyclic scaffold,[74] which was used toward the synthesis of spirolucidine.[75] Moreover, the C2 position can be utilized as

a handle to exert steric influence. Thus, the aforementioned manipulations can be greatly enhanced with stereoselectivity.

Most interestingly, cyclic enaminones possess a strong nucleophilicity at the C5 position. This unique nucleophilicity stems from both the electron-withdrawing feature of the enone moiety and the electron-donating feature of the enamine moiety. Hence, the polarized double bond in this *non-aromatic* ring structure displays a similar high reactivity towards electrophilic substitution as an *aromatic* compound. Halogenation at the C5 position is therefore a facile process. Comins[76] and Kunz[77] both have shown that the iodinated enaminones can undergo Pd-catalyzed cross-coupling reactions. Our group later reported that under microwave conditions a Suzuki-Miyaura coupling could easily take place to afford the arylated enaminones in excellent yields (Scheme 1-7).[78]

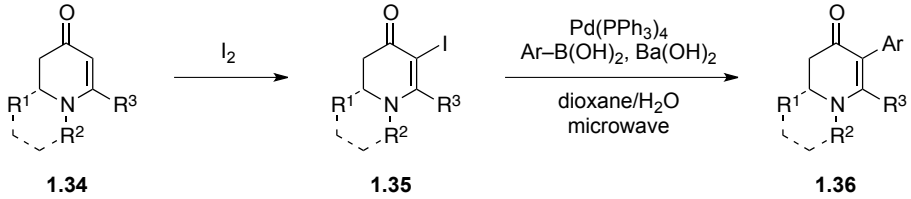

Scheme 1-7. Two-step arylation of cyclic enaminones.

1.5 C–H functionalization of cyclic enaminones in the Georg group

Given the intrinsic nucleophilicity of cyclic enaminones and the electrophilicity of cationic transition metal catalysts, these complementary properties inspired us to design a one-step process to arylate non-preactivated cyclic enaminones. This proposed arylation was first found by Ge and Niphakis using aryl trifluoroborates as the coupling partners (Scheme 1-8, top).[79] A series of electron-rich, mono- and bi-cyclic enaminones were arylated in this one-step process with excellent yields. It is worth noting that this new protocol prompted our efforts on extensive development of C–H functionalization of cyclic enaminones.

In order to expand the substrate scope, we continued to evaluate other aryl sources of more availability and less cost. A Hiyama-like protocol was therefore developed by Bi

using aryl triethoxysilanes (Scheme 1-8, middle).[80] Interestingly, CuF_2 served as a fluoride source to activate the silane and also as the reoxidant to convert Pd^0 to Pd^{II}. In 2012, Kim successfully applied aryl boronic acids as aryl coupling partners (Scheme 1-8, bottom).[81] A mixture of two Cu^{II} additives was found to be crucial for respectively assisting Pd^0 reoxidation and transmetalation through a putative [Ar–Cu] intermediate. Remarkably, both electron-rich and electron-poor aryl boronic acids were compatible with high yields. This is a significant improvement over the two previous methods that exhibited a strong preference for electron-rich aryl precursors.

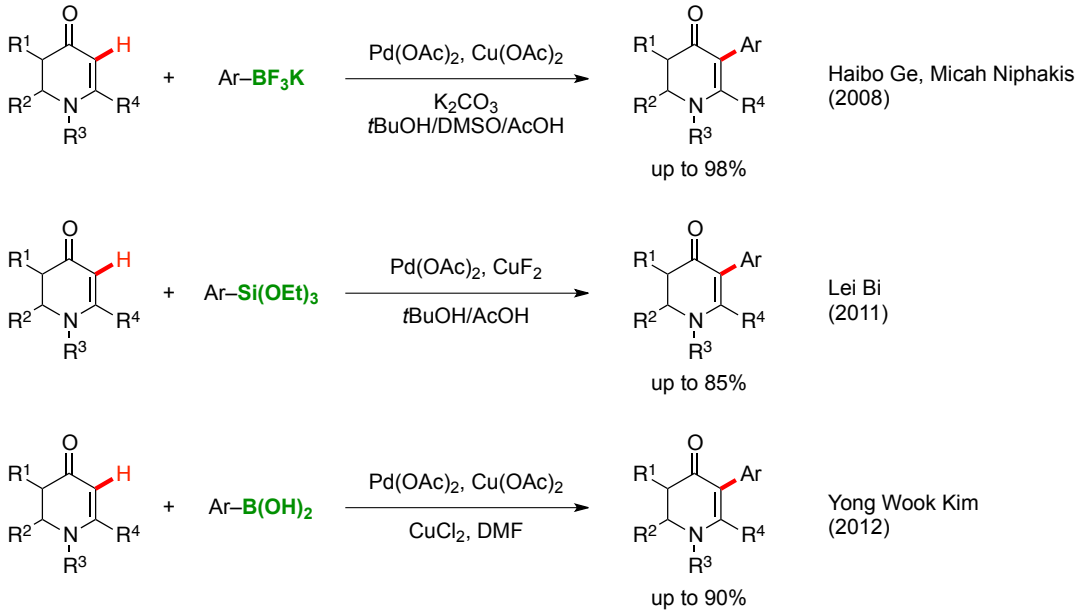

Scheme 1-8. Development of C–H arylation of cyclic enaminones.

The efficiency of these transformations via Pd catalysis have proven that cyclic enaminones are promising substrates for the ever-emerging C–H functionalization reactions. This new reactivity is an exciting addition to the already ample versatility of enaminones'. Further development in this regard will undoubtedly offer quick access to more highly functionalized enaminone derivatives for total synthesis and medicinal chemistry.

Chapter 2 Palladium-Catalyzed C–H Functionalization

C–C bond construction is the center of organic synthesis. Traditional transition metal-catalyzed C–C bond formation by cross-coupling reactions is a powerful method in synthetic applications.[82] These methods usually require stoichiometric amounts of pre-made nucleophilic organometallic reagents, represented as a C–M bond, as well as the pre-activation of precursors by halogenation or triflation, where the C–halide/triflate bond is represented as a C–X bond (Figure 2-1, left). However, there are many drawbacks of this "C–M/C–X" coupling strategy. (1) The preparation of both precursors is often a multi-step process, which is time-consuming and economically inefficient. (2) A stoichiometric amount of undesired metallic salts (MX) are generated as waste, which is environmentally hazardous. The need to improve efficiency and reduce hazardous waste has driven chemists to explore new catalytic reactions. One attractive solution to these problems is to treat C–H bonds as functional groups for direct transformations.[83-86] This strategy obviates the need for stoichiometric amounts of organometallic components, and the byproducts will be relatively more environmentally benign acids (HX) (Figure 2-1, right). On the other hand, C–H bonds are overall inert, rendering the direct utilization of C–H bonds very challenging. In addition, the ubiquity of C–H bonds in organic molecules introduces another fundamental obstacle—selectivity. Nevertheless, C–H functionalization chemistry has made tremendous progress in the past decade and it remains an area full of challenges and opportunities in the practice of organic synthesis.[87-93]

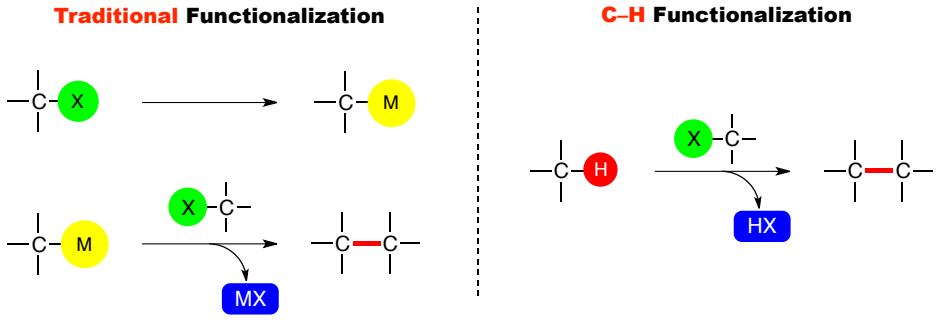

Figure 2-1. Traditional functionalization and C–H functionalization.[87]

2.1 "Innate" C–H functionalization and "guided" C–H functionalization

A multitude of research have addressed the inertness problem of C–H bonds for direct functionalization. Transition metals have been proven to react with C–H bonds to generate C–M bonds via "C–H activation".[84-87, 94-98] The resulting C–M bonds are much more reactive, and can be transformed to a variety of functional groups under mild conditions.

Selective activation of one specific C–H bond in a complex molecule is another key challenge associated with C–H functionalization. To date, two distinctive strategies have been developed to meet this challenge.[99] The most common strategy is to employ external reagents or directing groups to achieve specifically targeted C–H functionalization.[89, 91, 100, 101] This "guided" approach usually relies on coordination of heteroatoms to transition metals and selectively delivers the catalyst to the desired, proximal C–H bond. Nitrogen-containing groups, such as pyridinyl, have played an important role in the control of regioselectivity.[102, 103] Oxygen-containing groups, such as carboxylate, were also employed frequently in synthesis recently.[104, 105] Another powerful strategy is to solely capitalize on the intrinsic electronic nature of substrates without the presence of other directing forces.[79, 106] This "innate" approach is mostly applicable to the realm of heterocycles as heteroatoms easily induce electronic bias.[107]

It is worth noting that these two strategies are not superior but complementary to each other. The targeted molecule often dictates which strategy to be employed and in many cases a rational usage of both strategies can be very effective.

2.2 C–H functionalization via Pd catalysis

In the new millennium, the direct transformation of C–H bonds to C–C bonds has received much attention and significant progress has been made. Pd-catalyzed C–H functionalization has proven to be particularly effective.[91, 101, 108-112] It is the most widely studied reaction for many reasons: (1) Pd catalysts can install many types of bonds, including C–C, C–O, C–N, C–X, C–S bonds. Few other transition metal catalysts have shown such versatility. (2) Pd catalysts are compatible with many oxidants. (3)

Cyclopalladated intermediates can be selectively functionalized. (4) A variety of directing groups can bind with Pd catalysts. (5) A majority of Pd-catalyzed C–H functionalization reactions can be conducted in the presence of air and moisture. All these features set Pd apart from other transition metals in catalyzing C–H functionalization. In this regard, the current chapter will mainly focus on Pd-catalyzed C–C bond construction via C–H activation.

2.3 Plausible mechanisms for C–H activation

Pd-catalyzed C–H activation has been proposed to proceed through five distinct mechanisms (Figure 2-2): (1) Electrophilic palladation (S_EAr),[113-117] (2) a concerted S_E3 process,[118] (3) σ-bond metathesis,[114, 119, 120] (4) Heck carbopalladation,[114-117, 121, 122] (5) C–H oxidative addition.[119, 123]

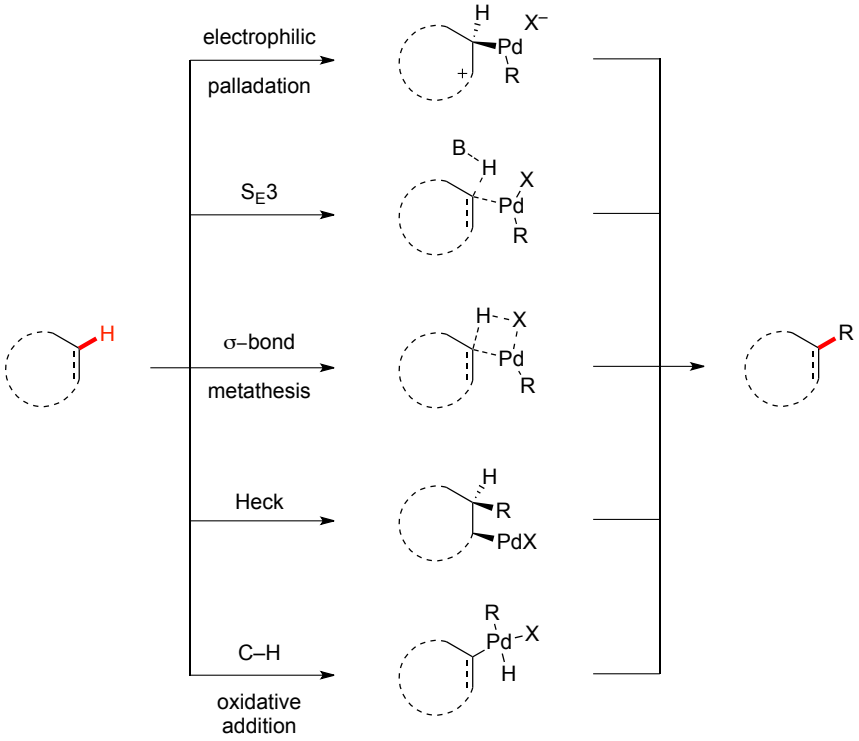

Figure 2-2. Plausible modes of C–H activation.

It should be noted that the exact mechanism for any given process depends largely on the nature of the substrates, Pd catalysts, additives, solvents, and ligands involved. Historically, S_EAr reactions, Heck processes, and C–H oxidative addition are favored in most cases. The S_EAr mechanism, however, has fundamental limitations, because not all the aromatics are sufficiently nucleophilic. Very recently, a number of experimental and computational studies supported the "concerted-metalation-deprotonation" (CMD) processes, involving a S_E3 process or σ-bond metathesis.[124-130] The key in these processes is the reactivity/acidity of the proton activated by the electron-withdrawing substituents. Hence, the C–H acidity could be used as a new parameter for tuning reactivity and regioselectivity, which offers an entirely different approach for designing C–H functionalization experiments.

2.4 Generic approaches for C–H functionalization

Over the course of the development of C–H functionalization chemistry, chemists have been striving to replace either C–M or C–X (or both) with C–H to improve the efficiency of cross coupling. Overall, there are three strategic routes to functionalize C–H bonds (Figure 2-3).

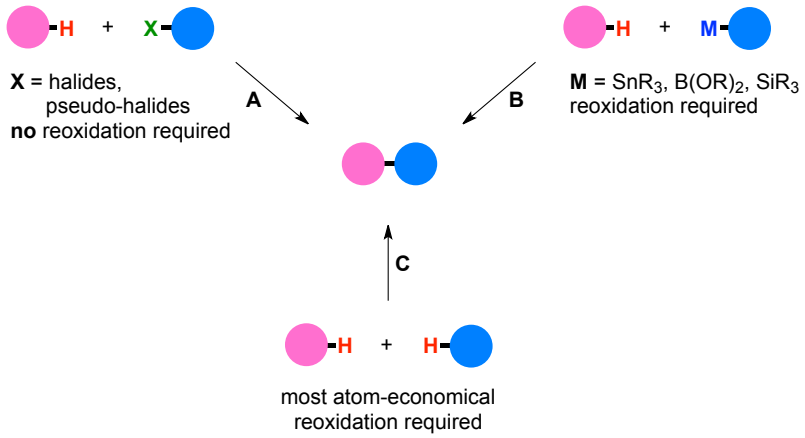

Figure 2-3. Three synthetic paths for C–H functionalization.

The most studied scenario involves direct C–H functionalization with organic halides/pseudohalides (Figure 2-3, Path A).[100, 109, 131, 132] As depicted in Figure 2-4, oxidative addition of organic halides/pseudohalides onto Pd^0 species initiates the catalysis. Next, one of the aforementioned mechanisms (Figure 2-2) can account for the subsequent C–H activation process, followed by reductive elimination to afford the coupling product and regenerate the Pd^0 catalyst. Variables such as ligands, bases, polar solvents, and high temperatures are critical in enabling these coupling reactions. Because hydrocarbons (C–H) are nucleophiles and organic halides/pseudohalides (C–X) are electrophiles, their coupling mechanism is a $Pd^{0/II}$ cycle, where no reoxidation is needed.

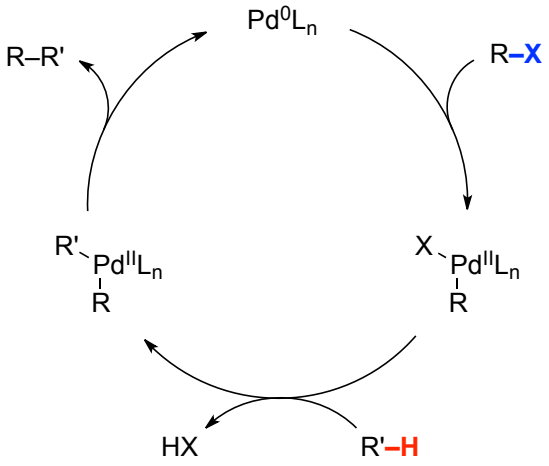

Figure 2-4. Generic mechanism of C–H functionalization with organic (pseudo)halides.

Recently, the cross-coupling reactions between hydrocarbons (C–H) and organometallic reagents (C–M) have started to gain more attention (Figure 2-3, Path B).[132-134] As the two coupling partners are both nucleophiles, these transformations apparently undergo a different process. Shown as a generic mechanism (Figure 2-5), C–H activation takes place first to generate the $R–Pd^{II}$ species. Transmetallation delivers the R' group onto the Pd center, followed by reductive elimination to furnish the coupling product, as well as the reduced Pd^0 species. To complete the catalytic cycle, oxidants are needed to reoxidize Pd^0 to Pd^{II}. Such a process is a $Pd^{II/0}$ cycle, defined as an *oxidative* cross-coupling. The challenges associated with this method are: (1) the homo-coupling of

organometallic reagents; (2) the incompatibility of the initial C–H activation and the following transmetallation; and (3) the instability of organometallic reagents under C–H activation conditions. Among the available organometallic reagents, Grignard reagents (organomagnesium), organolithium, organoaluminum, and organozinc reagents are highly reactive and therefore very unstable, which makes them hardly useful under C–H activation conditions. On the other hand, organoboron, organosilicon, and organotin reagents are superior candidates for C–H functionalization purposes.[133, 134]

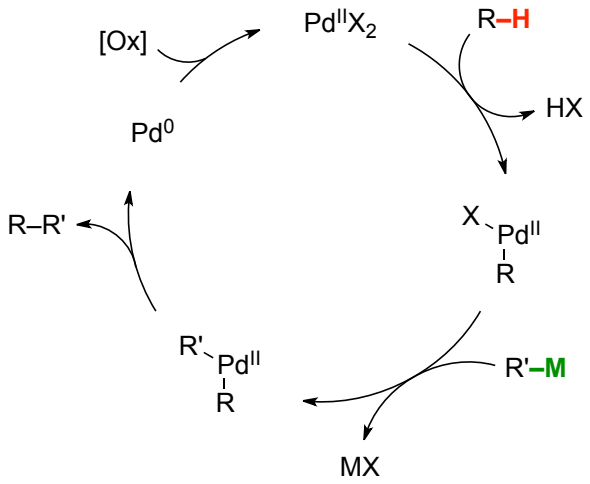

Figure 2-5. Generic mechanism of C–H functionalization with organometallic reagents.

Under the current trend of green chemistry, the best scenario to form a C–C bond is the coupling between two C–H bonds (Figure 2-3, Path C). This transformation is the most environmentally benign one in terms of ideal atom economy and minimal waste. Similar to Path B (in Figure 2-3), this coupling strategy also employs two nucleophiles and thus reoxidation is needed. However, this process is often extremely challenging and problematic with respect to regioselectivity. Mechanistically (Figure 2-6), the most difficult step is the *second* C–H activation (*i.e.* R'–H), because conditions must be found whereby the *second* C–H activation proceeds with complete reversal of chemoselectivity against the *first* C–H activation (*i.e.* R–H). This obstacle seems formidable at first glance because the competing homocoupling would be the most reasonable yet undesired

outcome. Fortunately, innovative solutions to this issue have been discovered. In recent years, there have been ever-increasing reports about these types of coupling reactions.[92, 133, 135-139] Overall, double C–H functionalization still remains much underdeveloped.

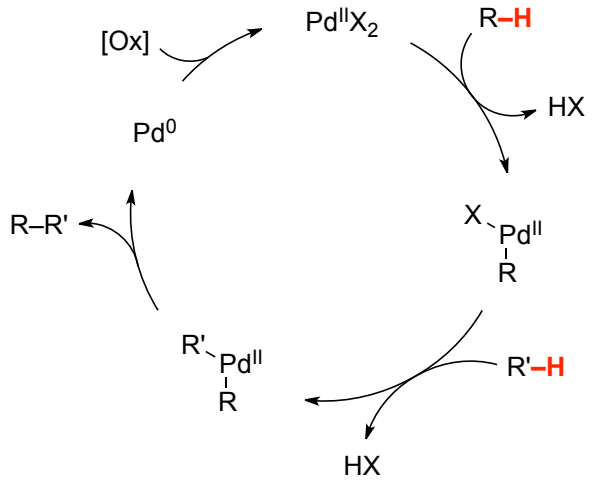

Figure 2-6. Generic mechanism of C–H functionalization with hydrocarbons.

In the following a brief review is provided that covers the most important advances of modern C–H functionalization chemistry, by highlighting the various coupling strategies. Given our goal to functionalize the C(sp^2)–H bond at the C5 position of 2,3-dihydropyridin-4(1*H*)-ones, the following review will be focusing on C(sp^2)–H functionalization.

2.5 Couplings between C(sp^2)–H and C–X

To date, numerous research efforts have been devoted to the coupling between nucleophiles (C–H) and electrophiles (C–X). Therefore, it is judicious to divide this section into four parts: C–H alkynylation, alkenylation, arylation, and alkylation.

2.5.1 C–H alkynylation with alkynyl (pseudo)halides – "Inverse Sonogashira"

Sonogashira cross-coupling reactions have been extremely valuable for preparing

functionalized (hetero)aryl alkynes, which are widely used in modern organic synthesis and material science.[140-142] The traditional version is a reaction between an aryl (or alkenyl) halide and a terminal alkyne. Recently, a complementary strategy was devised, namely an "inverse Sonogashira" coupling, which entails the direct C–H alkynylation of unactivated (hetero)arenes with readily available alkynyl halides.[143]

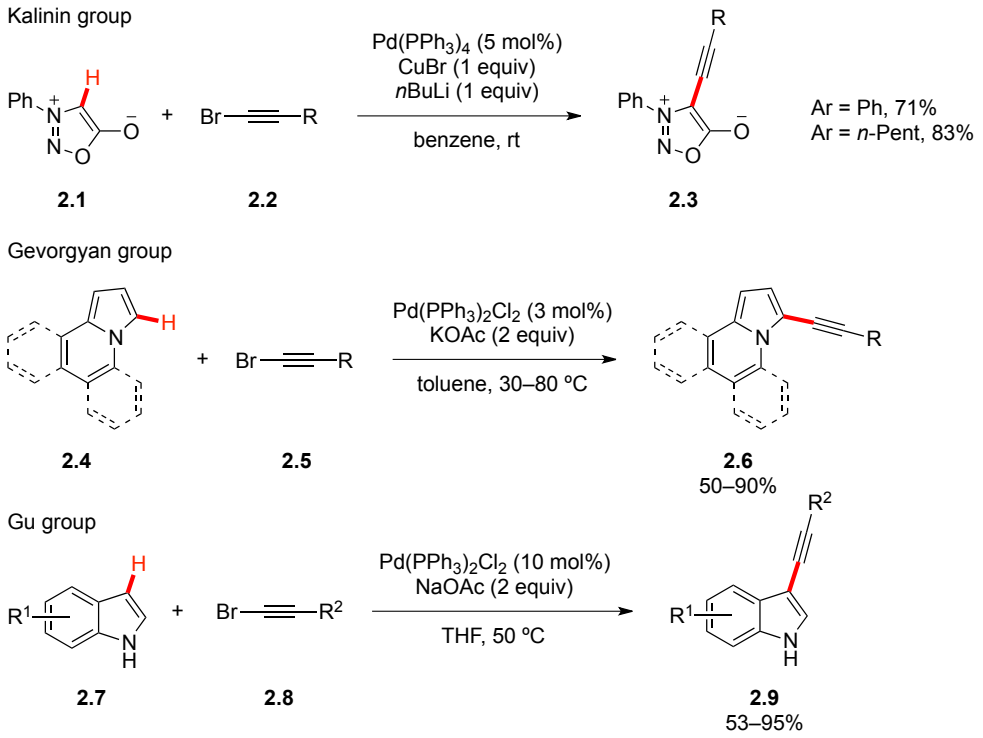

Scheme 2-1. "Inverse Sonogashira" reactions of heteroarenes.

The first example of this new alkynylation was developed on sydnones **2.1** in 1992 (Scheme 2-1, top).[144] This Pd^0-catalyzed protocol reported by Kalinin required a stoichiometric amount of Cu^I to form an organocopper intermediate for transmetallation. After that, the development of this coupling reaction almost halted until 2007, when Gevorgyan and co-workers reported a versatile protocol for the alkynylation of *N*-heteroarenes (Scheme 2-1, middle).[145] A series of electron-rich heterocycles **2.4** coupled with alkynyl bromides in high yields and regioselectivity. The authors showed that an alkynyl–Pd species, generated from the oxidative addition of Pd^0 into the alkynyl–Br

bond, was the key intermediate that enabled the installation of the alkynyl groups onto *N*-heterocycles by electrophilic substitution. Later, Gu reported a similar method to regioselectively alkynylate indoles at the C3-position with a wide range of substituted alkynyl bromides (Scheme 2-1, bottom).[146] The same electrophilic mechanism was proposed for this reaction as well.

In 2009, Chatani and co-workers reported the first Pd-catalyzed C–H alkynylation of anilides **2.10** (Scheme 2-2, top).[147] Directed by an acetamido group, *ortho*-alkynylation furnished a variety of aryl alkynes in good yields and excellent regioselectivity. Very recently, Chen applied the same strategy to directly alkynylate benzylamine picolinamides **2.13** (Scheme 2-2, bottom).[148] The picolinamide group-directed process attained excellent *ortho*-selectivity, and both electron-rich and electron-poor arenes afforded similar high yields.

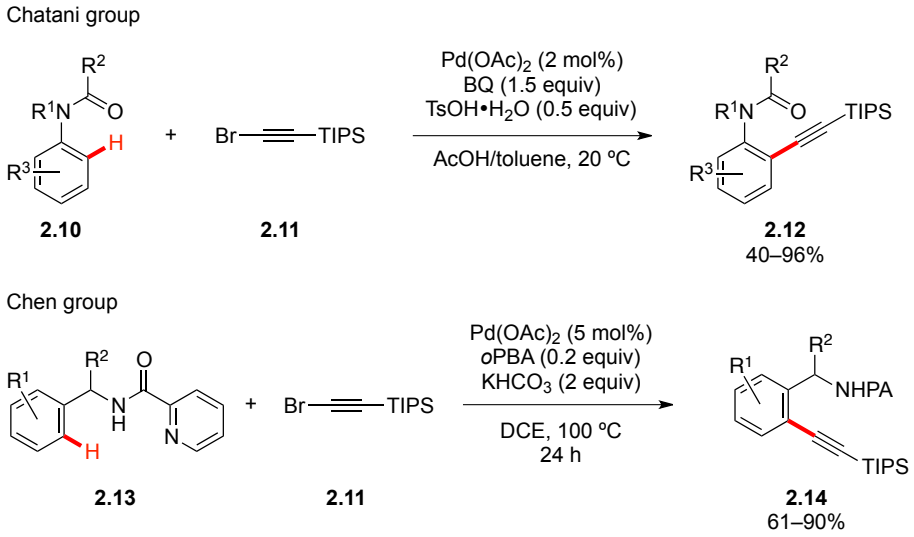

Scheme 2-2. "Inverse Sonogashira" reactions of benzenes.

2.5.2 C–H alkenylation with alkenyl (pseudo)halides – "Inverse Heck"

The Heck reaction was first introduced in 1971.[149] The reactants of Heck reactions typically involve an unsaturated (pseudo)halide and an alkene. As the traditional Heck reactions do not involve organometallic coupling partners, they hence possess better atom

economy compared to other related reactions, such as Suzuki, Negishi, and Still reactions. Due to the wide availability of substrates, the Heck reaction soon became one of the most useful coupling reactions in organic synthesis.[150-153]

Complementary to this approach is the "inverse Heck" reaction, which couples unfunctionalized arenes with alkenyl halides. This strategy expanded the substrate scope and provided alternative routes to alkenyl arenes. However, this approach has received much less attention.[154-160]

In 2005, Daugulis first reported a C–H alkenylation of anilides with haloolefines **2.16** (Scheme 2-3, top).[154] The authors proposed a C–H palladation/migratory alkenylation mechanism, which implied the feasibility of β-halide elimination, instead of β-H elimination, as the terminating step to regenerate the Pd catalyst. This acetamido group-directed coupling reaction afforded excellent *ortho*-selectivity and tolerated more functional groups compared to the traditional Heck reaction. Recently, Chen and co-workers employed a similar strategy to directly alkenylate benzylamine **2.13** (Scheme 2-3, bottom).[148] A broad scope of benzylamine picolinamides **2.13** and vinyl iodides was shown to be compatible with the Pd-catalyzed conditions and provided the reaction products in excellent regioselectivity and good to excellent yields.

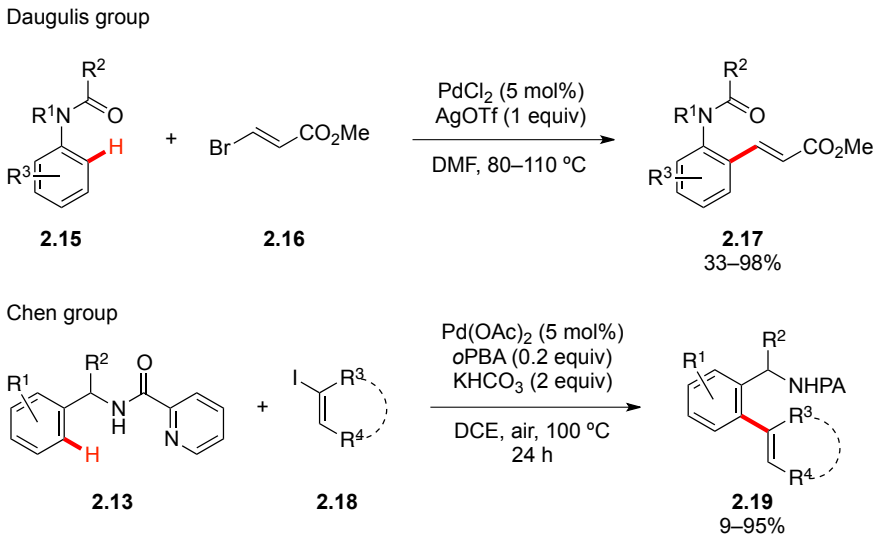

Scheme 2-3. "Inverse Heck" reactions of benzenes.

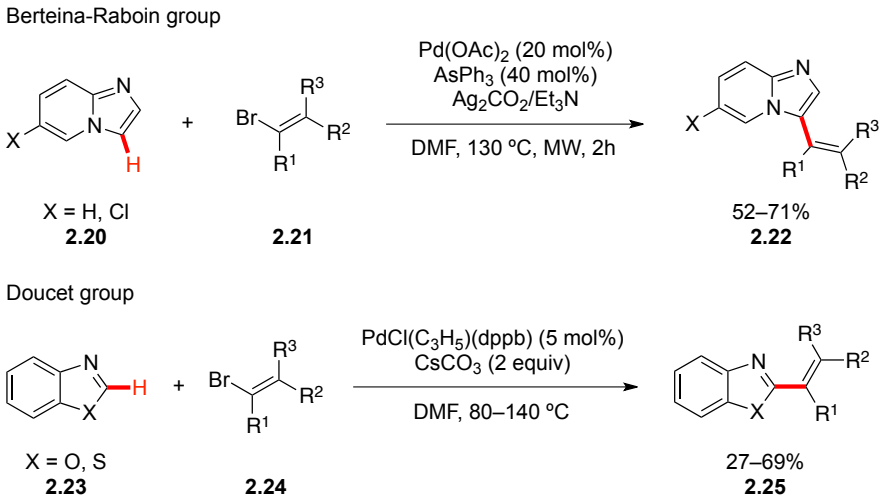

Scheme 2-4. "Inverse Heck" reactions of heteroarenes.

The "inverse Heck" reaction is also applicable to heteroarenes in the absence of directing groups. Berteina-Raboin and co-workers devised a Pd-catalyzed regioselective C–H alkenylation of imidazol[1,2-*a*]pyridines **2.20** under microwave conditions (Scheme 2-4, top).[160] The innate nucleophilicity of **2.20** enhanced the C3-regioselectivity. Different from the proposed mechanism for arenes with directing groups, Berteina-Raboin proposed a discrete route following an oxidative addition/electrophilic palladation/reductive elimination sequence. Later, Doucet extended the scope of heteroarenes to electron-rich benzoxazole and benzothiazole derivatives **2.23** (Scheme 2-4, bottom).[155] A set of alkenylated heteroarenes **2.25**, which was difficult to prepare before, was obtained in moderate yields, demonstrating the advantage of this coupling reaction. Similarly, Hoarau later reported that oxazoles were also suitable substrates for direct alkenylation.[157]

2.5.3 C–H arylation with aryl (pseudo)halides

Direct arylation with aryl (pseudo)halides is arguably the most studied C–H functionalization reaction. One reason is the importance of biaryl structural motifs in various natural products and pharmaceutical molecules.[82, 132, 161-163] Traditional arylation reactions have significant value for cross-coupling reactions, such as high regioselectivity

and reactivity, albeit with some drawbacks such as low atom-economy and poor substrate availability. Direct arylation with accessible and inexpensive aryl (pseudo)halides could overcome these disadvantages while retaining the desirable feature of high regioselectivity.

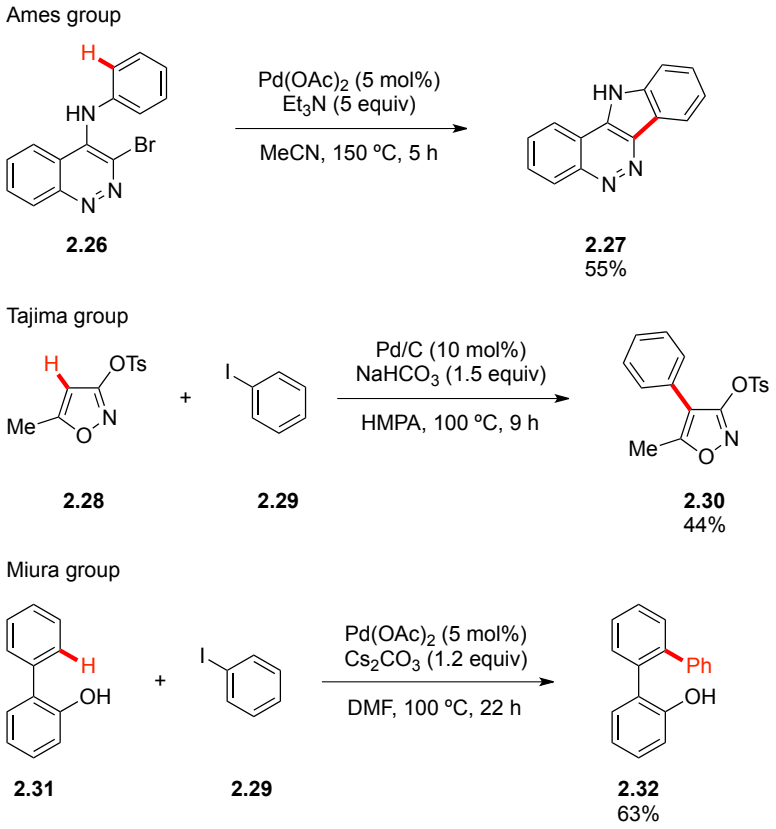

Scheme 2-5. Early examples of C–H arylation with aryl halides.

The early discovery of the direct arylation with aryl halides was made serendipitously. In 1982, Ames observed an intramolecular direct arylation product **2.27** when studying a Heck reaction with ethyl acrylate (Scheme 2-5, top).[164] Soon after, an intermolecular direct arylation with iodobenzene was observed on isoxazole **2.28** by Tajima and co-workers (Scheme 2-5, middle).[165] In 1997, Miura devised the first protocol of directing group-assisted regioselective intermolecular C–H arylation of 2-phenylphenol (**2.31**) with aryl iodides (Scheme 2-5, bottom).[166] These early

developments paved the road for the subsequent explorations of this valuable coupling strategy. Given the enormous amount of reports on this particular topic versus the limited space for this dissertation, the current section will only highlight the recent advance in direct arylation involving *challenging substrates* and *novel mechanistic strategies*.

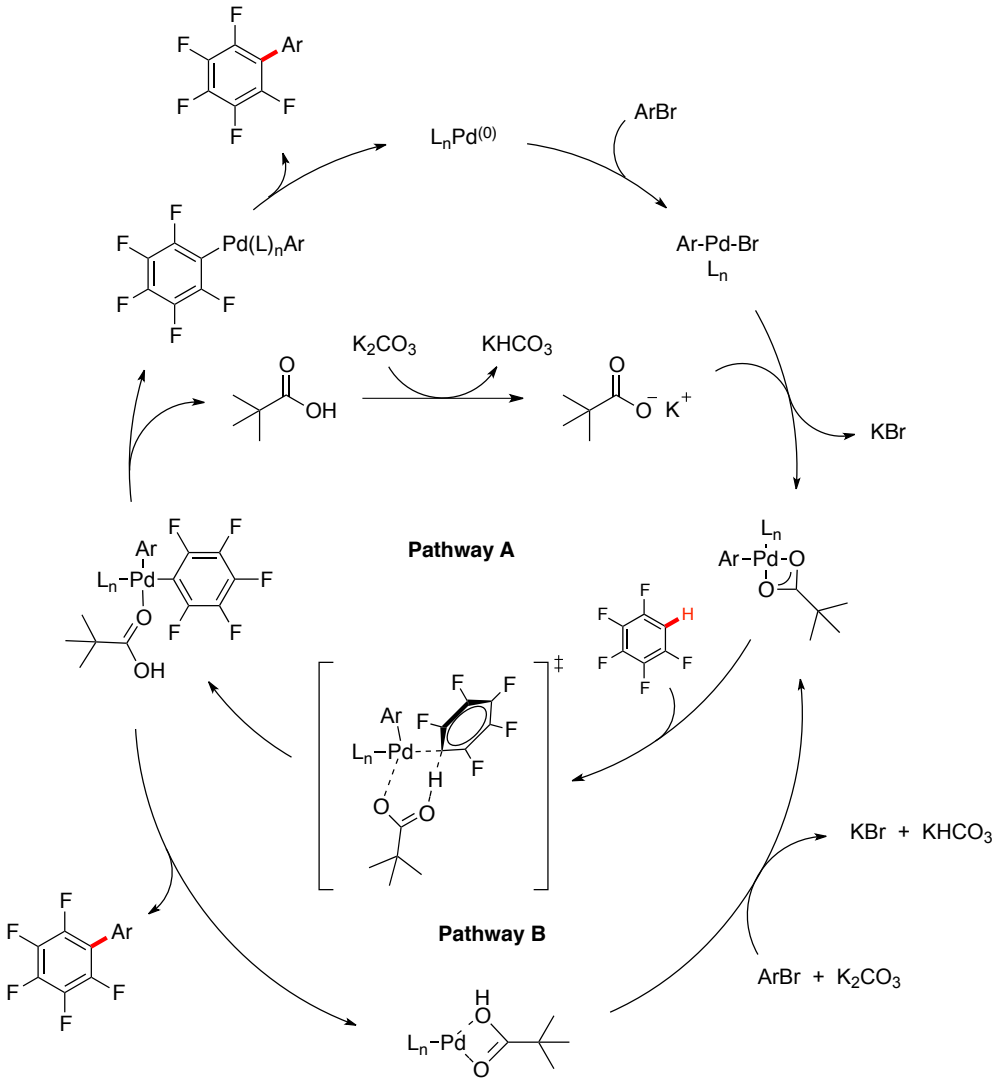

Figure 2-7. Proposed CMD mechanism with pivalic acid as a proton shuttle.

One major breakthrough in this field was the discovery of the concerted metalation–deprotonation (CMD) mechanism. Echavarren and co-workers first conducted a series of well-designed intramolecular competition experiments, which showed that the less

nucleophilic, thus more C–H acidic, fluorinated arenes were better substrates for direct arylation.[167-170] Meanwhile, Fagnou observed that electron-poor heteroarenes (*e.g.* pyridine *N*-oxide) underwent C2-regioselective direct arylation with aryl bromides.[171] Intermolecular competition experiments showed again that the less nucleophilic, thus more C–H acidic, heteroarenes were more reactive. In addition, the intermolecular kinetic isotope effect (KIE) was observed at 4.7 (*i.e.* primary KIE), which does not support an S_EAr mechanism.[171] Further experimental and computational studies indicated that the pivalate anion was a crucial component in the C–H cleavage, acting as a proton shuttle and lowering the transition state energy of C–H cleavage (Figure 2-7).[124, 126] In many cases, a direct correlation was found between the acidity of aromatic C–H bonds and the regioselectivity of the direct arylation.[126, 129] Electron-withdrawing substituents would increase the C–H acidity, thus activating those C–H bonds in the CMD process. Hence, the regioselectivity for direct arylation of (hetero)arenes, especially electron-deficient ones, could be predicted by the C–H acidities.[126, 129]

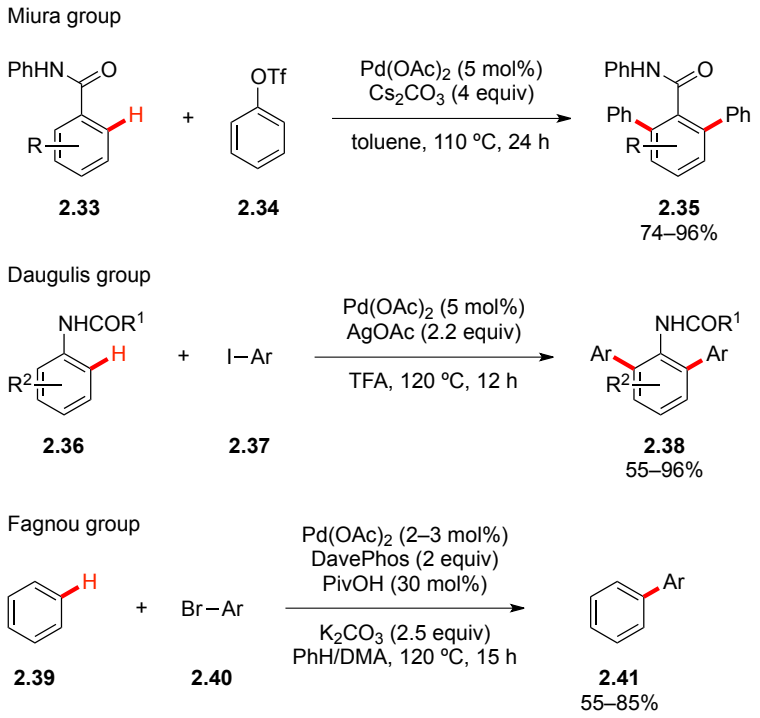

Scheme 2-6. Directed and non-directed C–H arylation of arenes.

The application of chelation control (*i.e.* directing groups) has also enabled intermolecular direct arylation of arenes with excellent *ortho*-selectivity. Following their original work,[166] Miura and co-workers continued to develop protocols for a variety of carbonyl directing groups, such as ketones, amides, and aldehydes (Scheme 2-6, top).[172, 173] Aryl bromides and triflates were used as good arylating reagents. Later, Daugulis expanded the scope of aryl halides to aryl iodides (Scheme 2-6, middle).[174] More substrates with other directing groups (*e.g.* acetamido, carboxylate, pyridine, etc.) were regioselectively functionalized with aryl iodides.[175-177] On the other hand, direct arylation of arenes without directing groups have been very rare. Fagnou and co-workers successfully arylated unactivated simple benzene through a CMD process with aryl bromides (Scheme 2-6, bottom).[124] Remarkably, this protocol furnished only mono-arylated benzenes **2.41**.

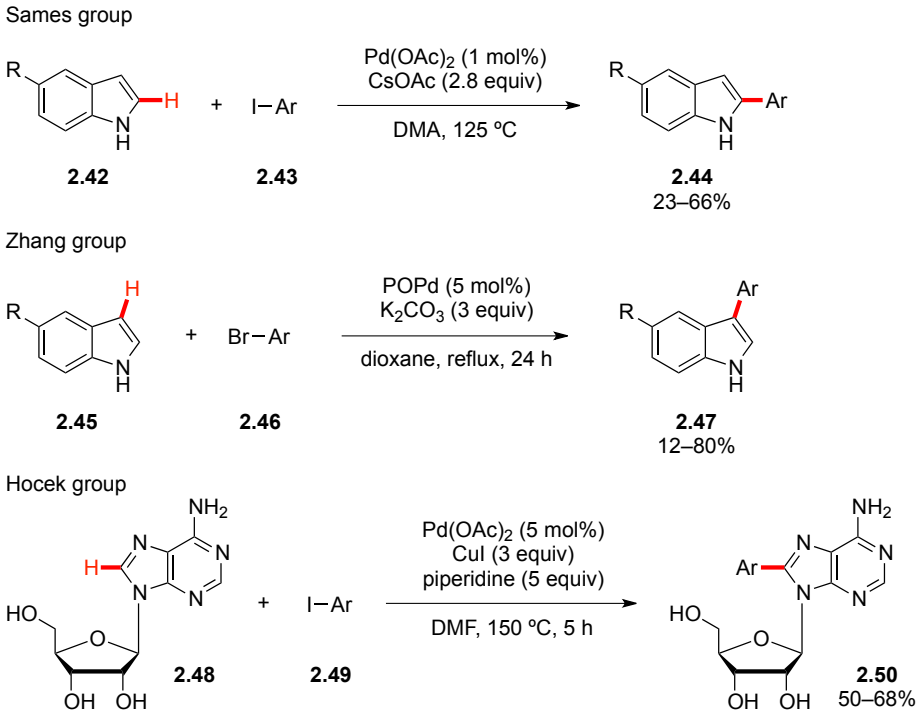

Scheme 2-7. Innate C–H arylation of heteroarenes with aryl halides.

Direct arylations of heteroarenes with aryl (pseudo)halides have also experienced fast

development. Indoles are arguably the most abundant heteroarene moieties in natural products.[178, 179] A significant amount of research has been carried out to functionalize this electron-rich heterocycle.[180] The direct arylation of indoles can take place at either the C2 or C3 positions. Sames and co-workers reported a ligand-free protocol for the direct C2-arylation of indoles (Scheme 2-7, top),[181] while later Zhang[182] and Bellina,[183] respectively, devised an efficient protocol for the regioselective C3-arylation of indoles (Scheme 2-7, middle). Many other heteroarenes (*e.g.* thiophenes,[184] azoles,[185] indolizines,[116] *etc*.) were all found to be good substrates for regioselective direct arylation without the assistance of directing groups. For example, Hocek and co-workers developed the first direct arylation of unprotected purine nucleosides **2.48**, thereby offering quick access to a variety of arylated adenine nucleosides **2.50** (Scheme 2-7, bottom).[186]

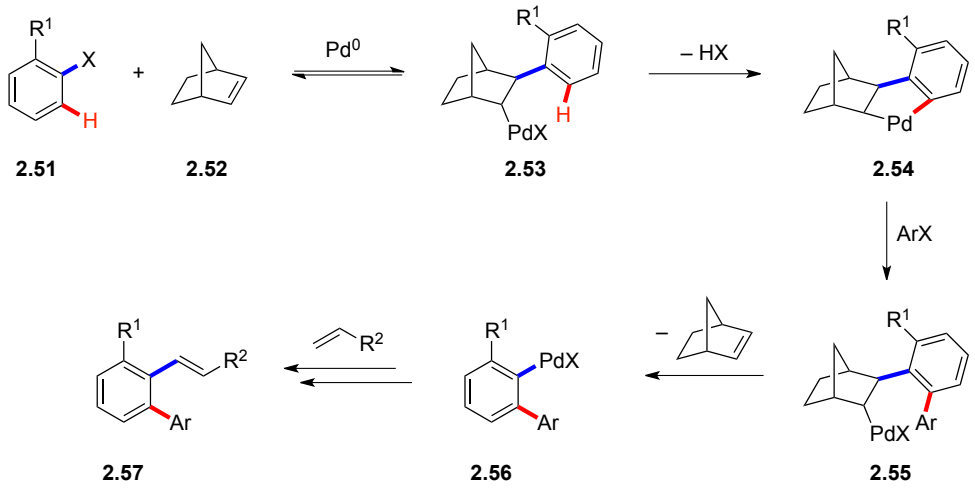

Scheme 2-8. Norbornene-mediated direct arylation.

Another elegant strategy for direct arylation is the use of strained norbornene **2.52** as a removable external directing group for sequential C–H functionalization.[187] Norbornene (**2.52**) forms palladacycle **2.54**, which directs the subsequent arylation and termination coupling selectively (Scheme 2-8). The installation of the R^1 group has two purposes: (1) Regioselectivity can be controlled at the other *ortho*-position; (2) The steric encumbrance in **2.55** exerted by the R^1 and Ar groups can facilitate the expulsion of norbornene. As

shown in Scheme 2-8, a Heck reaction can intercept the Pd species **2.56** in the end. The intermediate **2.56** can also be employed in other traditional coupling reactions to construct C–H, C–C, C–N, and C–O bonds.[187]

This novel concept has been used to quickly assemble complex molecules.[188] For example, Lautens applied this strategy to prepare a series of polycyclic 2*H*-indazoles such as **2.60** (Scheme 2-9, top).[189] Key features include one-pot procedures, high tolerance of functional groups, and readily available starting materials. Similarly, via a direct arylation/amination sequence, two C–C/C–N bonds were constructed regioselectively to form **2.63** in moderate yield (Scheme 2-9, bottom).[190]

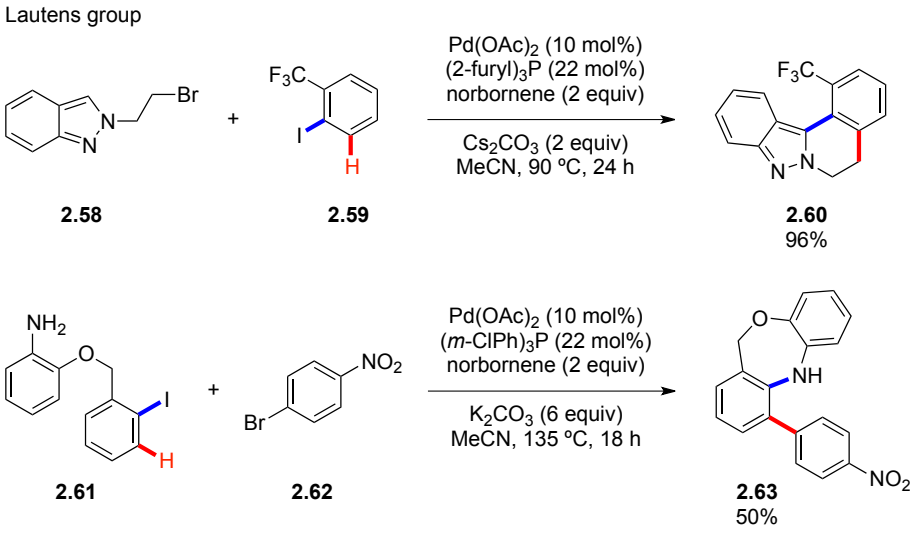

Scheme 2-9. Synthesis of polycycles via norbornene-mediated direct arylation.

Of all aryl (pseudo)halides, the chlorides are potentially the most accessible electrophiles due to their low cost and broad commercial availability. However, aryl chlorides have been very difficult to use for direct arylation. Until recently, examples of intermolecular direct arylation with aryl chlorides have been scarce.[191, 192] In 2006, Fagnou reported two examples of intermolecular direct arylation of 1,3-benzodioxole (**2.64**) using aryl chlorides (Scheme 2-10, top).[193] Later Daugulis disclosed a protocol for direct arylation of benzoic acids with aryl chlorides (Scheme 2-10, bottom).[194] Benzoic acids of any electronic nature can be employed in this reaction.

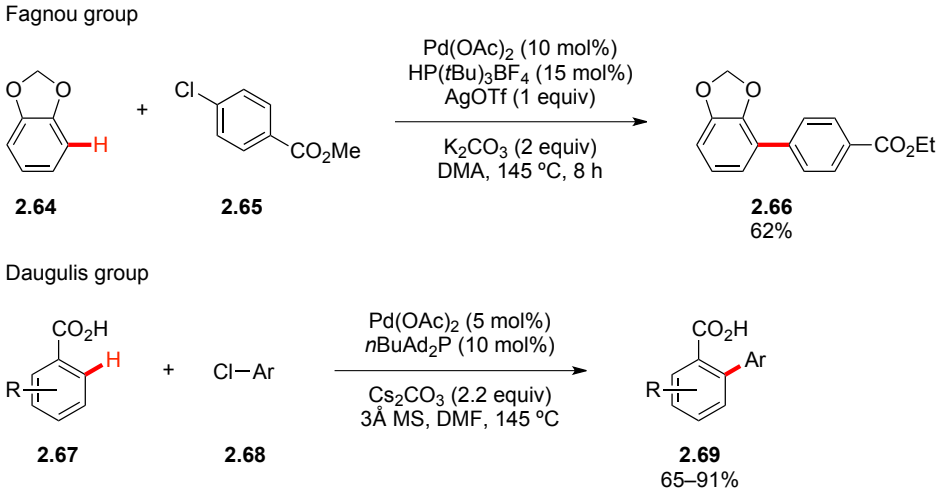

Scheme 2-10. Early examples of direct arylation with aryl chlorides.

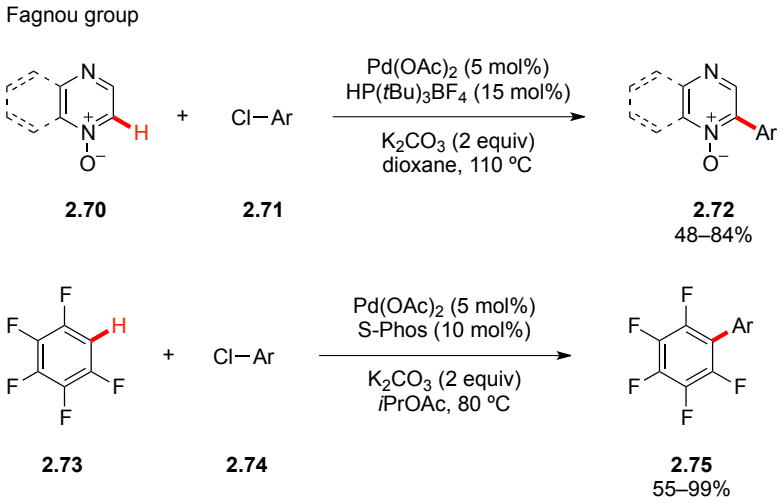

Scheme 2-11. Direct arylation of electron-deficient (hetero)arenes with aryl chlorides.

More recently, more electron-rich (hetero)arenes were also used for the direct arylation with aryl chlorides, such as benzoxazols,[195] thiazoles,[195] furans,[196] triazoles,[197] *etc*. Examples of electron-poor (hetero)arenes, albeit scarce, have also gained more attention. For example, diazine *N*-oxides **2.70** were regioselectively coupled with aryl chlorides in good yields via a CMD mechanism (Scheme 2-11, top).[198] These inexpensive and readily available substrates are good replacements for problematic diazine organometallic precursors for coupling reactions. In addition, mild and general protocols

were also established with aryl chlorides to functionalize perfluoroarenes (**2.73**, Scheme 2-11, bottom), a class of important structures particularly in material chemistry.[199, 200]

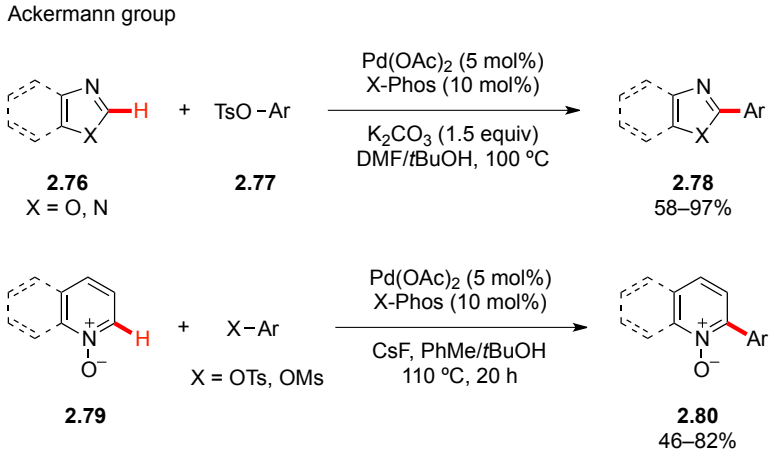

Scheme 2-12. Direct arylation using aryl pseudohalides.

Lately, other arylating electrophiles (pseudohalides) are emerging as good alternative aryl sources. Particularly, compared to aryl triflates,[201-203] aryl tosylates and mesylates are highly desirable, because they are stable towards hydrolysis and highly crystalline, thus easy to handle. These electrophiles can be prepared easily from inexpensive and readily available phenol derivatives. However, their good stability results in reduced reactivity towards coupling reactions. The development of these reagents for C–H functionalization has just begun to burgeon.[204-210] Ackermann and co-workers reported the first protocol using aryl tosylates in the C–H arylation of heteroarenes **2.76** in 2009 (Scheme 2-12, top).[209] Later, the protocol was modified for electron-poor heteroarenes **2.79** to provide excellent regioselectivity and high yields (Scheme 2-12, bottom).[208] The reaction conditions were also found to be applicable to reactions with aryl mesylates, which are more atom-economical than the tosylates. Very recently, aryl tosylates have also been effectively applied to the direct arylation of perfluoroarenes,[205, 207] as well as the intramolecular C–H arylation of simple arenes to construct a variety of heterocycles.[211]

2.5.4 C–H alkylation with alkyl (pseudo)halides

Conventional Pd-catalyzed alkylation requires the use of stoichiometrically metallated substrates and alkyl halides.[212-215] Its inherently low atom-economy and poor efficiency has motivated organic chemists to explore other coupling options, including direct C–H alkylation. However, a tremendous challenge associated with using alkyl (pseudo)halides is to eliminate the competing β-H elimination when β-hydrogens are present in the alkyl group. Contrary to the well developed use of aryl (pseudo)halides, the application of alkyl (pseudo)halides for intermolecular C–H alkylation is still in its infancy.[216-219]

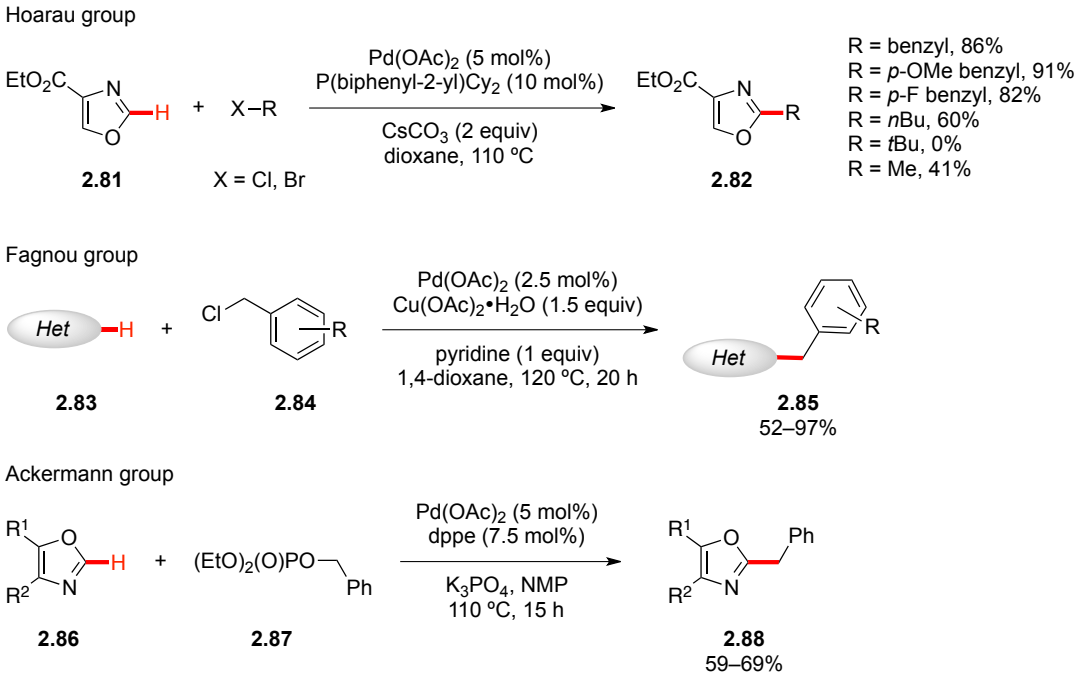

Scheme 2-13. Direct alkylation of heteroarenes using alkyl (pseudo)halides.

In recent years, remarkable progress has been made. Hoarau and co-workers reported the first intermolecular direct alkylation of heteroarenes in 2009.[157] The conditions they developed for the direct alkenylation of oxazoles **2.81** were also applicable for the direct alkylation and benzylation (Scheme 2-13, top), provided that the alkyl halides were in excess. Shortly thereafter, Fagnou significantly expanded the scope of heteroarenes for

direct benzylation (Scheme 2-13, middle).[220] A wide range of previously incompatible heterocycles, including thiazole, thiophene, 1,2,3-triazole, oxazole, furan, indolizidine, and imidazopyrimidine, were shown to regioselectively couple with benzyl chloride in excellent yields. Recently, Ackermann applied user-friendly benzyl phosphate **2.87** to replace the conventional benzyl halides as benzylating reagents (Scheme 2-13, bottom).[221] Similarly, Miura also demonstrated that benzyl carbonates can be used as electrophiles for the direct benzylation of azoles.[222]

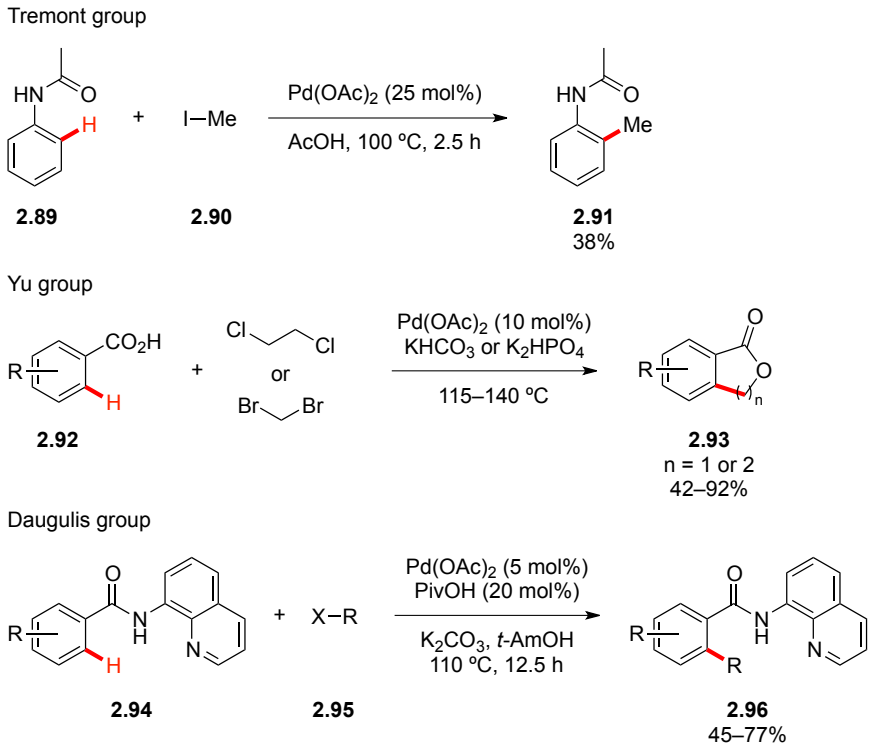

Scheme 2-14. Direct alkylation of arenes using alkyl halides.

Meanwhile, Tremont and co-workers first showed that C–H alkylation of acetanilide (**2.89**) could be achieved with methyl iodide, albeit in a low turnover number (1.5–1.8) (Scheme 2-14, top).[223] The mechanism was proposed to proceed through a Pd^{II}/Pd^{IV} cycle. However, the addition of excess AgOAc to regenerate more electrophilic Pd(OAc) catalyst significantly increased the TON to 10. In 2010, Yu devised a similar alkylation protocol for benzoic acids with 1,2-dichloroethane or dibromomethane to form

benzolactones **2.93** (Scheme 2-14, middle).[219] A mechanistic study showed that the initial reaction was an intermolecular *ortho*-C–H alkylation directed by the carboxylate group, which was followed by an intramolecular S_N2 cyclization. In contrast, Yu's protocol did not require Ag salts to regenerate the Pd catalyst. Unfortunately, monochloropentane (without the subsequent S_N2 cyclization) only furnished 26% of the desired *ortho*-alkylated product. In this regard, Daugulis developed a more applicable alkylation protocol between arenes and primary alkyl halides (Scheme 2-14, bottom).[224] Their auxiliary-assisted new protocol was also applicable for direct arylations with aryl halides.

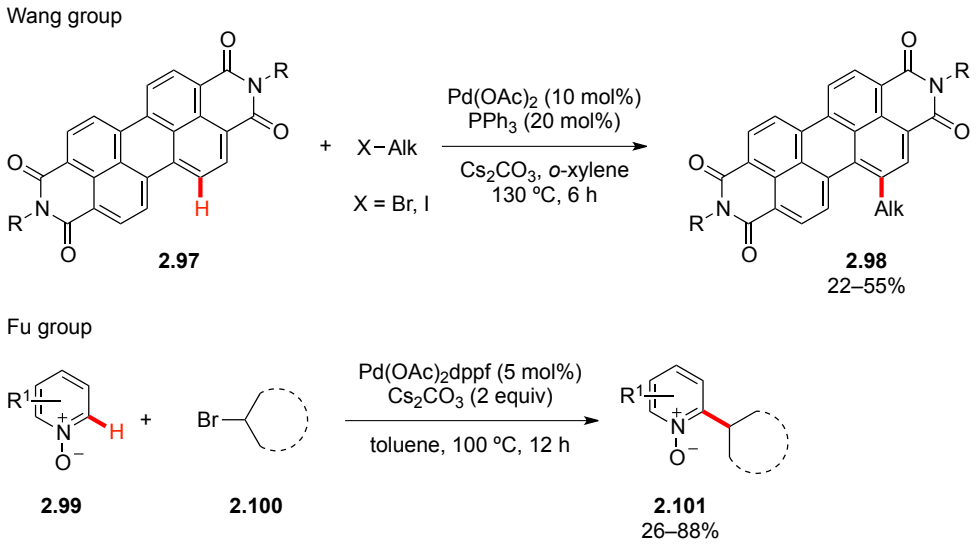

Scheme 2-15. New development in direct alkylations.

Most studies with arenes that have used primary alkyl electrophiles have achieved excellent *ortho*-selectivity thanks to the directing group effect. More recently, Wang and co-workers have shown that *meta*-selective C–H alkylation is also achievable (Scheme 2-15, top).[225] The electron-poor perylene bisimides **2.97** underwent C–H alkylation with open-chain alkyl halides in moderate yields but excellent regioselectivity. The authors proposed a CMD mechanism to account for the *meta*-selectivity. In regard to the difficulty of using *secondary* alkyl halides, one reason is that the Pd-catalyzed S_N2 process is sensitive to the steric bulk of the substrate. In 2013, Fu and co-workers demonstrated a remarkable protocol for direct alkylation using secondary and even

tertiary alkyl bromides **2.100** (Scheme 2-15, bottom).[226] Pyridine *N*-oxides were alkylated with high yields and excellent regioselectivity. Surprisingly, primary alkyl bromides were less reactive. A mechanistic study suggested a radical-type process for the C–Br bond cleavage, which may offer more opportunities for employing secondary and tertiary aliphatic electrophiles in Pd catalysis.

2.6 Couplings between C(sp^2)–H and C–M

Compared to the abundance of C–H functionalization protocols using (pseudo)halides, the application of organometallic reagents has just begun to be explored.[134] In addition to controlling regioselectivity, suppressing homo-coupling of organometallic reagents is another key matter. Due to the difference between organometallic reagents, the progress in this area will be highlighted accordingly. (Because the couplings between alkenes and organometallic reagents are known as *oxidative Heck* reactions,[151] these couplings are not technically C–H functionalization reactions. In that regard, the corresponding research will not be outlined in this thesis.)

2.6.1 Organoboron reagents

Suzuki-Miyaura reactions with organoboron reagents have been a powerful and convenient tool to build C–C bonds.[227-232] The wide applications of organoboron reagents in organic synthesis can be attributed to their nontoxicity, availability, stability, and ease of handling. Besides boronic acids, organoboron reagents also exist in other forms (Scheme 2-16), such as boronic esters, boroxines, and trifluoroborate salts, all of which have shown great reactivity in many cross-coupling reactions.[233-238]

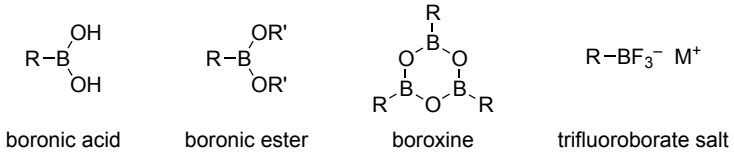

Scheme 2-16. Common forms of organoboron reagents.

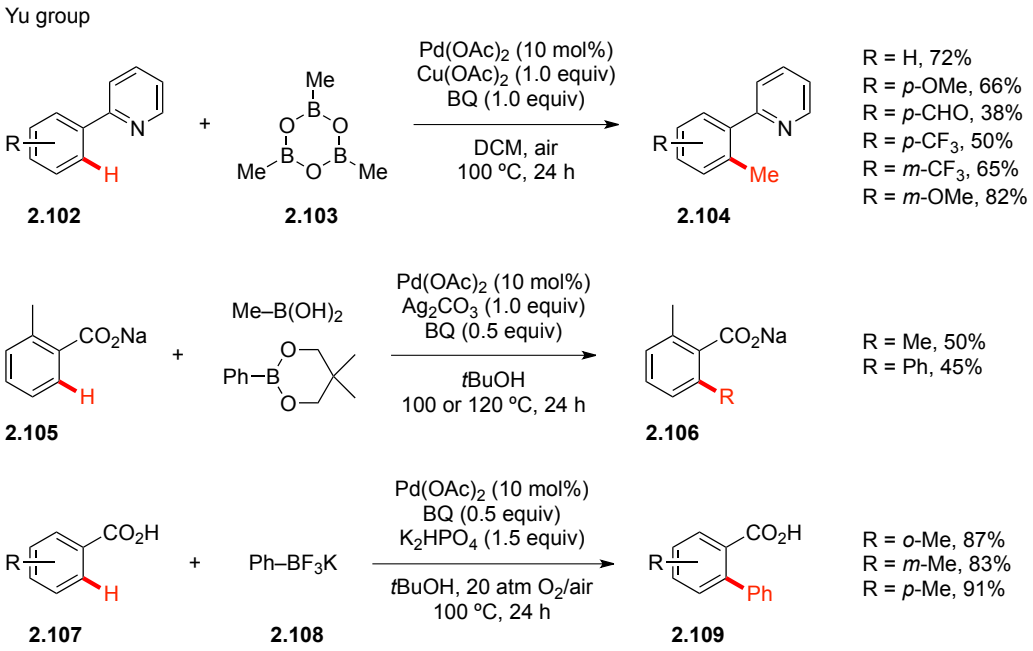

Scheme 2-17. "Guided" C–H functionalization using organoboron reagents in Yu's lab.

Reports about the "Suzuki-type" C–H functionalization are still rare, but recent advances have seen more application of organoboron reagents in this field. To date, using directing groups has been the best way to tune the reactivity and control the site selectivity. Prof. Jin-Quan Yu's work has been the most prominent.[239, 240] In 2006, his group first reported a Pd-catalyzed *ortho*-C–H alkylation of simple arenes directed by a pyridinyl group (Scheme 2-17, top).[239] Methylboroxine (**2.103**) was found to be the best methyl source. A variety of functional groups attached to the arene were compatible, although electron-withdrawing groups slightly lowered the yields. They were also able to use other alkylboronic acids to alkylate simple arenes under the same conditions, only replacing the Cu oxidant with Ag_2O and DCM solvent with *t*-AmOH. They later reported a similar transformation directed by a carboxylate group (Scheme 2-17, middle).[240] A sodium salt (**2.105**) of benzoic acids was crucial for reactivity. In order to use benzoic acids directly, the base K_2HPO_4 was essential to activate their reactivity in transmetallation by forming potassium salts *in situ*. However, the scope of this protocol was limited to only a few benzoic acids, and electron-poor arenes afforded very low yields. Hence, Yu and co-workers devised an improved method using aryltrifluoroborate

salts such as **2.108** (Scheme 2-17, bottom).[241] The scope and yield of the C–H arylation was greatly enhanced.

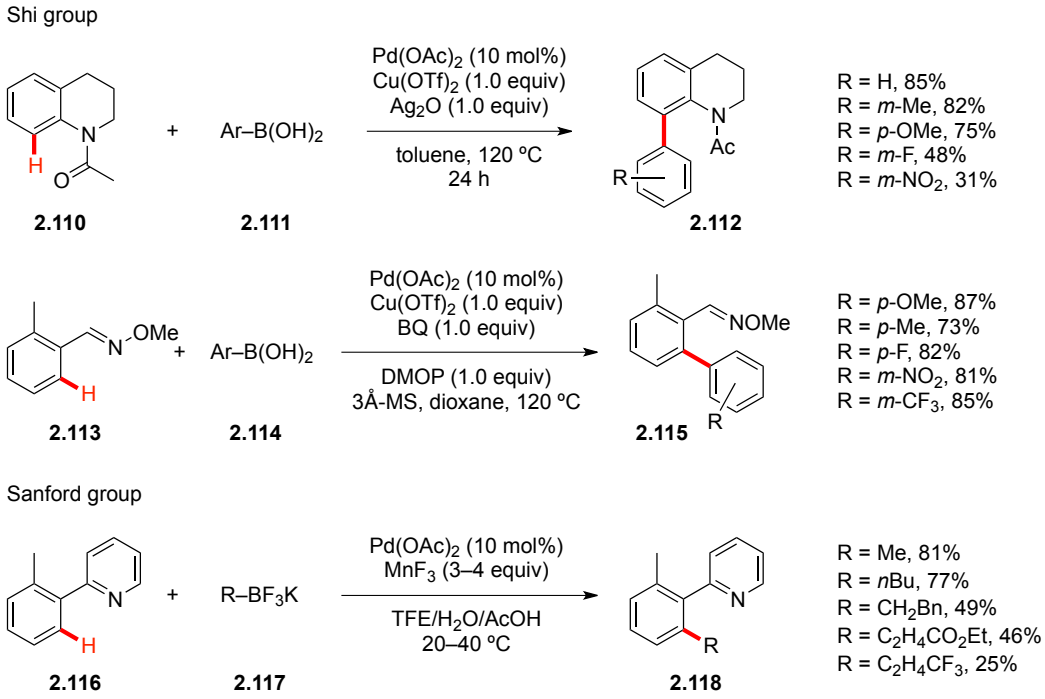

Scheme 2-18. "Guided" C–H functionalization with organoboron reagents.

In 2006, Shi and co-workers reported an acetamido-directed ortho-C–H arylation of acetanilide **2.110** (Scheme 2-18, top).[242] The coupling outcome was influenced by the electronics of the arylboronic acids. Electron-rich arylboronic acids afforded higher yields than the electron-poor ones. Later, they developed a similar *ortho*-arylation procedure, which was instead directed by *O*-methyl oximes (Scheme 2-18, middle).[243] They found that 2,6-dimethyloxypyridine (DMOP) was the most efficient base to improve the yield. In this protocol, the electronic properties of the aromatic substituents did not affect the yield very much. Moreover, other directing groups (*e.g.* oxazole, pyridylsulfinyl) were also reported to guide *ortho*-C–H arylation processes with arylboronic acids.[244, 245] Recently, Sanford and co-workers devised a mild method for ligand-directed C–H alkylation using MnF_3 in conjunction with organotrifluoroborates **2.117** (Scheme 2-18, bottom).[246] Their new method can install methyl and primary alkyl

groups onto substrates bearing either pyridine or amide directing groups. The mechanism was proposed to involve a more reactive R–Pd^{III} or R–Pd^{IV} intermediate, thereby addressing several of the key limitations of prior protocols (*e.g.* slow reductive elimination and high temperatures).

With regard to innate C–H functionalization with organoboron reagents, more reports have been emerging in recent years. In 2008, Shi reported an innate C–H arylation of mesitylenes **2.119** with phenylboronic acid (Scheme 2-19, top).[247] Electron-rich arenes showed good yields, although the substrate scope is quite limited. In fact, innate C–H functionalization is most suitable for heteroaromatic systems.[247, 248] A variety of electron-rich heteroarenes **2.122** underwent C–H arylation regioselectively with good yields (Scheme 2-19, bottom). However, the acetyl-protected indole afforded a poor yield, because the decrease of electron density disfavored the electrophilic palladation process.

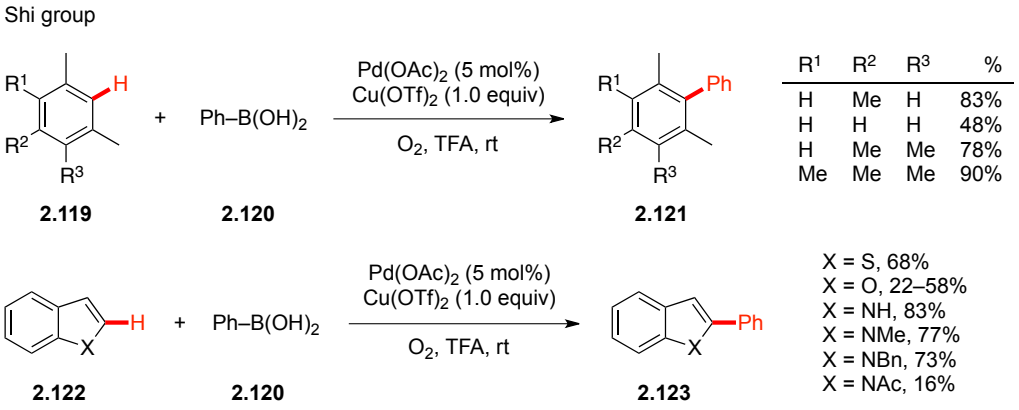

Scheme 2-19. "Innate" C–H functionalization with organoboronic acid.

2.6.2 Organotin reagents

Stille reactions with organotin reagents have been widely studied.[249-251] Because of their high tolerance of functional groups, moderate reactivity, and mild reaction conditions, organotin reagents have found many applications in total synthesis.[252-254] However, in regard to atom economy, only one of the four groups on Sn is actually delivered to the final product, rendering this process more costly. Lastly, the toxicity of

organotin reagents is another significant drawback that limits their applications.

Stille-type C–H functionalization by palladium catalysis was first reported by Yu and co-workers in 2005 (Scheme 2-20, top).[255] They found that Pd^{II}-catalyzed C–H alkylation of **2.124** could be achieved with alkyltin reagents by using stoichiometric amounts of $Cu(OAc)_2$ and benzoquinone (BQ) in MeCN under air. The oxazolinyl (Oxa) group served as the directing group and the dimethylated product was dominating. Interestingly, when the authors extended the directing group by one carbon, monoalkylation was achieved exclusively (Scheme 2-20, middle). A series of primary alkyl groups were installed in good yields. They noted that adding the organotin reagents in batches was crucial to eliminate homo-coupling products, which however led to extended reaction times.

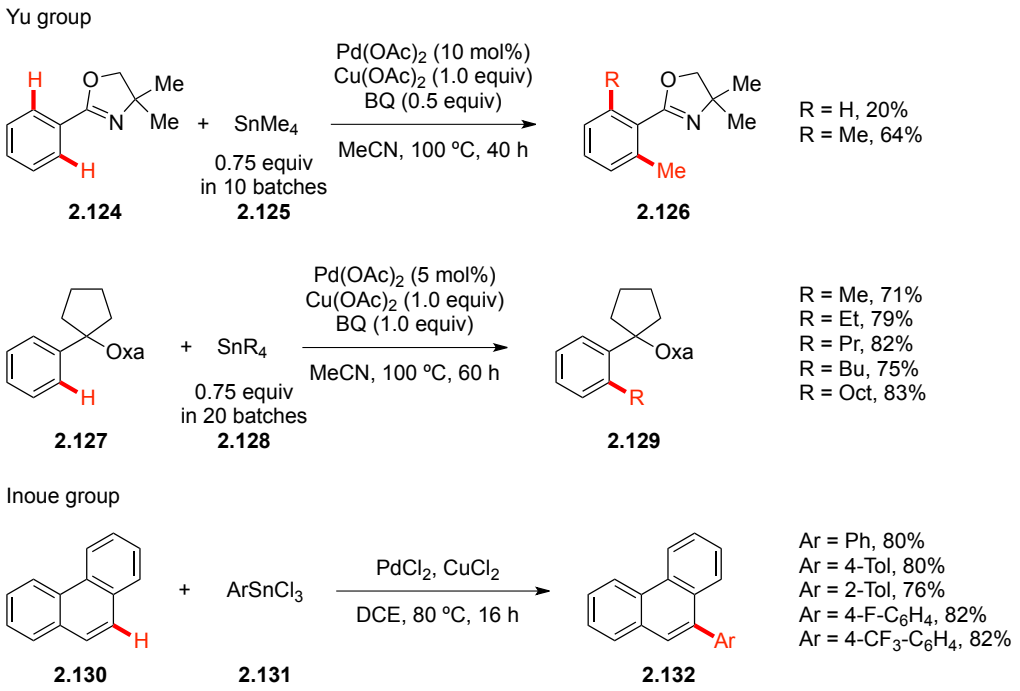

Scheme 2-20. C–H functionalization with organotin reagents.

Recently, the Inoue group reported a C–H arylation reaction on simple arene **2.130** with aryltin reagents (Scheme 2-20, bottom).[256] Notably, aryltin trichloride is much less toxic than triorganotins, the byproducts from using tetraorganotin reagents. $CuCl_2$ served

as both an activator and an oxidant for the Pd catalyst. Under the optimized condition, a variety of arylated phenanthrenes **2.132** were obtained. This transformation proceeded without a directing group, which greatly expanded the substrate scope. In 2012, Xue and Xiao group developed a room-temperature coupling protocol between aryl ureas and tetraarylstannanes, thus furnishing a mild approach for direct arylation.[257]

2.6.3 Organosilicon reagents

Hiyama reactions with organosilicon reagents are another important class of coupling reactions.[258-261] The C–Si bonds are only slightly polarized because there is little difference of electronegativity between carbon and silicon. Compared with other organometallic reagents, organosilicon reagents are the least reactive and as a result are better at tolerating a variety of functionalities. A common strategy to activate organosilicon reagents is using fluorides as additives to facilitate transmetallation. Hiyama couplings have been widely used in organic synthesis.[262-265]

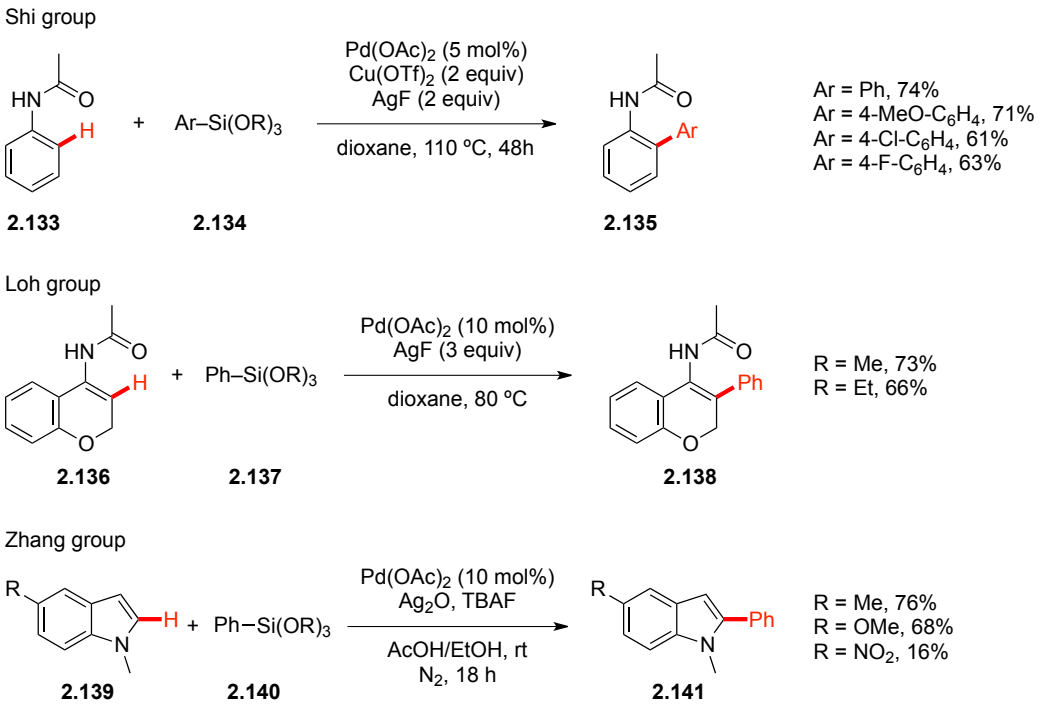

Scheme 2-21. C–H functionalization with organosilicon reagents.

In contrast, "Hiyama-type" oxidative C–H functionalization is very rare. In 2007, Shi and co-workers reported a Pd^{II}-catalyzed *ortho*-C–H arylation of acetanilide (Scheme 2-21, top).[266] The acetamido group was used as a directing group. AgF was proposed to serve as both a fluoride source and a co-oxidant. A series of arylsilicon reagents were used to install aryl groups in good yields. Later, the Loh group disclosed a similar *ortho*-C–H arylation reaction on cyclic enamines (Scheme 2-21, middle).[267] In this case, Cu oxidants were not necessary. $Pd(OAc)_2$ and AgF were proven to be the best combination.

As to heteroarenes, Zhang and co-workers reported an innate C–H arylation on indoles with arylsiloxanes (Scheme 2-21, bottom).[268] Ag_2O and TBAF were used as the oxidant and the fluoride source respectively. This protocol showed high regioselectivity at the C2 position of indole. As electron-rich indoles afforded higher yields than electron-poor ones, an electrophilic substitution mechanism was proposed.

2.7 Couplings between C(sp^2)–H and C–H

The ideal situation for C–H functionalization is the direct transformation of two C–H donors to a C–C bond, namely a dehydrogenative process. Despite the tremendous challenges, its green and sustainable features have attracted much attention.[90, 92, 136, 137, 139]

2.7.1 C(sp^2)–H and C(sp)–H cross-coupling

The cross-coupling between an sp^2 carbon and an *sp* carbon generates aryl acetylenes or enynes, which are important intermediates for total synthesis. The Sonogashira reaction has been the most efficient method for constructing C(sp^2)–C(sp) bonds by traditional Pd-catalysis.[140-142] In contrast, the dehydrogenative version of C(sp^2)–C(sp) coupling has been mostly catalyzed by Au and Cu.[137, 269-271] Pd-catalyzed cross-coupling reactions between C(sp^2)–H and C(sp)–H donors are very rare.[272] One main complication with this transformation is fast homocoupling of alkynes.

The first example using a Pd catalyst was reported by Li and co-workers in 2010 (Scheme 2-22, top).[273] Innate C–H alkynylation of 3-substituted indoles with terminal alkynes under an atmosphere of O_2 furnished a series of C2-alkynylated products in

moderate yields. To suppress the homocoupling of alkynes, slow addition of alkynes was required. Later, Chang demonstrated another Pd-catalyzed dehydrogenative alkynylation of azole heterocycles such as **2.145** with moderate to good yields (Scheme 2-22, middle).[274] Besides the critical choice of Pd catalysts and bases for optimal reaction efficiency, ambient air was successfully utilized as an environmentally benign oxidant. Shi and Larock also reported a similar innate dehydrogenative alkynylation on monosubstituted sydnones as **2.148** (Scheme 2-22, bottom).[275] A specific procedure for slow addition of alkynes and $Pd(OAc)_2$ was necessary to eliminate homo-coupling products as well as prolonging the lifetime of the active Pd species. Although this protocol has a limited scope of alkynes, it offers a convenient method to synthesize 4-alkynylsydnones.

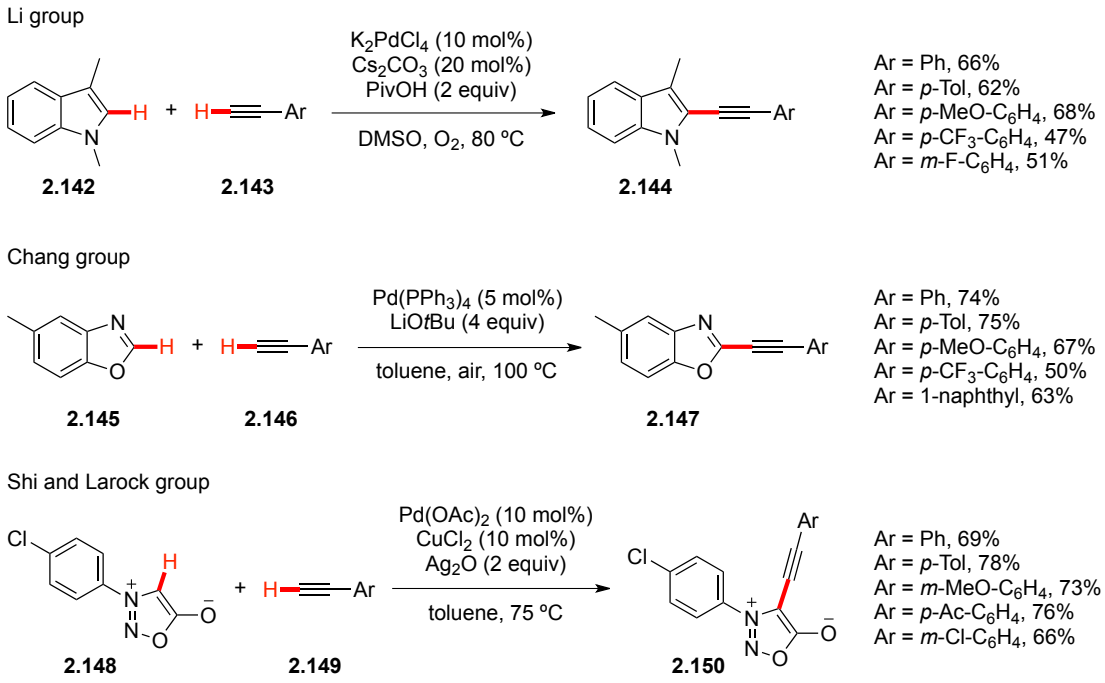

Scheme 2-22. Dehydrogenative alkynylation of heteroarenes.

Most recently, Murai and Shibahara developed a widely applicable C–H alkynylation protocol for 5-membered heteroarenes (Scheme 2-23).[276] With a combination of Pd catalysts and silver salts, imidazole, benzimidazole, imidazo[1,5-*a*]pyridine, oxazole,

benzoxazole, thiazole, and benzothiazole could all be effectively alkynylated. Interestingly, the C–H alkynylation conditions left the bromine atom on the substrates intact, not susceptible to the traditional Sonogashira reaction. Based on these results, they further devised a straightforward route to dialkynylate imidazo[1,5-*a*]pyridines and thiazole via C–H functionalization. In early 2013, Su and co-workers tackled the homocoupling problem by reducing the catalyst loading down to 0.2 mol %.[277] They found alkynylation conditions for heterocycles such as thiophenes and furans, which were not suitable substrates for direct alkynylation before.

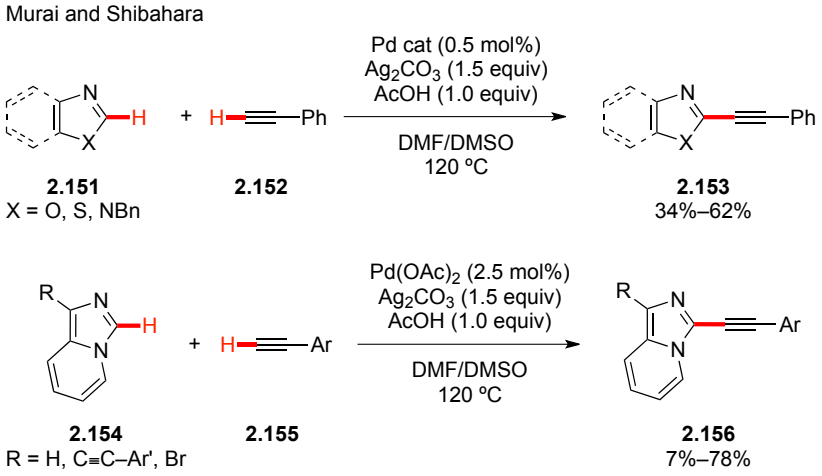

Scheme 2-23. Recent examples of dehydrogenative alkynylation of heteroarenes.

Similarly, the synthesis of enynes in a dehydrogenative fashion was not reported until recently. Jung reported the first example of constructing conjugated enynones **2.159** via Pd catalysis (Scheme 2-24, top).[278] Remarkably, molecular oxygen was used as the only oxidant to reoxidize Pd^0. A series of terminal alkyl- or aryl-alkynes were employed under the optimized conditions providing *E*-selectivity and yields of up to 92%. However, the scope of alkenes **2.157** was limited to acrylates and vinyl ketones. In 2012, Zhang and Zhong reported an efficient method using unactivated allylic ethers **2.160** as substrates for direct alkynylation (Scheme 2-25, bottom).[279] Various arylalkynes could participate in the coupling and interestingly afforded *Z*-enynes **2.162** in moderate to good yields.

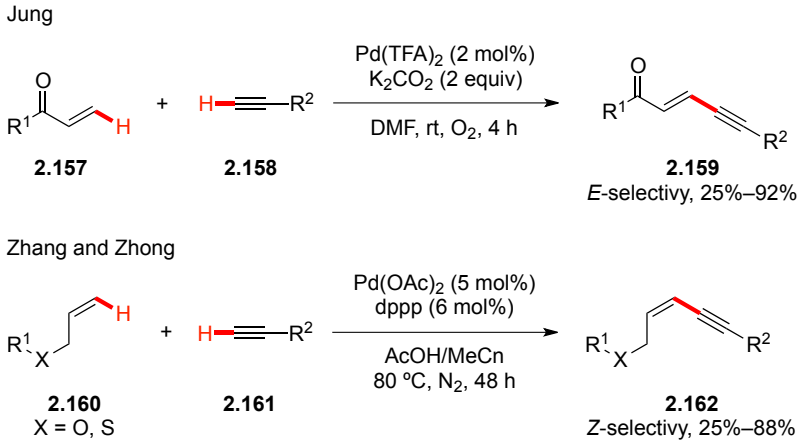

Scheme 2-24. Dehydrogenative alkynylation of alkenes.

2.7.2 C(sp^2)–H and C(sp^2)–H cross-coupling

Cross dehydrogenative couplings of two C(sp^2)–H bonds are the most widely studied.[133, 136, 138, 151] The first example of double C(sp^2)–H functionalization dates back to 1967.[280, 281] Fujiwara and Moritani used benzene and styrene without any preactivation to produce the coupling product **2.165** (Scheme 2-25). Although the reaction used 1.0 equiv of $Pd(OAc)_2$, their findings revolutionized C(sp^2)–H functionalization and guided the research for the following decades.

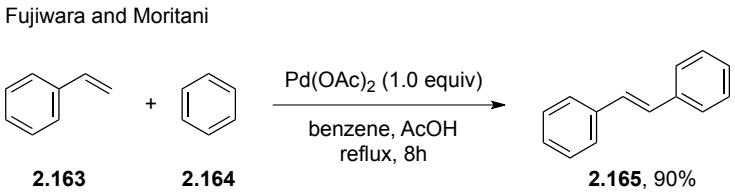

Scheme 2-25. Fujiwara-Moritani reaction.

Due to the enormous amount of research conducted towards this type of cross-coupling, this section will be divided into three parts: the dehydrogenative couplings between an arene and an arene, between an arene and an alkene, and between an alkene and an alkene.

2.7.2.1 Arene and arene coupling

Biaryl linkages are embedded in a plethora of natural products, pharmaceuticals, and materials. The most attractive approach towards the formation of biaryls would be the direct oxidative coupling of two aryl C–H donors. The study on dehydrogenative coupling between arenes started with the oxidative homocoupling of benzene in the presence of stoichiometric amounts of $PdCl_2$ by VanHelden and Verberg.[282] Since then, organic chemists have made significant progress in terms of using catalytic amounts of Pd catalysts, applying green conditions, controlling the regioselectivity, and achieving cross-coupling between different arenes, *etc*.[283-285]

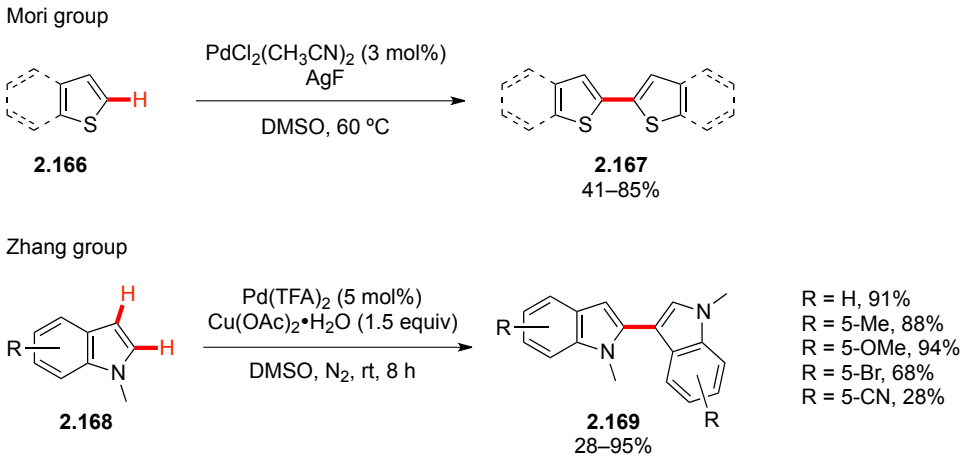

Scheme 2-26. Dehydrogenative homocouplings of heteroarenes.

In 2000, Sasson and co-workers developed a protocol for the Pd-catalyzed homocoupling of substituted benzenes under mild aerobic oxidation.[286] Different from earlier protocols that required extreme conditions, such as high O_2 pressure and temperatures, they combined two sets of catalysts (*i.e.* $PdCl_2$ for the coupling reaction, and $Co^{II}/Mn^{II}/Zr^{IV}$ salts to activate molecular oxygen) in a one-pot procedure, which therefore enabled low O_2 pressure.[287] However, regioselectivity was an issue. As to heteroarenes, their dehydrogenative homocoupling was developed earlier,[288] but their catalytic transformations were not reported until recently. In 2003, Mori first reported thiophenes underwent C–H homocoupling in the presence of 3 mol % of $PdCl_2(CH_3CN)_2$

(Scheme 2-26, top).[289] A series of bithiophenes **2.167** were obtained regioselectively in good yields. In addition to symmetric C–H homocouplings, unsymmetrical homocouplings of arenes are also possible in the presence of more than one active C–H bond. For example, Zhang developed mild conditions for unsymmetrical homocoupling of substituted indoles **2.168** with high yields and excellent regioselectivity (Scheme 2-26, bottom).[290] Electron-rich and moderately electron-poor indoles were compatible.

In order to control regioselectivity, a widely applicable strategy is employing directing groups. The pyridyl group has been very useful in directing Pd catalysts to the desired reaction site. For example, Sanford reported an oxidative homocoupling of substituted benzenes directed by a pyridyl group with high levels of regioselectivity (Scheme 2-27).[291] The coupling proceeded at room temperature and tolerated halide groups.

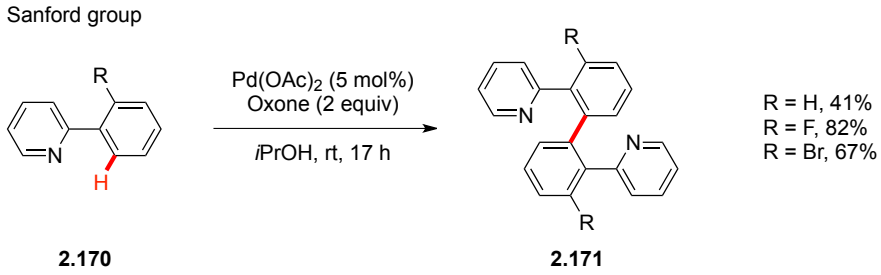

2.170 **2.171**

Scheme 2-27. Directing group-assisted regioselective C–H homocouplings.

Cross dehydrogenative couplings of two different arenes are much more problematic than homocoupling because both homo- and cross-coupling products can be obtained. Current strategies often include (1) introducing directing groups and (2) tuning the substrate's properties. The Sanford group first introduced a regioselective protocol for Pd-catalyzed oxidative cross-coupling of arenes aided by a directing ligand (Scheme 2-28, top).[292] Based on their findings in dehydrogenative homocoupling of **2.170** (Scheme 2-27),[291] the intermediate palladacycle after the first C–H activation was unreactive towards homocoupling, which enhanced the chemoselectivity for cross-coupling products. Their results showed that the reactivity of two C–H activation processes were

controlled by proximity to a ligand (for the first C–H activation) and the adjacent steric environment (for the second C–H activation) respectively.[293] Later, Shi and co-workers introduced the acetamido group to direct the dehydrogenative cross-coupling of arenes (Scheme 2-28, bottom).[294] Similar to Sanford's strategy, the high regioselectivity of this work was also controlled by the directing group and the steric hindrance in the corresponding C–H activation steps. Other directing groups, such as oxazoline and *O*-carbamate, were also shown to direct dehydrogenative coupling of different arenes in high regioselectivity.[295-297]

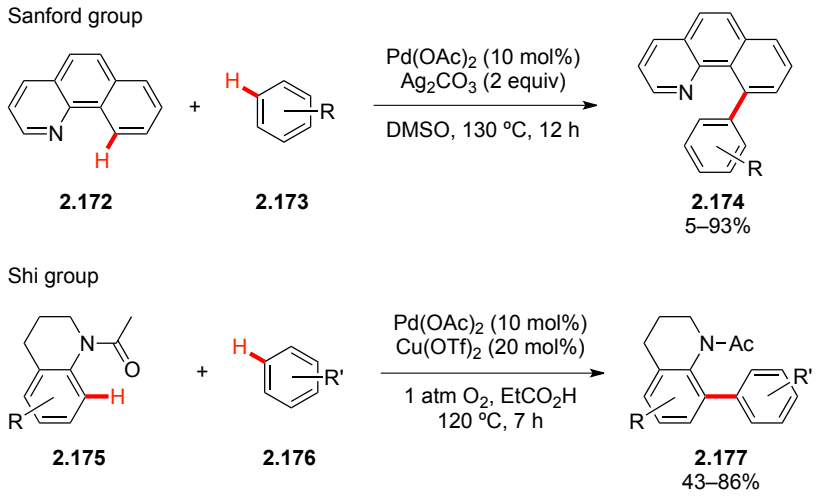

Scheme 2-28. Cross dehydrogenative couplings of arenes.

In the absence of a directing group, Lu and co-workers made the first attempt in 2006 to synthesize 1-arylnaphthalenes **2.180** directly from benzene and naphthalene (Scheme 2-29, top).[298] The concentrations of arenes and TFA were found critical. In spite of the low yields, the chemoselectivity of **2.180** was very good. In the following year, Fagnou reported a groundbreaking result of the dehydrogenative coupling between benzene and indoles in high selectivity and yields (Scheme 2-29, middle).[125] The *N*-substituent of indole was vital to the reactivity. Free *N*-H indole did not react at all while *N*-methylindole predominantly furnished a homocoupling product. In contrast, indoles bearing electron-withdrawing groups (as in **2.181**) exhibited superb reactivity and yields.

Interestingly, replacing $Cu(OAc)_2$ with AgOAc reversed the regioselectivity favoring the C2-position of indole. Concurrently, DeBoef reported a similar cross-coupling between benzofuran and benzene (Scheme 2-29, bottom).[299] O_2 was used as the green oxidant. The regioselectivity was controlled at the C2-position of benzofuran. In contrast to Fagnou's results, DeBoef's protocol was applicable to *N*-methylindole.

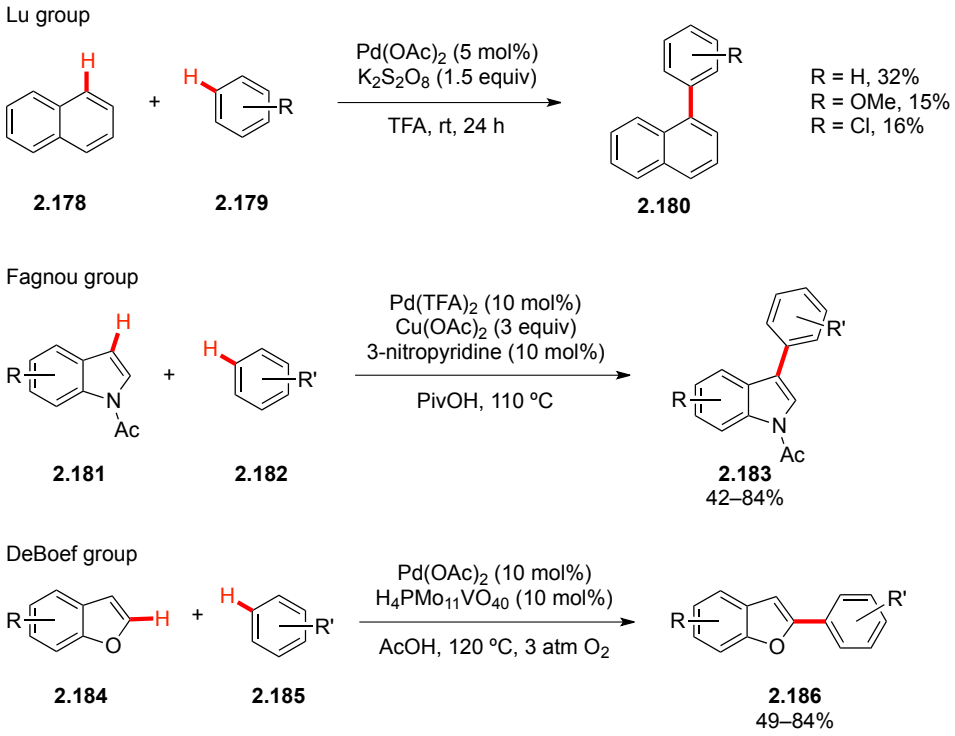

Scheme 2-29. Cross dehydrogenative couplings of arenes without directing groups.

Recently, more Pd-catalyzed cross dehydrogenative couplings between (hetero)arenes have been explored.[300] In 2010, Hu and You reported the first example between two heteroaryl C–H donors (Scheme 2-30, top).[301] A series of electron-rich and electron-poor *N*-heteroarenes (*e.g.* azoles, xanthines, indolizines, pyridine *N*-oxides, *etc.*) were compatible to furnish products with high regioselectivity and yields. Later, electron-deficient **2.190** was also successfully coupled to other (hetero)arenes in Zhang's and Su's groups respectively (Scheme 2-30, bottom).[302, 303] Further developments are directed towards finding additional substrates and milder conditions.[304-306]

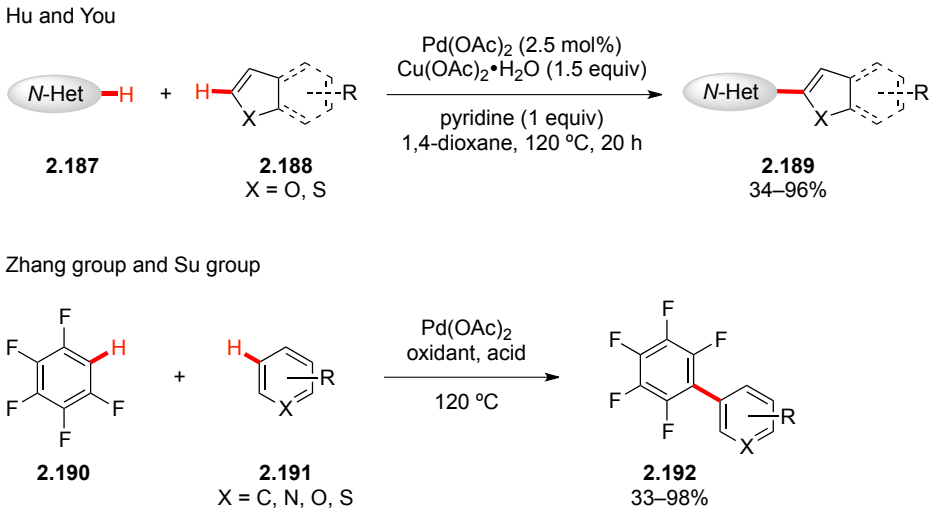

Scheme 2-30. Recent examples of cross dehydrogenative couplings of arenes.

2.7.2.2 Arene and alkene coupling

Ever since Fujiwara and Moritani reported the seminal example of dehydrogenative coupling of arenes with alkenes in the 60s, a broad range of arenes have undergone direct coupling with alkenes.[138, 151] For many years, early oxidative coupling reactions were usually assisted by stoichiometric amounts of Pd. In order to develop catalytic protocols, stoichiometric amounts of oxidants were used to regenerate Pd catalysts in later development.

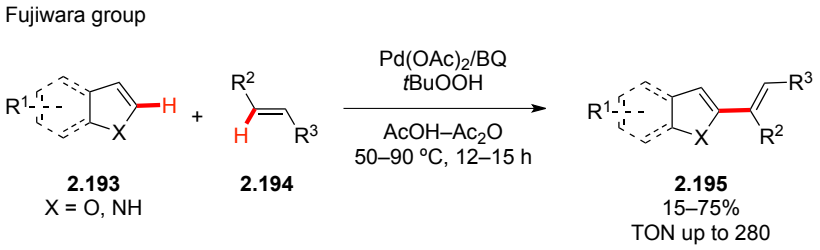

Scheme 2-31. Early example of catalytic dehydrogenative alkenylation.

Conventional oxidants include metal salts (*e.g.* Ag^{I} and Cu^{II} salts) and organic peroxides (*e.g.* *t*BuOOH and $PhCO_3tBu$). The application of these oxidants significantly reduced the loading of Pd catalysts.[138] For example, in 1999, Fujiwara and co-workers

reported an efficient dehydrogenative coupling between arenes and alkenes with only 1 mol % of $Pd(OAc)_2$ with *t*-butyl hydroperoxide as the oxidant.[307] Their protocol was particularly effective for heteroarenes **2.193** (*e.g.* furans and indoles) with excellent regio- and stereoselectivity (Scheme 2-31). With benzoquinone as a co-catalyst, impressive turnover numbers (TON) up to 280 were achieved.

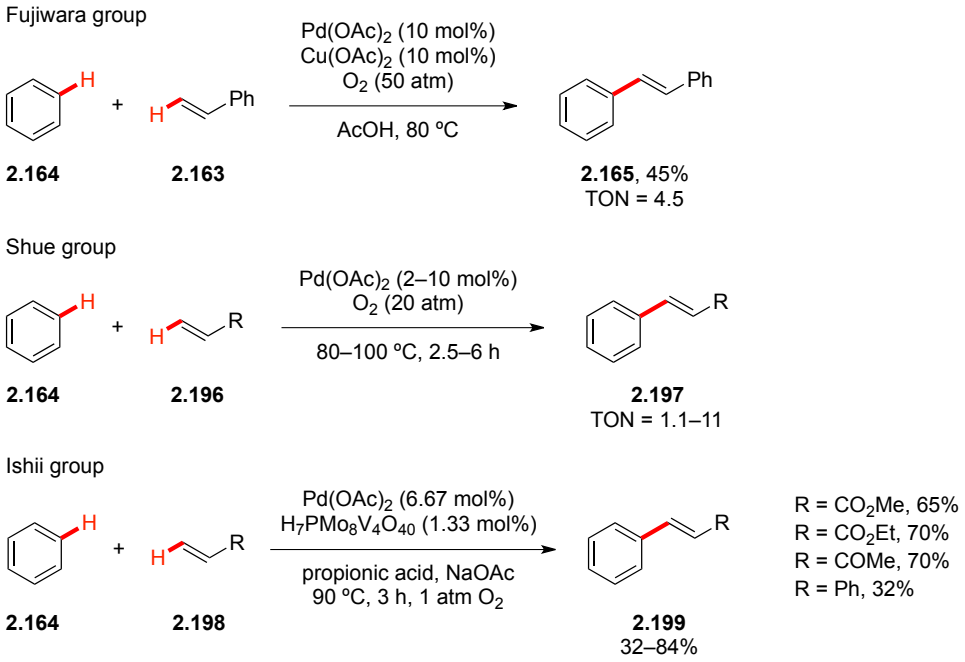

Scheme 2-32. Green conditions of dehydrogenative alkenylation using O_2.

In the interests of green chemistry, molecular oxygen is undoubtedly the optimal terminal oxidant.[308, 309] Initially, Fujiwara discovered that in the presence of oxygen or air, $Cu(OAc)_2$ or AgOAc could catalytically assist $Pd(OAc)_2$ in catalyzing oxidative cross-couplings (Scheme 2-32, top).[310] The first example of using oxygen as the sole oxidant was disclosed in 1971 by Shue and co-workers (Scheme 2-32, middle).[311] The drawback was that the pressure of oxygen required much more than 1 atm, which unfortunately was a common issue for many earlier conditions. The main reason was that the concentration of molecular oxygen was low in solutions and Pd^0 therefore could not be oxidized effectively. Recent improvement on oxidative couplings often involved

oxygen "activators/co-catalysts" under much lenient conditions.[309] For example, molybdovanadophosphoric acid (HPMoV) was applied as a co-catalyst in Ishii's report in 2002 (Scheme 2-32, bottom).[312] In this mild protocol, dehydrogenative coupling of benzene with acrylates was achieved under 1 atm of O_2. Other activators, such as benzoquinone and catechol, also showed good efficiency in assisting the reoxidation of Pd^0.[312, 313]

From a mechanistic perspective, the two C–H activation processes involved in dehydrogenative alkenylation of arenes are discrete in nature. Compared to the perplexing chemoselectivity in dehydrogenative cross-couplings of arenes, the chemoselectivity of C–H alkenylation of arenes has not been a key issue. On the other hand, the regioselectivity remains problematic.

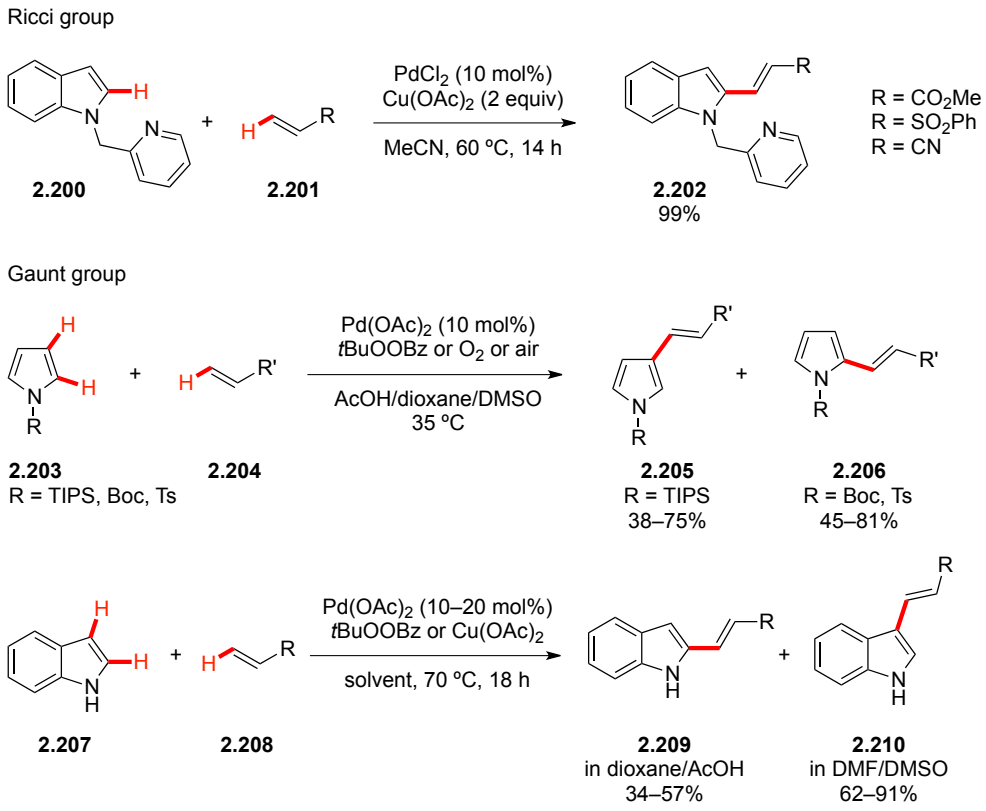

Scheme 2-33. Regioselectivity of dehydrogenative alkenylation of heteroarenes.

For heteroarenes, the regioselectivity of alkenylation can be tuned with either a directing group or their innate electronic and steric properties. Ricci first reported an *N*-substituent-directed alkenylation of indoles with excellent C2-regioselectivity (Scheme 2-33, top).[123] Gaunt and co-workers demonstrated another *N*-substituent-controlled oxidative alkenylation of pyrroles under aerobic conditions (Scheme 2-33, middle).[314] Electron-withdrawing *N*-substituents, such as *N*-Boc and *N*-Ts, regioselectively afforded C2-arylated pyrroles **2.206** due to reduced nucleophilicity, while sterically bulky *N*-TIPS group shielded the C2-position and predominantly afforded C3-alkenylated products **2.205**. In addition, the choice of solvents also significantly affected the regioselectivity (Scheme 2-33, bottom).[315] As Gaunt noted, oxidative coupling reactions carried out in polar solvent such as DMSO and DMF produced C3-alkenylated indoles **2.210**, while the nonpolar solvent dioxane with AcOH as a cosolvent showed C2-regioselectivity (*e.g.* **2.209**) instead.

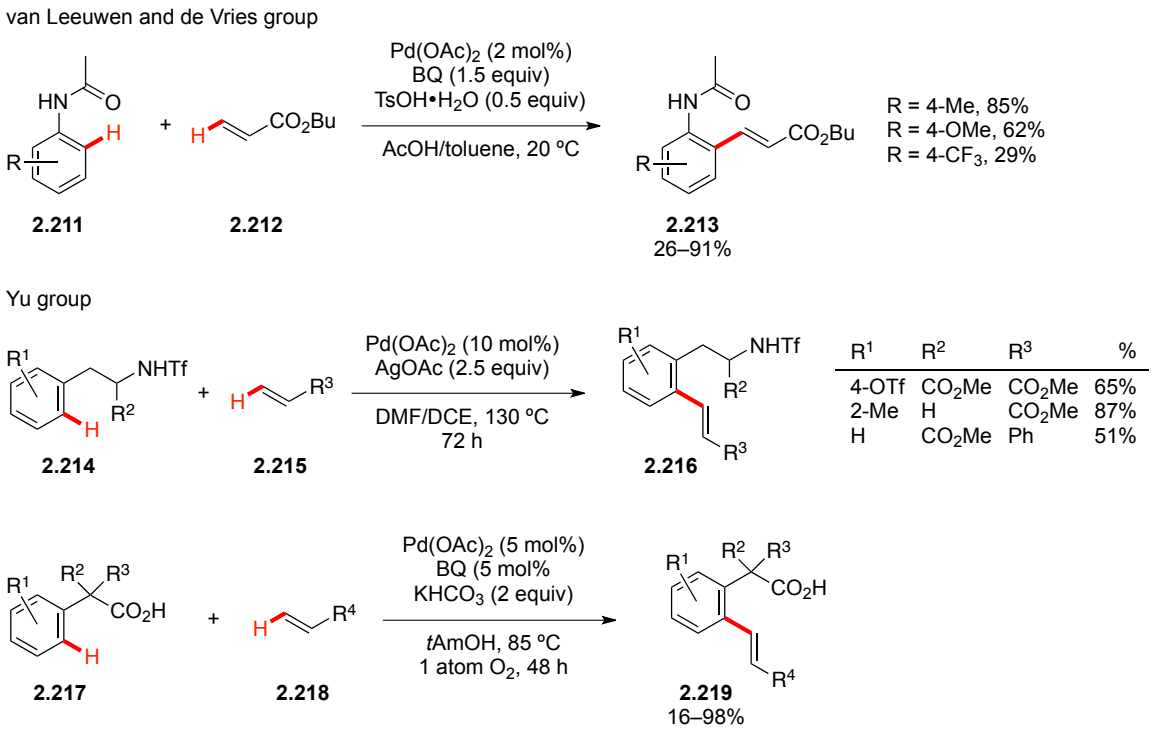

Scheme 2-34. Regioselectivity of dehydrogenative alkenylation of arenes.

For C–H alkenylation of arenes, using a directing group is very effective to achieve excellent regioselectivity. van Leeuwen and de Vries first reported using an acetamido group to direct the C–H alkenylation (Scheme 2-34, top).[316] Only *ortho*-alkenylation was observed, where electron-rich arenes afforded higher yields than electron-poor ones. Yu also employed triflamido and carboxyl groups as directing groups and achieved excellent regioselectivity (Scheme 2-34, bottom).[317, 318] A wide range of 2-phenylethylamines **2.214** and phenylacetic acids **2.217** were employed for *ortho*-C–H alkenylation reactions with high yields. Intriguingly, they found a significant ligand-promoted reactivity/selectivity when mono-*N*-protected amino acids were used. The strange ligand effect was later attributed to the acceleration of the C–H cleavage step, where the original electrophilic palladation mechanism was changed to a CMD process.[319] In addition, other functional groups (*e.g.* urea, sulfonamido, and hydroxyl) have been excellent in directing regioselective C–H alkenylation through weak ligation.[320]

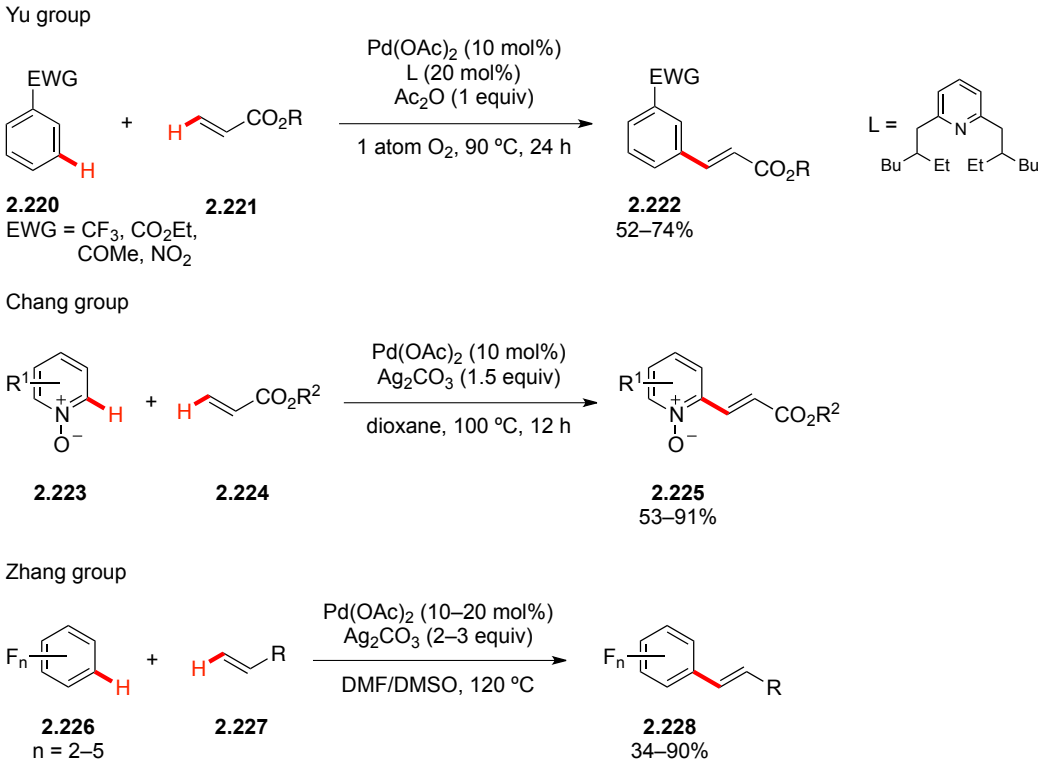

Scheme 2-35. Dehydrogenative alkenylation of electron-deficient (hetero)arenes.

Because electrophilic palladation is the dominant pathway for C–H activation, most (hetero)arenes involved in dehydrogenative alkenylation are electron-rich. On the contrary, electron-deficient (hetero)arenes are more difficult substrates for C–H activation due to their poor coordination with $Pd(OAc)_2$.[219] Hence, fewer reports are available.[219, 321-323] Yu developed the first protocol to *meta*-alkenylate electron-poor arenes in 2009 (Scheme 2-35, top).[219] 2,6-dialkylpyridine as the ligand was vital to the *meta*-selectivity. Although the origin of this ligand effect is unclear, the loss of reactivity at the *ortho*-position might be attributed to a steric effect. An electrophilic substitution appears to be a plausible rational for the *meta*-selectivity over para-selectivity. In another example, Chang and co-workers unveiled an efficient protocol for *ortho*-alkenylation of pyridine *N*-oxides in high yields (Scheme 2-35, middle).[322] The coupling proceeded with excellent regio-, stereo- and chemoselectivity. As to perfluoroarenes **2.226**, Zhang and co-workers reported an efficient protocol, which succeeded with a variety of activated and unactivated alkenes in moderate to high yields (Scheme 2-35, bottom).[323]

2.7.2.3 Alkene and alkene coupling

Polyenes and conjugated dienes are important structural motifs found in many pharmaceutically active compounds and natural products, such as carotenes, vitamin A, bombykol, *etc.* Synthesis of these compounds can be categorized into two classes: (1) carbonyl alkenylation reactions,[324] represented by the Wittig reaction;[325] (2) Cross alkenylation couplings, represented by the Heck reaction.[326] Compared with the aforementioned two coupling modes between C(sp^2)–H and C(sp^2)–H, dehydrogenative alkenylation of alkenes is still a very underdeveloped area. Examples of this sort are very limited.[136] The earliest example involved the dehydrogenative homocoupling of camphene reported by Gusevskaya.[327]

Research on dehydrogenative cross-couplings of alkenes has started to gain more attention very recently. Ishii first demonstrated the oxidative cross-coupling of vinyl acetate **2.229** and acrylates **2.230** in 2004 (Scheme 2-36, top).[328] This protocol used O_2 as the terminal oxidant with HPMoV as the co-catalyst. A series of linear dienes were

efficiently constructed in good yields, albeit with moderate stereoselectivity. Five years later, Loh and co-workers reported a similar protocol involving acrylates and styrene derivatives under mild conditions (Scheme 2-36, middle).[329] The stereoselectivity was improved, favoring the *E*-configuration. However, only 2-substituted styrenes **2.232** were compatible in the reaction. In 2010, Yu reported another cross-coupling between α-oxoketene dithioacetals **2.235** with terminal alkenes (Scheme 2-36, middle).[330] A series of functionalized 1,3-dienes were obtained in high yields with excellent *E*-selectivity. Most recently, Liu's group expanded the substrate scope to electron-rich alkenes **2.239** for dehydrogenative cross-coupling (Scheme 2-36, bottom).[331] Common leaving groups were tolerated under their conditions. Different from Loh's results, styrene without 2-substituents worked well under Liu's protocol with good yields.

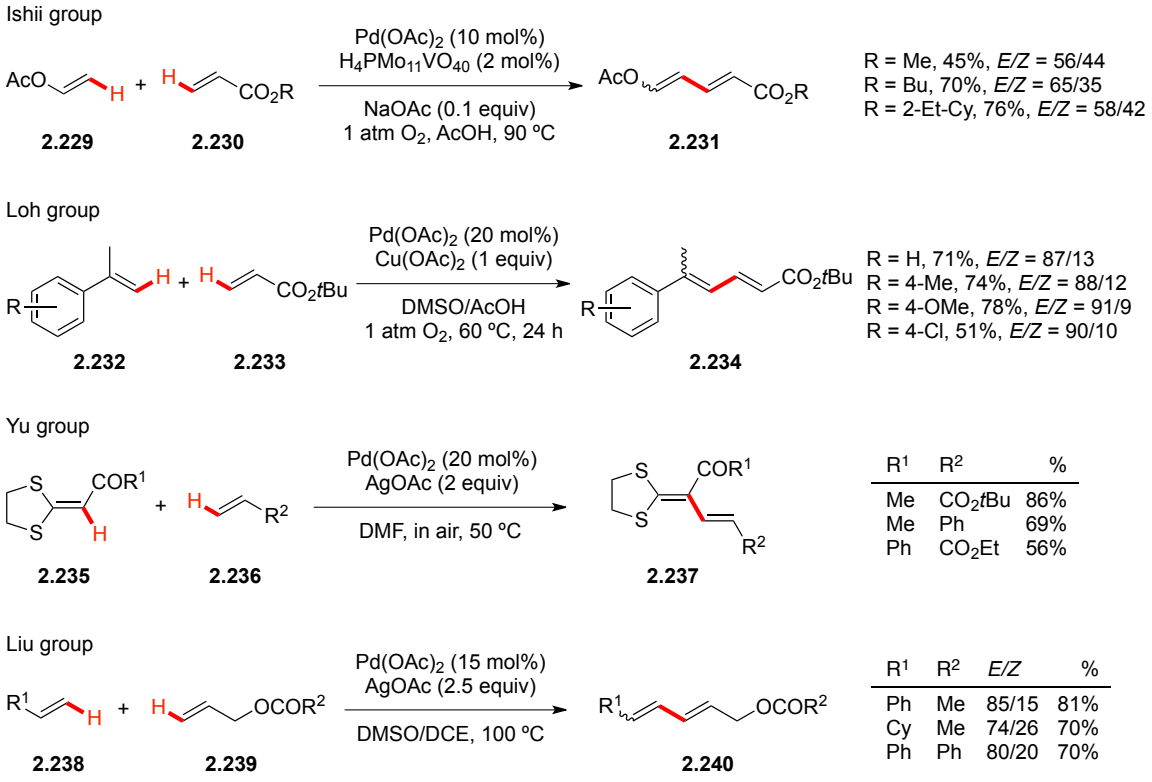

Scheme 2-36. Dehydrogenative alkenylation of linear alkenes.

In addition to linear alkenes, cyclic alkenes have also been shown to participate in

dehydrogenative coupling reactions. In 2011, Liu and co-workers first disclosed an effective method to directly alkenylate glycals as **2.241** with excellent regioselectivity and stereoselectivity (Scheme 2-37, top), which could be valuable for synthesizing pyran-containing natural products.[332] Similarly, when nonaromatic cyclic enamides as **2.244** was subjected to oxidative alkenylation conditions, high yields and excellent regio- and stereoselectivity were achieved (Scheme 2-37, bottom).[333]

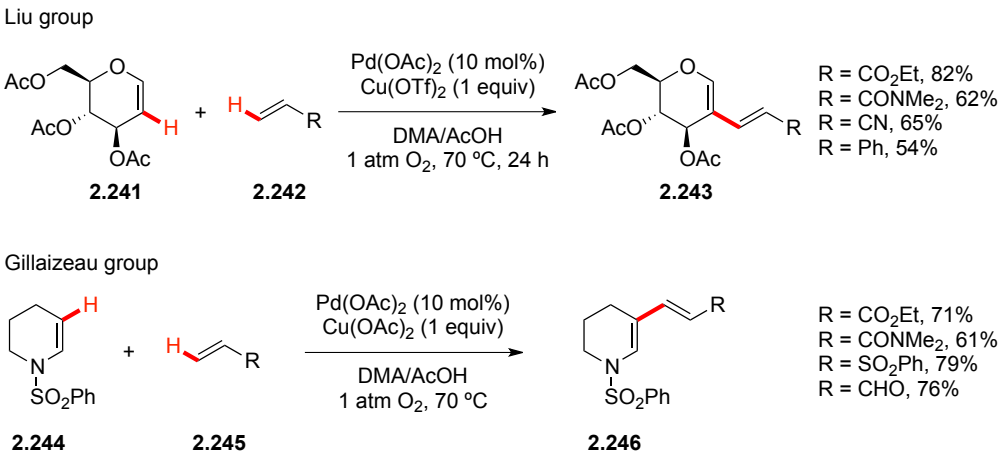

Scheme 2-37. Dehydrogenative alkenylation of cyclic alkenes.

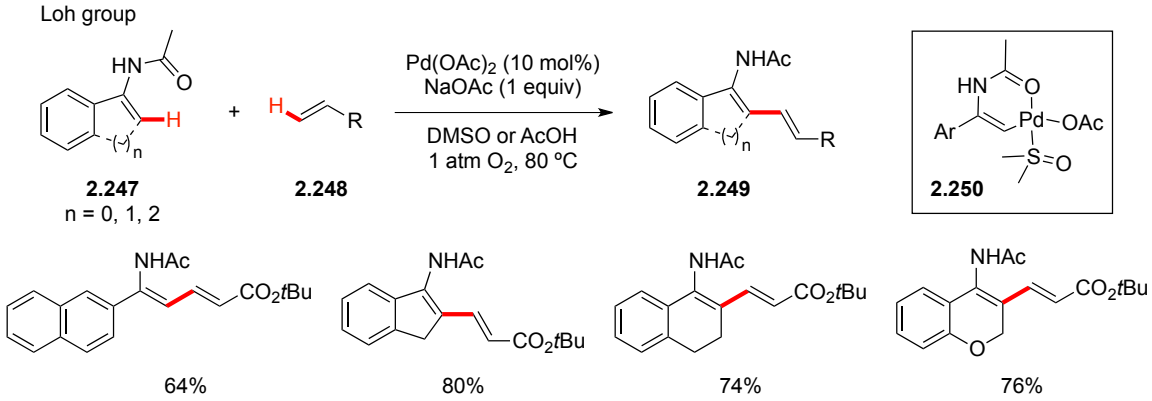

Scheme 2-38. Directing group-assisted dehydrogenative cross-alkenylation.

The excellent regioselectivity shown in the above examples relied on the innate electronic properties of the substrates. Although the stereoselectivity (of *E*/*Z* isomers)

was superior for cyclic alkenes, it still remains a significant challenge for linear alkenes. One solution is using directing groups. So far, only one example with directing group assistance was reported (Scheme 2-38).[334] Good yields and excellent selectivity were achieved. A vinylpalladium cyclic species **2.250** was isolated (when Ar = 2-naphthyl) and proposed to be the possible intermediate after the first C–H activation.

2.7.3 C(sp^2)–H and C(sp^3)–H cross-coupling

Unlike C(sp^2)–H bonds, C(sp^3)–H bonds do not have empty low-energy orbitals or filled high-energy orbitals that could readily interact with orbitals of the metal. Therefore, C(sp^3)–H activation is significantly more challenging. So far, many transition metal catalysts have been used to catalyze dehydrogenative alkylation of (hetero)arenes or alkenes.[90, 92, 137, 335] Most of the C(sp^3)–H donors involve active sp^3 carbon centers, such as α-amino carbons and allylic/benzylic carbons,[336, 337] much less attention has been devoted to non-acidic C–H bonds of alkyl groups.[338]

For Pd-catalyzed intermolecular dehydrogenative alkylation only a few examples are known so far. Bao and co-workers reported the first case involving a Pd catalyst to achieve dehydrogenative allylic indolation (Scheme 2-39, top).[337] DDQ was found to be the most effective oxidant and the reaction needed to be carried out at 0 ºC to obtain the best yields. Indoles bearing electron-withdrawing groups afforded better yields. The regioselectivity revealed that the C3 position of indole was the most active site. Widenhoefer and co-workers reported the first example of a Pd-catalyzed addition of stabilized carbon nucleophiles **2.254** to ethylene and propylene (Scheme 2-39, middle).[339] The pressure of ethylene and propylene gas was critical in controlling the desired coupling and suppressing the competing protonolysis. Very recently, Cui and Wu developed a dehydrogenative C2-alkylation of quinoline *N*-oxides **2.257** with ethers in good yields (Scheme 2-39, bottom).[340] The mechanism was proposed to involve a Pd^{III} species via a radical process. This method offers a new and simple way to synthesize useful quinoline *N*-oxide derivatives.

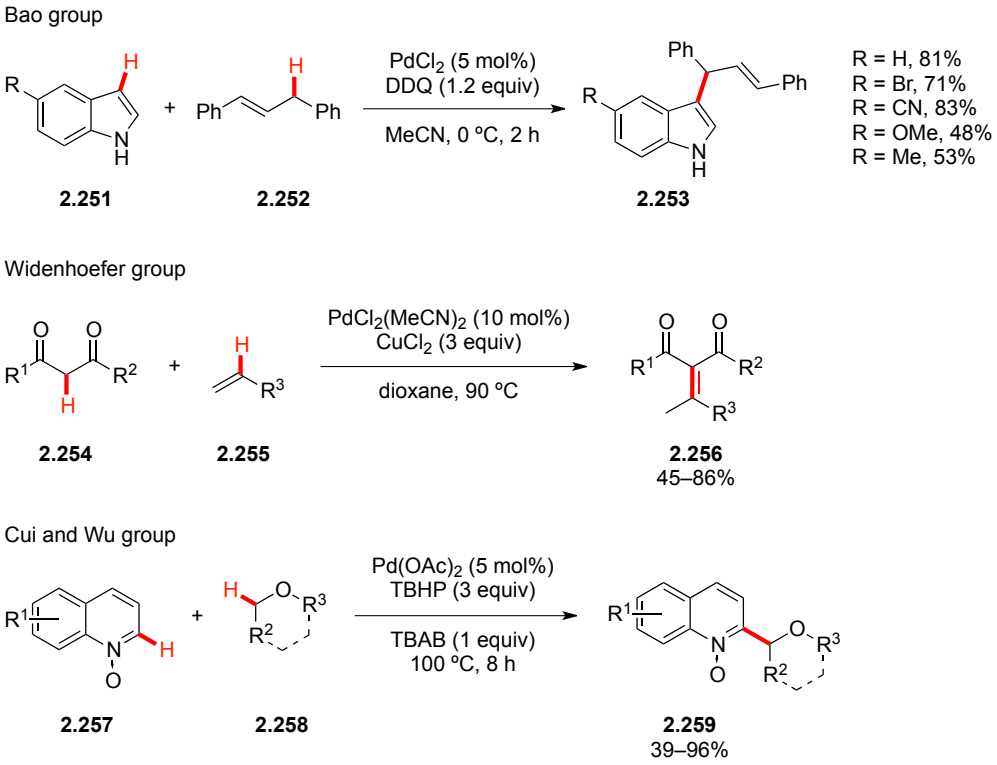

Scheme 2-39. Dehydrogenative alkylation reactions.

2.8 Summary

C–H functionalization reactions are attractive methods in organic chemists. The ubiquity of C–H bonds makes such chemistry very promising, yet at the same time very challenging. A useful C–H functionalization protocol must be able to activate a targeted C–H bond in a selective manner that only one of the many will react.

Over the past decade, this field has seen remarkable progress. First, more transition metals have been introduced as catalysts to activate C–H bonds. Palladium as a traditional catalyst has found new applications in various C–H coupling systems beyond traditional coupling reactions. Second, "innate" and "guided" approaches have effectively delivered excellent regioselectivity. More directing groups have been designed. For instance, weak coordination is becoming a new, powerful means for selective C–H functionalization. Third, new mechanisms have been discovered, leading to the development of new protocols for substrates not suitable for C–H functionalization

before. Notably, the discovery of the CMD mechanism opened the door for functionalizing C–H bonds of electron-deficient (hetero)arenes, a class of important molecules which were not compatible substrates not so long ago. Fourth, C–H functionalization is moving towards even "greener" directions. For example, molecular oxygen is being used as the terminal oxidant, room temperature conditions are becoming more available, and more research efforts are devoted to dehydrogenative cross-couplings with ideal atom economy. Lastly but not least, C–H functionalization are changing our way in designing organic synthesis. Many common linkages in natural products and pharmaceuticals, such as biaryls, can now be conveniently assembled with different choices thanks to a myriad of methods available. Their permeation in modern total synthesis has proven again the tremendous potential of C–H functionalization chemistry.

However, the accessible tools for manipulating C–H bonds are far from sophistication. Many difficult tasks still remain. For example, functionalization of sp^3 C–H bonds continues to be challenging compared to their *sp* and sp^2 counterparts. Directing groups are often needed for selective C–H activation. The development of removable or convertible directing groups is hence preferable. In addition, the field of dehydrogenative cross-couplings is still in its infancy. Topics like controlling chemoselectivity and regioselectivity await innovative solutions. Finally, reducing use of expensive catalysts or abandoning use of catalysts entirely is essential for future practicality.

Regardless of the challenges faced at the present stage, future exciting advances of this rapid evolving area can be expected undoubtedly. The increasing importance of this new chemistry will propel methodology development and further application in organic synthesis, materials sciences, and in the pharmaceutical industry.

Chapter 3 Pd-Catalyzed C–H Arylation of Cyclic Enaminones with Aryl Iodides

3.1 Introduction

Cyclic enaminones, namely 2,3-dihydropyrid-4(1*H*)-ones, have displayed a distinctive reactivity profile, including notably a strong innate nucleophilicity.[78, 341-344] As piperidine surrogates, these non-aromatic substrates have been exploited as versatile synthetic intermediates in the syntheses of various heterocycles and heterocyclic natural products.[61, 345-348] As our laboratory continues to investigate the pharmaceutical applications of phenanthropiperidine alkaloids, the syntheses of these natural products and analogs entail a regioselective C5-arylation of cyclic enaminone **3.1** as a key step (Scheme 3-1).[59, 60, 65, 349] Our strategy has been employing direct C–H arylation reactions because of their convenience and efficiency.

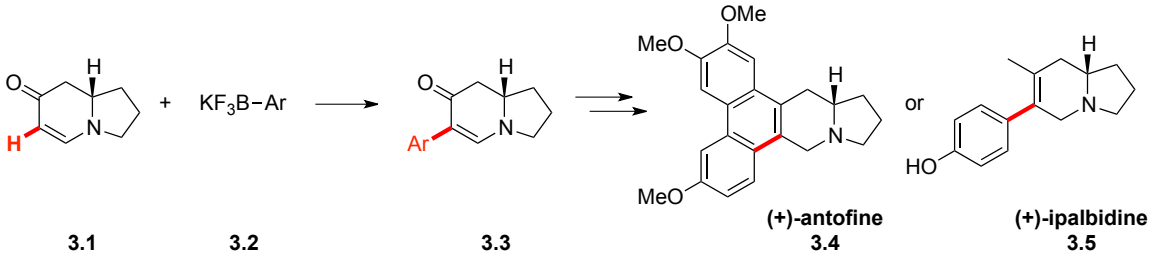

Scheme 3-1. C–H functionalization in alkaloid syntheses.

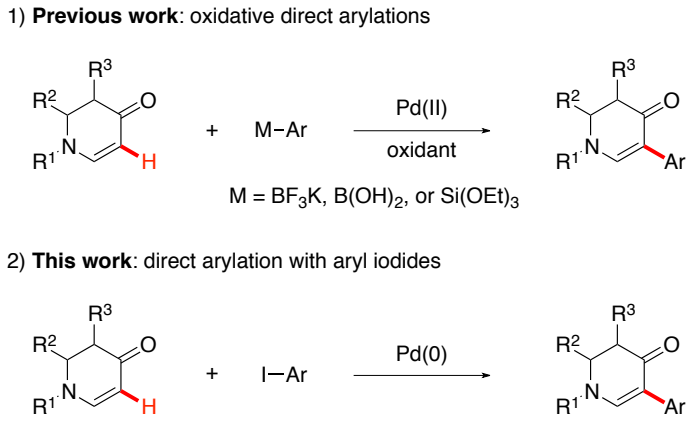

Scheme 3-2. Direct arylation of cyclic enaminones.

Direct C–H arylation chemistry has been extensively studied over the years due to the ubiquity of heterocycle-aryl linkages in pharmaceuticals.[88, 89, 91, 99, 108, 350, 351] Our earlier syntheses have demonstrated that the regioselective C5-arylation of cyclic enaminones can be achieved through convenient and high yielding C–H arylation protocols via oxidative Pd catalysis (Scheme 3-2.1).[79-81] In these protocols, aryl metal precursors were used (*i.e.* aryl boronic acids,[81] silanes,[80] and trifluoroborates[79]). Issues of limited commercial availability or high cost led us to explore the widely available aryl iodides as alternative reagents (Scheme 3-2.2).[109, 352-356]

3.2 Coupling strategy

Among the possible C–H activation mechanisms,[100, 117, 126] our past study suggested that an electrophilic palladation pathway was more likely involved in reactions with the nucleophilic enaminones (Figure 3-1, top).[341] However, a carbopalladation process is also feasible and would lead to C6-arylation as the double bond in the *non-aromatic* enaminone scaffold could be a Heck-donor (Figure 3-1, bottom). [117, 357] Therefore, the regioselectivity of the coupling reaction presented another challenge. The following studies describe the development of a C5 regioselective direct C–H arylation of cyclic enaminones using aryl iodides.

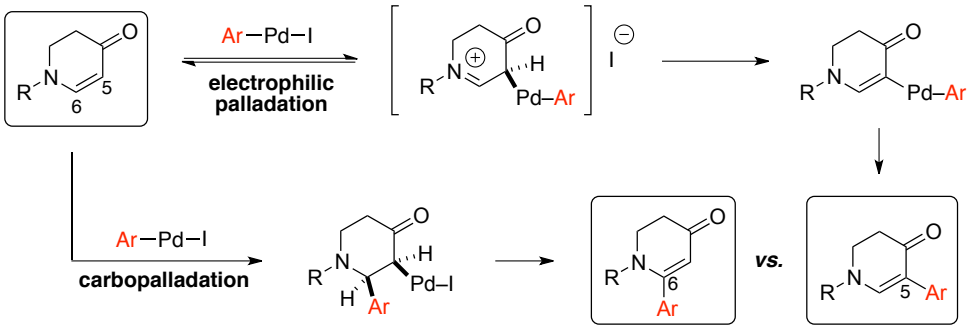

Figure 3-1. Postulated competing pathways for direct C–H arylation.

3.3 Condition optimization

3.3.1 Initial trials

Table 3-1. Initial screen of direct C–H arylation conditions

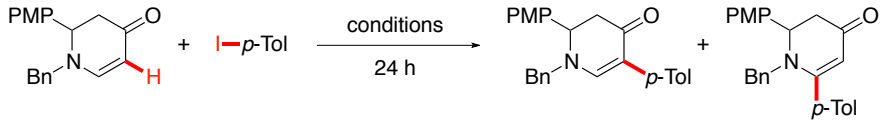

3.6 **3.7** **3.8** **3.9**

Entry[a]	Catalytic Conditions	**3.8** (%)	**3.9** (%)
1	$Pd(PPh_3)_4$ (10 mol %), TEA (2.0 equiv), CH_3CN, 80 °C, 18 h	0	1
2	$Pd_2(dba)_3$ (10 mol %), Bu_4NCl (2.0 equiv), NMP, 100 °C, 18 h	8	1
3	$Pd(dba)_2$ (10 mol %), Bu_4NCl (1.0 equiv), $NaHCO_3$ (2 equiv), DMF, 80 °C, 18 h	11	2
4	$PdCl_2(PPh_3)_2$ (10 mol %), $AgNO_3$ (1.0 equiv), KF (2.0 equiv), DMSO, 100 °C, 24 h	16	4
5	$[Pd(dppf)Cl_2]CH_2Cl_2$ (10 mol%), Ag_2CO_3 (2.0 equiv), DMSO, 80 °C, 24 h	0	0
6	$Pd(OAc)_2$ (10 mol%), PPh_3 (40 mol %), TEA (2.0 equiv), $AgNO_3$ (1.5 equiv), CH_3CN, 80 °C, 18 h	0	1
7	$Pd(OAc)_2$ (10 mol%), $NaHCO_3$ (3.0 equiv), Bu_4NCl (1.0 equiv), DMF, 80 °C, 18 h	30	2
8	CuCl (10 mol %), Li*O*tBu (2.0 equiv), DMF, 140 °C, 22 h	0	0
9	DMEDA (20 mol%), KO*t*Bu (3.0 equiv), dioxane, 80 °C, 23 h	0	0
10	KO*t*Bu (2.5 equiv), dioxane, 140 °C, 23 h	0	0

[a] NMR yields with Ph_3SiMe (1.0 equiv) as the internal standard (*p*-Tol = *para*-tolyl).

We initiated our study by examining a collection of C–H arylation conditions (Table 3-1). Pd^0 catalysts showed very limited catalytic activity (entries 1–3). Triphenylphosphine as a strong stabilizing ligand failed to furnish any desired product **3.8**, possibly because it stabilizes the electrophilic Pd^{II} oxidative adduct and thus inhibits the succeeding electrophilic palladation process (entry 1). Based on this analysis, a less electron-donating ligand should help activate the catalysis. Indeed, Pd^0 with dibenzylideneacetone (dba) afforded product **3.8**, although the yield was only around 10% (entries 2–3). The ligand effect was also prominent with Pd^{II} catalysts (entries 4–7). PPh_3 and dppf respectively showed inhibitory effect on yields (entries 4–6), whereas a ligand-free protocol (*i.e.* the Jeffery conditions[358]) provided 30% of desired compound **3.8** (entry 7). It is worth noting that the Jeffery conditions were initially developed for classic Heck reactions. As anticipated, in addition to the desired C5-arylated **3.8**, C6-arylated **3.9** was observed as well. However, the Heck byproduct **3.9** was interestingly not favored compared to **3.8** under the current conditions (entry 7). Moreover, a Cu^I-catalyzed method was also tested in addition to two other metal-free conditions (entries 8–10), but no desired product was observed. Therefore, we proceeded with the Jeffery conditions for further optimization.

3.3.2 Detailed optimization

We then undertook a thorough optimization of the arylation conditions (Table 3-2). A survey of seven solvents (entries 1–7) revealed that DMSO favored the formation of **3.8** via the presumed electrophilic palladation pathway (*e.g.* 50% in DMSO, entry 7 *vs.* 10% in dioxane, entry 2), whereas toluene (entry 1) significantly increased the formation of **3.9**. Indeed, DMSO provided the highest yield and the best regioselectivity (entry 7). The choice of the base was also important (entries 8–15). $NaHCO_3$ (entry 7) and Na_2CO_3 (entry 9) were more effective in facilitating the deprotonation process than NaOAc (entry 8). Addition of pivalic acid (PivOH) with Na_2CO_3 did not improve the yield (entry 10). The evaluation of carbonate salts showed that the sodium cation had beneficial effects on direct arylation (entries 11–13). Unsurprisingly, strong bases such as NaOH (entry 14) or

NaO*t*Bu (entry 15) decomposed the enaminones. Thus, the originally chosen $NaHCO_3$ provided the best outcome (50%, entry 7). Next, the reaction temperature was tuned from 20 ºC to 140 ºC in 30-degree intervals (entries 16–19). We found that 80 °C was the optimal temperature to activate the transformation without decomposing the heat-sensitive enaminones. Moreover, several tetraalkylammonium salts were assessed as phase-transfer agents in order to enhance yields and selectivities (entries 20–22).[358] The absence of Bu_4NBr indeed resulted in a lower yield of **3a** and a reduced regioselectivity (entry 20). Interestingly, Bu_4NCl (entry 21) provided a better regioselectivity than Bu_4NI (entry 22) or Bu_4NBr (entry 7). Lastly, the ligand effect was investigated. Phosphine ligands (*i.e.* PPh_3, $P(OPh)_3$ and $P(C_6F_5)_3$), regardless of their electronic properties, were detrimental to catalysis (entries 23–25). Amino acids (*i.e.* Boc-L-alanine and Boc-L-phenylalanine), supposedly coordinating to the Pd center through weak ligation,[359] showed no improvement in either yields or regioselectivity (entries 26–27).

Table 3-2. Detailed optimization of direct C–H arylation of cyclic enaminones

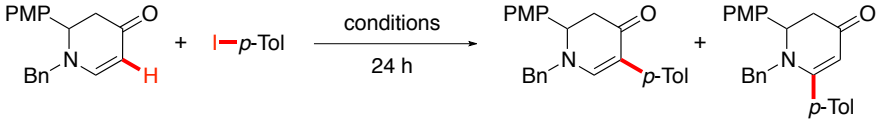

3.6 **3.7** **3.8** **3.9**

Entry[a]	Ligand	Additive	Base	Temp (°C)	Solvent	**3.8** (%)[b]	**3.9** (%)[b]
1	—	Bu_4NBr	$NaHCO_3$	80	toluene	14	18
2	—	Bu_4NBr	$NaHCO_3$	80	dioxane	10	12
3	—	Bu_4NBr	$NaHCO_3$	80	*t*BuOH	8	12
4	—	Bu_4NBr	$NaHCO_3$	80	NMP	15	7
5	—	Bu_4NBr	$NaHCO_3$	80	DMF	29	7
6	—	Bu_4NBr	$NaHCO_3$	80	DMA	22	8
7	—	Bu_4NBr	$NaHCO_3$	80	DMSO	50	6
8	—	Bu_4NBr	NaOAc	80	DMSO	36	5
9	—	Bu_4NBr	Na_2CO_3	80	DMSO	49	8
10[c]	—	Bu_4NBr	Na_2CO_3	80	DMSO	51	8

11	—	Bu_4NBr	Li_2CO_3	80	DMSO	29	3
12	—	Bu_4NBr	K_2CO_3	80	DMSO	16	0
13	—	Bu_4NBr	Cs_2CO_3	80	DMSO	0	0
14	—	Bu_4NBr	NaOH	80	DMSO	0	0
15	—	Bu_4NBr	NaO*t*Bu	80	DMSO	0	0
16	—	Bu_4NBr	$NaHCO_3$	20	DMSO	8	2
17	—	Bu_4NBr	$NaHCO_3$	50	DMSO	31	3
18	—	Bu_4NBr	$NaHCO_3$	110	DMSO	46	9
19	—	Bu_4NBr	$NaHCO_3$	140	DMSO	35	7
20	—	—	$NaHCO_3$	80	DMSO	40	12
21	—	Bu_4NCl	$NaHCO_3$	80	DMSO	**49**	**3**
22	—	Bu_4NI	$NaHCO_3$	80	DMSO	35	16
23	PPh_3	Bu_4NCl	$NaHCO_3$	80	DMSO	0	0
24	$P(OPh)_3$	Bu_4NCl	$NaHCO_3$	80	DMSO	0	0
25	$P(C_6F_5)_3$	Bu_4NCl	$NaHCO_3$	80	DMSO	0	0
26[d]	Boc-Ala-OH	Bu_4NCl	$NaHCO_3$	80	DMSO	52	6
27[d]	Boc-Phe-OH	Bu_4NCl	$NaHCO_3$	80	DMSO	45	4

[a] **3.6** (0.2 M), **3.7** (1.5 equiv), $Pd(OAc)_2$ (20 mol %), ligand (40 mol %), additive (1.0 equiv), base (3.0 equiv) in DMSO (1 mL). (*p*-Tol = *para*-tolyl) [b] NMR yields with Ph_3SiMe (1.0 equiv) as the internal standard. [c] With PivOH (40 mol %). [d] **3.7** (3.0 equiv), Bu_4NCl (0.5 equiv) and $NaHCO_3$ (1.0 equiv).

3.3.3 The effect of silver salts

Next, we examined eight silver salts as additives (Table 3-3). Silver salts are often used to irreversibly abstract halide anions from Pd complexes thus rendering them more electrophilic and preventing the formation of mostly inactive PdI_2.[360-362] Indeed, the regioselectivity was enhanced in the presence of a silver salt (entries 1–8). We found that AgCl not only increased the yield of **3.8**, but also promoted exclusive reaction at the C5-position (entry 6).

Table 3-3. Silver effect on the regioselectivity of C–H arylation of cyclic enaminone

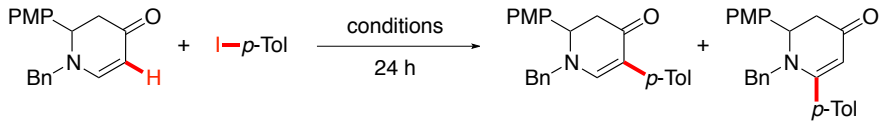

3.6 **3.7** **3.8** **3.9**

Entry[a]	Ag Salt	**3.8** (%)[b]	**3.9** (%)[b]
1	AgTFA	33	<1
2	AgF_2	14	0
3	$AgNO_3$	32	0
4	AgOAc	30	<1
5	Ag_2CO_3	30	<1
6	AgCl	65	0
7[c]	Ag_2O + benzoic acid	30	0
8[c,d]	Ag_2O + pivalic acid	49	3
9	–	49	3

[a] **3.6** (0.2 M), **3.7** (3.0 equiv), $Pd(OAc)_2$ (20 mol %), Bu_4NCl (1.0 equiv), $NaHCO_3$ (3.0 equiv), silver salt (1.2 equiv) in DMSO (1 mL) at 80 ºC. (*p*-Tol = *para*-tolyl) [b] NMR yields with Ph_3SiMe (1.0 equiv) as the internal standard. [c] Ag_2O (0.75 equiv), acid (1.5 equiv), no $NaHCO_3$. [d] No Bu_4NCl.

3.3.4 Fine-tuning the stoichiometry

Lastly, we proceeded to tune the reagent stoichiometry extensively (Table 3-4). First, the concentration of Bu_4NCl was tested from 0.1 to 3.0 equiv (entries 1–5). Arylation conditions with 0.5 equiv of Bu_4NCl generated a comparable yield of **3.8** (64%, entry 2) as those with originally chosen 1.0 equiv of Bu_4NCl (65%, entry 3). Further lowering and increasing the amount of Bu_4NCl both resulted in a yield decrease of **3.8**. Second, the loading of AgCl was changed from 0.1 to 3.0 equiv (entries 6–9). The highest yield was observed in the presence of 1.2 equiv of AgCl. Third, we controlled the amount of aryl iodide **3.7** (entries 10–15). As expected, the yield climbs from 52% when the addition of **3.7** increases from 1.1 equiv. However, the yield plateaued at 64% after 3.0 or more equiv of **3.7** were added. Adding **3.7** to the reaction in up to 15.0 equiv unfortunately

showed no beneficial effect. We also altered the concentration of $NaHCO_3$ from 1.0 to 10.0 equiv (entries 16–19). Even though no higher yield was obtained, we were able to reduce the loading of $NaHCO_3$ from originally 3.0 to 1.0 equiv with the same yield (64%, entry 16). In addition, the loading of $Pd(OAc)_2$ was examined from 0.1 to 30 mol % (entries 20–24). We found that the reaction ceased with only 0.1 mol % of catalyst, while being the most productive (64%) in the presence of 20 mol % of $Pd(OAc)_2$. We also monitored the reaction progress over a 24-h period (entries 25–30). The yield curve revealed that the C–H arylation reaction proceeded slowly in the first 12 hours and then stopped without decomposition of **3.8**. Lastly, we evaluated the effect of the reaction scale from 0.067 to 0.4 M (entries 31–34). We were pleased to find that the reaction on a 0.2 M scale in 0.5 mL of DMSO furnished the best yield of desired product **3.8** (72%, entry 32). It is worth mentioning that the byproduct **3.9** was not observed in most of the tested conditions.

Table 3-4. Extensive optimization of reaction stoichiometry and time

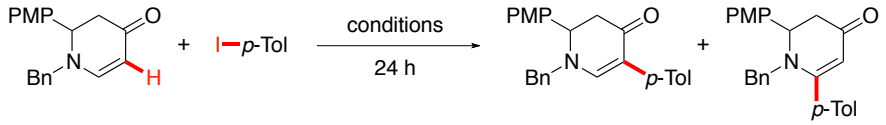

3.6 **3.7** **3.8** **3.9**

Entry[a]	**3.6** (mmol)	**3.7** (equiv)	$Pd(OAc)_2$ (mol %)	AgCl (equiv)	$NaHCO_3$ (equiv)	Bu_4NCl (equiv)	DMSO (mL)	*t* (h)	**3.8** (%)	**3.9** (%)
1	0.2	3.0	20	1.2	3.0	**0.1**	1.0	24	48	0
2	0.2	3.0	20	1.2	3.0	**0.5**	1.0	24	64	0
3	0.2	3.0	20	1.2	3.0	**1.0**	1.0	24	65	0
4	0.2	3.0	20	1.2	3.0	**2.0**	1.0	24	36	0
5	0.2	3.0	20	1.2	3.0	**3.0**	1.0	24	19	0
6	0.2	3.0	20	**0.1**	3.0	0.5	1.0	24	57	3
7	0.2	3.0	20	**0.5**	3.0	0.5	1.0	24	58	1
8	0.2	3.0	20	**2.0**	3.0	0.5	1.0	24	54	0
9	0.2	3.0	20	**3.0**	3.0	0.5	1.0	24	55	0
10	0.2	**1.1**	20	1.2	3.0	0.5	1.0	24	52	0

11	0.2	**1.5**	20	1.2	3.0	0.5	1.0	24	60	0
12	0.2	**2.0**	20	1.2	3.0	0.5	1.0	24	63	0
13	0.2	**4.0**	20	1.2	3.0	0.5	1.0	24	64	0
14	0.2	**6.0**	20	1.2	3.0	0.5	1.0	24	64	0
15	0.2	**15.0**	20	1.2	3.0	0.5	1.0	24	63	0
16	0.2	3.0	20	1.2	**1.0**	0.5	1.0	24	64	0
17	0.2	3.0	20	1.2	**2.0**	0.5	1.0	24	61	0
18	0.2	3.0	20	1.2	**5.0**	0.5	1.0	24	59	0
19	0.2	3.0	20	1.2	**10.0**	0.5	1.0	24	59	0
20	0.2	3.0	**0.1**	1.2	1.0	0.5	1.0	24	0	0
21	0.2	3.0	**5**	1.2	1.0	0.5	1.0	24	46	0
22	0.2	3.0	**10**	1.2	1.0	0.5	1.0	24	56	0
23	0.2	3.0	**15**	1.2	1.0	0.5	1.0	24	61	0
24	0.2	3.0	**30**	1.2	1.0	0.5	1.0	24	60	0
25	0.2	3.0	20	1.2	1.0	0.5	1.0	**0.5**	34	0
26	0.2	3.0	20	1.2	1.0	0.5	1.0	**1**	47	0
27	0.2	3.0	20	1.2	1.0	0.5	1.0	**2**	57	<1
28	0.2	3.0	20	1.2	1.0	0.5	1.0	**4**	58	<1
29	0.2	3.0	20	1.2	1.0	0.5	1.0	**8**	62	<1
30	0.2	3.0	20	1.2	1.0	0.5	1.0	**12**	64	<1
31	**0.2**	3.0	20	1.2	1.0	0.5	**0.5**	24	64	0
32	**0.1**	3.0	20	1.2	1.0	0.5	**0.5**	24	**75 (72[b])**	**<1**
33	**0.2**	3.0	20	1.2	1.0	0.5	**2.0**	24	55	0
34	**0.2**	3.0	20	1.2	1.0	0.5	**3.0**	24	52	0

[a] NMR yields with Ph_3SiMe (1.0 equiv) as the internal standard. (*p*-Tol = *para*-tolyl) [b] Isolated yield.

In short, we decided to use the following optimized conditions for the investigation of the reaction scope: cyclic enaminone (0.1 M), aryl iodide (3.0 equiv), $Pd(OAc)_2$ (20 mol

%), Bu_4NCl (0.5 equiv), $NaHCO_3$ (1.0 equiv), AgCl (1.2 equiv) in DMSO (0.5 mL) at 80 ºC.

3.4 Investigation of the reaction scope

3.4.1 Scope of aryl iodides

Table 3-5. Scope of aryl iodides for the Direct C–H arylation[a]

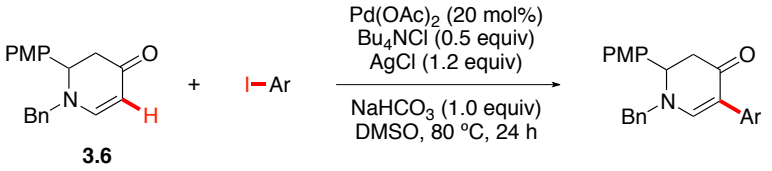

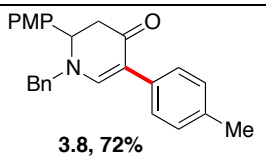

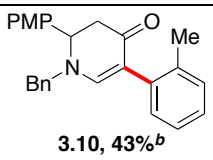

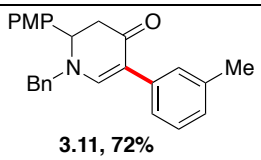

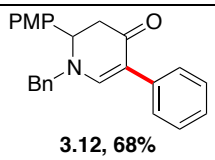

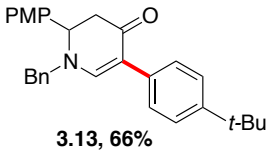

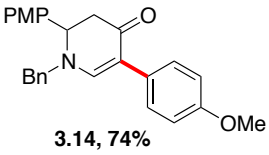

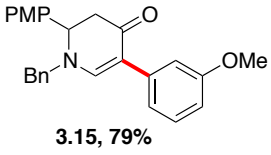

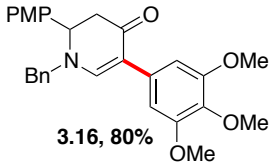

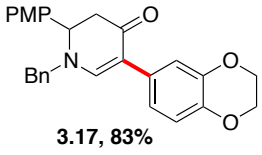

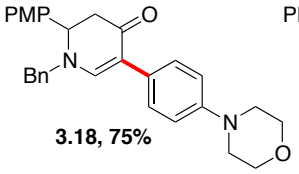

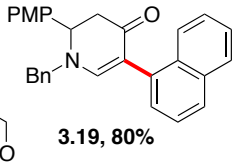

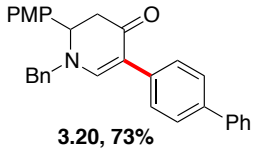

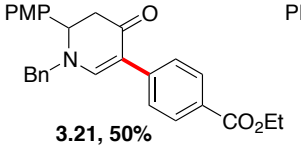

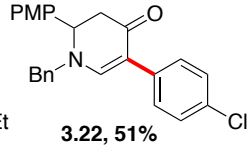

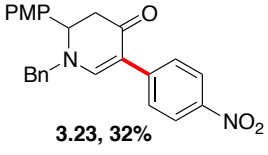

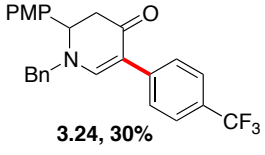

[a] **3.6** (0.2 M), aryl iodide (3.0 equiv), $Pd(OAc)_2$ (20 mol %), Bu_4NCl (0.5 equiv), $NaHCO_3$ (3.0 equiv), AgCl (1.2 equiv) in DMSO (0.5 mL), 24 h. Isolated yields with full consumption of **3.6**, unless otherwise noted. [b] 14% recovered **3.6**.

Next we explored the scope of aryl iodides in this reaction using the optimized conditions (Table 3-5) and found that the electronic properties of the aryl iodides affected

reaction yields significantly. Good yields were generally obtained with electron rich aryl iodides (**3.8**–**3.20**). Electron poor aryl iodides afforded slightly lowered yields (**3.21**–**3.24**). Reactions of aryl iodides with strongly electron-withdrawing substituents, *e.g.* NO_2 (**3.23**) and CF_3 (**3.24**), resulted in low yields. Steric hindrance, as expected, impeded the effectiveness of the cross coupling. For instance, compared to the 4-tolyl derivative (**3.8**), 2-tolyl iodide afforded a lower yield (**3.10**) with 14% recovered **3.6**. In addition, arylation of bifunctional 4-chlorophenyliodide proceeded exclusively at the iodine terminus with the chlorine terminus intact (**3.22**), which may be subjected to sequential cross-coupling reactions.[363-366] It is worth mentioning that phenyl bromide was tested under the optimized conditions and afforded an inferior yield (21% with 32% recovered **3.6**) compared to phenyl iodide, which afforded **3.12** in 68%. Neither 4-chlorotoluene nor phenyl triflate functioned as arylating reagents to afford the desired product.

3.4.2 Scope of cyclic enaminones

Given the high coupling efficiency of electron-rich aryl iodides, a series of cyclic enaminones was subjected to the optimized conditions with 4-iodoanisole (**3.25**, Table 3-6). Consistent with our previous results,[79-81, 341] electron-rich and monocyclic and bicyclic enaminones were all compatible with the optimized conditions (**3.26**–**3.31)**. Compared to *N*-benzylenaminone **3.26**, *N*-phenylenaminone **3.27** was formed in a decreased yield probably due to its attenuated nucleophilicity. Notably, these mildly basic conditions did not compromise the stereochemical integrity of the epimerizable enaminone **3.31**. In contrast, no reaction took place on either the *N*-unprotected enaminone or the *E*-enaminone to form products **3.32** or **3.33**.[79-81, 341] Electron-deficient enaminones also failed to furnish desired 5-arylated products **3.34** or **3.35**.

Notably, cyclic enaminones with *N*-electron-withdrawing groups underwent C6-arylation exclusively in sharp contrast to their lack of reactivity observed previously (Scheme 3-3).[79-81] We postulate that the diminished nucleophilicity of enaminones blocks electrophilic palladation, thus rendering the carbopalladation pathway favorable.

Table 3-6. Scope of cyclic enaminones for the direct C–H arylation[a]

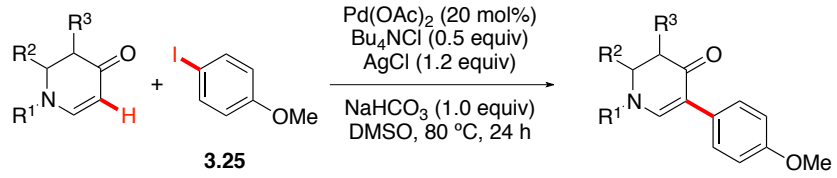

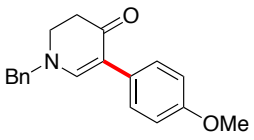

3.26, 78%

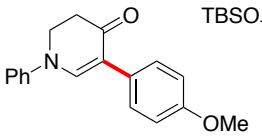

3.27, 50%

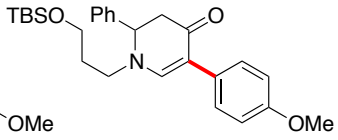

3.28, 45%

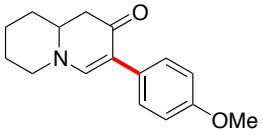

3.29, 63%

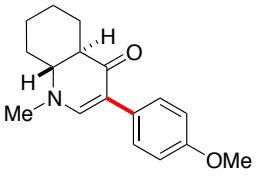

3.30, 48%

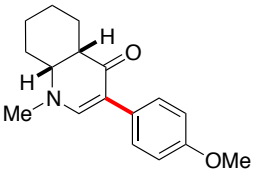

3.31, 60%

Incompatible:

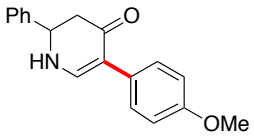

3.32, 0%[b]

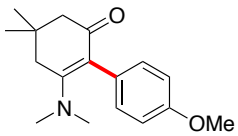

3.33, 0%[c]

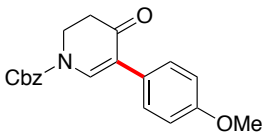

3.34, 0%[d]

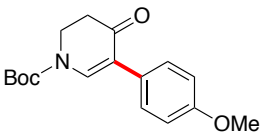

3.35, 0%[e]

[a] cyclic enaminone (0.2 M), **3.25** (3.0 equiv), $Pd(OAc)_2$ (20 mol %), Bu_4NCl (0.5 equiv), $NaHCO_3$ (3.0 equiv), AgCl (1.2 equiv) in DMSO (0.5 mL), 24 h. Isolated yields. [b] 60% recovered starting enaminone. [c] 65% recovered starting enaminone. [d] 15% recovered starting enaminone. [e] 27% recovered starting enaminone.

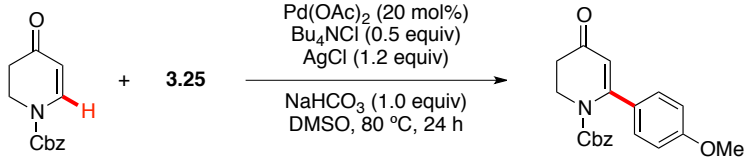

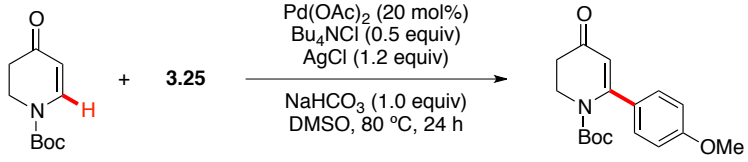

Scheme 3-3. C6-arylation of electron-deficient cyclic enaminones.

3.5 Mechanistic discussion

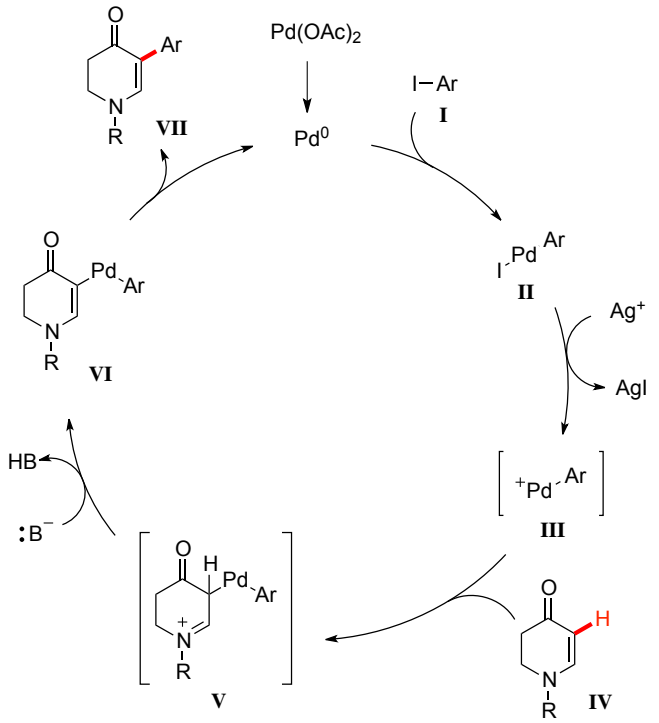

Figure 3-2. Proposed mechanism of direct arylation of cyclic enaminones.

Mechanistically, the aforementioned electrophilic palladation pathway (Figure 3-1) for direct arylation can account for the observed C5-regioselectivity, the silver salt effect, the solvent dependency, and the substituent effects. Presumably, AgCl abstracts the iodide from the Pd oxidative adduct (*i.e.* Ar–Pd–I) to generate a cationic $[Ar–Pd]^+$ complex, whose electrophilicity matches the innate C5-nucleophilicity of enaminones to yield C5-arylated enaminones. This unique C5-regioselectivity is enhanced by DMSO because the cationic $[Ar–Pd]^+$ species should be stabilized by this highly polar and coordinating solvent. In addition, the $[Ar–Pd]^+$ species should also be stabilized by electron-donating substituents, which would lead to less catalyst degradation and subsequently higher yields (*e.g.* 80% of **3.16** *vs.* 32% of **3.23**). It is worth noting that a concerted-metalation-deprotonation (CMD) mechanism cannot be excluded at this time. However, the lack of reactivity of the electron-deficient enaminones (**3.36** and **3.38)**

indicates a low possibility for this process, which often works well on electron-deficient substrates.[367] In addition, a Pd^{II}/Pd^{IV} catalytic cycle, albeit not ruled out, is also less likely because (1) more than one catalytic turnover was observed in the absence of silver salts (*e.g.* Table 3-2, entry 7, TON = 2.5), suggesting that silver salts did not serve to regenerate the Pd catalyst;[194] (2) our initial optimization also demonstrated that other Pd^0 catalysts (*e.g.* Table 3-1, entries 2-3, $Pd(dba)_2$ or $Pd_2(dba)_3$) would catalyze C5-arylation as well, albeit in low yields (8–11%).

Therefore, we propose the following mechanism (Figure 3-2): First, the pre-catalyst $Pd(OAc)_2$ is reduced *in situ* to Pd^0, which undergoes oxidative addition with iodide **I** to form the adduct **II**. Silver chloride then abstracts the iodide anion from the Pd center and presumably generates a cationic Pd^{II} species **III**, which subsequently palladates the strongly nucleophilic enaminone **IV** to form the key intermediate **VI** after deprotonation by a base. Finally, reductive elimination furnishes the desired C5-arylated product **VII** with the regeneration of Pd^0.

3.6 Summary

We have developed a straightforward method for the regioselective C–H arylation of cyclic enaminones with aryl iodides. In spite of showing reduced but nevertheless good yields compared to our earlier arylation protocols, the new method reported herein utilizes aryl iodides with broader commercial availability. This transformation tolerates a wide range of substrates and presents an alternative approach to synthesize 3-arylpiperidine derivatives.

Chapter 4 Pd^{II}-Catalyzed Dehydrogenative Alkenylation of Cyclic Enaminones

4.1 Introduction

In order to further elaborate the cyclic enaminone scaffold and enhance its synthetic utility, we began to investigate a C–H alkenylation reaction on the C5-position. Following the strategy of C–H arylation of cyclic enaminones with aryl trifluoroborates (Figure 4-1, route a),[79] we planned to use alkenyl trifluoroborates to synthesize the alkenylated enaminone **VI** (Figure 4-1, route b). Unfortunately, no desired product was observed. We speculated that the rate of transmetallation with the alkenyl reagents surpassed that of C5-palladation and as a result homocoupling depleted the alkenyl precursors and reoxidants.

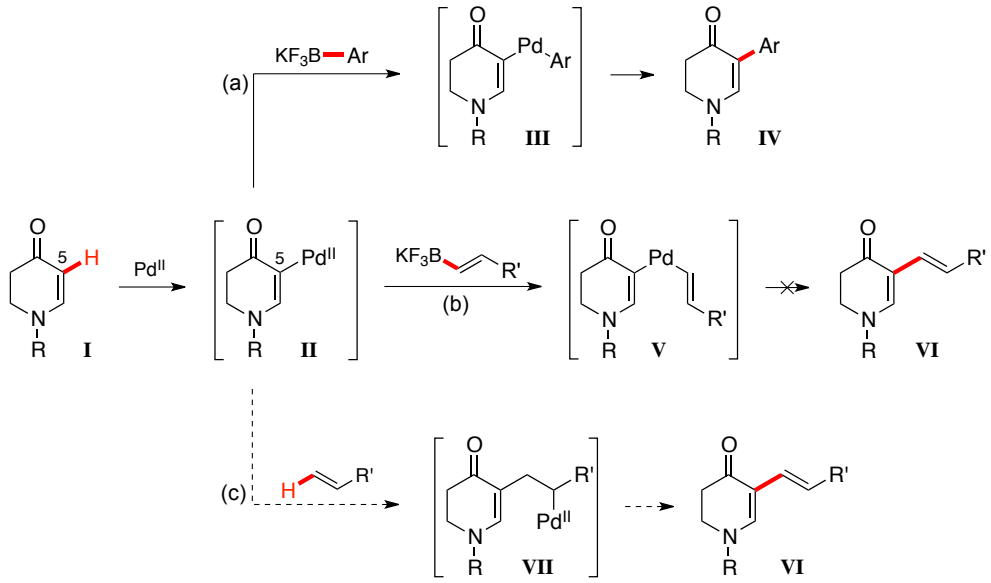

Scheme 4-1. Pd^{II}-catalyzed cross-coupling reactions of cyclic enaminones.

4.2 Coupling strategy

To address this problem, we examined the feasibility of a dehydrogenative alkenylation reaction (Figure 4-1, route c) to access 5-alkenyl enaminone derivatives. Notably, dehydrogenative processes of this sort that use two C–H bonds to form a new

C–C bond are highly sought after, because they require no prefunctionalization of either substrate and as a result have high atom economy.[90, 92, 137, 138, 335] Key to this strategy would be the use of alkenes with complementary reactivity. We envisioned that the palladated enaminone **II** could be orthogonally intercepted by an electron-deficient alkene to furnish product **VI**.

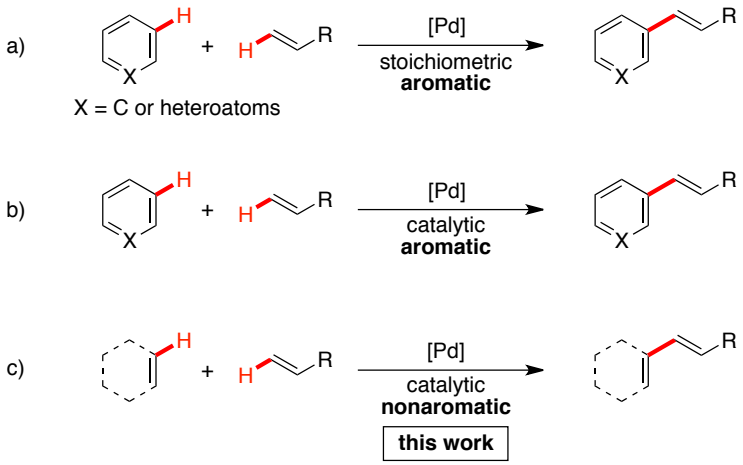

Scheme 4-2. Development of the Fujiwara-Moritani reaction.

The Fujiwara-Moritani reaction is a process by which aromatic substrates undergo intermolecular dehydrogenative alkenylation. As mentioned in Chapter 2.7.2, this reaction was initially developed using stoichiometric amounts of Pd^{II} (Figure 4-2a),[280] but soon thereafter was shown to also take place with catalytic amounts of Pd^{II} (Figure 4-2b).[310, 368] In recent years, the scope of the Fujiwara-Moritani reaction has been expanded to a plethora of aromatic substrates.[369-372] However, only a small number of dehydrogenative reactions involving two *alkenyl* C–H donors (Figure 4-2c) have been reported.[136, 328, 330-333, 373] They are largely limited to select substrates, require high Pd loading, and need long reaction time. The realization of dehydrogenative alkenylation of cyclic enaminones will not only furnish convenient access to 3-alkenyl piperidine scaffolds, but also provide new examples to the field of cross-dehydrogenative coupling.

4.3 Condition optimization

We selected enaminone **4.1** as the substrate and examined its reaction with *tert*-butyl acrylate (**4.2**) (Table 4-1). $Pd(OAc)_2$ (10 mol %) was initially selected because of its well-established reactivity.[79, 374]

4.3.1 Solvent study

Table 4-1. Solvent effect on the dehydrogenative alkenylation

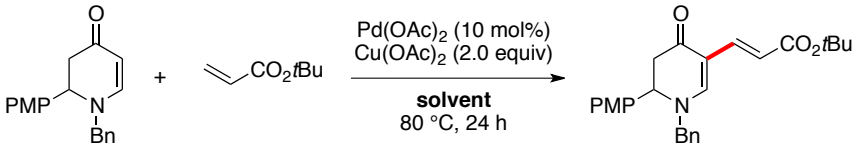

4.1 **4.2** **4.3**

Entry[a]	Solvent	% Consumption[b]	% Yield[c]
1	toluene	52	33
2	*t*AmOH	100	67
3	*t*BuOH	100	55
4	dioxane	100	64
5	DMSO	100	53
6	DMF	97	78
7	NMP	100	78
8	AcOH	92	8
9	DMA	100	70
10	CH_3CN	97	67
11	DMF/DMSO (20:1)	100	75
12	NMP/DMSO (20:1)	100	75
13	DMF/AcOH (4:1)	58	47
14	DMF/AcOH/DMSO (20:5:1)	60	51

[a] Other reaction conditions: enaminone **4.1** (0.4 mmol), **4.2** (2.0 equiv), $Pd(OAc)_2$ (10 mol%), $Cu(OAc)_2$ (2.0 equiv) without additives under N_2 at 80 °C through 24 h. [b] NMR % conversion of the starting enaminone with Ph_3SiMe (1.0 equiv) as the internal standard. [c] NMR % yield with Ph_3SiMe (1.0 equiv) as the internal standard.

An array of common solvents was examined (Table 4-1), and the choice of solvents showed significant effect on the yields.[375, 376] Except for toluene (entry 1), all other single solvent systems proceeded with greater than 90% consumption, providing 8–78% of the desired product (entries 2–10). The acidic medium, acetic acid (entry 8), gave the poorest yield (8%), presumably due to the instability of the enaminones in an acidic environment. The highest yield (78%) was obtained in the presence of DMF (entry 6) or NMP (entry 7). Together with DMA (entry 9), these three examples indicate that a nitrogen-containing solvent may facilitate the catalytic process. Presumably this is because their coordinating ability may contribute to the stability of the Pd^{II} catalyst.

Multi-solvent media were also examined. Mixing DMSO with either DMF or NMP gave the same yield after 100% consumption of enaminone **4.1** (entries 11–12). Although aprotic polar DMSO can function as a good ligand for the Pd catalyst, the 20:1 formula failed to improve the outcome. Neither did the combination of DMP, AcOH and DMSO (entries 13–14), where the consumption and yield both dropped to 50–60%. We again attribute this to the instability of enaminones in AcOH. As solvent mixtures were inferior to single solvents, less costly DMF was chosen for the subsequent optimization studies.

4.3.2 Reoxidant study

Eight more reoxidants were assessed in addition to $Cu(OAc)_2$ (Table 4-2). $CuCl_2$ and $Cu(OTf)_2$ yielded no product at all (entries 2–3). Reducing the loading of $Cu(OAc)_2$ to 1.0 equiv under air or O_2 resulted in similar consumption of **4.1**, but lowered the yields to 60–70% (entries 4–5). It is interesting to note that the yield obtained under an O_2 atmosphere was lower than that attained under air. Possibly, excess O_2 could oxidize the enaminones *in situ*, therefore decreasing the yield. Ag^I salts, *tert*-butyl benzoperoxoate, and duroquinone were also tested and were not successful in increasing the yield of **4.3** (entries 6–9). Hence, we continued to use $Cu(OAc)_2$ as the most effective reoxidant.

Table 4-2. Reoxidant effect on the dehydrogenative alkenylation

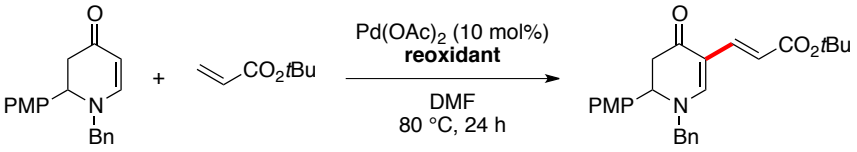

Entry[a]	Reoxidant (equiv)	% Consumption[b]	% Yield[c]
1	$Cu(OAc)_2$ (2.0)	97	78
2	$CuCl_2$ (2.0)	77	0
3	$Cu(OTf)_2$ (2.0)	72	0
4	$Cu(OAc)_2$ (1.0) + air	94	70
5	$Cu(OAc)_2$ (1.0) + O_2	98	60
6	AgOAc (2.0)	81	43
7	Ag_2O (1.0)	41	6
8	$PhCO_3tBu$ (1.0)	98	59
9	duroquinone (1.0)	23	5

[a] Other reaction conditions: enaminone **4.1** (0.4 mmol), **4.2** (2.0 equiv), $Pd(OAc)_2$ (10 mol%) without additives in DMF under N_2 at 80 °C through 24 h. [b] NMR % conversion of the starting enaminone with Ph_3SiMe (1.0 equiv) as the internal standard. [c] NMR % yield with Ph_3SiMe (1.0 equiv) as the internal standard.

4.3.3 Additive study

Table 4-3 summarizes the effect of various additives on the alkenylation. The yield of **4.3** was improved in most cases. The addition of lithium salts guaranteed a 100% consumption of **4.1** with the yields around 78% (entries 2–3). Three chloride additives showed varied results, indicating group I metals could be a good cation source (entries 3–5), which is echoed by the comparable yields from the acetate salts of three group I metals (entries 6–8). We also tested carbonate and phosphate salts but no yield improvement was observed (entries 9–11). When KTFA was employed (entry 12), we obtained the highest yield (85%), which was verified by the isolated yield (81%). Surprisingly, the acid-sensitive enaminone tolerated the presence of 1.0 equiv of the strong acid TFA and afforded a similar yield (80%, entry 13). We speculate that the anion

exchange between TFA and OAc of $Pd(OAc)_2$ may render the Pd^{II} center more electrophilic, thus more prone to electrophilic palladation. In addition, we also investigated the effect of varied additive concentrations. 1.0 equiv of KTFA was found the most effective in regard to the consumption and the yield (entries 12 and 14–15).

Table 4-3. Additive effect on the dehydrogenative alkenylation

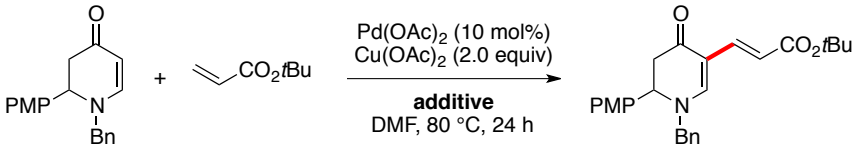

4.1 **4.2** **4.3**

Entry[a]	Additive (equiv)	% Consumption[b]	% Yield[c]
1	—	97	78
2	$LiBF_4$ (1.0)	100	80
3	LiCl (1.0)	100	76
4	$BiCl_3$ (1.0)	96	39
5	$MgCl_2$ (1.0)	86	51
6	NaOAc (1.0)	94	78
7	CsOAc (1.0)	92	77
8	KOAc (1.0)	95	82
9	Cs_2CO_3 (1.0)	94	79
10	K_2CO_3 (1.0)	82	68
11	K_3PO_4 (1.0)	90	75
12	KTFA (1.0)	100	85 (81[d])
13	TFA (1.0)	100	80
14	KTFA (0.5)	94	80
15	KTFA (2.0)	98	80

[a] Other reaction conditions: enaminone **4.1** (0.4 mmol), **4.2** (2.0 equiv), $Pd(OAc)_2$ (10 mol%), $Cu(OAc)_2$ (2.0 equiv) with additives in DMF under N_2 at 80 °C through 24 h. [b] NMR % conversion of the starting enaminone with Ph_3SiMe (1.0 equiv) as the internal standard. [c] NMR % yield with Ph_3SiMe (1.0 equiv) as the internal standard. [d] Isolated yield.

4.3.4 Temperature effect

With the best solvent, reoxidant, and additive in hand, we continued to investigate the temperature impact on catalysis (Figure 4-1). Raising temperature from room temperature to 110 °C at 30 °C intervals increased the consumption of the starting material from 72% up to 100% (red bars). The yield followed a similar pattern (green bars), while the peak (85%) occurred at 80 °C. Further increasing the temperature up to 110 °C lowered the yield by 16%, presumably due to the thermal decomposition of enaminones.

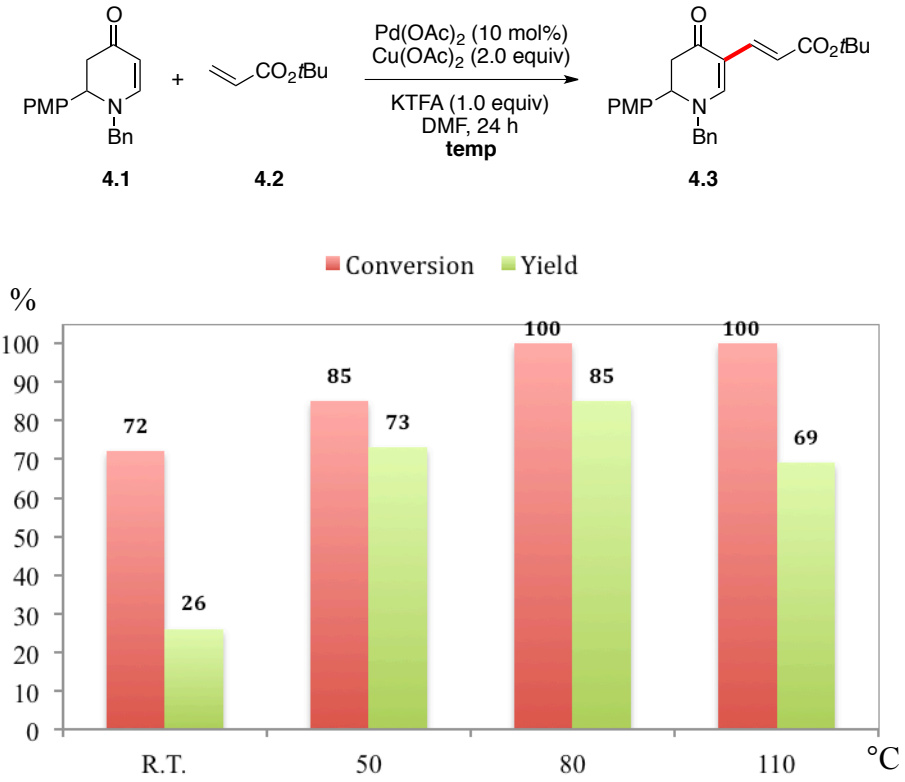

[a] Other reaction conditions: enaminone **4.1** (0.4 mmol), **4.2** (2.0 equiv), $Pd(OAc)_2$ (10 mol%), $Cu(OAc)_2$ (2.0 equiv) with KTFA (1.0 equiv) in DMF under N_2 through 24 h. NMR % conversion of the starting enaminone and NMR % yield with Ph_3SiMe (1.0 equiv) as the internal standard.

Figure 4-1. Temperature effect on the dehydrogenative alkenylation.[a]

4.3.5 Reaction time control

Figure 4-2 illustrates the coupling process in a 24 h period. The consumption of the starting material was monitored with ^{1}H NMR by testing every 0.1 ml aliquot from the mixture when the reaction reached 0.5, 1, 3, 5, 9, 12, and 24 h respectively. As indicated in the graph, the reaction went to completion within 3 h. During the succeeding 21 h, the yield remained constant, suggesting that the product was stable under the reaction conditions. The marginal deviations in yields may be attributed to the stochastic errors of ^{1}H NMR integration measurement.

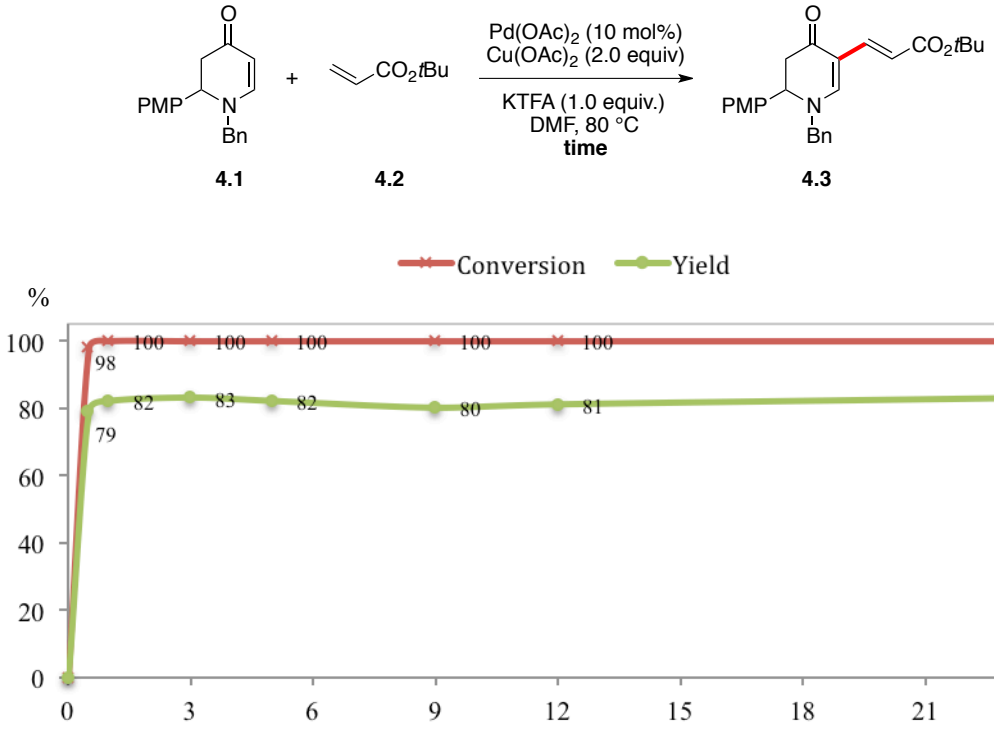

[a] Other reaction conditions: enaminone **4.1** (0.4 mmol), **4.2** (2.0 equiv), $Pd(OAc)_2$ (10 mol%), $Cu(OAc)_2$ (2.0 equiv) with KTFA (1.0 equiv) in DMF under N_2 at 80 °C. NMR % conversion of the starting enaminone and NMR % yield with Ph_3SiMe (1 equiv) as the internal standard.

Figure 4-2. Reaction time effect on the dehydrogenative alkenylation.[a]

4.3.6 Stoichiometry investigation

Finally, the effect of stoichiometry was probed (Table 4-4). It is worth mentioning that the reaction time was kept at 24 h for the purpose of consistency. Entries 1–4 demonstrate that by lowering the catalyst concentration not only did the consumption rate drop significantly, but the yield also decreased to 30%. In addition, the decrease of the alkene concentration furnished less product (entries 5–6). Lastly, we found that the variation of the reaction scale had no positive influence on yields (entries 7–9).

Therefore, the optimized conditions for C–H alkenylation of enaminones are Pd(OAc) (10 mol %) with alkene (2.0 equiv), $Cu(OAc)_2$ (2.0 equiv), and KTFA (1.0 equiv) in DMF at 80 ºC on a 0.4 M scale.

Table 4-4. Stoichiometry study on the dehydrogenative alkenylation

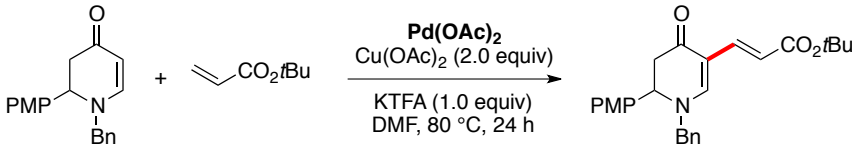

4.1 **4.2** **4.3**

Entry[a]	**4.1** (M)	**4.2** (equiv)	$Pd(OAc)_2$ (mol %)	% Consumption[b]	% Yield[c]
1[d]	0.4	2.0	10	100	85 (81[e])
2	0.4	2.0	5	100	83
3	0.4	2.0	2.5	88	72
4	0.4	2.0	1	48	30
5	0.4	1.5	5	98	76
6	0.4	1.1	5	93	68
7	0.1	2.0	5	98	76
8	0.2	2.0	5	99	81
9	0.8	2.0	5	98	71

[a] Other reaction conditions: $Cu(OAc)_2$ (2.0 equiv) with KTFA (1.0 equiv) in DMF under N_2 at 80 °C through 24 h. [b] NMR % conversion of the starting enaminone with Ph_3SiMe (1 equiv) as the internal standard. [c] NMR % yield with Ph_3SiMe (1 equiv) as the internal standard. [d] The best conditions after the previous screens. [e] Isolated yield.

4.4 Investigation of the reaction scope

With the optimized reaction conditions in hand, we embarked on exploring the substrate scope. A series of substituted alkenes and cyclic enaminones were evaluated.

4.4.1 Alkene scope

Table 4-5. Scope of alkenes for dehydrogenative alkenylation of cyclic enaminones[a]

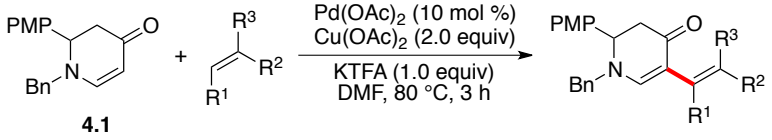

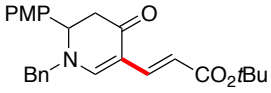

4.3, 81%

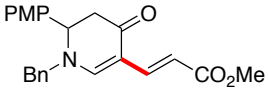

4.4, 82%

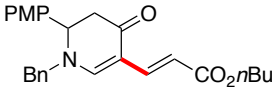

4.5, 87%

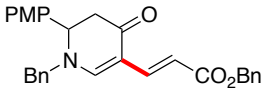

4.6, 91%

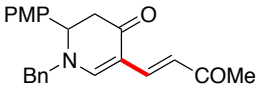

4.7, 85%

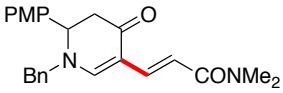

4.8, 95%

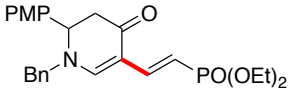

4.9, 68%

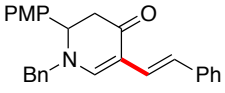

4.10, 66%

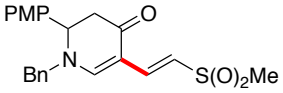

4.11, 56%

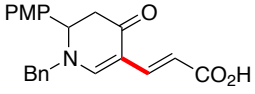

4.12, ≤3%

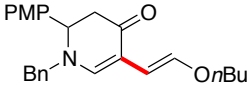

4.13, ≤3%

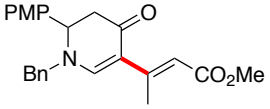

4.14, 42%

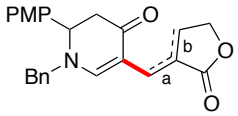

4.15
(83%, a:b = 1:2.5[b])

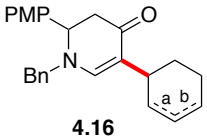

4.16
(49%, a:b = 1:1.1[c])

[a] Conditions: **4.1** (0.4 M), alkene (2.0 equiv), $Pd(OAc)_2$ (10 mol %), $Cu(OAc)_2$ (2.0 equiv), KTFA (1.0 equiv) in DMF under N_2 at 80 °C for 3 h. Isolated yield. [b] Isolated ratio. [c] ^1H NMR ratio.

We were pleased to find that this direct alkenylation protocol was amenable to reaction with a variety of electron-deficient alkenes (Table 4-5). Acrylate esters and vinyl ketones readily reacted with **1**, providing the desired dienes (**4.3–4.7**) in excellent yields up to 91%. Notably, the highest yield (95%) was observed with *N*,*N*-dimethylacrylamide (**4.8**). Phosphonates, styrene and sulfones were also viable coupling partners, yet furnishing the products (**4.9–4.11**) in slightly lower yields. Acrylic acid and vinyl ethers, however, failed to afford the desired products **4.12** or **4.13**.

Double bond isomerization in coupling products was observed in the cases of multi-substituted alkenes bearing more than one β-hydrogen. Although methyl crotonate only formed a single *E*-isomer (**4.14**), α-methylene-γ-lactones afforded both the conjugated and unconjugated (to enaminone) diene products with a greater preference for the latter (**4.15a**:**4.15b**=1:2.5). This preference for the formation of unconjugated dienes has been previously noted.[377-379] Interestingly, alkenylation of cyclohexene yielded two inseparable, unconjugated dienes (**4.16a**/**4.16b**). Mechanistically, we speculated that **4.16b** was generated from **4.16a** through *in situ* Pd–H insertion and immediate β-H elimination.[380]

4.4.2 Cyclic enaminone scope

We next assessed a series of cyclic enaminones (Table 4-6). We found that this reaction could be extended to monocyclic and bicyclic, electron-rich enaminones (**4.17–4.22**, **4.25**) with yields up to 92%. Notably, compared to *N*-alkylenaminones, *N*-phenylenaminone could afford a slightly decreased yield of **4.17** despite its attenuated nucleophilicity. Bicyclic enaminones generally gave lower yields than their monocyclic counterparts, where the indolizidine enaminone (**4.20**, 73%) appeared to be less effective in this reaction than the quinolizidine scaffold (**4.21**, 86%). Possibly, the conjugation between the lone pair of the nitrogen and the *p*-orbitals of the double bond is impaired due to the more constrained 5,6-bicyclic scaffold of **4.20**, which results in a less nucleophilic enaminone towards electrophilic palladation. We were glad to find that alkenylation of the diastereomeric substrates (**4.22**/**4.25**) took place without epimerization

of the stereocenters and with virtually the same yields. However, the installation of a C6-methyl substituent on the cyclic enaminone significantly decreased the yield of **4.23** presumably due to the steric repulsion to either palladation or migratory insertion.

Table 4-6. Scope of enaminones for dehydrogenative alkenylation of cyclic enaminones[a]

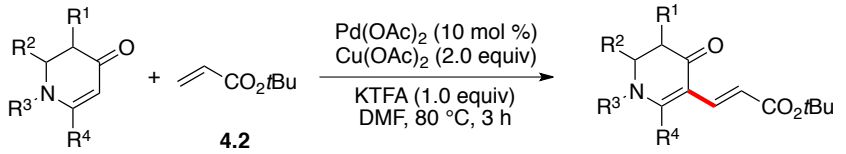

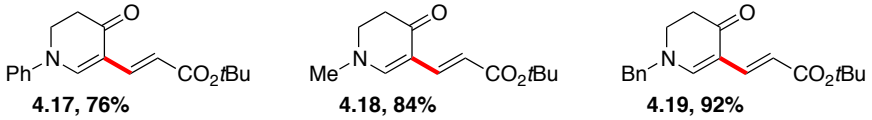

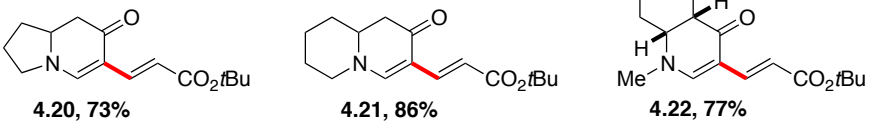

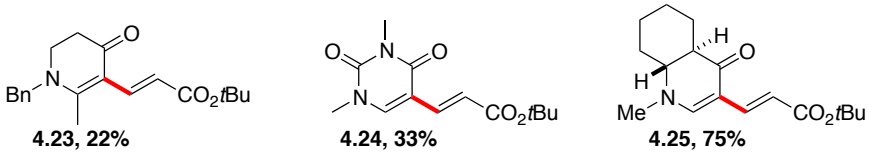

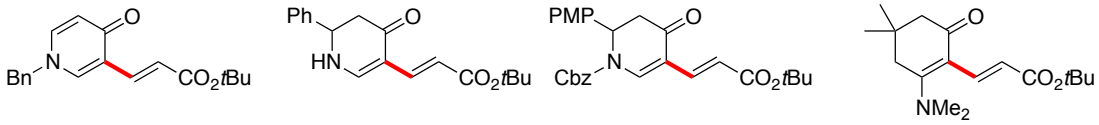

[a] Conditions: enaminone (0.4 M), **4.2** (2.0 equiv), $Pd(OAc)_2$ (10 mol %), $Cu(OAc)_2$ (2.0 equiv), KTFA (1.0 equiv) in DMF under N_2 at 80 °C for 3 h. Isolated yield.

A small collection of cyclic enaminones was found incompatible under the optimized conditions. Interestingly, 4-pyridone was found to furnish a mono-coupling product **4.26** albeit in only 7% yield. The *N*-unsubstituted enaminone only furnish 6% of the desired product **4.27** possibly due to the Pd catalyst poisoning by the free *N*-H group. *N*-Cbz enaminone (**4.28**) also showed no reactivity. We speculate that the electron-withdrawing nature of the Cbz group may significantly hamper the enaminone's nucleophilicity, which

is vital for electrophilic palladation. An *E*-enaminone was also tested, but product **4.29** was not observed. These results, however, are consistent with our previous findings.[79-81]

As structurally akin to the enaminone scaffold, 1,3-dimethyluracil was also subjected to the optimized conditions. To our disappointment, only 33% of the desired alkenylated uracil **4.24** was formed with a large amount of 1,3-dimethyluracil remaining. We presume that the nucleophilicity of uracils is tempered by aromatic delocalization and the electron-withdrawing C2-carbonyl. Our ^{1}H NMR study revealed that the chemical shifts for the two alkenyl protons from *N*-methylenaminone were 4.92 (C5) and 6.98 (C6) ppm, whereas those from 1,3-dimethyluracil were 5.74 (C5) and 7.17 (C6) ppm (Scheme 4-3). The chemical shift differences of the enaminone (2.06 ppm) *vs.* those of the uracil (1.43 ppm) indicate a more polarized double bond (*i.e.* a more nucleophilic C5 and a more electrophilic C6). This preliminary observation may help to understand the reduced reactivity of 1,3-dimethyluracil. Nevertheless, due to the medicinal importance of 5-alkenyluracils,[381-385] the development of a high-yielding dehydrogenative alkenylation method for uracils was pursued and will be discussed in Chapter 5.

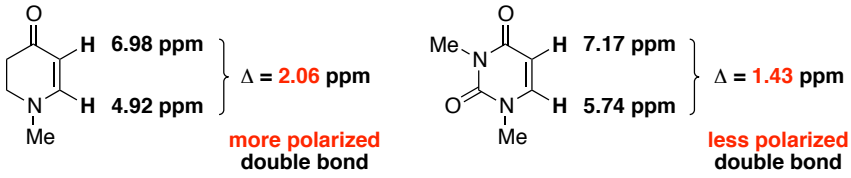

Scheme 4-3. Chemical shifts of C5- and C6-protons from enaminone and uracil.

4.5 Mechanistic study

To probe the alkenylation mechanism, a mechanistic analysis of the initial interaction of Pd^{II} with enaminone **4.1** was carried out by ^{1}H NMR (in DMSO-d_6 at room temperature, Figure 4-3). 50 mol % of $Pd(OAc)_2$ with **4.1** (Figure 4-3.2) furnished intermediate **4.30** at room temperature along with the same amount of acetic acid and unreacted **4.1**. With 100 mol % of $Pd(OAc)_2$ (Figure 4-3.3), a complete conversion of **4.1** was observed after only 20 min, furnishing only **4.30** and acetic acid. The full spectrum is shown in Figure 4-4.

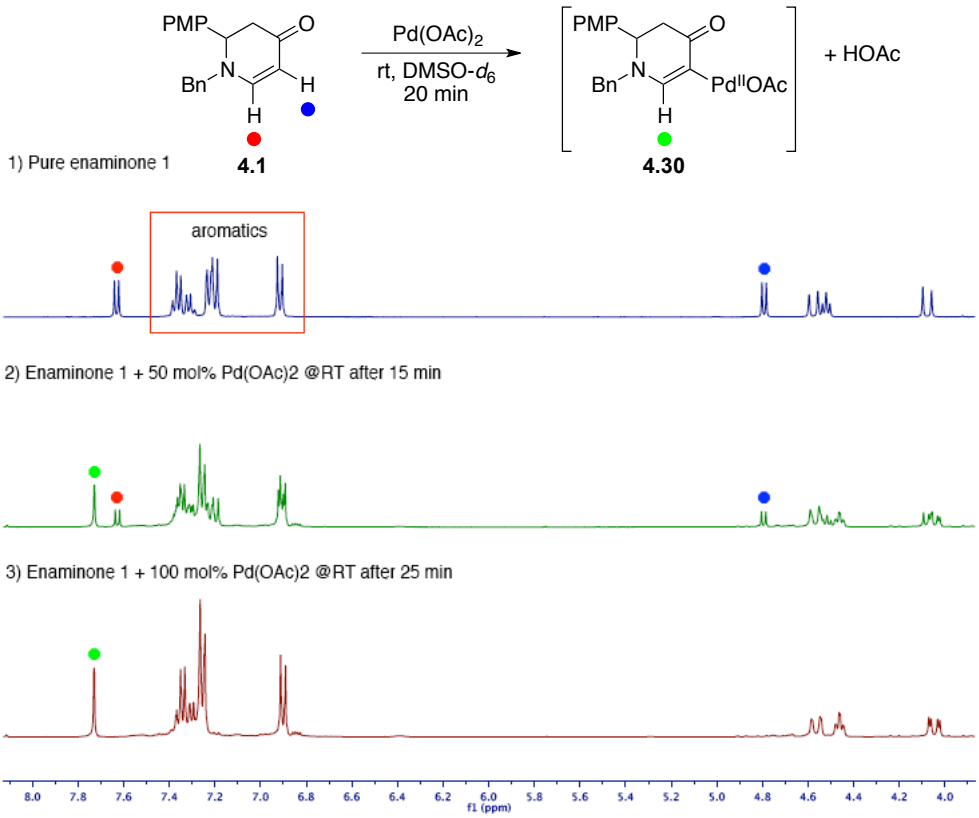

Figure 4-3. Palladation monitored by ^{1}H NMR (in DMSO-d_6).

Intermediate **4.30** was further converted to product **4.3** under the treatment of 2.0 equiv of acrylate **4.2** (Table 4-7). Surprisingly, DMSO showed a strong stabilizing effect on **4.30** and only afforded 7% of **4.3** at the optimized temperature (80 ºC, entry 1). Raising the temperature did increase the yield presumably by breaking down the ligation of DMSO to activate the intermediate (entries 2–4). However, due to the thermal instability of **4.3** seen in Figure 4-1, the conversion (20%) at 140 ºC is not optimal. Nevertheless, the proposed intermediate **4.30** is proven to furnish the desired product. This suggests that the C–C bond formation may be the rate-limiting step. It is worth noting that intermediate **4.30** was not detected when DMF-d_7 was used as the solvent, presumably because DMF does not stabilize **4.30** as well as DMSO.[386] The discrepancy of their stabilizing effect as solvents was also shown in the yield of **4.3**, where 78% was produced in DMF compared to 53% in DMSO (Table 4-1, entries 5 and 6).

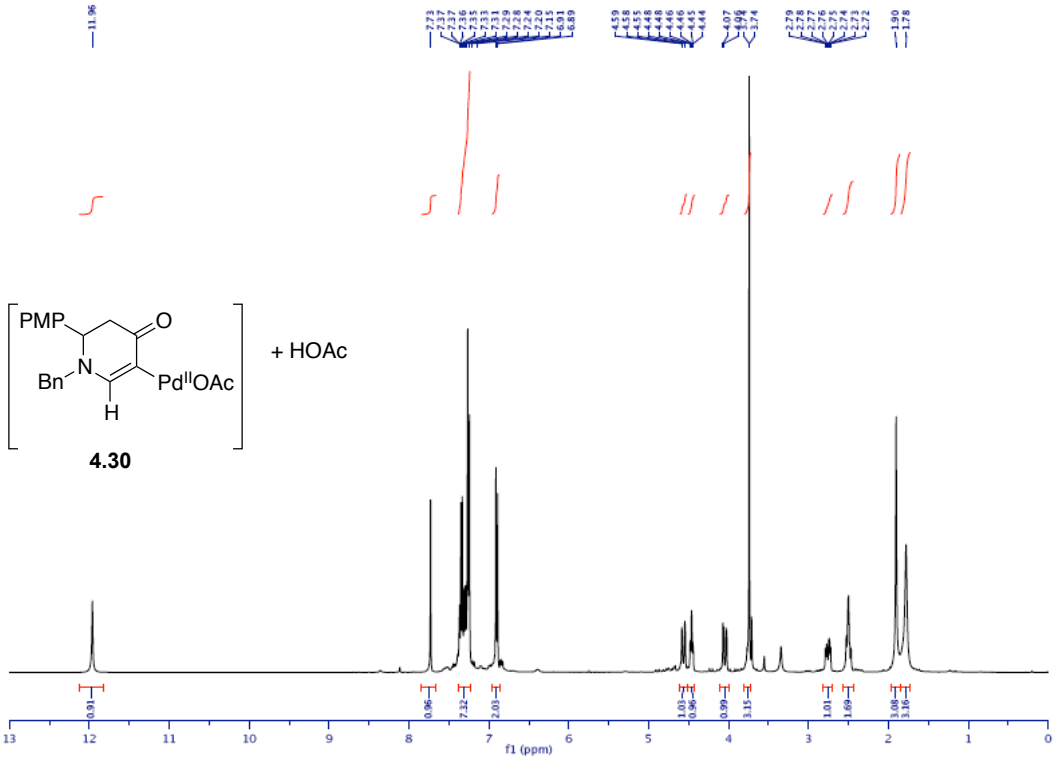

Figure 4-4. ^{1}H NMR spectrum of palladation with $Pd(OAc)_2$ (100 mol %, in DMSO-d_6).

Table 4-7. Conversion of product **4.3** from intermediate **4.30**

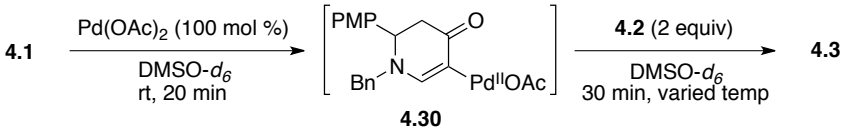

Entry[a]	Temp (ºC)	% Yield[b]
1	80	7%
2	100	10%
3	120	18%
4	140	20%

[a] Procedure: **4.1** (29.3 mg, 0.10 mmol) was mixed with 100 mol % of $Pd(OAc)_2$ in DMSO-d_6 (1.0 mL) at rt under N_2 for 20 min, followed by the addition of **4.2** (2.0 equiv). Reaction was further stirred at different temperatures for 30 min. The reaction was then quenched with 0.5 g of K_2CO_3 and filtered. The filtrate was concentrated and subjected to ^{1}H NMR analysis. [b] ^{1}H NMR % yield with Ph_3SiMe (1.0 equiv) as the internal standard.

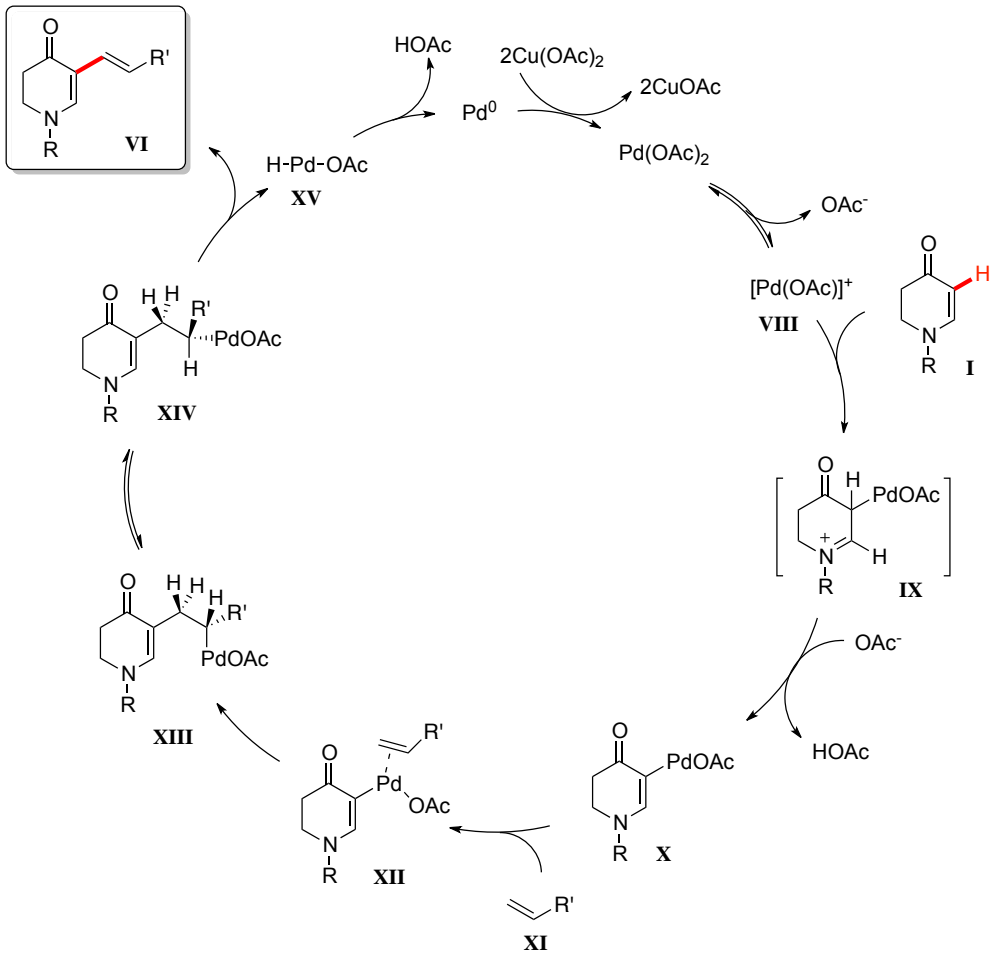

Figure 4-5. Proposed mechanism of dehydrogenative alkenylation of cyclic enaminones.

We therefore suggest a detailed catalytic cycle of the dehydrogenative alkenylation reaction (Figure 4-5). The key steps are: (1) The dissociation of $Pd(OAc)_2$ forms an electrophilic cationic species **VIII**. (2) The electrophilic attack of $[Pd(OAc)]^+$ onto the C=C bond of cyclic enaminone **I** followed by deprotonation generates the palladated intermediate **X**. (3) The alkene **XI** inserts into the newly formed Pd–C bond in a *syn* fashion. (4) β-Hydride *syn*-elimination occurs in the suitable conformer **XIV** as a result of the C–C bond rotation to furnish the final product **VI** along with palladium hydride **XV**. (5) The reductive elimination releases HOAc to form Pd^0, which is then reoxidized by $Cu(OAc)_2$ to regenerate the Pd^{II} catalyst.

4.6 Summary

We developed a convenient and highly atom-economic approach for the dehydrogenative coupling of cyclic enaminones and unfunctionalized alkenes. This method addressed the problem of using alkenyl trifluoroborates as the alkene source, and expanded the reaction mode of cyclic enaminones from direct arylation to alkenylation. The generality of this transformation presents a useful strategy for directly cross-coupling alkenes and offers an attractive new approach to prepare 3-alkenyl piperidine scaffolds.

Chapter 5 Pd^{II}-Catalyzed Dehydrogenative Alkenylation of Uracils

5.1 Introduction

Functionalization of uracils at the C5-position is of interest for the purpose of labeling[387-389] and the preparation of bioactive uracil derivatives.[390-393] The C5-position of pyrimidines is the location of choice for structural modification because this site is not involved in Watson-Crick base pairing.[394] 5-Alkenyluracils have been shown to exhibit antitumor[381, 395] and potent antiviral activities (Scheme 5-1).[382-385] Structure-activity relationship (SAR) studies demonstrated that the antiviral activity was enhanced when the C5-position was equipped with an unsaturated, *E*-configured substituent bearing a hydrophobic electronegative functionality (such as an amide) in conjugation with the pyrimidine ring.[396, 397]

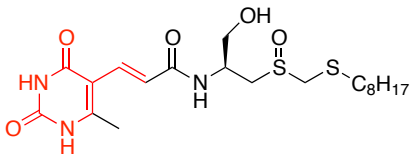

5.1

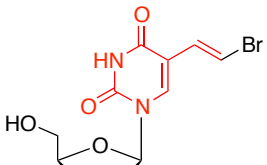

5.2

Antitumor	Leukemia L1210
ID_{50} (μg/mL)	0.05

Antiviral	HSV-1 (KOS)	VZV (YS)
MIC (μg/mL)	0.02	0.001

Scheme 5-1. Antitumor and antiviral activities of 5-alkenyluracils.

C5-alkenylation of uracils has in the past typically involved transition metal-catalyzed cross-coupling reactions between pre-activated uracils (*e.g.* 5-iodo[398, 399], 5-triflated[400] uracils) and metallated alkenes (*e.g.* stannane[387], boron[401]). These methods rely on multistep reaction sequences, lack atom economy, and are therefore of low efficiency. In addition, toxic stannane impurities could be problematic for biological studies. Direct alkenylation of uracils in a dehydrogenative way would address all the above problems and provide an efficient method to synthesize 5-alkenylated uracils.[90, 92, 137, 138, 335]

5.2 Research progress on C–H functionalization of uracils

Direct C–H functionalization chemistry has emerged as a powerful new tool to functionalize uracils. Hocek and co-workers first reported a protocol to regioselectively arylate uracils at the C5 position using aryl iodides (Scheme 5-2, top).[402, 403] Interestingly, they also found that the coupling reaction in the presence of CuI furnished predominant C6-aryl derivatives. However, the yields and selectivity of C5-aryluracils were not satisfactory, and aryl iodides bearing electron-withdrawing groups were not compatible under their conditions. Later, Kim and co-workers devised another arylation protocol based on aryl bromides (Scheme 5-2, bottom).[404] Although electron-deficient aryl bromides were tolerated in the new protocol, the yields and regioselectivity were moderate in most cases.

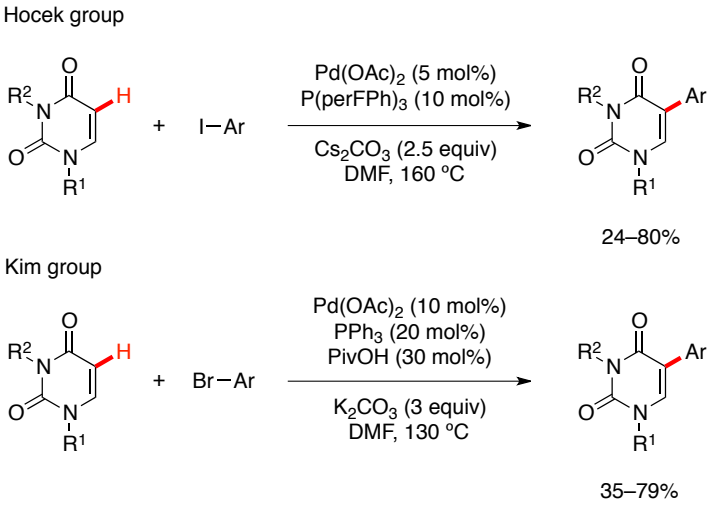

Scheme 5-2. Direct C–H arylation of uracils.

During their study of the uracil substrate, Kim and co-workers also reported a Pd-catalyzed C–H acetoxylation reaction (Scheme 5-3, top).[405] This protocol can be applied to a collection of uracils and uridines with moderate to good yields. The mechanism was thought to proceed through an electrophilic palladation pathway. The Pd^{II} intermediate was further oxidized by PIDA (phenyliodonium diacetate) to form a Pd^{IV} species with high reactivity towards reductive elimination to generate the desired product. In addition,

the same group later examined the synthesis of uracil dimers (Scheme 5-3, bottom).[406] They found three types of homo-coupling dimers (*i.e.,* C5–C5', C5–C6', and C6–C6' linked dimers), the yield distribution of which largely depended on the reaction temperatures and time. Good yields were obtained for a series of uracil derivatives, including uracil nucleosides.

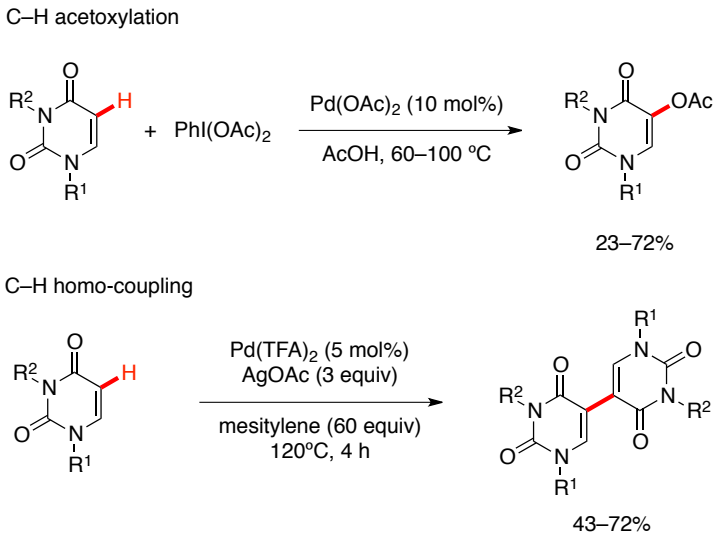

Scheme 5-3. C–H acetoxylation and homo-coupling of uracils.

Moreover, innate C–H trifluoromethylation was also achieved on uracils. MacMillan and co-workers developed a remarkable method via photoredox catalysis using $Ru(phen)_3Cl_2$ (Scheme 5-4, top).[407] This trifluoromethylation reaction undergoes a radical-mediated mechanism under very mild conditions and has broad utility for trifluoromethylating a variety of non-preactivated aromatic and heteroaromatic systems, including 1,3-dimethyluracil with excellent yields. Meanwhile, Baran and co-workers employed peroxides to initiate a similar radical process for direct trifluoromethylation of a broad scope of electron-rich and electron-deficient heterocycles (Scheme 5-4, bottom).[106] Their robust protocol is operationally simple, scalable, and proceeds at room temperature. Notably, uracil and 2'-deoxyuridine can also be trifluoromethylated without *N*- or *O*-protection.

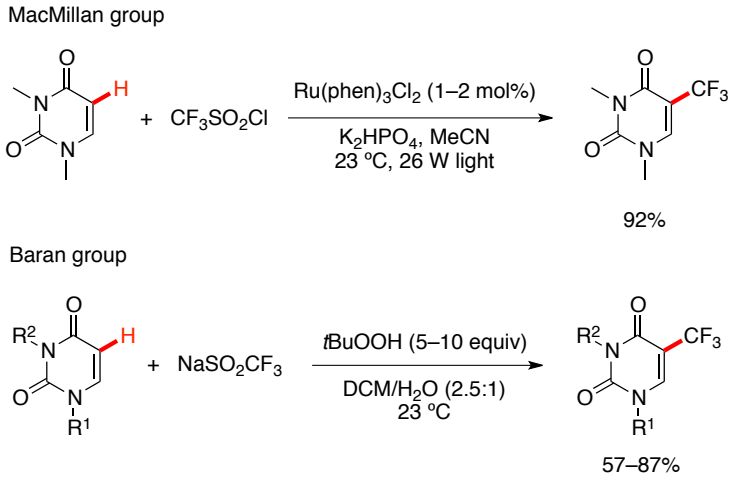

Scheme 5-4. C–H trifluoromethylation of uracils.

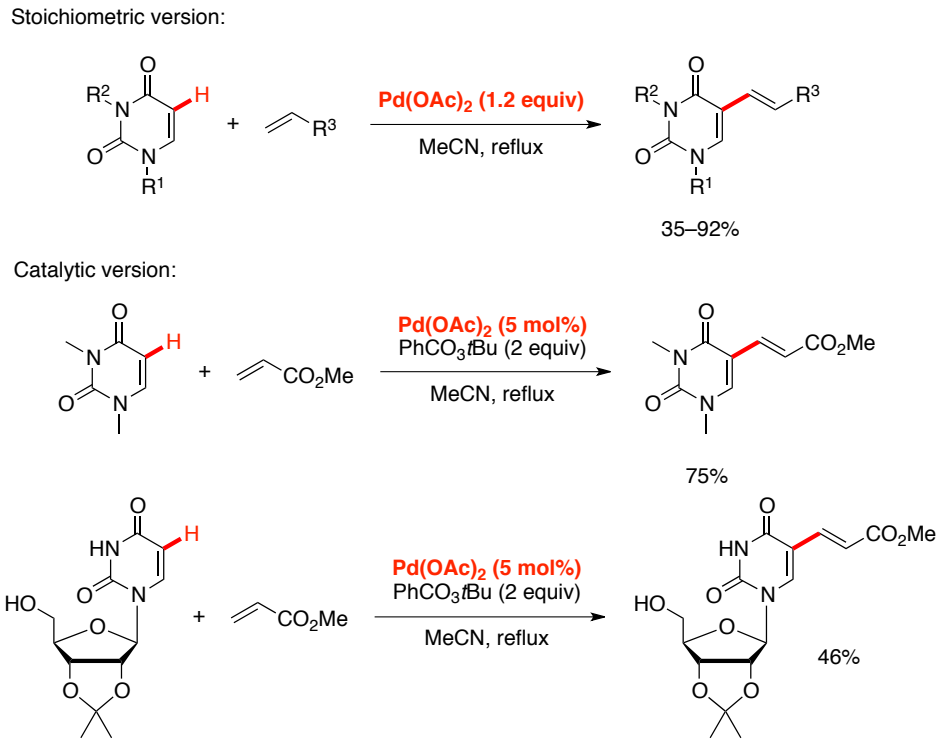

Scheme 5-5. Research advances for the C–H alkenylation of uracils.

In contrast, C–H alkenylation of uracils has been typically achieved using *stoichiometric* amounts of Pd (Scheme 5-5, top). So far only one report has appeared that describes two examples employing *catalytic* Pd loading, using *tert*-butyl perbenzoate as

the reoxidant (Scheme 5-5, bottom).[408] We therefore decided to investigate the substrate scope of the Pd-*catalyzed* direct C5-alkenylation in more detail. Herein, we disclose the development of an efficient dehydrogenative alkenylation of unactivated uracils with various alkenes via Pd-catalysis.

5.3 Condition optimization

We initiated our investigation with an extensive optimization of the alkenylation conditions (Table 5-1). Adapted from our alkenylation protocol for cyclic enaminones, 1,3-dimethyluracil (**5.3**) and *t*-butyl acrylate (**5.4**) were chosen as test substrates with $Pd(TFA)_2$ as the catalyst and DMF as the solvent.

5.3.1 Reoxidant screening

We first investigated the effect of reoxidants (Table 5-1). Alkenylation with $Cu(OAc)_2$, as used in the enaminone protocol,[341] only afforded a moderate yield (52%, entry 1). Additional Cu^{II} oxidants led to significantly reduced consumption of the starting uracil and yields (entries 2–4). Meanwhile, a few common organic oxidants were tested (entries 5–6). Duroquinone was chosen instead of *o*-quinone because *o*-quinone could react as an alkene coupling partner to compete with **5.4**. (This was confirmed later in the study of the scope of the reaction, see **5.15**.) Unfortunately, only 4% of the desired product was formed with duroquinone (entry 5). *t*-Butyl perbenzoate, used in the reported examples (Scheme 5-5),[408] also failed to improve the coupling efficiency (entry 6). We then turned to Ag oxidants. Initial trials with a series of Ag salts showed very poor yields (entries 7–12). The use of Ag_2CO_3 increased the TON to 2, but the yield was still low (entry 13). In comparison, AgOBz (entry 14) showed better oxidation capability and provided a similar yield (55%) to that of $Cu(OAc)_2$ (52%, entry 1). To our delight, AgOAc significantly improved the consumption of the starting uracil and increased the yield to 68% (entry 15).

Table 5-1. Reoxidant effect on the dehydrogenative alkenylation

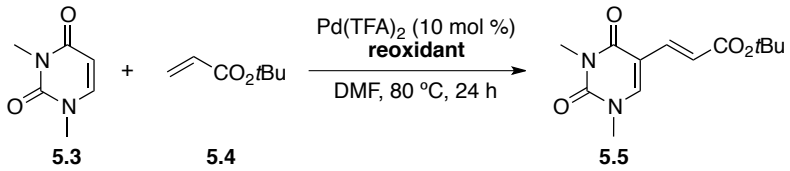

5.3 5.4 5.5

Entry[a]	Reoxidant (equiv)	% Consumption[b]	% Yield[c]
1	$Cu(OAc)_2$ (2.0)	74	52
2	$CuCl_2$ (2.0)	9	0
3	$Cu(OTf)_2$ (2.0)	8	6
4	$Cu(TFA)_2$ (2.0)	10	0
5	duroquinone (2.0)	15	4
6	$PhCO_3tBu$ (2.0)	60	45
7	AgF_2 (2.0)	0	0
8	AgCl (2.0)	7	0
9	$AgNO_3$ (2.0)	10	3
10	$AgSbF_6$ (2.0)	32	0
11	AgOTf (2.0)	27	0
12	Ag_2O (1.0)	26	11
13	Ag_2CO_3 (1.0)	37	20
14	AgOBz (2.0)	64	55
15	**AgOAc (2.0)**	**86**	**68**

[a] Reaction conditions: uracil **5.3** (0.2 M), acrylate **5.4** (2.0 equiv), $Pd(TFA)_2$ (10 mol%), oxidant, DMF (0.5 mL) under air at 80 °C, 24 h. [b] ^1H NMR % Consumption of the starting uracil with Ph_3SiMe (1.0 equiv) as the internal standard. [c] ^1H NMR % yield with Ph_3SiMe (1.0 equiv) as the internal standard.

5.3.2 Additive study

We next examined the effect of additives (Table 5-2). Addition of K_2CO_3 was detrimental to the reaction, where significant reduction of yield was observed (entry 2). With regard to acids, the strong acid TFA showed similar reaction inhibition as K_2CO_3 did (entry 3). The use of the weak acid AcOH virtually has no effect on the alkenylation

yield (70%, entry 4 *vs.* 68%, entry 1). When a weaker acid, pivalic acid (PivOH), was used, the consumption of the starting uracil was almost complete, which furnished the desired 5-alkenyluracil in a 77% yield (entry 5). Given the above results, we speculated that the OAc anion had little effect on the coupling process and AgOPiv formed *in situ* by anion exchange might be the real effective oxidant/additive. Therefore, the combination of Ag_2O and PivOH was assessed to generate AgOPiv *in situ* for direct alkenylation of uracils. Indeed, a comparable yield was recorded, albeit slightly lower (entry 6).

Table 5-2. Additive effect on the dehydrogenative alkenylation

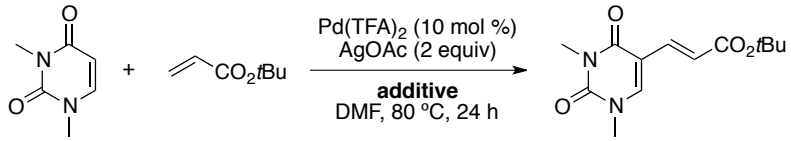

5.3 **5.4** **5.5**

Entry[a]	Reoxidant (equiv)	Additive (equiv)	% Consumption[b]	% Yield[c]
1	AgOAc (2.0)	–	86	68
2	AgOAc (2.0)	K_2CO_3 (2.0)	37	19
3	AgOAc (2.0)	TFA (2.0)	34	24
4	AgOAc (2.0)	AcOH (2.0)	86	70
5	**AgOAc (2.0)**	**PivOH (2.0)**	**96**	**77**
6	Ag_2O (1.0)	PivOH (2.0)	88	74

[a] Reaction conditions: uracil **5.3** (0.2 M), acrylate **5.4** (2.0 equiv), $Pd(TFA)_2$ (10 mol%), AgOAc (2.0 equiv), additive, DMF (0.5 mL) under air at 80 °C, 24 h. [b] ^1H NMR % Consumption of the starting uracil with Ph_3SiMe (1.0 equiv) as the internal standard. [c] ^1H NMR % yield with Ph_3SiMe (1.0 equiv) as the internal standard.

The effectiveness of this Pd/Ag/PivOH combination, employed in many recent C–H activation reactions,[130, 333, 409, 410] can be attributed to both lowered transition state energies and increased basicity of its conjugated base serving as a proton shuttle.[124-126] However, the concerted-metalation-deprotonation (CMD) mechanism[125] is less likely because the uracil C6-proton is more acidic than the C5-proton,[411] which would predict C6-alkenylation if this mechanism was at work, but does not correlate with the observed

exclusive C5-regioselectivity. Nonetheless, we cannot rule out the possibility of a Pd 1,2-migration.

5.3.3 Solvent effect

An array of solvents was also examined (Table 5-3). DMSO showed significant coupling inhibition (entry 1). Possibly, its strong coordinating ability decreased the electrophilicity of the Pd^{II} catalyst and impeded the electrophilic palladation process. Other polar solvents gave better but similar yields, while less polar solvents (*e.g.* dioxane) gave slightly lower yields (entries 2–7). Among all the solvents, the initially chosen DMF turned out to be optimal (entry 4).

Table 5-3. Solvent effect on the dehydrogenative alkenylation

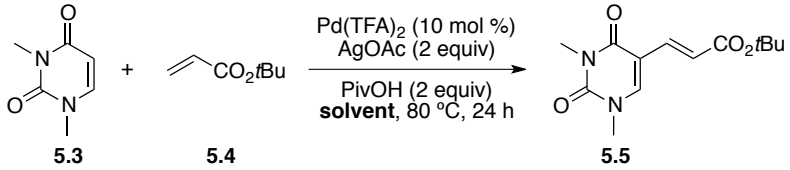

5.3 **5.4** **5.5**

Entry[a]	Solvent (0.5 mL)	% Consumption[b]	% Yield[c]
1	DMSO	38	24
2	MeCN	76	62
3	NMP	92	64
4	**DMF**	**96**	**77**
8	DMA	90	72
5	THF	94	66
6	dioxane	100	58
7	*t*BuOH	78	52

[a] Reaction conditions: uracil **5.3** (0.2 M), acrylate **5.4** (2.0 equiv), $Pd(TFA)_2$ (10 mol%), AgOAc (2.0 equiv), PivOH (3.0 equiv), solvent, under air at 80 °C, 24 h. [b] ^1H NMR % Consumption of the starting uracil with Ph_3SiMe (1.0 equiv) as the internal standard. [c] ^1H NMR % yield with Ph_3SiMe (1.0 equiv) as the internal standard.

5.3.4 Catalyst choice

Table 5-4. Catalyst efficiency on the dehydrogenative alkenylation[a]

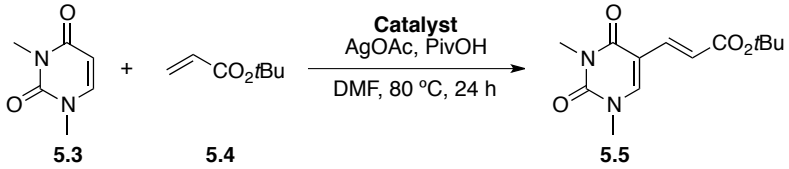

5.3 5.4 5.5

Entry	Catalyst (mol%)	AgOAc (equiv)	PivOH (equiv)	% Consumption[b]	% Yield[c]
1	$Pd(TFA)_2$ (10)	2.0	2.0	96	77
2	$Pd(OAc)_2$ (10)	1.1	2.0	76	58
3	$Pd(OAc)_2$ (10)	2.0	2.0	95	80
4	$Pd(OAc)_2$ (10)	2.5	2.0	100	85
5	$Pd(OAc)_2$ (10)	3.0	2.0	100	85
6	$Pd(OAc)_2$ (1)	2.5	2.0	73	66
7	$Pd(OAc)_2$ (1)	4.0	2.0	65	57
8	$Pd(OAc)_2$ (5)	1.5	2.0	79	67
9	$Pd(OAc)_2$ (5)	2.0	2.0	93	83
10	**$Pd(OAc)_2$ (5)**	**2.5**	**2.0**	**100**	**84**
11	$Pd(OAc)_2$ (5)	3.0	2.0	100	82
12	$Pd(OAc)_2$ (5)	2.5	0.5	94	79
13	$Pd(OAc)_2$ (5)	2.5	2.5	100	83
14	$Pd(OAc)_2$ (5)	2.5	3.0	100	83
15[d]	$[Cp^*RhCl_2]_2$ (5)	–	–	20	0

[a] Reaction conditions: uracil **5.3** (0.2 M), acrylate **5.4** (2.0 equiv), catalyst, AgOAc, PivOH, DMF (0.5 mL) under air at 80 °C, 24 h. [b] ^{1}H NMR % Consumption of the starting uracil with Ph_3SiMe (1.0 equiv) as the internal standard. [c] ^{1}H NMR % yield with Ph_3SiMe (1.0 equiv) as the internal standard. [d] With $AgSbF_6$ (20 mol%) and $Cu(OAc)_2$ (2.0 equiv) in THF.

The reason we chose $Pd(TFA)_2$ as the initial catalyst was because of the beneficial effect of KTFA in our C–H alkenylation protocol for cyclic enaminones (Table 4-3, entry 12). We assumed that the anionic ligand exchange between $Pd(OAc)_2$ and KTFA would form $Pd(TFA)_2$ *in situ*, producing a more electron-deficient thus more reactive Pd^{II} center

for electrophilic palladation. Our hypothesis was later supported by a tentative $Pd(TFA)_2$-catalyzed alkenylation of cyclic enaminone with a similar yield (83%) compared to 81% under the optimized $Pd(OAc)_2$/KTFA conditions.

As mentioned in Section 5.3.2, more basic anionic ligands were beneficial to the current alkenylation. We hence returned to $Pd(OAc)_2$ as the catalyst, which indeed showed better catalytic efficacy (Table 5-4). With the same loading (10 mol %), $Pd(OAc)_2$ afforded a slightly better yield (80%, entry 3) than $Pd(TFA)_2$ (77%, entry 1). Increasing the concentration of oxidant AgOAc helped to increase the yield to 85% (entries 2–5).

We then studied the effect of reduced Pd loadings. Alkenylation using only 1 mol % of $Pd(OAc)_2$ gave significantly poorer outcome (66%, entry 6), and adding more oxidant (up to 4.0 equiv) failed to improve the yield (57%, entry 7). However, we were pleased to find that 5 mol % of $Pd(OAc)_2$ exhibited equally excellent efficacy as that of 10 mol % of $Pd(OAc)_2$ (entry 9 *vs*. entry 3). Fine-tuning the oxidant and additive concentrations (entries 8–14) revealed that 2.5 equiv of AgOAc and 2.0 equiv of PivOH could push the reaction to completion and produce the desired product in excellent yield (84%, entry 10). Additionally, we also tested a Rh-catalyzed protocol, which unfortunately failed to yield product, presumably due to the absence of a directing group (entry 15).[412, 413]

5.3.5 Effect of reactant concentration

The influence of reactant concentrations was probed as well (Table 5-5). First, the concentration of acrylate **5.4** was modified (entries 1–3). 2.0 equiv of acrylate **5.4** was found to be optimal (entry 2). Then we tested the concentration of **5.3** at 0.1 M and 0.5 M. Virtually the same outcome was observed (entries 2, 4–5), which indicates the robustness of the alkenylation reaction to substrate concentrations within this range.

5.3.6 Temperature effect

In the interest of green chemistry, we next explored the possibility of lowering the reaction temperature preset at 80 ºC (Table 5-6). At 50 ºC, excellent yields up to 87%

were achieved by manipulating the mixture ratio of AgOAc and PivOH (entries 1–3). However, the consumption of the starting uracil was never complete. Hence, we raised the temperature to 60 ºC. The extra 10 ºC heat combined with the similar tuning on AgOAc and PivOH concentrations enabled 100% consumption of **5.3** and afforded better yields up to 91% (entries 4–8). In addition, we also tested temperatures from 70 ºC up to 100 ºC (entries 9–12). Although the starting uracil **5.3** was consumed, slightly lower yields (up to 88%) were obtained. Therefore, we determined that the optimal temperature was 60 ºC.

Table 5-5. Reaction scale of the dehydrogenative alkenylation

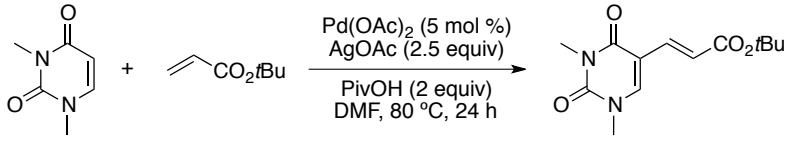

5.3 **5.4** **5.5**

Entry[a]	**5.3** (M)	**5.4** (equiv)	% Consumption[b]	% Yield[c]
1	0.2	1.1	100	78
2	**0.2**	**2.0**	**100**	**84**
3	0.2	3.0	97	81
4	0.1	2.0	100	84
5	0.5	2.0	100	82

[a] Reaction conditions: uracil **5.3** (0.1 mmol), acrylate **5.4**, $Pd(OAc)_2$ (5 mol%), AgOAc (2.5 equiv), PivOH (2.0 equiv), DMF (0.2–1.0 mL) under air at 80 °C, 24 h. [b] ^1H NMR % Consumption of the starting uracil with Ph_3SiMe (1.0 equiv) as the internal standard. [c] ^1H NMR % yield with Ph_3SiMe (1.0 equiv) as the internal standard.

5.3.7 Reaction time

Lastly, we monitored the reaction over a 24 h period. Figure 5-1 revealed that the reaction proceeded slowly in the course of the first 12 h. After that, only a minimum amount of catalytic activity was observed, which led to a merely 3% increase of the yield. Presumably, this could be attributed to the reduced concentration of **5.3** as well as the inactivation of the Pd^{II} catalyst by the aggregation of black Pd^0 over time before

reoxidation. Nevertheless, the desired 5-alkenyluracil **5.5** was shown to be stable under the current conditions over the course of 24 h.

Table 5-6. Temperature effect on the dehydrogenative alkenylation

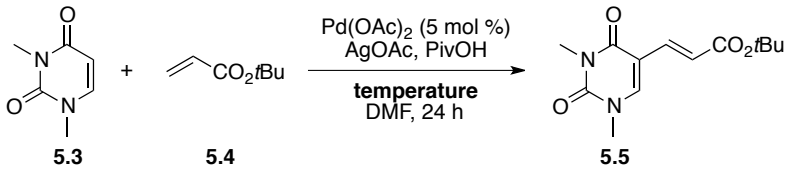

5.3 **5.4** **5.5**

Entry[a]	AgOAc (equiv)	PivOH (equiv)	Temp (ºC)	% Consumption[b]	% Yield[c]
1	2.5	2.0	50	86	80
2	2.5	2.0	50	86	78
3	3.0	3.0	50	92	87
4	2.5	2.0	60	100	86
5	3.0	2.0	60	100	91
6	2.5	2.5	60	100	87
7	2.5	3.0	60	100	91
8	**3.0**	**3.0**	**60**	**100**	**91**
9	2.5	2.0	70	100	88
10	3.0	3.0	70	100	87
11	2.5	2.0	80	100	84
12	2.5	2.0	100	100	74

[a] Reaction conditions: uracil **5.3** (0.2 M), acrylate **5.4** (2.0 equiv), $Pd(OAc)_2$ (5 mol%), AgOAc, PivOH, DMF (0.5 mL) under air, 24 h. [b] ^1H NMR % Consumption of the starting uracil with Ph_3SiMe (1.0 equiv) as the internal standard. [c] ^1H NMR % yield with Ph_3SiMe (1.0 equiv) as the internal standard.

It is worth noting that all the above reactions proceeded in a capped vial under ambient air. In comparison, direct alkenylation under N_2 afforded a marginally lower yield (87%), indicating that O_2 might serve as a minor oxidant.

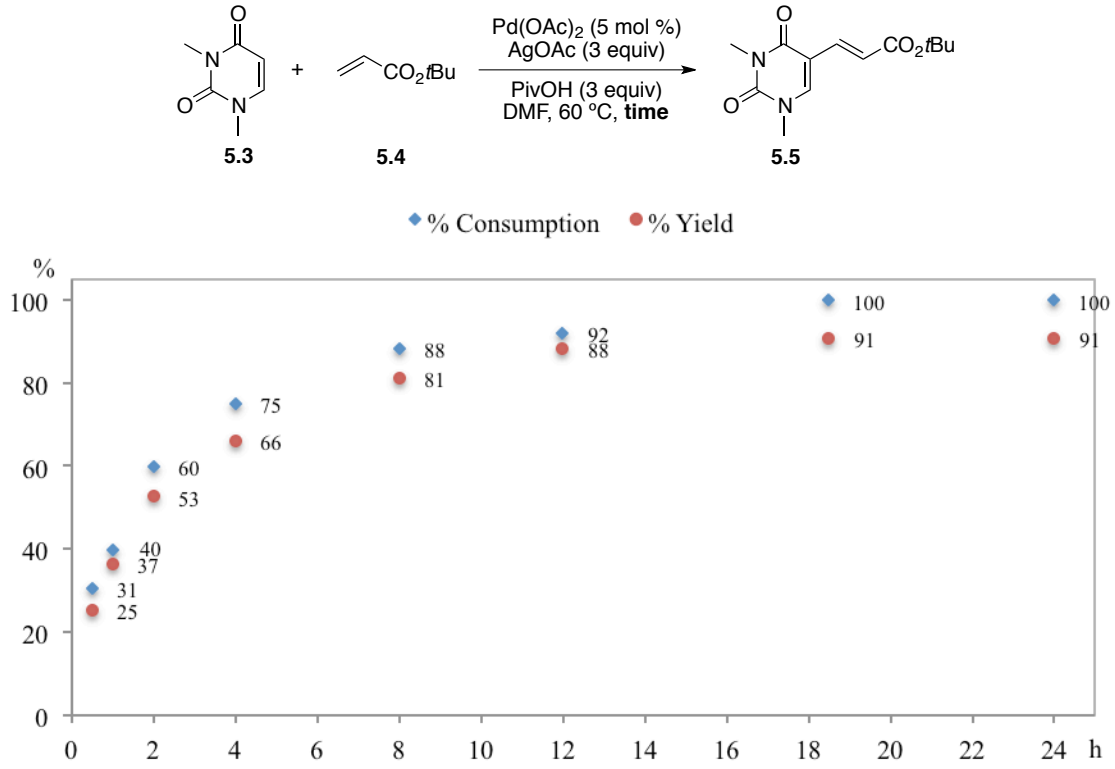

[a] Reaction conditions: uracil **5.3** (0.2 M), acrylate **5.4** (2.0 equiv), $Pd(OAc)_2$ (5 mol%), AgOAc (3.0 equiv), PivOH (3.0 equiv), DMF (0.5 mL), under air at 60 °C, 0–24 h. ^{1}H NMR % Consumption of the starting uracil with Ph_3SiMe (1.0 equiv) as the internal standard. ^{1}H NMR % yield with Ph_3SiMe (1.0 equiv) as the internal standard. 92% isolated yield.

Figure 5-1. Effect of reaction time on the dehydrogenative alkenylation.[a]

5.4 Investigation of the scope

5.4.1 Alkene scope

Utilizing these optimized catalytic conditions, a broad range of alkenes was found to undergo dehydrogenative coupling with uracil **5.3** in good to excellent yields (Table 5-7). The newly formed 5-alkenyluracils were obtained with absolute regio- and stereoselectivity (*E*-isomers), and a variety of functionalities were tolerated. Acrylate esters and styrene furnished excellent yields (**5.5**–**5.9**). Remarkably, quantitative consumption was observed when acrylamide was employed (**5.10**). Acrolein, dimethyl vinylphosphonate, and methylvinylketone were also good alkenylating partners albeit

showing slightly lowered yields (**5.11**–**5.13**). Notably, acrolein and acrolein diethyl acetal furnished the same aldehyde **5.11**/**5.11'** with comparable yields, presumably due to *in situ* hydrolysis by PivOH of the acetal functional group. As for disubstituted alkenes, overall moderate yields were observed, possibly due to the steric repulsion exerted by the substituents (**5.14**–**5.15** and **5.17**–**5.18**). As expected, when more than one β-hydrogen was present, final products **5.16**–**5.18** showed double bond tautomerization with a preference for *unconjugated* (to uracil) 5-allyluracils **5.17b** and **5.18b**.[341, 377-379] However, allyl acetate predominantly afforded the *conjugated* 5-alkenyluracil **5.16a**. As documented previously,[331, 414, 415] the coordination between O (from the acetyl) and Pd locks the conformation and subsequently favors H_a for *syn*-elimination (Scheme 5-6). In addition, double C–H activation was observed in by-product **5.18c** to our surprise (Scheme 5-7). We speculate that **5.18b** served as an alkene for subsequent coupling with uracil **5.3** to furnish **5.18c**, albeit in a low yield.

5.4.2 Uracil scope

We next probed the scope of uracils[416-423] under the optimized conditions (Table 5-8). In addition to *N*-methyl groups (**5.5**), uracil can be protected with other electron-donating groups, such as benzyl (**5.19**), methoxymethyl (MOM) (**5.20**), and *p*-methoxybenzyl (PMB) (**5.22**), and provide reaction products in good to excellent yields. The new protocol was also effectively applied to 1-benzyl-3-(3',5'-dimethylbenzyl)uracil (to furnish **5.21**), which has exhibited potent antiviral activity against the human immunodeficiency virus (HIV-1) and the human cytomegalovirus (HCMV).[424, 425] On the other hand, electronically-attenuated uracils (with electron-withdrawing groups or without protecting groups) were unreactive in the alkenylation process (**5.25**–**5.27**). Although poor solubility may play a role, we presume that decreased nucleophilicity of the uracils is the reason for the observed lack of reactivity. In further investigations we found that protected uridine and 2'-deoxyuridine were also good substrates (**5.23** and **5.24**), demonstrating the practicality of our reaction protocol to uracil-based nucleosides.

Table 5-7. Scope of alkenes for dehydrogenative alkenylation[a]

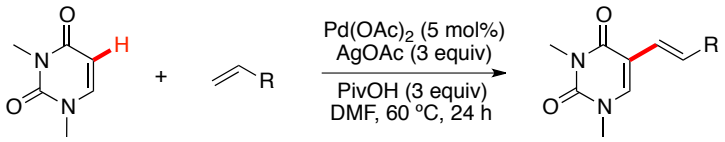

5.3

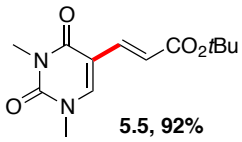
5.5, 92%

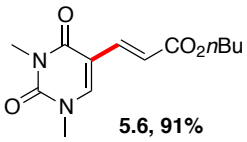
5.6, 91%

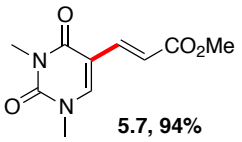
5.7, 94%

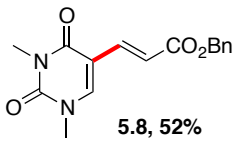
5.8, 52%

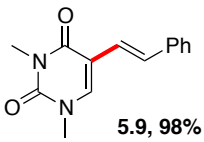
5.9, 98%

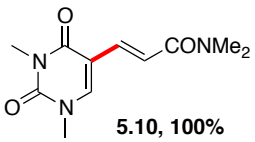
5.10, 100%

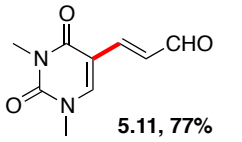
5.11, 77%
5.11', 79%[b]

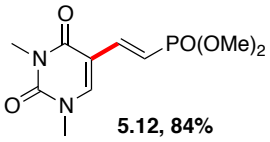
5.12, 84%

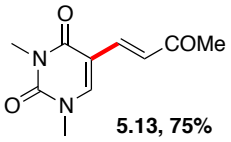
5.13, 75%

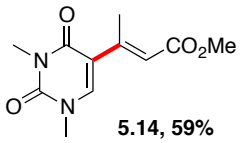
5.14, 59%

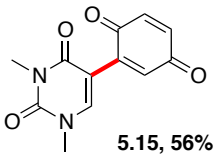
5.15, 56%

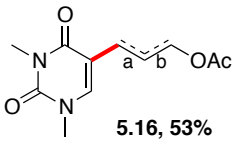
5.16, 53%
(a:b = 8.7:1)[c]

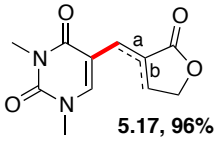
5.17, 96%
(a:b = 1:4.3)[c]

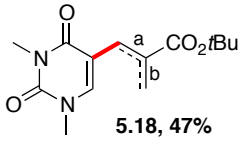
5.18, 47%
(a:b = 1:2.5)[c]

[a] Conditions: uracil **5.3** (0.2 M), alkene (2.0 equiv), $Pd(OAc)_2$ (5 mol%), AgOAc (3.0 equiv), PivOH (3.0 equiv), DMF (0.5 mL) under air at 60 °C, 24 h. Isolated yields. [b] Acrolein diethyl acetal (2.0 equiv) was used as the alkene. [c] Ratio determined by ^1H NMR.

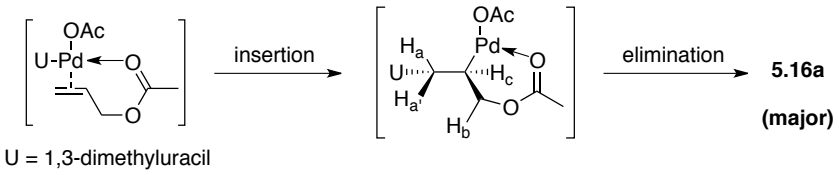

Scheme 5-6. Dehydrogenative alkenylation with allyl acetate.

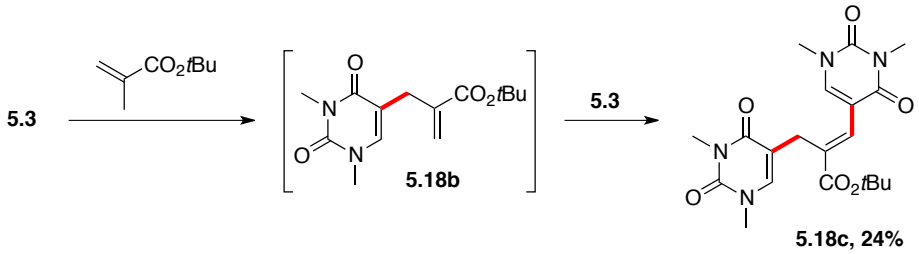

Scheme 5-7. Double C–H activation of uracil **5.3**.

Table 5-8. Scope of uracils for dehydrogenative alkenylation[a]

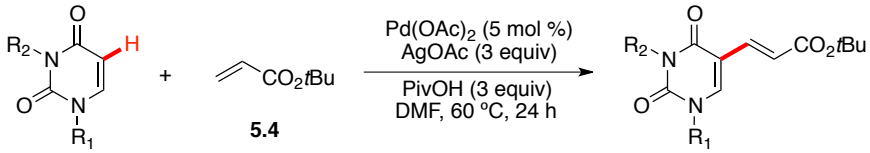

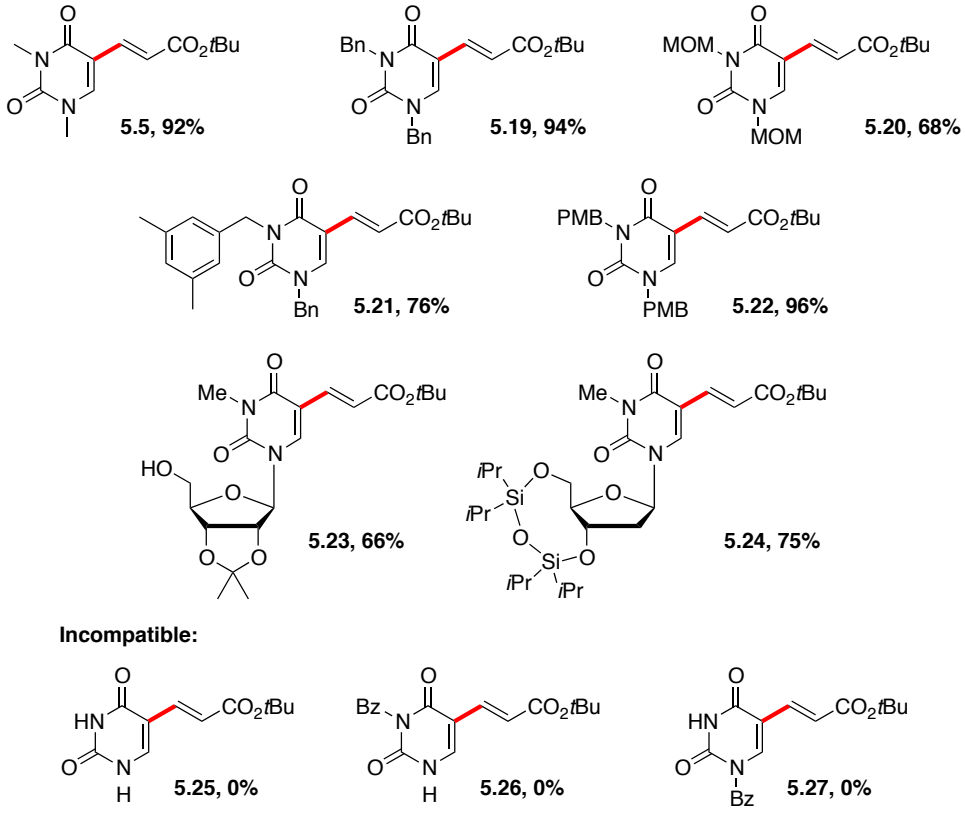

[a] Conditions: uracil (0.2 M), acrylate **5.4** (2.0 equiv), $Pd(OAc)_2$ (5 mol %), AgOAc (3.0 equiv), PivOH (3.0 equiv), DMF (0.5 mL) under air at 60 °C, 24 h. Isolated yields.

5.5 Proposed mechanism

In light of both the exclusive C5-regioselectivity and the lack of reactivity from electron-poor uracils, an electrophilic palladation pathway[138] was envisaged (Figure 5-2). Similar to our previously investigated enaminone system,[341] uracil's nucleophilic C5-position is most likely first attacked by the Pd(II) species, although prior coordination of Pd(II) to the carbonyl group or the double bond is a possibility as well.[426, 427] Deprotonation by the more basic pivalate ligand then forms a palladated uracil **II**, which then undergoes migratory alkene insertion. Subsequent *β*-H elimination delivers the desired 5-alkenyluracil **IV**. Reductive elimination and reoxidation by Ag^{I} regenerates Pd^{II} to resume the catalytic cycle.

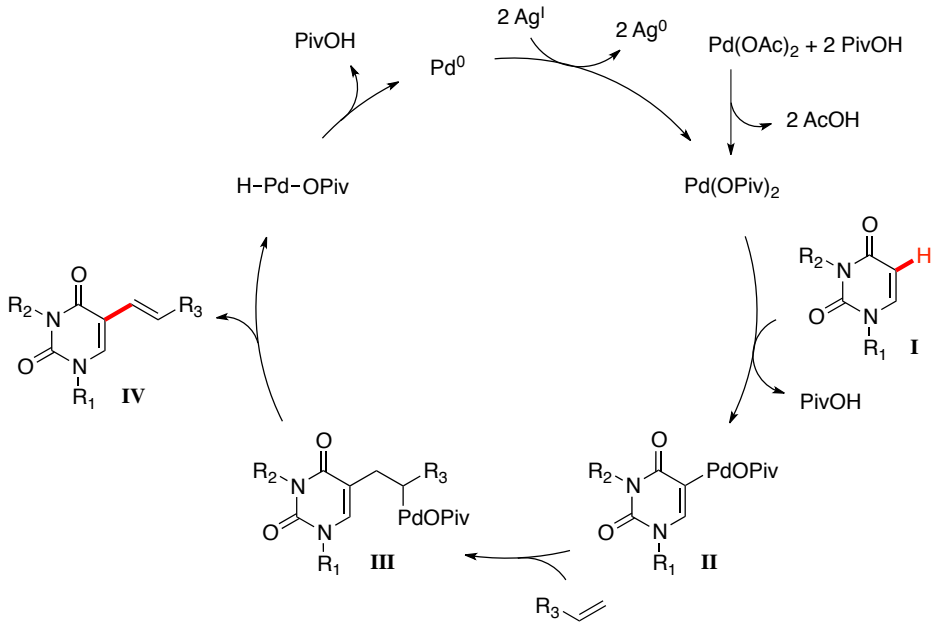

Figure 5-2. Proposed mechanism for the dehydrogenative alkenylation of uracils.

5.6 Summary

We have developed an efficient and highly atom-economical protocol for cross-dehydrogenative coupling of uracils and alkenes. The generality of this transformation

provides a promisingly direct route to synthesize 5-alkenyluracils, which are of importance in medicinal chemistry.

Chapter 6 Biomimetic Aerobic C–H Alkenylation of Cyclic Enaminones at Room Temperature: Development toward the Synthesis of 1,3,5-Trisubstituted Arenes

6.1 Introduction

An important task in modern organic chemistry is the development of green, mild, and efficient methods for broad synthetic applications. In the interests of sustainable chemistry, new methods that generate a minimal amount of waste are highly sought-after.[308, 309] In the field of transition metal-catalyzed C–C construction, dehydrogenative reactions are arguably the flagship of all cross-coupling reactions, because they activate two C–H bonds with no prefunctionalization, thus significantly reducing byproducts and wastes by releasing, in theory, a stoichiometric amount of hydrogen gas.[92, 133, 137-139]

Since dehydrogenative reactions entail two C–H nucleophiles, an oxidant is required to achieve catalytic turnover (see discussion in Chapter 2.4). We recently developed an efficient Pd-catalyzed dehydrogenative alkenylation of cyclic enaminones,[341] the distinctive reactivity profile of which has been exploited extensively for heterocycle synthesis (Chapter 4).[59, 61, 65, 345-349] Despite the high-yielding feature and broad scope, our protocol requires stoichiometric amounts of a Cu^{II} oxidant and an additive at an elevated temperature (80 ºC). Unfortunately, this demand for stoichiometric amounts of sacrificial heavy metal oxidants is very common in current research and is ironically contradictory to the goal of C–H functionalization (*e.g.* reducing heavy metal waste).[133, 137-139] In search of alternative green oxidants, molecular oxygen is regarded as the ideal candidate because of its inexpensive and eco-friendly nature.[308, 309]

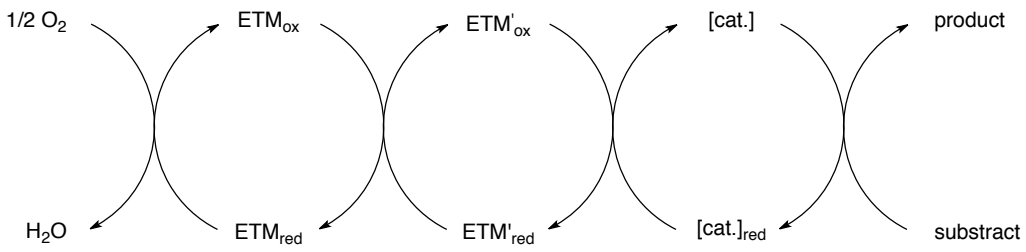

Scheme 6-1. Biomimetic O_2 activation with ETMs.

The obstacle of applying O_2 as the sole oxidant is the high activation energy and low concentration of O_2 in solutions which significantly impedes the direct oxidation of Pd^0. Hence, in early development, the pressure of O_2 was often applied much higher than 1 atm.[138, 308] To circumvent high pressure, new protocols have been devised with catalytic amounts of oxygen activators (*i.e.* electron transfer mediators, ETM), such as molybdovanadophosphoric acid (HPMoV) and benzoquinone, to facilitate oxidation in a biomimetic approach.[138, 309, 428] Mechanistically, this biomimetic strategy divides the oxidation process into several interconnected redox cycles and therefore effectively reduces the initial high-energy barrier for electron transfer (Scheme 6-1).[428] For example, Hosokawa and co-workers discovered that the use of catalytic amounts of inexpensive catechol and Cu^{II} under O_2 could remarkably enhance Pd^{II} catalysis (Scheme 6-2).[313, 429] Because catechol was readily oxidized to *o*-quinone under O_2 in the presence of the $Pd(OAc)_2$–$Cu(OAc)_2$ catalyst, the authors proposed that the *o*-quinone could serve as a Cu^{II} ligand.

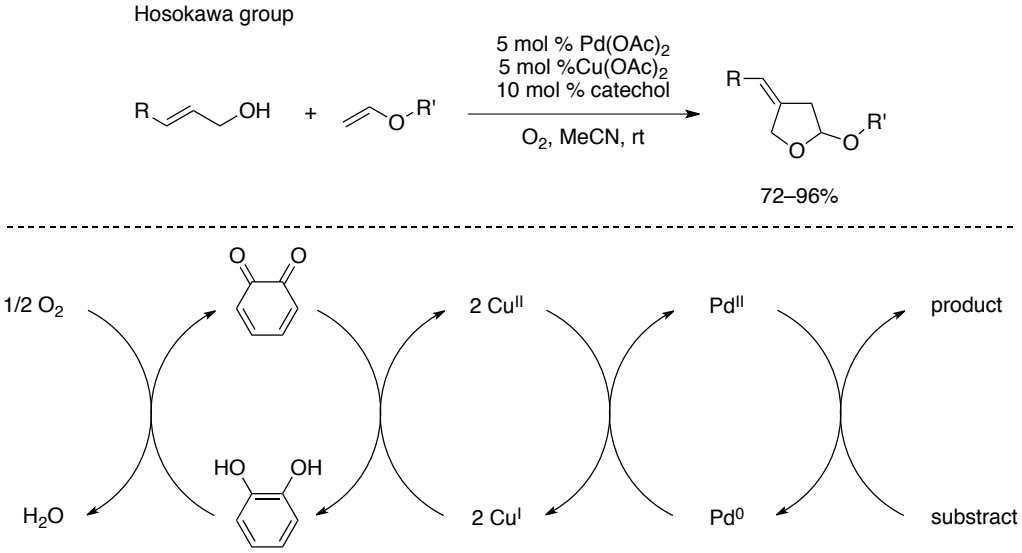

Scheme 6-2. Biomimetic O_2 activation by catechol and Cu^{II} salt.

The synthesis of 1,3-dienes and polyenes through dehydrogenative cross-coupling between alkenes surprisingly did not attract much attention until very recently, despite

their importance in organic and medicinal chemistry, and material science.[136] The use of O_2 as the terminal oxidant in this type of coupling is very rare, and to the best of our knowledge there has been no report yet about a dehydrogenative cross-coupling of alkenes proceeding at room temperature.[328, 329, 332, 334, 430] Bäckvall and co-workers reported a versatile biomimetic aerobic reaction between two alkenyl C–H donors under low catalyst loading.[430] Unfortunately, their protocol involving acidic media, failed to deliver a satisfactory outcome with cyclic enaminone substrates,[430] which as piperidine surrogates are valuable synthetic intermediates.[59, 61, 65, 345-349] In light of the recent advances in this field, we aimed at developing a greener and milder method for the dehydrogenative alkenylation of cyclic enaminones at room temperature. We envisioned the alkenylated enaminones (*i.e.* 1,3-dienes) undergoing a Diels-Alder reaction to gain rapid access to hydroquinolines, a key structural motif in several major classes of alkaloids.[431-436] Serendipitously, we instead found a Diels-Alder tandem reaction to furnish a series of 1,3,5-trisubstituted arenes, including chalcones, which are a major class of flavonoids and exhibit a wide range of pharmacological activities, including antiproliferative, antioxidant, anti-inflammatory and anticancer effects.[437-439] Herein, we disclose the development of a biomimetic aerobic C–H alkenylation of cyclic enaminones at *room temperature* using O_2 as the terminal oxidant and its unexpected application for the synthesis of 1,3,5-trisubstituted arenes.

6.2 Alkenylation optimization

6.2.1 Initial trials

We started probing the aerobic conditions under atmospheric pressure (Table 6-1). The initial reaction conditions were adapted from our first protocol: enaminone **6.1** and alkene **6.2** (2 equiv) were mixed with $Pd(OAc)_2$ (10 mol %) and KTFA (1 equiv) in DMF under air for 24 h. Without Cu^{II} oxidants, the starting material consumption and product yield dropped significantly under air (entry 1). Changing the reaction atmosphere to pure O_2 improved the yield to 44% (entry 2). Addition of 20 mol % of $Cu(OAc)_2$ to the

reaction did not improve the yield (entry 3). Amino acids as ligands were also examined, but did not improve the outcome of the reactions (entries 4–5).

Table 6-1. Initial attempts of aerobic oxidative alkenylation of cyclic enaminones

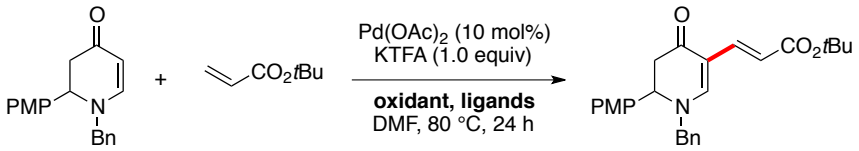

6.1 **6.2** **6.3**

Entry[a]	Cu^{II} (0.2)	Oxidant[b]	Ligand (0.2)	% Consumption[c]	% Yield[d]
1	–	air	–	50	27
2	–	O_2	–	71	44
3	$Cu(OAc)_2$	O_2	–	91	41
4	–	O_2	Boc-β-Ala-OH	85	49
5	–	O_2	Boc-Phe-OH	76	45

[a] Other conditions: **6.1** (0.2 M), **6.2** (2 equiv), $Pd(OAc)_2$ (10 mol %), KTFA (1 equiv) in DMF (0.5 mL) at 80 ºC through 24 h. [b] The pressure was 1 atm. [c] NMR % conversion of the starting enaminone with Ph_3SiMe (1.0 equiv) as the internal standard. [d] NMR % yield with Ph_3SiMe (1.0 equiv) as the internal standard.

6.2.2 Introduction of catechol

In order to activate O_2, catalytic amounts of catechol were added to the reaction mixture (Table 6-2). Initially, a 1:1:2 ratio of the $Pd(OAc)_2$/$Cu(OAc)_2$/catechol mixture was tested at 80 ºC, which failed to increase the yield (40% from entry 1 *vs.* 44% from Table 4.8, entry 2). We also ran the same reaction at room temperature but recorded an even lower yield (36%, entry 2). Thus, we modified the catalyst formula and used a 1:2:4 ratio, but only observed a slight increase of yield to 47% (entry 3). A significant increase of yield to 78% was attained after the loading of $Pd(OAc)_2$ was doubled to 10 mol % (entry 4). We saw a similar trend when the reactions were performed under air, albeit with lower yields respectively (entries 5–6). Additional tuning of the ratio of $Pd(OAc)_2$/$Cu(OAc)_2$/catechol did not afford higher yields (entries 7–8), which suggests that the optimal ratio is 1:1:2.

Table 6-2. Aerobic oxidative alkenylation of cyclic enaminones with catechol

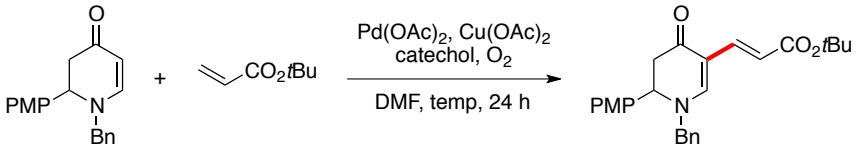

6.1 **6.2** **6.3**

Entry[a]	$Pd(OAc)_2$ (mol %)	$Cu(OAc)_2$ (mol %)	Catechol (mol %)	Oxidant (1 atm)	Temp (ºC)	% Consumption[b]	% Yield[c]
1	5	5	10	O_2	80	69	40
2	5	5	10	O_2	rt	49	36
3	5	10	20	O_2	rt	47	47
4	10	10	20	O_2	rt	**85**	**78**
5	5	10	20	air	rt	49	44
6	10	10	20	air	rt	79	72
7	10	10	10	O_2	rt	78	72
8	10	20	40	O_2	rt	77	69

[a] Other conditions: **6.1** (0.2 M), **6.2** (4 equiv) in DMF (0.5 mL) through 24 h. [b] NMR % conversion of the starting enaminone with Ph_3SiMe (1.0 equiv) as the internal standard. [c] NMR % yield with Ph_3SiMe (1.0 equiv) as the internal standard.

6.2.3 Solvent screen

Then we screened a series of common solvents. Except for the initially chosen DMF, all the other solvents failed to improve the alkenylation outcome (Table 6-3). The relatively high yields from DMF, MeCN and DMSO (entries 1–3) indicate that the coordinating ability of the solvents may help extend the catalyst lifespan, as reflected by the higher coupling yields.

6.2.4 Alkene concentration

The concentration of alkenes also proved to be critical. *tert*-Butyl acrylate was investigated on a scale from 1 equiv to 8 equiv (Table 6-4). The most effective

concentration was recorded at 4 equiv (entry 4). Attempts to push the reaction to completion by adding more alkenes, did not improve yields. (entries 5–7).

Table 6-3. Solvent effect on the aerobic oxidative alkenylation of cyclic enaminones

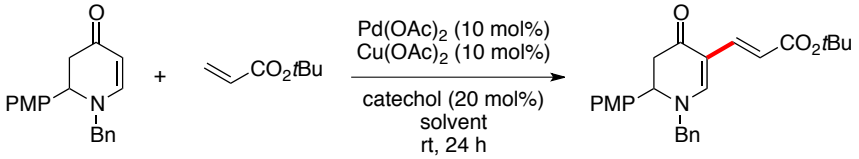

6.1 **6.2** **6.3**

Entry[a]	Solvent	% Consumption[b]	% Yield[c]
1	DMF	**85**	**78**
2	MeCN	73	65
3	DMSO	70	62
4	NMP	51	43
5	THF	42	39
6	toluene	65	57

[a] Other conditions: **6.1** (0.2 M), **6.2** (4 equiv), $Pd(OAc)_2$ (10 mol %), $Cu(OAc)_2$ (10 mol %), catechol (20 mol %) in DMF (0.5 mL) at rt under O_2 (1 atm) through 24 h. [b] NMR % conversion of the starting enaminone with Ph_3SiMe (1.0 equiv) as the internal standard. [c] NMR % yield with Ph_3SiMe (1.0 equiv) as the internal standard.

6.2.5 Catalyst combination

As Hosokawa had reported the importance of anionic ligands to catalyst efficacy,[429] we next examined the effect of a few anionic ligands (*i.e.* TFA^-, OAc^-, and Cl^-, Table 6-5). In single anion systems (entry 1–3), OAc^- afforded a better yield (78%) than TFA^- (63%) or Cl^- (55%). Gratifyingly, the use of $Pd(TFA)_2$ and $Cu(OAc)_2$ improved the yield to 81% (entry 4). When the anionic ligands were switched, the use of $Pd(OAc)_2$ and $Cu(TFA)_2$ gave the same yield (81%, entry 5). This yield similarity was also observed in the combination of OAc^-/Cl^- and TFA^-/Cl^- systems (entry 6–9), albeit furnishing lower yields respectively. This similarity suggests that the anionic ligands shall be exchangeable between Pd^{II} and Cu^{II} in the solution.

Table 6-4. Alkene concentration on the aerobic oxidative alkenylation of cyclic enaminones

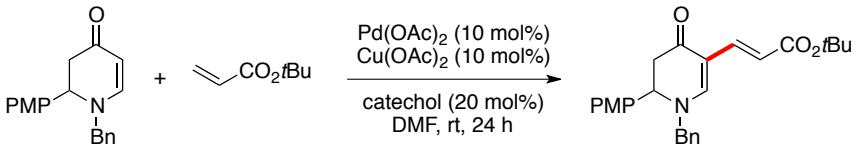

6.1 **6.2** **6.3**

Entry[a]	**6.2** (equiv)	% Consumption[b]	% Yield[c]
1	1.0	59	57
2	2.0	72	69
3	3.0	69	62
4	4.0	**85**	**78**
5	5.0	77	74
6	6.0	82	74
7	8.0	77	77

[a] Other conditions: **6.1** (0.2 M), $Pd(OAc)_2$ (10 mol %), $Cu(OAc)_2$ (10 mol %), catechol (20 mol %) in DMF (0.5 mL) at rt under O_2 (1 atm) through 24 h. [b] NMR % conversion of the starting enaminone with Ph_3SiMe (1.0 equiv) as the internal standard. [c] NMR % yield with Ph_3SiMe (1.0 equiv) as the internal standard.

6.2.6 Additional optimization

We also investigated the role of bases, reactant ratios, and additives (Table 6-6). First, a few common bases were added to the reaction mixture (entry 1–5). It soon became clear that bases inhibited the dehydrogenative coupling by reducing the yield to 16%. Since bases will neutralize the stoichiometric amounts of AcOH/TFA formed as byproducts, it echoed our earlier findings that acids enhanced the coupling efficiency of cyclic enaminones presumably by assisting anionic ligand dissociation.[79] Next, we adjusted the reaction concentration from 0.03 M to 0.4 M and found that more concentrated solutions were favorable in general (entries 6–9), which is not uncommon for intermolecular coupling reactions. Moreover, Stahl and co-workers had reported that the addition of molecular sieves was beneficial for Pd-catalyzed aerobic alcohol oxidation.[440] They found molecular sieves could provide a heterogeneous surface that hindered bulk

aggregation of Pd^0 metal to increase the catalyst stability. Indeed, the presence of 4Å MS in the current aerobic protocol promoted a full consumption of **6.1**, as well as an optimal isolated yield at 89% (entry 10).

Table 6-5. Catalyst screen for the aerobic oxidative alkenylation of cyclic enaminones

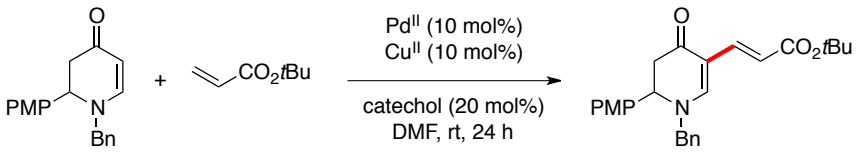

6.1 **6.2** **6.3**

Entry[a]	Pd^{II} (10 mol %)	Cu^{II} (10 mol %)	% Consumption[b]	% Yield[c]
1	$Pd(OAc)_2$	$Cu(OAc)_2$	85	78
2	$Pd(TFA)_2$	$Cu(TFA)_2$	73	63
3	$PdCl_2$	$CuCl_2$	53	55
4	$Pd(TFA)_2$	$Cu(OAc)_2$	**90**	**81**
5	$Pd(OAc)_2$	$Cu(TFA)_2$	86	81
6	$PdCl_2$	$Cu(OAc)_2$	61	57
7	$Pd(OAc)_2$	$CuCl_2$	48	37
8	$PdCl_2$	$Cu(TFA)_2$	43	33
9	$Pd(TFA)_2$	$CuCl_2$	38	27

[a] Other conditions: **6.1** (0.2 M), **6.2** (4 equiv), catechol (20 mol %) in DMF (0.5 mL) at rt under O_2 (1 atm) through 24 h. [b] NMR % conversion of the starting enaminone with Ph_3SiMe (1.0 equiv) as the internal standard. [c] NMR % yield with Ph_3SiMe (1.0 equiv) as the internal standard.

6.3 Investigation of the scope of the dehydrogenative alkenylation

With the optimal conditions in hand, we embarked on a study of the scope of the reaction (Table 6-7). Acrylates were excellent alkene sources with yields up to 89% (**6.3**–**6.6**). Vinyl phosphonate, vinyl ketone, acrylamide, and styrene were all well tolerated (**6.7**–**6.10**). Disubstituted alkenes afforded significantly lower yields (**6.11**–**6.13**), possibly because the sterics exerted by the substituents hindered the migratory insertion. Interestingly, double bond isomerization was not observed when more than one β-hydride

was present in the alkenes. Only conjugated (to enaminone) diene isomers (**6.12** and **6.13**) were isolated. This is in contrast to our first alkenylation protocol, where unconjugated (to enaminone) diene isomers were favored at an elevated temperature (80 ºC). We postulate that β-hydride elimination is a kinetically controlled process to furnish the conjugated diene isomers, whereas the unconjugated diene isomers are thermodynamically more favorable.

Table 6-6. Further study on the aerobic oxidative alkenylation of cyclic enaminones

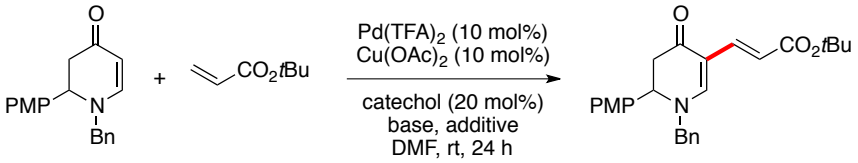

6.1 **6.2** **6.3**

Entry[a]	**6.1** (M)	Base (0.2 equiv)	Additive	% Consumption[b]	% Yield[c]
1	0.2	–	–	90	81
2	0.2	pyridine	–	20	16
3	0.2	Et_3N	–	52	51
4	0.2	Na_2CO_3	–	72	69
5	0.2	$NaHCO_3$	–	77	73
6	0.4	–	–	100	86
7	0.1	–	–	58	43
8	0.05	–	–	77	68
9	0.03	–	–	61	52
10	0.2	–	4Å MS	**100**	**91** (**89**[d])

[a] Other conditions: **6.2** (4 equiv), $Pd(TFA)_2$ (10 mol %), $Cu(OAc)_2$ (10 mol %), catechol (20 mol %) in DMF (0.5 mL) at rt under O_2 (1 atm) through 24 h. [b] NMR % conversion of the starting enaminone with Ph_3SiMe (1.0 equiv) as the internal standard. [c] NMR % yield with Ph_3SiMe (1.0 equiv) as the internal standard. [d] Isolated yield.

A collection of enaminones was assessed under the optimized conditions as well (Table 6-7). Bicyclic, electron-rich enaminones offered moderate yields (**6.14**–**6.15**). Remarkably, our new conditions do not compromise the preexisting stereocenters of **6.15**.

Replacing the 2-aryl group (*i.e.* PMP) with an alkyl group (*i.e. i*Pr) retained a good yield (83%, **6.16**). Surprisingly, the removal of the 2-PMP group caused a significant decline in yield (to 57%, **6.17**). The reason behind this observation is yet to be elucidated. As we reported earlier, *N*-phenylenaminone is a less effective substrate possibly due to its attenuated nucleophilicity. Indeed, it afforded a lower yield (32%, **6.18**) compared to the *N*-benzyl analogue (57%, **6.19**). It is worth mentioning that the *E*-enaminone, *N*-H enaminone, and *N*-Cbz enaminone were all incompatible under the current aerobic conditions (**6.19**–**6.21**), albeit consistent with our previous studies. Our attempts on the uracil scaffold (**6.22**) were unfortunately not successful either.

6.4 Unexpected formation of chalcones

6.4.1 Initial trials

In our continuous efforts to synthesize enaminone-based pilot scale libraries, we hypothesized that the Diels-Alder reaction could be an effective approach to quickly transform the alkenylated products of cyclic enaminones to hydroquinoline analogues, a common structural feature in many alkaloids.[431-436] In fact, amino-substituted dienes have been employed as substrates to construct the octahydroquinoline scaffold (Scheme 6-3). Comins and co-workers reported that cyclic enaminone **6.23** underwent the Diels-Alder transformation with a variety of dienophiles to afford novel octahydroquinolines **6.25** as single diastereomers.[441, 442]

Because our dehydrogenative alkenylation method installed electron-deficient alkenes onto cyclic enaminones, two of the three substituents on enaminone dienes (*e.g.* **6.3**) are electron-withdrawing. It is uncertain whether the proposed Diels-Alder reaction would be normal-electron-demand (NED) or inverse-electron-demand (IED). Accordingly, we treated the alkenylated enaminone **6.3** with both electron-rich and electron-deficient dienophiles (**6.26** and **6.27**, Scheme 6-4). To our disappointment, no desired product was observed in either scenario. Most of enaminone **6.3** was consumed when subjected to an electron-deficient dienophile, while it did not react in the presence of an electron-rich dienophile. These intriguing results led us to first investigate the electronic nature of

enaminone dienes affected by the unique substitution pattern.

Table 6-7. Scope of aerobic dehydrogenative alkenylation of cyclic enaminones[a]

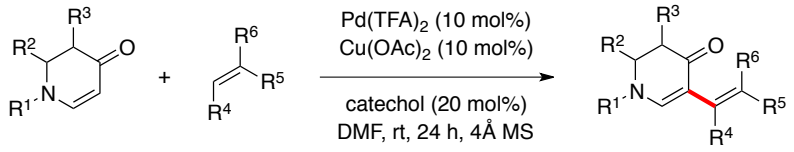

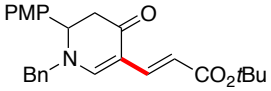

6.3, 89%

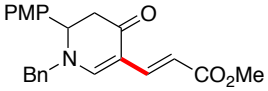

6.4, 78%

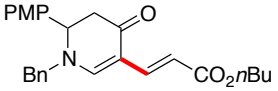

6.5, 85%

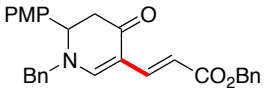

6.6, 87%

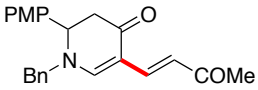

6.7, 69%

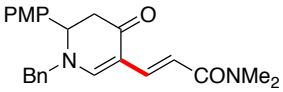

6.8, 80%

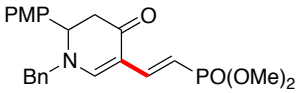

6.9, 68%

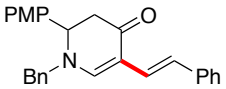

6.10, 46%

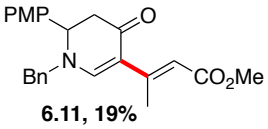

6.11, 19%

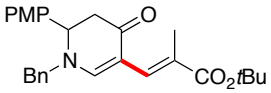

6.12, 37%

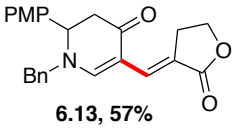

6.13, 57%

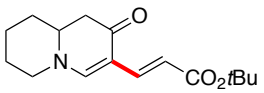

6.14, 59%

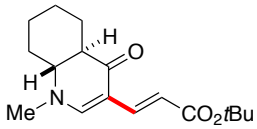

6.15, 59%

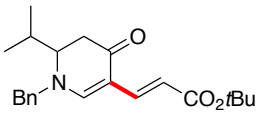

6.16, 83%

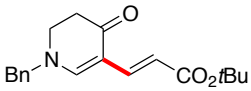

6.17, 57%

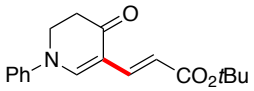

6.18, 32%

Incompatible:

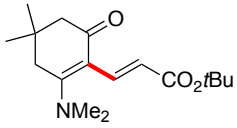

6.19, 0%

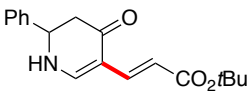

6.20, 0%

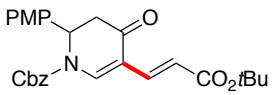

6.21, 0%

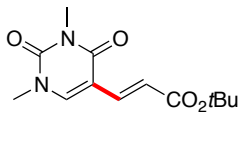

6.22, 0%

[a] Conditions: enaminone (0.2 M), acrylate (4 equiv), catechol (20 mol %), $Pd(OAc)_2$ (10 mol %), $Cu(OAc)_2$ (10 mol %), catechol (20 mol %) with 4Å MS in DMF (0.5 mL) at rt under O_2 (1 atm) through 24 h. Isolated yield.

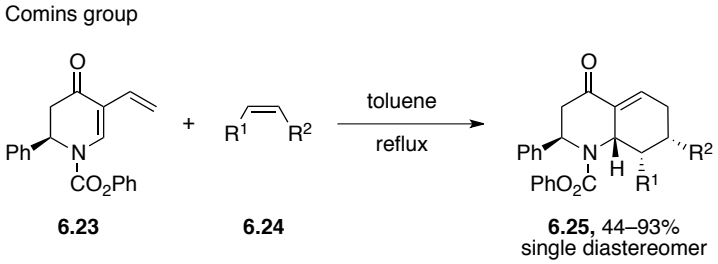

Scheme 6-3. Examples of the Diels-Alder reaction to prepare octahydroquinolines.

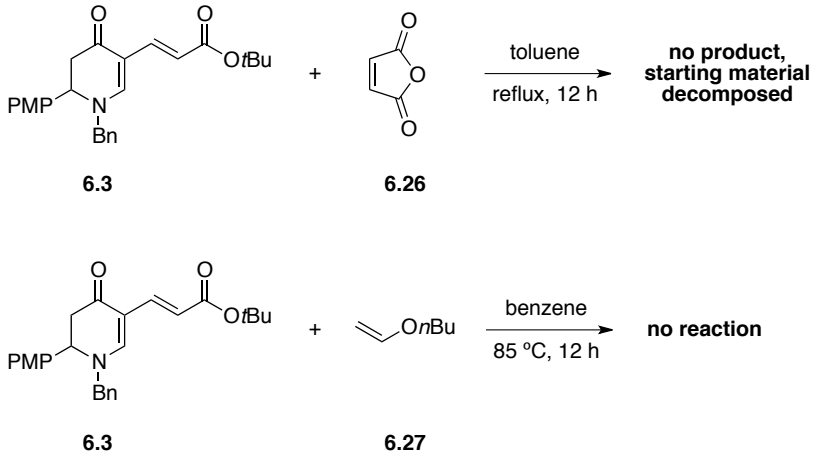

Scheme 6-4. Failed attempts toward Diels-Alder cycloaddition.

6.4.2 Theoretical prediction on the nature of the Diels-Alder reaction

We turned to computational chemistry to explore the nature of the proposed Diels-Alder reaction. Computational chemistry has made tremendous progress in the past two decades. It has enabled chemists to understand fundamental correlation between structures and properties (*e.g.* QSAR) and also predicted unknown reactivities that assist experimental chemists in rational compound design (*e.g.* drug design and catalyst). In particular, for small- to medium-size organic compounds (<30 first row atoms), computation using quantum chemical methods, such as the density functional theory, are now capable of predicting molecular properties with a precision approaching that of experiments.[443-446]

A series of representative diene substrates were selected (Scheme 6-5). Dienes **6.28**

and **6.23** are known to undergo NED cycloaddition,[441, 442, 447] while dienes **6.29** and **6.30** are reported to undergo IED cycloaddition.[448-452] *Ab initio* calculations were performed with the Gaussian 09 program suite.[453] Geometry optimizations were performed with the B3LYP/6-31G(d) method without any constraint. Frequency calculations were carried out at the same B3LYP/6-31G(d) level of theory to confirm convergence to appropriate local minima or saddle points on the energy surface. Single-point energies were calculated with the UB3LYP/6-31+G(d,p) method. The HOMO and LUMO energies are shown in Figure 6-1.

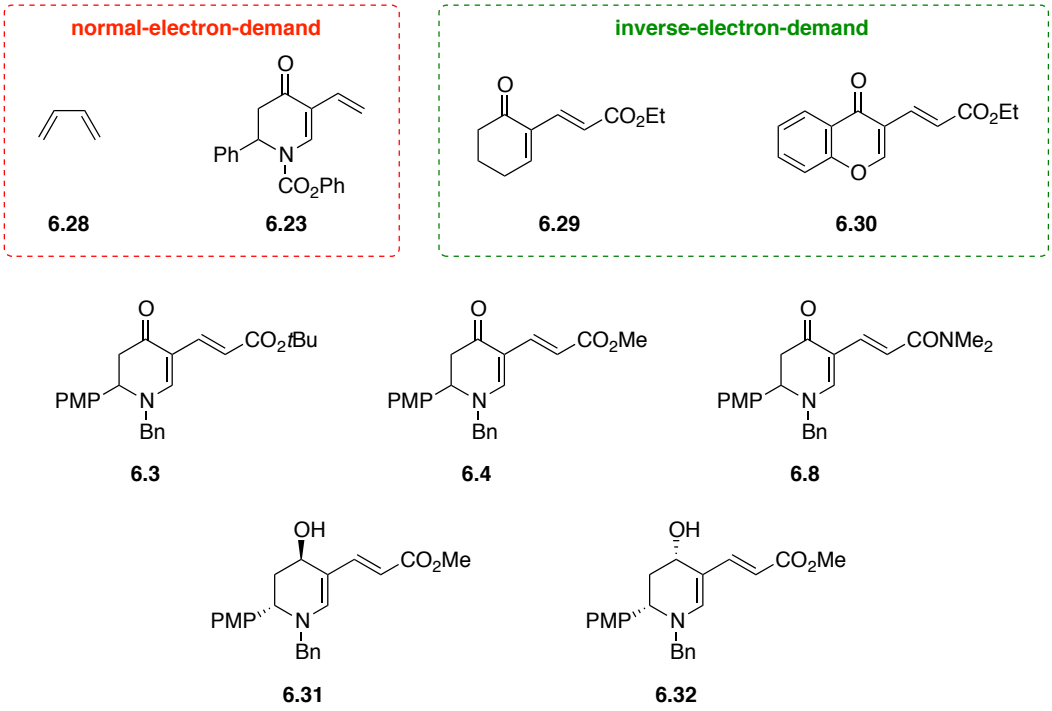

Scheme 6-5. Representative diene substrates for computational calculation.

The calculation results revealed that the alkenylated enaminones should thermodynamically favor NED Diels-Alder reactions. All the HOMO energies of selected enaminones (**6.3**, **6.4**, **6.8**, **6.31**, and **6.32**) are higher than those of electron-rich dienes (**6.28** and **6.23** in the red dashed box) that undergo NED Diels-Alder reactions. In comparison, **6.29** and **6.30** (in the green dashed box) should have lowered LUMO energies because they undergo IED Diels-Alder reactions,[448-452] which was indeed

confirmed by our calculation. Therefore, the reduced HOMO-LUMO energy gaps between enaminones and dienophile **6.26** predict that the Diels-Alder reaction of alkenylated enaminones would proceed in a NED manner.

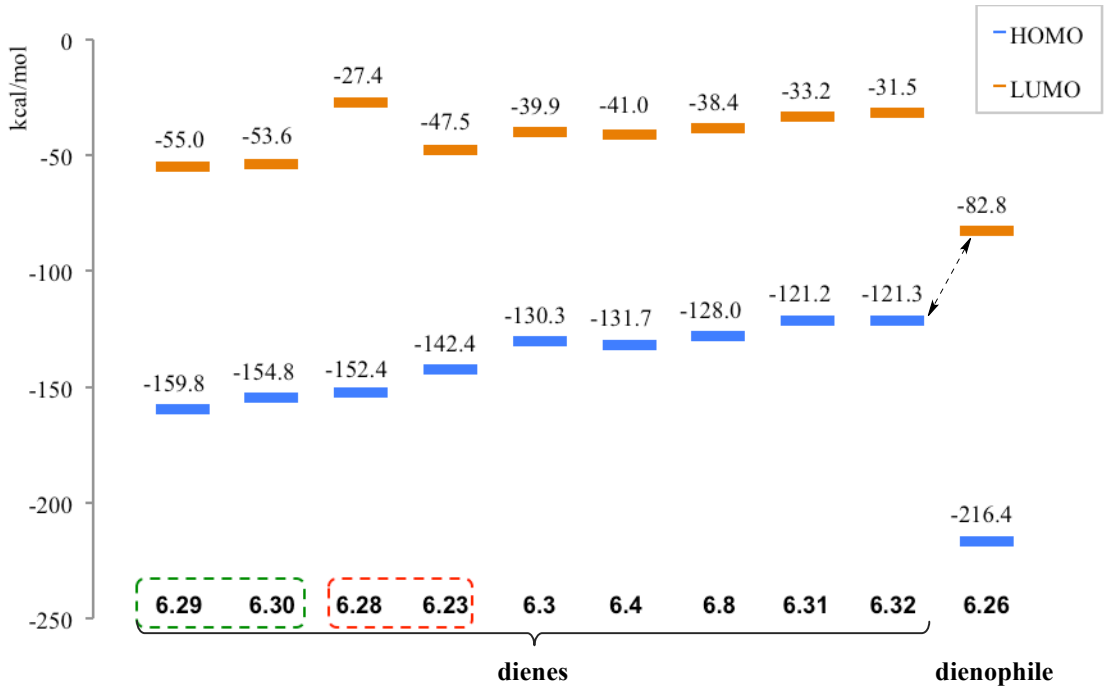

Figure 6-1. Calculated energies of HOMOs and LUMOs.

6.4.3 Unexpected chalcone formation

As we reexamined the NED Diels-Alder reaction between **6.33** and **6.34**, we were surprised to isolate a large amount of much less polar compound **6.36** instead of the expected **6.35** (Scheme 6-6). Presumably, the multiple electron-withdrawing substituents and the amino leaving group in cycloadduct **6.35** promoted aromatization.[441, 447, 450] Afterwards a retro-Michael fragmentation released methylamine and afforded chalcone **6.36**.

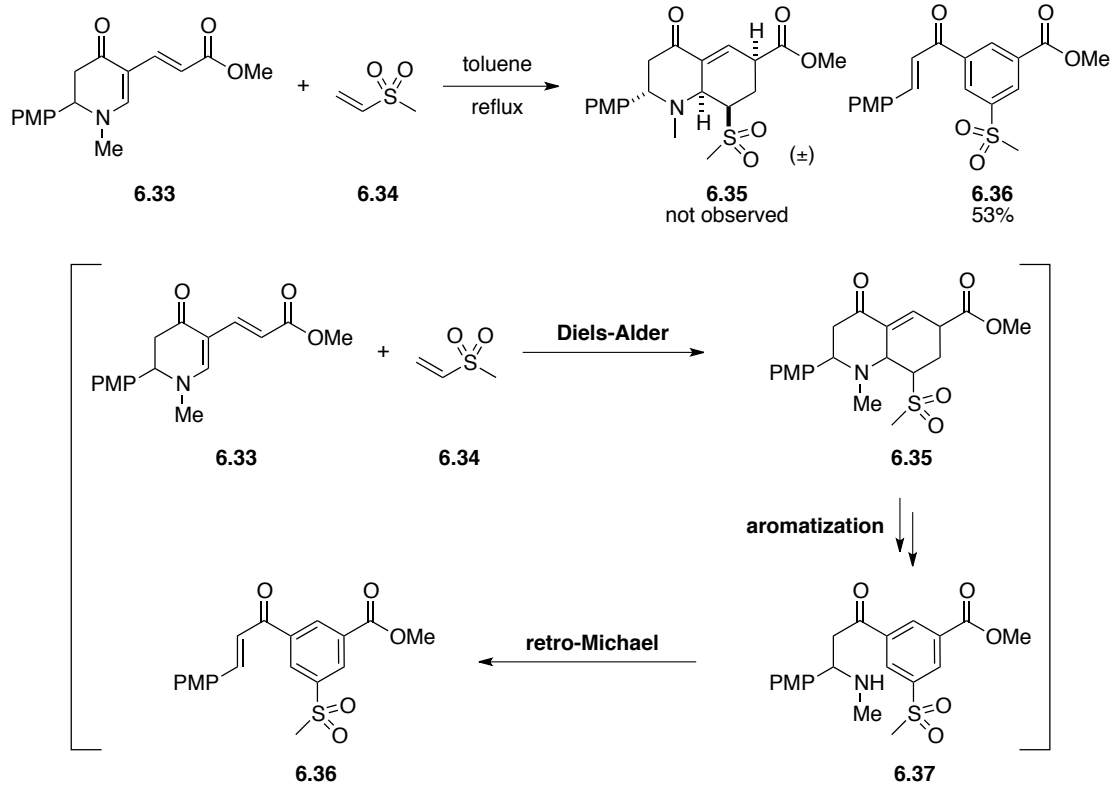

Scheme 6-6. Proposed mechanism for unexpected chalcone formation.

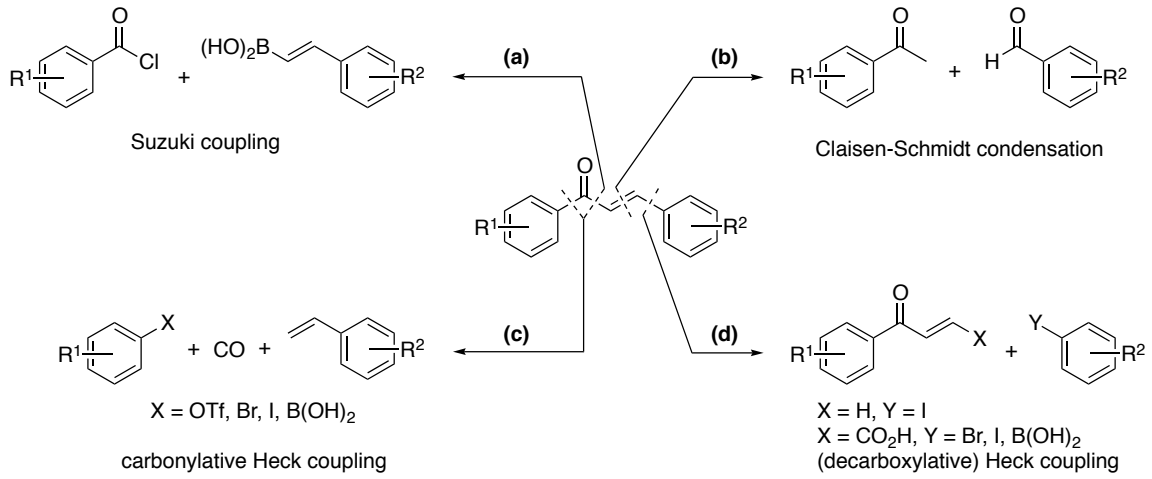

Scheme 6-7. Representative strategies for chalcone synthesis.

Conventionally, chalcones have been synthesized by the Claisen-Schmidt condensation (Scheme 6-7, path b).[454, 455] The reaction efficiency and functionality

tolerance are usually low due to the strongly basic conditions. Although new Pd-catalyzed cross-coupling methods, such as Suzuki (path a),[456] carbonylative Heck (path c),[457-459] and (decarboxylative) Heck reactions (path d),[460, 461] have been developed for chalcone syntheses, their utilization has mostly depended on the availability of aryl coupling precursors and the necessity for pressurized carbon monoxide. In order to diversify the chalcone scaffold for library production, chemo- and regioselective functionalization of the aryl rings requires innovative strategies.

Hence, the task of diversifying the chalcone core ultimately relies on the methods of functionalizing arenes. In spite of the high efficiency of the classic functionalization methods, such as electrophilic, nucleophilic and radical aromatic substitution, it is still of fundamental importance to devise novel methods for regioselective functionalization of arenes.[462] Transition metal-catalyzed coupling reactions have become highly effective,[463] and direct C–H functionalization of arenes has been heavily studied in recent years.[88, 91, 132, 161, 350, 464-466] In many of these couplings, a directing group is required to achieve excellent regioselectivity.

In particular, 1,3,5-trisubstituted benzenes are important structural motifs in material science and medicinal chemistry because of their unique symmetry. The symmetrical 1,3,5-trisubstituted benzenes have been used in liquid crystals,[467, 468] macromolecules,[469] and organic light-emitting devices (OLEDs),[470, 471] while the unsymmetrical counterparts have been studied as thrombin inhibitors,[472] γ-turn mimics,[473, 474] and anticancer agents,[475] etc. A majority of the methods for synthesizing 1,3,5-trisubstituted benzenes employ commercially available 1,3,5-trihalobenzenes or alike as precursors, where the substitution pattern is established in the beginning.[467, 469, 470, 476, 477] The regioselectivity is often problematic in order to produce unsymmetrical 1,3,5-trisubstituted benzenes. The sequential functionalization of each position sometimes also requires protection schemes, which are undesirable with poor atom economy.[472] With regard to the advanced C–H activation chemistry of arenes, *ortho*-functionalization prevails, while *meta*-functionalization is still in its infancy.[478-484] Due to the synthetic difficulty, there is a lack of a general, regioselective method for synthesizing unsymmetrical 1,3,5-trisubstituted benzenes.

Inspired by our preliminary results, we decided to explore the potential of the Diels-Alder tandem reaction to devise an alternative useful method to synthesize 1,3,5-trisubstituted benzenes, including polysubstituted chalconoids.

6.5 Condition optimization for the Diels-Alder tandem reaction

6.5.1 Solvent screen

We first tested a series of solvents for the Diels-Alder tandem reaction (Table 6-8). Due to the incomplete conversion of enaminone **6.33**, all the reactions were run for 5 days. An extended reaction time however led to more side reactions. Nevertheless, less polar solvents such as toluene and DCE furnished better yields (entries 1–2). More polar solvents such as MeCN, THF, and DMAc did not measure up (entries 3–5), while no product **6.39** was formed in THF (entry 6). As toluene has a higher boiling point than DCE, we chose toluene as the solvent for the subsequent study.

Table 6-8. Study of solvent effect on the Diels-Alder tandem reaction

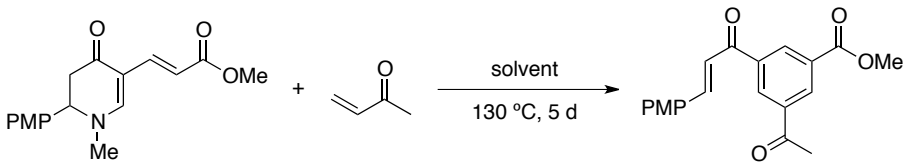

6.33 **6.38** **6.39**

Entry[a]	Solvent (1 mL)	% Yield
1	toluene	44
2	DCE	45
3	MeCN	36
4	dioxane	35
5	DMAc	28
6	THF	0

[a] Conditions: Enaminone **6.33** (0.07 M), alkene **6.38** (2 equiv) at 130 °C for 5 d. ^{1}H NMR yield based on 1.0 equiv of Ph_3SiMe as the internal standard.

6.5.2 Reaction time and temperature

Table 6-9. Study of reaction time and temperature

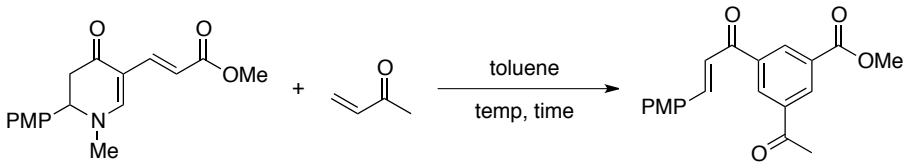

6.33 **6.38** **6.39**

Entry[a]	Time (h)	Temp (ºC)	% Yield
1[b]	0.5	180	17
2[b]	2	180	44
3[b]	4	180	48
4[b]	8	180	51
5[b]	10	180	52
6[b]	2	200	46
7[b]	4	200	19
8	24	150	31
9	24	160	56
10	24	170	40
11	24	180	45
12	15	180	43

[a] Conditions: Enaminone **6.33** (0.07 M), alkene **6.38** (4 equiv) in toluene (1 mL). ^{1}H NMR yield based on 1.0 equiv of Ph_3SiMe as the internal standard. [b] Under microwave.

Next, we explored the feasibility of applying the microwave technique to facilitate the reaction (Table 6-9). The reaction was first exposed to an elevated temperature (180 ºC) for 0.5 h. To our disappointment, only 17% of **6.39** was observed (entry 1). As we prolonged the reaction time, it quickly became clear that the tandem transformation proceeded slowly (entries 1–5) Attempts to accelerate the reaction by increasing the temperature to 200 ºC resulted in decomposition (entries 6–7). Hence, the microwave technique is not suitable for this transformation. The conventional heating technique was

then adopted and the reaction temperature was controlled from 150 ºC to 180 ºC in 10 ºC intervals (entries 8–12). 160 ºC was found to be the most suitable temperature (entry 9).

6.5.3 Stoichiometry

Lastly, the reagent stoichiometry was examined (Table 6-10). The concentration of dienophile **6.38** was controlled from 1.1 equiv up to 30.0 equiv (entries 1–6). Apparently, 8.0 equiv of **6.38** reached the apparent "saturation" level and afforded the highest yield (entry 4). Adding more dienophile showed no beneficial effect (entries 5–6). Attempts to extend the reaction time to 48 h and to use less dienophile **6.38** (2.0 equiv) were not successful (entry 7). It was also found that an oxygen atmosphere was detrimental to the Diels-Alder tandem reaction (entry 8).

Table 6-10. Study of reagent stoichiometry

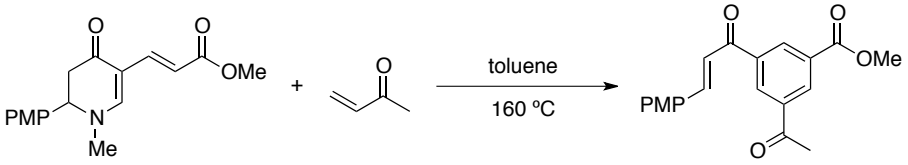

6.33 **6.38** **6.39**

Entry[a]	**6.37** (equiv)	Time (h)	% Yield
1	1.1	24	27
2	2.0	24	42
3	4.0	24	56
4	8.0	24	**63** (**66**[b])
5	15.0	24	59
6	30.0	24	61
7	2.0	48	43
8[c]	2.0	24	17

[a] Other conditions: Enaminone **6.33** (0.07 M) in toluene (1 mL) at 160 ºC. ^{1}H NMR yield based on 1.0 equiv of Ph_3SiMe as the internal standard. [b] Isolated yield. [c] Under 1 atm O_2.

6.6 Study of the scope of the 1,3,5-trisubstituted arene synthesis

The scope of the tandem reaction was then explored (Table 6-11). The Diels-Alder reaction exhibited excellent regioselectivity, furnishing a distinctive 1,3,5-trisubstitution pattern. A wide range of electron-deficient dienophiles (*e.g.* vinyl sulfone, vinyl ketone, acrylates, acrylonitrile, vinyl phosphonate) were compatible with yields up to 86% (**6.36**, **6.39**–**6.44**). Surprisingly, maleimide was not well tolerated, generating **6.45** in a low yield (16%). When acrylic acid was used, decarboxylation occurred to form **6.46** (Scheme 6-8). Although styrene was not reactive as a dienophile, the flexibility of our protocols allowed us to install styrene (as R^3) beforehand via dehydrogenative alkenylation, and the tandem reaction thereafter could furnish the phenylated chalcones (**6.47**–**6.48**). Surprisingly, diene **6.14** generated a distinct benzene **6.49**. A structural search of 1,3,5-trisubstituted benzenes bearing ketone, ester and cyano functionalities obtained only one precedence.[474] Due to the unique structural feature in **6.56**, we presume that a retro-Mannich reaction took place instead of a retro-Michael fragmentation (Scheme 6-9). It is worth noting that no octahydroquinoline products (as **6.35**) were left after any of these transformations.

The advantages of this new tandem reaction in regioselectively functionalizing benzenes are four-fold:

(1) The new protocol provides a straightforward pathway to synthesize unsymmetrical 1,3,5-*electron-withdrawing-group*-substituted benzenes. The synthesis of this type of arenes is not simple via conventional approaches. For instance, the classics electrophilic substitution could work in theory, but the deactivation of reactivity by every additional electron-withdrawing group significantly devalues this strategy. Metal-catalyzed/mediated functionalization would require meticulously prefunctionalized benzenes with different (pseudo)halogens on 1,3,5-positions respectively;[473-475] Otherwise, regioselectivity is difficult to control. As to C–H functionalization, *meta*-selectivity has very few reports so far with a limited substrate scope.[478-484]

(2) The tandem reaction tolerates a series of electron-withdrawing functionalities. Due to the nature of the dehydrogenative alkenylation and NED Diels-Alder reaction, a variety of electron-deficient alkenes are compatible in both reactions (Tables 6-6 and 6-11). In particular, functionalities such as sulfone (**6.36**) and phosphonate (**6.44**) can be

installed onto the phenyl ring in one step from commercially available vinyl reagents, which eliminates the prefunctionalization step (*e.g.* halogenation) required in previous methods.[485-491]

Table 6-11. Scope of the Diels-Alder tandem reaction[a]

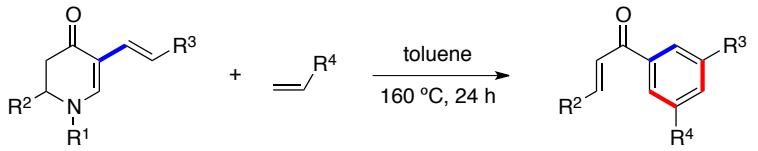

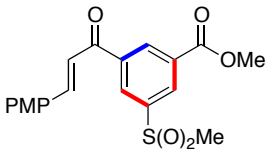

6.36, 82%

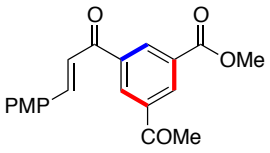

6.39, 66%

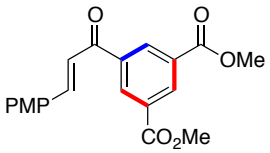

6.40, 73%

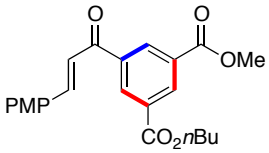

6.41, 75%

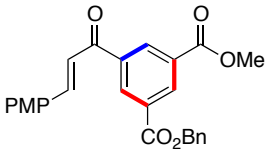

6.42, 86%

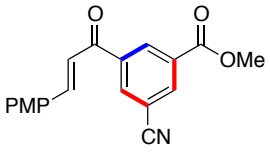

6.43, 80%

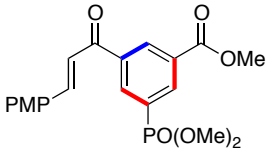

6.44, 23% (57%[b])

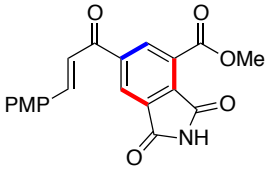

6.45, 16%

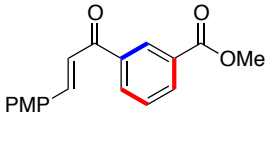

6.46, 33%

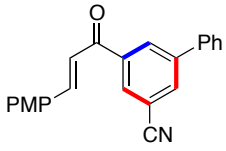

6.47, 46%[c]

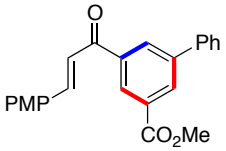

6.48, 52%[c]

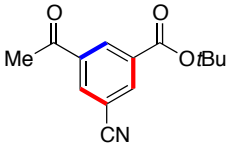

6.49, 48%[d]

[a] Conditions: Enaminone **6.33** (0.07 M), alkene (8.0 equiv) in toluene at 160 °C for 24 h. Isolated yield. [b] Based on recovered starting material **6.33**. [c] Enaminone **6.10** was used. [d] Enaminone **6.14** was used.

(3) This two-step scheme (*i.e.* the dehydrogenative alkenylation and Diels-Alder tandem reaction) is complementary and flexible. As mentioned above, compounds **6.47**

and **6.48** have demonstrated the feasibility of changing the sequence of alkenes used in each step to afford satisfactory yield. In addition, the choice of alkenes in each step can simply construct symmetrical and unsymmetrical 1,3,5-trisubstituted benzenes (*e.g.* symmetrical **6.40** vs. unsymmetrical **6.43**). Thus, the distribution of functional groups can be easily manipulated. Remarkably, several products, such as **6.49**, have three different functional groups that might be modified in a chemoselective manner.

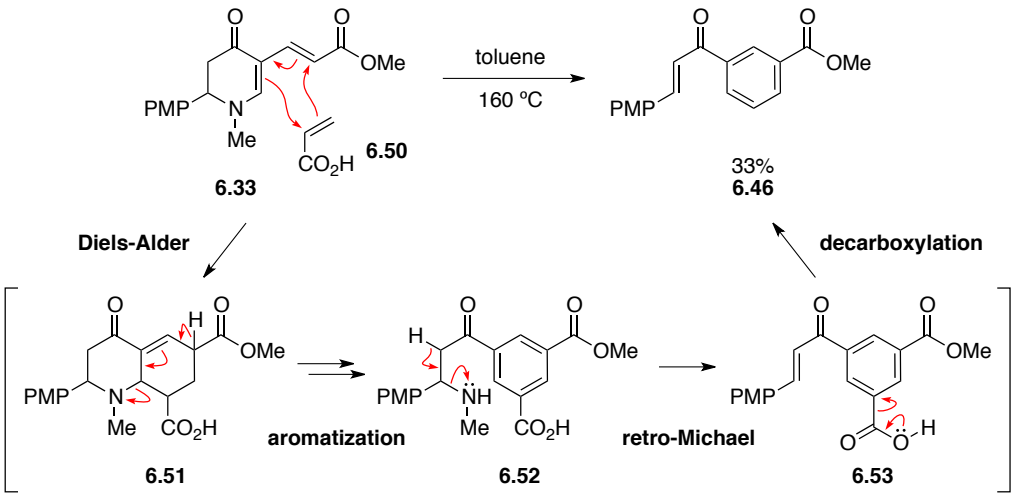

Scheme 6-8. A tandem sequence with decarboxylation.

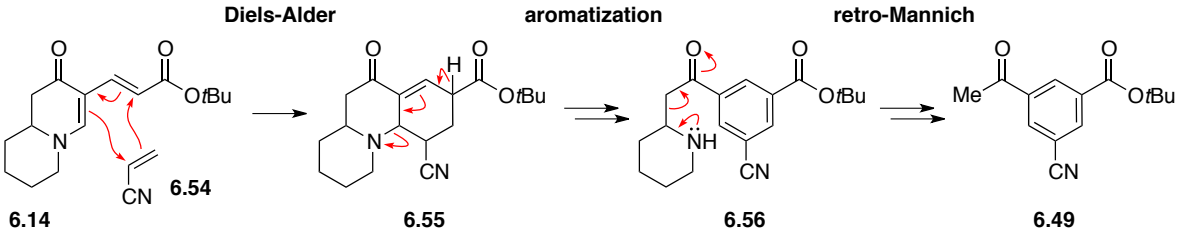

Scheme 6-9. A tandem sequence with retro-Mannich fragmentation.

(4) With respect to chalcone synthesis, the current approach focuses on the diversification of chalcone aryl rings, contrary to previous methods that paid most attention to the construction of the vinylketone linkage in chalcones (Scheme 6-7). Since the tandem reaction construct one of the two phenyl rings in chalcones, our approach does not depend as heavily as other methods on the availability of aryl precursors. In

addition, all the aforementioned advantages for the 1,3,5-trisubstituted benzene synthesis can facilitate the generation of unique chalcone libraries for medicinal study.

6.7 Conclusion

In this study, we successfully improved our dehydrogenative alkenylation method for cyclic enaminones in a biomimetic approach by adopting catechol as an O_2 activator. The current protocol uses using O_2 as a green oxidant and significantly reduces the heavy metal oxidant $Cu(OAc)_2$ to a catalytic level. Remarkably, the new aerobic C–H alkenylation reaction shows comparable scope and proceeds efficiently at room temperature, which we believe is the first example in the field of dehydrogenative cross-coupling. Interestingly, our synthetic development on alkenylated cyclic enaminones discovered a tandem reaction, which constructed a series of unique 1,3,5-trisubstituted benzenes through a Diels-Alder/aromatization/retro-Michael sequence. This unexpected transformation can provide an alternative approach to synthesize multisubstituted chalconoids in good yields.

Chapter 7 Progress on C–H Trifluoromethylation of Cyclic Enaminones

7.1 Introduction

Even though inorganic fluorides are abundant on Earth, no more than a dozen of the compounds created by nature contain fluorine atom(s).[492] In contrast, 30–40% of all commercial agrochemicals and 20–30% of all pharmaceuticals are decorated with at least one fluorine atom.[493] Among all the fluorinated compounds, molecules bearing a trifluoromethyl (CF_3) group constitute an important class of compounds and have attracted broad attention because of their unique properties such as elevated electronegativity, hydrophobicity, and metabolic stability, *etc.*[493, 494] Hence, molecular modification with a CF_3 group is now common in the pharmaceutical and agrochemical industries (Scheme 7-1).[493, 495] Classic methods to synthesize trifluoromethylated compounds largely undergo Lewis acid-promoted exchange of chloride by fluoride via the Swarts-type reaction (Scheme 7-2).[496, 497] The harsh conditions significantly limit their synthetic application. With the increasing importance of fluorinated compounds, new synthetic methods are urgently needed.

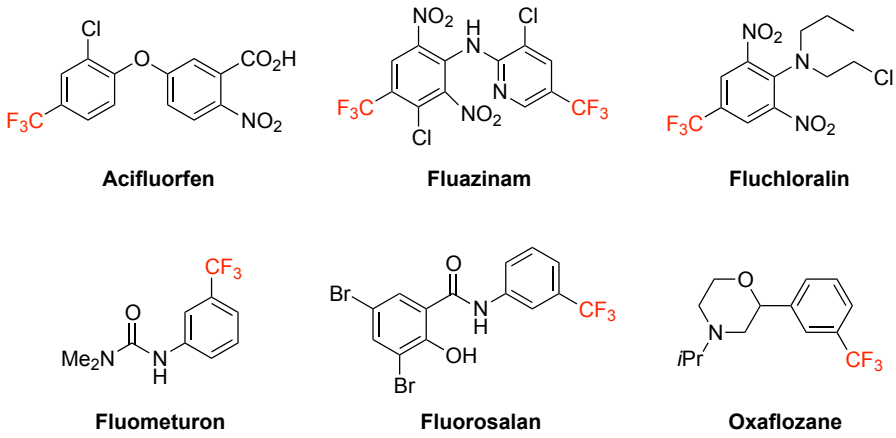

Scheme 7-1. Examples of CF_3-containing pharmaceuticals.

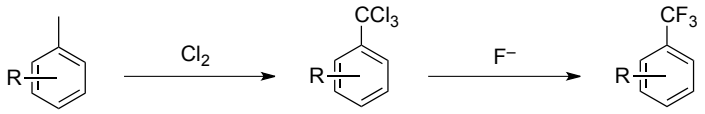

Scheme 7-2. Traditional methods for trifluoromethylation.

Transition metal-catalyzed trifluoromethylation in this regard is very promising in terms of regioselectivity, functionality tolerance, and reaction efficiency.[498-504] Palladium- and copper-catalyzed cross-coupling reactions in particular have proven to be an efficient strategy to introduce the CF_3 functionality.[498-504] These reactions often require substrate prefunctionalization with halogen or boron substituents. Although these reactions could afford excellent regioselectivity due to prefunctionalization, their low atom-economy would confine their industrial applications. A more desirable approach for trifluoromethylation via direct C–H activation would bypass the prefunctionalization step and offer a more straightforward and economical pathway. Unfortunately, direct C–H trifluoromethylation is very challenging. Mild and robust methods had not been available until very recently.[505-508]

7.2 Recent development

7.2.1 Direct trifluoromethylation of sp^2 C–H bonds

Due to the wide application of trifluoromethylated (hetero)arenes in pharmaceuticals, agrochemicals and advanced materials, direct trifluoromethylation of sp^2 C–H bonds is currently the most studied and in fact the most straightforward method to synthesize CF_3-containing (hetero)arenes.[498, 501, 503, 506, 508] The developed protocols can be categorized into three classes based on the three CF_3 sources used: CF_3^+, CF_3^-, and CF_3•.[509]

7.2.1.1 Trifluoromethylation involving CF_3^+ reagents

Yu and co-workers first reported a directed electrophilic *ortho*-trifluoromethylation reaction of arenes using Umemoto's reagent (**7.1**, a trifluoromethyl sulfonium salt, Scheme 7-3, top).[510] *N*-heterocycles, such as pyridine, pyrimidine, imidazole, and

thiazole, could be used as the directing groups. This pioneering work was catalyzed via a proposed Pd^{II}/Pd^{IV} cycle, and therefore a stoichiometric amount of $Cu(OAc)_2$ as the oxidant was required. Subsequently, the same group developed a similar electrophilic trifluoromethylation reaction using an amido group as the directing group.[511] In particular, *N*-methylformamide as an additive was crucial for the coupling process. Similarly, Shi and co-workers successfully applied the acetamino group as an alternative directing group to achieve regioselective *ortho*-trifluoromethylation of arenes (Scheme 7-3, bottom).[512]

Mechanistically, Sanford and co-workers later reported that the oxidation of the cyclometalated Pd^{II} dimer with CF_3^+ reagents could produce a monomeric CF_3–Pd^{IV} intermediate, which would underwent selective reductive elimination to form a C–CF_3 bond.[513]

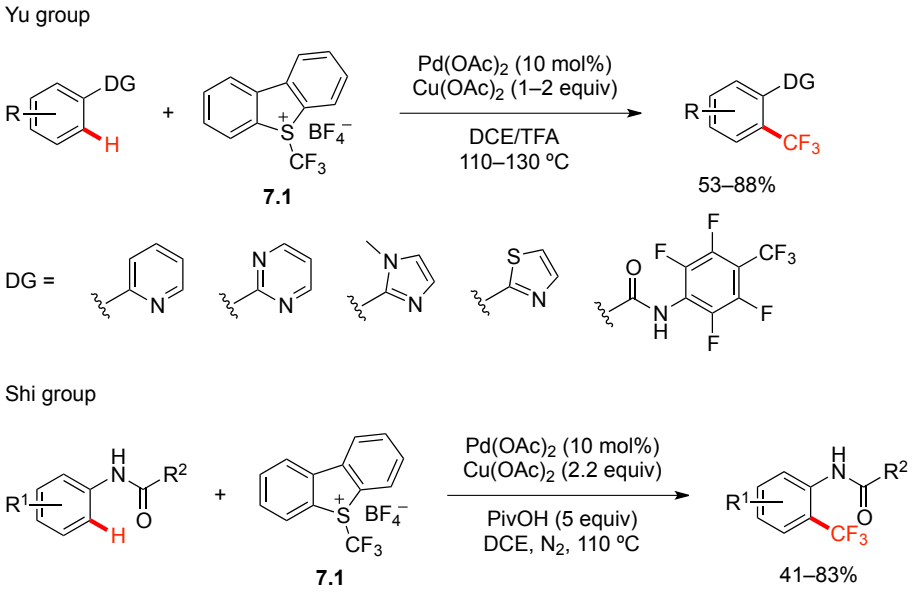

Scheme 7-3. Electrophilic *ortho*-trifluoromethylation using Umemoto's reagent.

Another class of CF_3^+ sources is Togni's reagent (**7.2**, a hypervalent iodine compound). Initially, Togni and co-workers reported that no catalysts were needed for electrophilic aromatic trifluoromethylation on a broad range of arenes and *N*-heteroarenes, although **7.2** showed increased electrophilicity in the presence of a Lewis

acid.[514] Hence, Sodeoka and co-workers later developed a CuOAc-catalyzed regioselective trifluoromethylation of indole derivatives using Togni's reagent under very mild conditions (Scheme 7-4, top).[515] Very recently, Sodeoka reported a difunctionalization-type trifluoromethylation reaction of activated alkenes bearing allylic protons using Togni's reagent.[516] This Cu^{I}-catalyzed protocol provides trifluoromethylated carbocycles and heterocycles in good to excellent yields. As for C–H trifluoromethylation of alkenes, Loh and co-workers reported the first example of this reaction (Scheme 7-4, bottom).[517] A series of enamides was converted with Togni's reagent to their β-trifluoromethyl substituted derivatives by Cu^{I} catalysis in good to excellent yields.

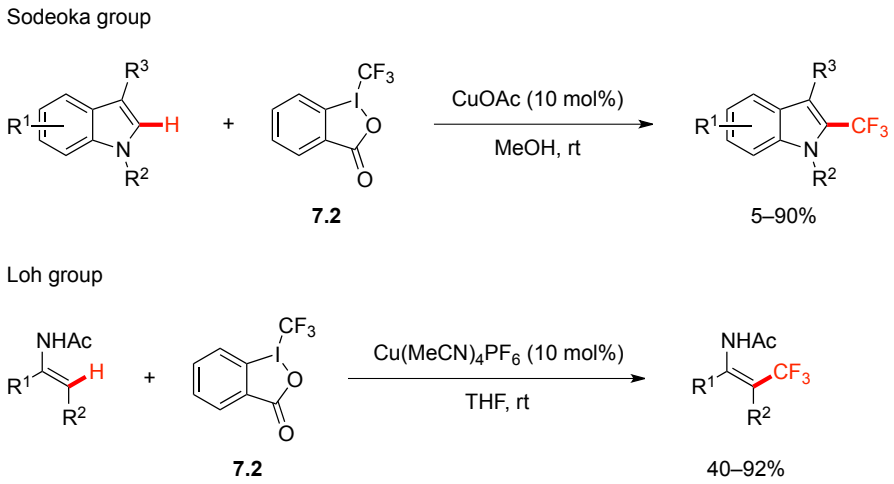

Scheme 7-4. Electrophilic trifluoromethylation using Togni's reagent.

7.2.1.2 Trifluoromethylation involving CF_3^- reagents

The most used CF_3^- reagent is $TMSCF_3$ (the Ruppert-Prakash reagent). Liu and co-workers developed a Pd-catalyzed oxidative trifluoromethylation of indoles using $TMSCF_3$ (Scheme 7-5, top).[518] $PhI(OAc)_2$ was used as an oxidant as this reaction was proposed to take place via a Pd^{II}/Pd^{IV} mechanism. Using very similar conditions, the same group continued to develop a tandem oxidative aryltrifluoromethylation of activated alkenes.[519] This difunctionalization reaction afforded a variety of CF_3-containing

oxindoles in good yields. More recently, Qing and co-workers described a Cu-catalyzed C–H trifluoromethylation reaction of heteroarenes and electron-deficient arenes with $TMSCF_3$ (Scheme 7-5, bottom).[520] The acidity of the targeted C–H proton is the key to this regioselective transformation. A wide range of aromatic compounds, including oxadiazoles, benzoxazoles, benzothiazoles, benzoimidazoles, indoles, and perfluoroarenes, were compatible under the optimized conditions.

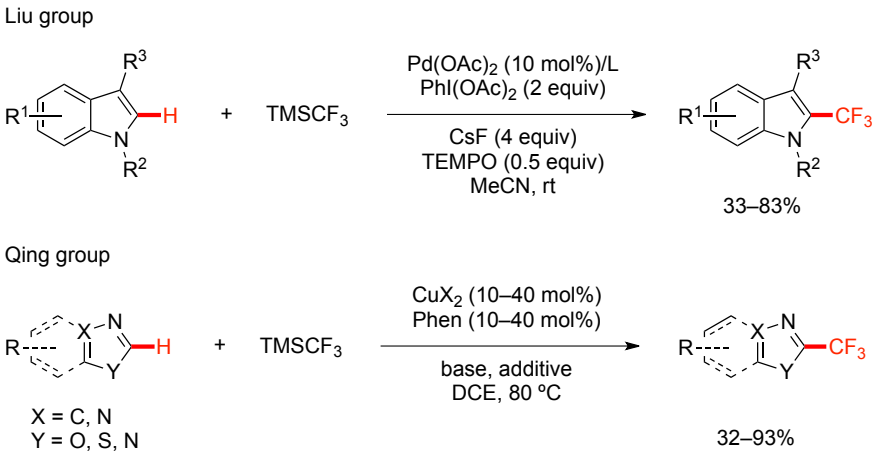

Scheme 7-5. Nucleophilic trifluoromethylation using $TMSCF_3$.

7.2.1.3 Trifluoromethylation involving CF_3• reagents

In 2010, Yamakawa and co-workers demonstrated the use of CF_3I in the presence of a Fe^{II} catalyst, H_2O_2 and DMSO in trifluoromethylating various (hetero)aromatic compounds.[521] The regioselectivity is largely directed by the general trend of aromatic electrophilic substitution. Later, the Sanford group reported a silver-mediated direct trifluoromethylation of arenes with $TMSCF_3$ (Scheme 7-6, top).[522] An Ag–CF_3 species was proposed as a key intermediate to produce the CF_3• radical. Although a wide scope of substrates was tolerated, this protocol has a few drawbacks including the use of stoichiometric amounts of Ag salts and problematic regioselectivity. Bräse and co-workers extended this silver-mediated protocol to aryl triazene substrates and achieved good *ortho*-selectivity (Scheme 7-6, bottom).[523] Thanks to the versatility of triazenes, a variety of CF_3–containing building blocks are therefore available.

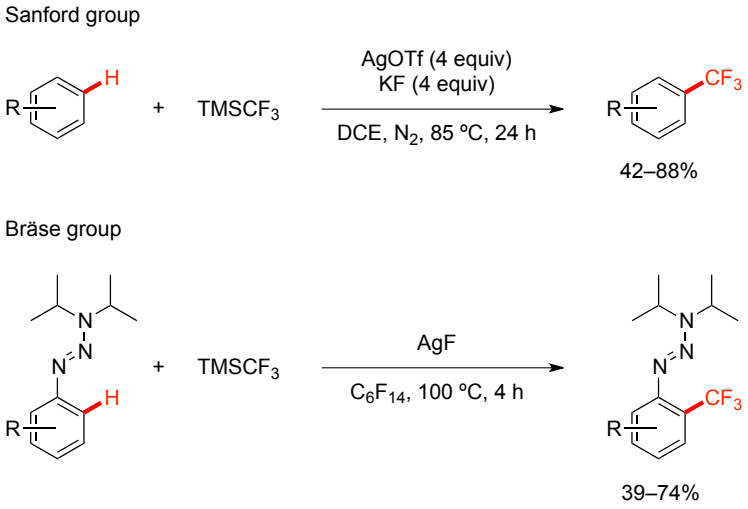

Scheme 7-6. Silver-mediated C–H trifluoromethylation.

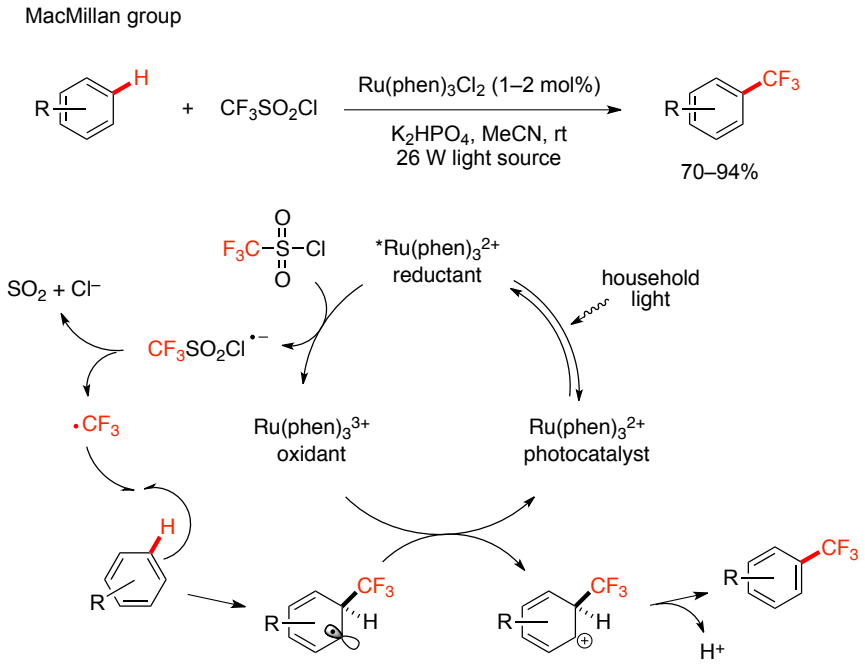

Scheme 7-7. MacMillan's radical-based trifluoromethylation protocol.

A recent breakthrough in direct C–H trifluoromethylation is the advance of radical approaches with inexpensive reagents and mild conditions.[499, 524] MacMillan and co-workers devised a novel photoredox protocol that promoted Ru^{II}-catalyzed direct C–H trifluoromethylation on an array of arenes and heteroarenes (Scheme 7-7).[407] CF_3SO_2Cl

(*i.e.* TfCl) was used as the CF_3• source. The low cost of TfCl and the mild conditions rendered this protocol very promising. Since then, a series of subsequent developments based on this photoredox protocol was achieved. For instance, Cho and co-workers used CF_3I as the CF_3• source in the direct trifluoromethylation of a wide range of heteroarenes with good to excellent yields.[525]

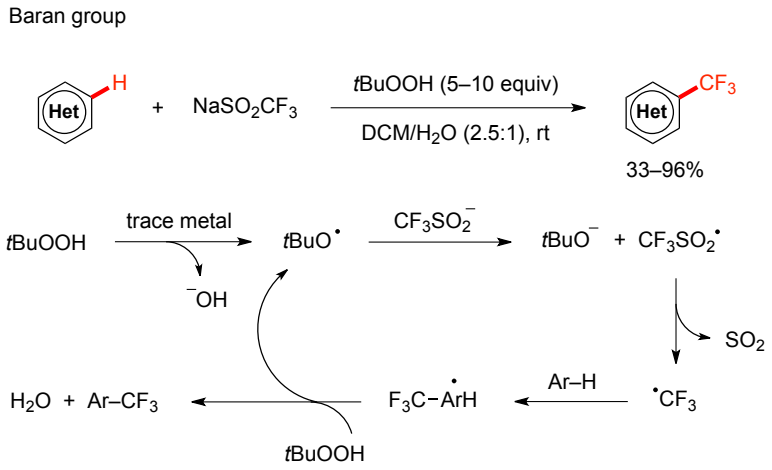

Scheme 7-8. Baran's radical-based trifluoromethylation protocol.

Meanwhile, Baran's group successfully employed CF_3SO_2Na (the Langlois reagent), a benchtop-stable and inexpensive solid, in a metal-free trifluoromethylation reaction with peroxides as radical initiators (Scheme 7-8).[106] Both electron-rich and electron-deficient heteroarenes can be used efficiently and with high functional group tolerance. However, the regioselectivity was modest, but the choice of solvent sometimes could help tune the innate substrate reactivity. These two methods are very beneficial for medicinal chemistry because their robust conditions and wide functional group tolerance allow late stage trifluoromethylation to diversify drug candidates.[524]

7.2.2 Direct trifluoromethylation of *sp* C–H bonds

The examples of direct C–H trifluoromethylation on *sp* carbon centers are very limited. As mentioned in Chapter 2, the dimerization of alkynes is a main problem. In

2010, Qing and co-workers reported the fist example of a Cu-mediated oxidative trifluoromethylation of terminal alkynes with $TMSCF_3$ (Scheme 7-9).[526] Stoichiometric amounts of CuI were needed for the reaction to proceed efficiently. Remarkably, the same group later reduced the usage of Cu^I to a catalytic amount by slow addition of reagents through a syringe pump.[527] Subsequently, the Qing group reported an improved procedure for trifluoromethylation of terminal alkynes. This protocol used (phen)Cu(CF_3) generated *in situ* and proceeded smoothly at room temperature with a smaller amount of $TMSCF_3$.[528]

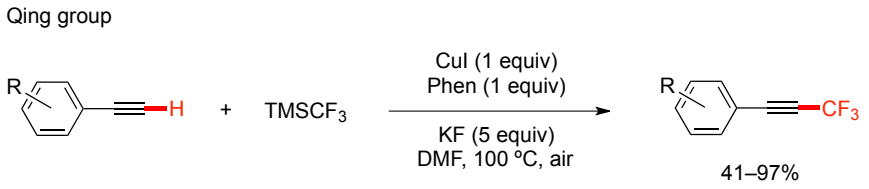

Scheme 7-9. First example of a C–H trifluoromethylation of alkynes.

7.2.3 Direct trifluoromethylation of sp^3 C–H bonds

Similar to its *sp* counterpart, direct trifluoromethylation of sp^3 C–H bonds is extremely challenging. The current available methods are applicable to only a few substrate prototypes, *e.g.* allylic C–H bonds and α-carbonyl C–H bonds.[529-538]

Liu and Fu first reported a Cu^I-catalyzed C–H trifluoromethylation of terminal alkenes via allylic C–H activation using Umemoto's reagent (Scheme 7-10, top).[532] Their mechanistic calculation showed that the reaction might proceed through a Heck-like four-membered transition state. This method can work on a variety of terminal alkenes without 2-substitutents, whereas 2-substituted terminal alkenes or internal (including cyclic) alkenes were not viable. Meanwhile, Buchwald[533] and Wang[534] independently reported Cu^I-catalyzed allylic C–H trifluoromethylation reactions using Togni's reagent (Scheme 7-10, middle). These methods tolerate a wide range of functional groups and proceed with good yields. Interestingly, branched terminal alkenes and cyclic alkenes were not compatible with Buchwald's method, but worked well using Wang's conditions, albeit

requiring a higher temperature. In addition, Qing and co-workers developed a Cu-catalyzed oxidative trifluoromethylation of terminal alkenes using $TMSCF_3$ (Scheme 7-10, bottom).[535] This method provides a complementary pathway for direct allylic trifluoromethylations without using Umemoto's reagent or Togni's reagent.

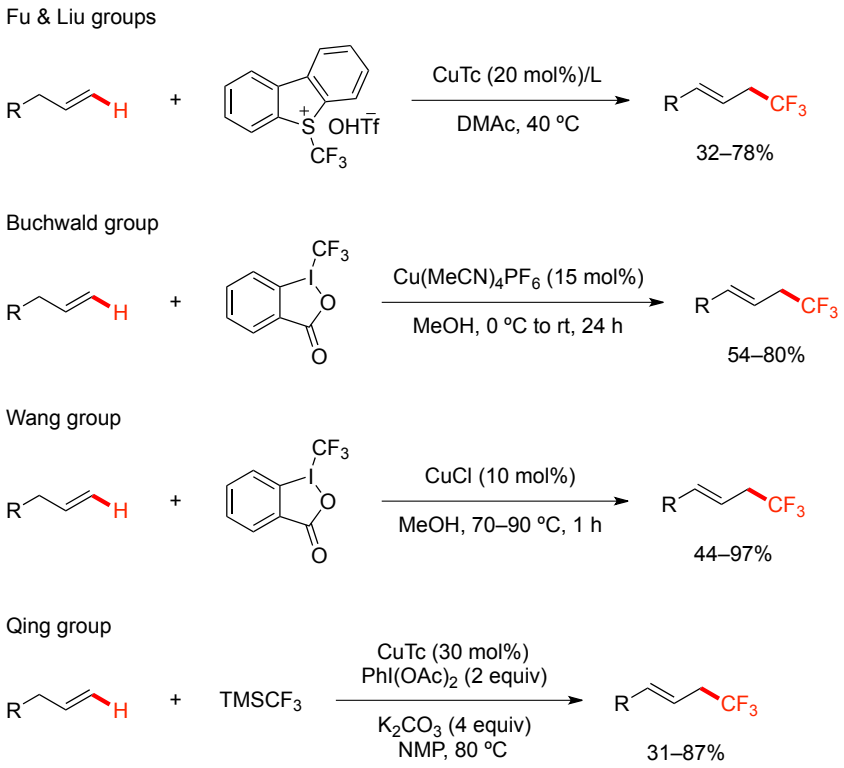

Scheme 7-10. Allylic C–H trifluoromethylation.

MacMillan and co-workers pioneered the direct trifluoromethylation of α-carbonyl C–H bonds using their aforementioned photoredox chemistry. They first reported their discovery in 2009 using CF_3I as a CF_3• source (Scheme 7-11).[536] A series of aldehydes were α-trifluoromethylated enantioselectively. Later, they applied Togni's reagents to replace CF_3I in a non-photolytic approach to achieve enantioselective α-trifluoromethylation of aldehydes.[537] Recently, they expanded the substrate scope from aldehydes to ketones, esters, and amides with very good yields, which further enhanced the utility of this novel protocol.[538]

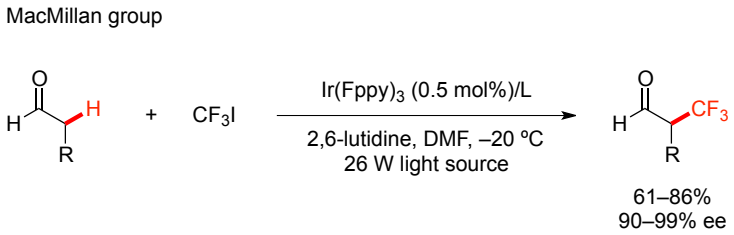

Scheme 7-11. Enantioselective α-trifluoromethylation of aldehydes.

Despite the rapid advance in this field, existing methods and substrates are still inadequate. In particular, direct trifluoromethylation of alkenyl C–H bonds is very rare. Only one method involving enamides was reported so far by Loh and co-workers (Scheme 7-4, bottom).[517] Trifluoromethylation of internal or cyclic alkenes has not been developed. With the innate nucleophilicity that favors Pd-catalysis, *non-aromatic* cyclic enaminones offer a promising platform to assess the feasibility of direct trifluoromethylation of cyclic alkenyl C–H bonds, which would potentially furnish a straightforward path to access 3-trifluoromethylpiperidine derivatives.

Table 7-1. Trifluoromethylation of cyclic enaminone **7.3** using Umemoto's reagent

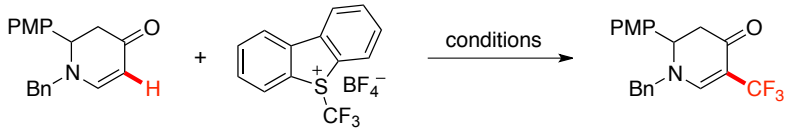

7.3 **7.1** **7.4**

Entry[a]	$Pd(OAc)_2$ (mol%)	$Cu(OAc)_2$ (equiv)	Additive (equiv)	Solvent	Temp. (°C)	Time (h)	% Yield[b]
1	10	2	KTFA (1)	DMF	100	24	0
2	10	2	TFA (10)	DCE	100	24	0
3	10	2	TFA (10)	dioxane	100	24	0
4	10	2	TFA (1)	DCE	100	24	0
5	—	—	—	DMF	rt	3	0
6	—	—	—	DMF	80	3	0

[a] Conditions: enaminone **7.3** (0.1 mmol), **7.1** (2.0 equiv), $Pd(OAc)_2$, $Cu(OAc)_2$, additive, in solvent (1 mL). [b] ^1H NMR yields with Ph_3SiMe (1.0 equiv) as the internal standard.

Table 7-2. Trifluoromethylation of cyclic enaminone **7.3** using Togni's reagent

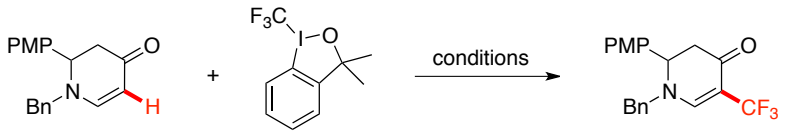

7.3 **7.5** **7.4**

Entry[a]	Lewis Acid (equiv)	Additive (equiv)	Solvent	Temp (ºC)	Time (h)	% SM Consumption[b]	% Yield[b]
1	–	Bu_4NI (0.5)	MeCN	rt	24	26	12
2	–	Bu_4NI (0.5)	MeCN	80	24	54	15
3	–	Bu_4NI (0.5)	DMF	rt	24	28	11
4	–	Bu_4NI (0.5)	MeOH	rt	24	30	15
5	$Cu(OAc)_2$ (2)	–	MeOH	rt	3	68	25

[a] Conditions: enaminone **7.3** (0.1 mmol), **7.5** (2.0 equiv), Lewis acid, additive, in solvent (1 mL). [b] ^1H NMR yields with Ph_3SiMe (1.0 equiv) as the internal standard.

7.3 Reaction optimization

7.3.1 Screen of existing protocols

We first subjected cyclic enaminone **7.3** to the existing methods in order to determine the most effective protocol. Electrophilic trifluoromethylation using Umemoto's reagent failed to proceed in the desired manner (Table 7-1). Altering the additives and solvents did not yield any trifluoromethylated product **7.4** (entries 1–4). Our attempts to use metal-free conditions were not successful either (entries 5–6). Therefore, we turned to Togni's reagent (**7.5**) as the alternative CF_3^+ source (Table 7-2). We first tested metal-free conditions, which afforded the desired product **7.4** in only 12% (entry 1). As the consumption of the starting material **7.3** was low, we increased the temperature to 80 ºC, which unfortunately failed to provide a satisfactory conversion (entry 2). We also changed the solvent to DMF and MeOH, only the latter of which furnished a marginally higher yield (entries 3–4). As Cu salts were reported to catalyze trifluoromethylation reactions involving Togni's reagent, $Cu(OAc)_2$ was added to the reaction, which afforded

7.4 in 25% yield (entry 5). Overall, the electrophilic trifluoromethylation protocols did not meet our expectation.

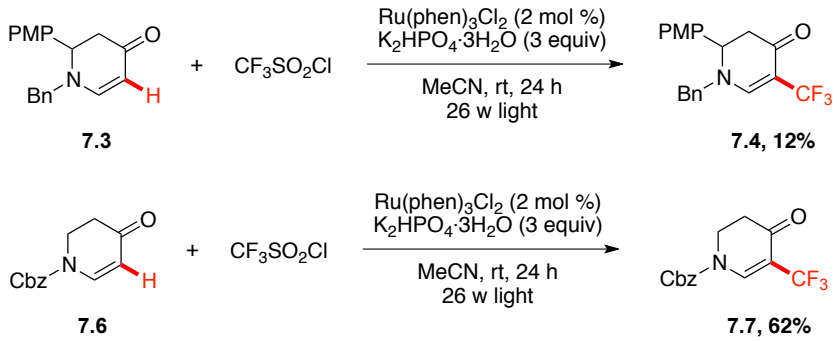

Scheme 7-12. Radical trifluoromethylation of cyclic enaminone by photoredox catalysis.

Table 7-3. Trifluoromethylation of cyclic enaminone **7.3** using *t*BuOOH

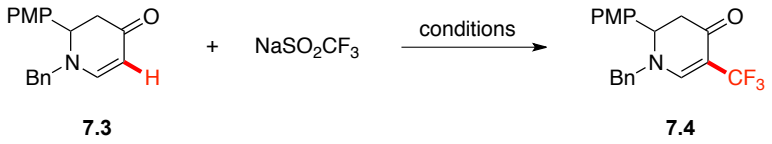

Entry[a]	Catalyst (equiv)	Solvent	Time (h)	% Yield[b]
1	—	DCM/H_2O (2.5:1)	48	1
2	—	$DMSO/H_2O$ (2.5:1)	48	40
3	$AgNO_3$ (0.1)	$DMSO/H_2O$ (2.5:1)	21	8
4	$CuSO_4$ (0.1)	$DMSO/H_2O$ (2.5:1)	21	44
5	$Fe_2(SO_4)_3$ (0.1)	$DMSO/H_2O$ (2.5:1)	21	37

[a] Conditions: enaminone **7.3** (0.1 mmol), $NaSO_2CF_3$ (3.0 equiv), catalyst, *t*BuOOH (5 equiv) in solvent (1 mL) at rt. [b] ^{19}F NMR yields with C_6F_6 (1.0 equiv) as the internal standard.

Next, we examined the existing radical-based protocols. MacMillan's photoredox chemistry showed discrete results (Scheme 7-12). Electron-rich enaminone **7.3** only produced 12% of the desired product **7.4**. In contrast, electron-deficient enaminone **7.6** afforded a much better yield (62%). It is the first example of an electron-deficient enaminone being compatible with C–H functionalization at the C5 position. We presume

that the electron-withdrawing Cbz group may contribute to stabilizing the enaminone radical intermediate formed in the reaction (Scheme 7-7), thus averting decomposition and increasing the yield.

Meanwhile, Baran's radical protocol also gave varied yields (Table 7-3). The reported solvent mixture (DCM/H_2O) only generated a trace amount of product **7.4** over an extended period of time (entry 1). Replacing DCM with a more polar solvent (DMSO) increased the yield to 40% (entry 2). As several reports showed beneficial effects from catalytic metal salts, we then introduced Ag^{I}, Cu^{II}, and Fe^{III} salts to the reactions. It quickly became apparent that metal additives were not required for a productive reaction (entries 3–5).

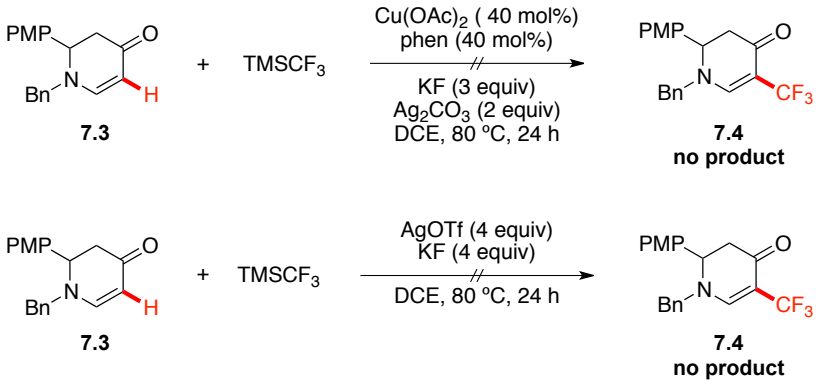

Scheme 7-13. Failed trifluoromethylation of cyclic enaminone using $TMSCF_3$.

Next, we tested a few $TMSCF_3$-based protocols. Unfortunately, Cu-catalyzed trifluoromethylation of **7.3** failed to furnish any desired product (Scheme 7-13, top). Attempts to adopt Sanford's protocol involving stoichiometric amounts of AgOTf did not yield any desired product either (Scheme 7-13, bottom). Lastly, we tried a Pd-catalyzed, PIDA-mediated protocol developed by Liu and coworkers (Table 7-4). The addition of TEMPO improved the yield of **7.4** by 10% (entry 2), while using PIFA instead of PIDA inhibited trifluoromethylation (entry 3).

In all, two existing protocols afforded satisfactory yields after our preliminary investigation: 1) Baran's *t*BuOOH-mediated radical trifluoromethylation (Table 7-3), and

2) Liu's PIDA-mediated nucleophilic trifluoromethylation (Table 7-4). Although both methods use operationally easy procedures and readily available reagents, Liu's protocol offers more variables for optimization. Hence, we decided to pursue a C–H trifluoromethylation method for cyclic enaminones based on Liu's protocol.

Table 7-4. Nucleophilic trifluoromethylation of cyclic enaminone **7.3** using $TMSCF_3$

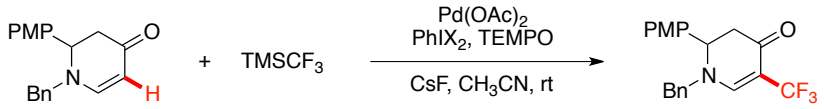

7.3 **7.4**

Entry [a]	$PhIX_2$ (equiv)	TEMPO (equiv)	% SM Consumption[b]	% Yield[b]
1	$PhI(OAc)_2$ (2.0)	–	64	32
2	$PhI(OAc)_2$ (2.0)	TEMPO (0.5)	60	41
3	$PhI(TFA)_2$ (2.0)	TEMPO (0.5)	84	0

[a] Conditions: enaminone **7.3** (0.1 mmol), $TMSCF_3$ (4.0 equiv), $Pd(OAc)_2$ (10 mol %), CsF (4.0 equiv), $PhIX_2$, TEMPO in MeCN (1 mL) at rt for 24 h. [b] ^1H NMR yields with Ph_3SiMe (1.0 equiv) as the internal standard.

7.3.2 Further optimization

7.3.2.1 Ligand selection

We first surveyed a series of *N*-containing ligands (Table 7-5). The yields of **7.4** revealed the beneficial effect of ligands compared to the ligandless conditions (32%, entry 12). Although these data do not provide definitive information on the best class of ligands, oxazole-based bidentate ligands (**L4**–**L7**) showed relatively higher yields (entries 4–7). In particular, indenooxazole ligand **L4** offered the highest yield at 61% (entry 4).

7.3.2.2 Solvent survey

Table 7-6 shows the survey results of nine solvents. To our surprise, more polar solvents, such as DMSO and NMP, only furnished a trace amount of **7.4** (entries 1–2). DMF and acetone (entries 3–4) did not provide comparable yields to that of MeCN (61%,

entry 5). Interestingly, using EtOAc as a medium offer a better yield (68%, entry 6). Further attempts involving dioxane, THF and DCM did not increase the formation of **7.4** (entries 7–9).

Table 7-5. Ligand effect on C–H trifluoromethylation of cyclic enaminone **7.3**

Entry [a]	**L** (15 mol%)	% SM Consumption[b]	% Yield[b]
1	**L1**	75	46
2	**L2**	41	6
3	**L3**	41	8
4	**L4**	**69**	**61**
5	**L5**	71	51
6	**L6**	68	57
7	**L7**	72	55
8	**L8**	69	51
9	**L9**	67	49
10	**L10**	69	56
11	**L11**	72	54
12	–	64	32

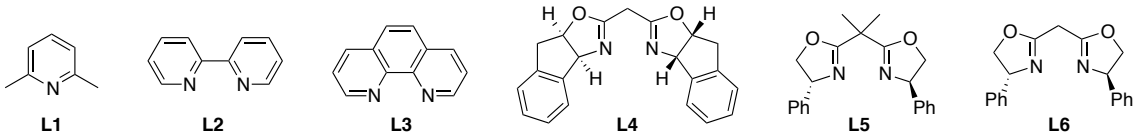

[a] Conditions: enaminone **7.3** (0.1 mmol), $TMSCF_3$ (4.0 equiv), $Pd(OAc)_2$ (10 mol %), ligand (15 mol %), $PhI(OAc)_2$ (2 equiv), CsF (4.0 equiv), TEMPO (0.5 equiv) in MeCN (1 mL) at rt for 24 h. [b] ^1H NMR yields with Ph_3SiMe (1.0 equiv) as the internal standard.

Table 7-6. Solvent effect on C–H trifluoromethylation of cyclic enaminone **7.3**

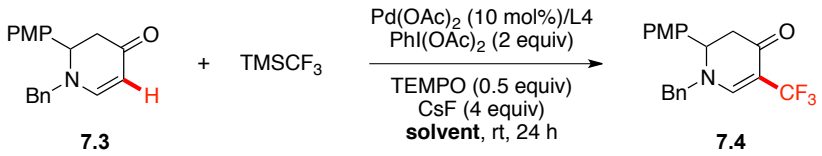

Entry[a]	Solvent (1 mL)	% SM Consumption[b]	% Yield[b]
1	DMSO	17	3
2	NMP	22	3
3	DMF	43	31
4	acetone	22	11
5	MeCN	69	61
6	EtOAc	**76**	**68**
7	dioxane	48	19
8	THF	33	9
9	DCM	70	37

[a] Conditions: enaminone **7.3** (0.1 mmol), $TMSCF_3$ (4.0 equiv), $Pd(OAc)_2$ (10 mol %), **L4** (15 mol %), $PhI(OAc)_2$ (2 equiv), CsF (4.0 equiv), TEMPO (0.5 equiv) in solvent (1 mL) at rt for 24 h. [b] ^1H NMR yields with Ph_3SiMe (1.0 equiv) as the internal standard.

7.3.2.3 Oxidant screen

In addition to phenyliodine diacetate (PIDA), seven other oxidants were examined for their effectiveness (Table 7-7). Unfortunately, no other oxidant showed any reactivity. Strongly oxidizing reagents like PIFA and Selectfluor largely decomposed **7.3** without any conversion to **7.4** (entries 2–3). The other oxidants showed total reaction inhibition (entries 4–8).

7.3.2.4 Base effect

We also found that the choice of the metal cation for the F^- sources was crucial (Table 7-8). Main group I metals (*i.e.* Na^+, K^+ and Cs^+) were examined and only KF and CsF afforded **7.4** (entries 1–3). Other fluoride salts, such as AgF, CuF_2, ZnF_2 and NiF_2,

were not effective either (entries 4–7). The commonly used TBAF also proved to be unsuitable (entry 8). We also tested a few non-fluoride metal salts (entries 9–11), and only K_3PO_4 provided **7.4** but with an inferior yield of 20% (entry 9).

Table 7-7. Oxidant screen for C–H trifluoromethylation of cyclic enaminone **7.3**

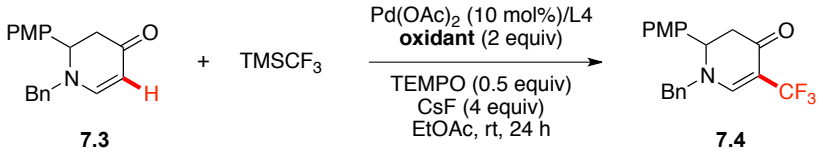

Entry[a]	Oxidant (2.0 equiv)	% SM Consumption[b]	% Yield[b]
1	$PhI(OAc)_2$	**86**	**69**
2	$PhI(TFA)_2$	89	0
3	Selectfluor	100	0
4	duroquinone	5	0
5	$K_2S_2O_8$	4	0
6	Oxone	5	0
7	$Cu(OAc)_2$	6	0
8	AgOAc	5	0

[a] Conditions: enaminone **7.3** (0.1 mmol), $TMSCF_3$ (4.0 equiv), $Pd(OAc)_2$ (10 mol %), **L4** (15 mol %), oxidant (2 equiv), CsF (4.0 equiv), TEMPO (0.5 equiv) in EtOAc (1 mL) at rt for 24 h. [b] ^1H NMR yields with Ph_3SiMe (1.0 equiv) as the internal standard.

7.3.2.5 Additive effect

Next, a series of additives were introduced to the reaction conditions (Table 7-9). $Yb(OTf)_3$ presented a beneficial effect in an earlier example of aryltrifluoromethylation of alkenes,[519] but significantly inhibited the current trifluoromethylation of **7.3** (14%, entry 2). Weak carboxylic acids, especially benzoic acid, increased the yield to 68% (entries 3–4). As reported earlier, radical side reactions were observed with indoles.[519] We thus tested a few radical scavengers, such as TEMPO and 2,6-di-*t*-butyl-4-methylphenol (entries 5–6). Intriguingly, 2,6-di-*t*-butyl-4-methylphenol failed to improve the yield, while TEMPO increased the yield to 69%. Following attempts to find the most

effective concentration of TEMPO quickly revealed a deleterious effect from TEMPO, whereby 2.0 equiv of TEMPO caused a total inhibition of trifluoromethylation (entry 6–9). Therefore, 0.5 equiv of TEMPO turned out to be the most effective additive.

Table 7-8. Base screen for C–H trifluoromethylation of cyclic enaminone **7.3**

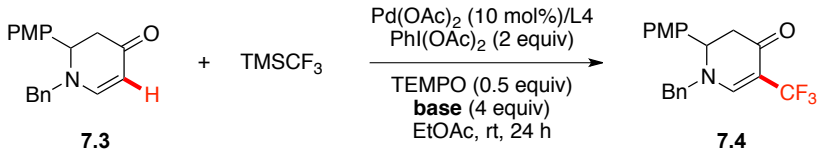

Entry[a]	Base (4.0 equiv)	% SM Consumption[b]	% Yield[b]
1	NaF	73	0
2	KF	87	61
3	CsF	**86**	**69**
4	AgF	43	0
5	ZnF_2	64	0
6	NiF_2	70	0
7	CuF_2	70	0
8	TBAF	26	0
9	K_3PO_4	83	20
10	K_2CO_3	64	0
11	NaOAc	77	0

[a] Conditions: enaminone **7.3** (0.1 mmol), $TMSCF_3$ (4.0 equiv), $Pd(OAc)_2$ (10 mol %), **L4** (15 mol %), $PhI(OAc)_2$ (2 equiv), base (4.0 equiv), TEMPO (0.5 equiv) in EtOAc (1 mL) at rt for 24 h. [b] ^1H NMR yields with Ph_3SiMe (1.0 equiv) as the internal standard.

7.3.2.6 Temperature effect

Given the incomplete consumption of **7.3**, the reaction temperature was raised from room temperature to 80 ºC (Table 7-10). Unexpectedly, both the consumption rates and product yields were affected adversely. We presumed that the higher temperatures might weaken the stability of the palladated intermediate and cause more side reactions. Thus, reaction at room temperature proved to be the best of the conditions examined.

Table 7-9. Additive effect on C–H trifluoromethylation of cyclic enaminone **7.3**

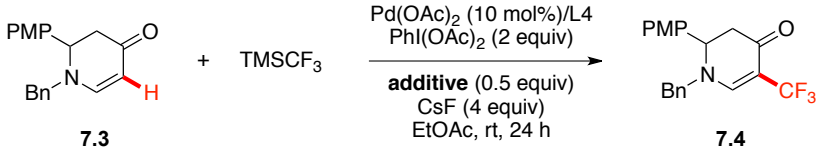

7.3 **7.4**

Entry[a]	Additive (equiv)	% SM Consumption[b]	% Yield[b]
1	–	86	58
2	$Yb(OTf)_3$ (0.5)	76	14
3	benzoic acid (0.5)	84	68
4	pivalic acid (0.5)	84	57
5	2,6-di-*t*-butyl-4-methylphenol (0.5)	70	49
6	TEMPO (0.5)	**86**	**69**
7	TEMPO (0.2)	89	60
8	TEMPO (1.0)	76	52
9	TEMPO (2.0)	27	0

[a] Conditions: enaminone **7.3** (0.1 mmol), $TMSCF_3$ (4.0 equiv), $Pd(OAc)_2$ (10 mol %), **L4** (15 mol %), $PhI(OAc)_2$ (2 equiv), CsF (4.0 equiv) and additive in EtOAc (1 mL) at rt for 24 h. [b] ^1H NMR yields with Ph_3SiMe (1.0 equiv) as the internal standard.

Table 7-10. Temperature effect on C–H trifluoromethylation of cyclic enaminone **7.3**

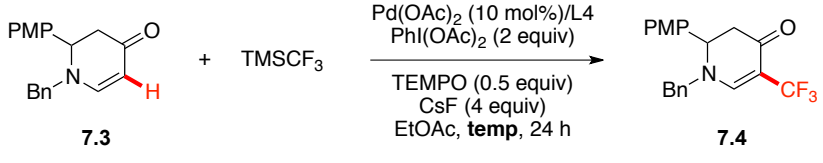

7.3 **7.4**

Entry[a]	Temp (ºC)	% SM Consumption[b]	% Yield[b]
1	rt	**86**	**69**
2	40	85	59
3	60	83	51
4	80	77	47

[a] Conditions: enaminone **7.3** (0.1 mmol), $TMSCF_3$ (4.0 equiv), $Pd(OAc)_2$ (10 mol %), **L4** (15 mol %), $PhI(OAc)_2$ (2 equiv), CsF (4.0 equiv) and TEMPO (0.5 equiv) in EtOAc (1 mL) for 24 h. [b] ^1H NMR yields with Ph_3SiMe (1.0 equiv) as the internal standard.

7.3.2.7 Choice of catalyst

Table 7-11. Catalyst choice for C–H trifluoromethylation of cyclic enaminone **7.3**

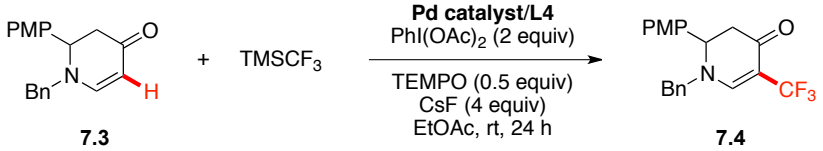

Entry[a]	Pd Catalyst/**L** (mol %)	% SM Consumption[b]	% Yield[b]
1	$PdCl_2$/**L4** (10/15)	77	61
2	$Pd(TFA)_2$/**L4** (10/15)	84	67
3	$Pd(OAc)_2$/**L4** (10/15)	**86**	**69 (70[c])**
4	$Pd(OAc)_2$/**L4** (5/7.5)	80	60
5	$Pd(OAc)_2$/**L4** (15/22.5)	84	62
6	$Pd(OAc)_2$/**L4** (20/30)	80	60
7	–	**78**	**60**

[a] Conditions: enaminone **7.3** (0.1 mmol), $TMSCF_3$ (4.0 equiv), Pd catalyst and **L4** (1:1.5) $PhI(OAc)_2$ (2 equiv), CsF (4.0 equiv) and TEMPO (0.5 equiv) in EtOAc (1 mL) at rt for 24 h. [b] ^1H NMR yields with Ph_3SiMe (1.0 equiv) as the internal standard. [c] Isolated yield.

Lastly, we screened a few common Pd^{II} catalysts in addition to $Pd(OAc)_2$ (Table 7-11). According to the yields, $PdCl_2$ showed inferior catalytic efficacy, while $Pd(TFA)_2$ afforded comparable outcome to reaction with $Pd(OAc)_2$ (entries 1–3). Attempts to manipulate the Pd loading indicated no or little correlation between the yield and the Pd loading (entries 3–6). This prompted us to evaluate the feasibility of metal-free conditions (entry 7). As anticipated, a moderate yield (60%) was recorded in the absence of the catalyst and ligand.

7.4 Mechanistic implication

The comparable yield (60%) from the metal-free conditions (Table 7-11, entry 7) prompted us to reevaluate our results. We propose two competing pathways (Figure 7-1). Alongside with the Pd^{II}/Pd^{IV} catalysis (path **a**), a PIDA-mediated process (path **b**) is also feasible. However, the almost identical results from Table 7-11 entry 1 and entry 7

suggest that $PdCl_2$ essentially had no catalytic activity towards **7.3**. The beneficial effect from adding $Pd(TFA)_2$ and $Pd(OAc)_2$ is not significant either (within 10% yield increase, Table 7-11, entries 2–3), indicating that Pd catalysis only played a minor role in the C–H trifluoromethylation. Path **b** is likely to be more favorable in the competing processes.

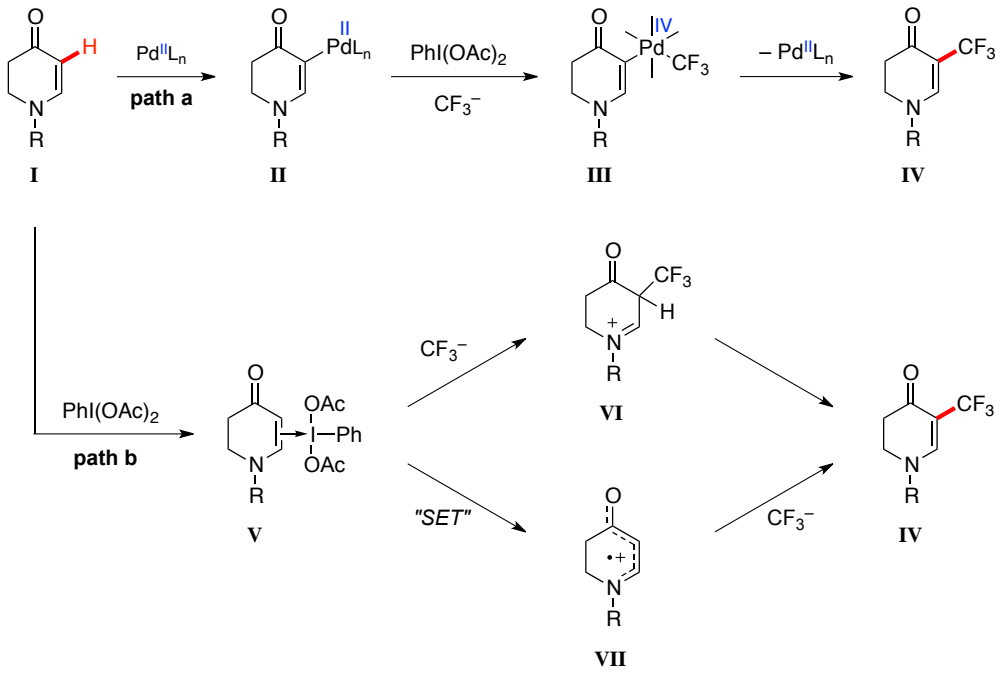

Figure 7-1. Plausible mechanisms for C–H trifluoromethylation of cyclic enaminones.

Under ligandless conditions we observed a 32% yield of **7.4** (Table 7-5, entry 12), lower than that (61%) from the equivalent conditions in the presence of ligand **L4** (Table 7-5, entry 4). We presume that the lack of ligands significantly destabilized the active Pd^{IV} intermediate **III**, whose decomposition resulted in decreased formation of **IV**.

On the other hand, although ligands are essential to stabilize intermediate **III**, they unfortunately seem to retard the palladation process to form **II**. The mechanistic study in Chapter 4 (section 4.5) revealed fast palladation between $Pd(OAc)_2$ and enaminone **7.3** *in the absence of ligands*. We postulate that ligands would reduce the electrophilicity of the Pd^{II} center and thus hamper the fast palladation, resulting in impeding path **a** and directing trifluoromethylation towards path **b**. This detrimental effect of ligands was also seen in our C–H arylation project (Chapter 3, section 3.3.2). Hence, the direct

trifluoromethylation of cyclic enaminones by Pd catalysis is overall not favored compared to the metal-free PIDA-mediated protocol.

The key for the high reactivity of PIDA is the strong electrophilicity of the hypervalent iodine(III) center, which is complementary in nature to the strong nucleophilicity of the cyclic enaminones. Two tentative mechanisms are plausible for the metal-free protocol (path **b**). One is the nucleophilic substitution via intermediate **VI**, while the other is a single-electron-transfer (SET) process via intermediate **VII**.[539-543] Although the mechanism is yet to be elucidated, the total reaction inhibition caused by 2.0 equiv of TEMPO may indicate a radical-based process (Table 7-9, entry 9).

It is worth noting that metal-free $PhI(OAc)_2$-mediated C–H trifluoromethylation of arenes has been reported very recently.[539] We reckon it is more advantageous to devise a green and mild trifluoromethylation method for cyclic enaminones under metal-free conditions at room temperature. The ensuing development is being conducted by Adwait Ranade in our laboratory.

7.5 Summary

Our preliminary study on C–H trifluoromethylation has showed good yields from both electron-rich and electron-deficient cyclic enaminones. A Pd^{IV}-catalyzed protocol was initially studied employing electron-rich enaminones. However, we later found that the key effective ingredient was $PdI(OAc)_2$, which led to the discovery of a metal-free protocol with comparable yields. In addition, a Ru-catalyzed photoredox protocol was found very effective for electron-deficient enaminones. It is the first time that we are able to functionalize the C5–H bond on electron-deficient enaminones. Further studies are underway.

Chapter 8 Experimental Data

8.1 General information

All reactions were carried out in clear vials used without drying the vial. All chemicals were purchased and were directly used without further purification. Anhydrous solvents were used as purchased without further drying. Flash column chromatography was carried out on silica gel (230–400 mesh). TLC was conducted on 250 micron, F_{254} silica gel plates. ^{1}H NMR spectra were recorded at 400 MHz and ^{13}C NMR spectra at 100 MHz with complete proton decoupling. Chemical shifts are reported as ppm relative to chloroform ($CHCl_3$: 7.26 ppm for ^{1}H, 77.16 ppm for ^{13}C). Data are reported as follows: chemical shift, multiplicity (s = singlet, d = doublet, t = triplet, q = quartet, br = broad, m = multiplet), coupling constants (Hz) and integration. IR Spectra of liquids were directly taken on a NaCl plate. IR spectra of solids were obtained by dissolving the sample in CH_2Cl_2 on a NaCl plate. High-resolution mass spectrometry was performed on an ESI-TOF instrument. Melting points were uncorrected.

8.2 Preparation of starting materials

8.2.1 Synthesis of *N*-benzyl-2-(*p*-methoxyphenyl)-2,3-dihydropyridin-4(1*H*)-one

Step 1) Preparation of *N*-benzyl-4-pyridone

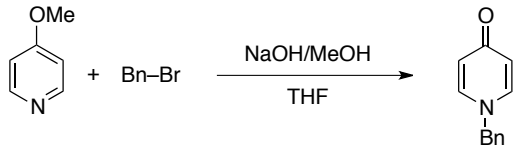

To a solution of 4-methoxypyridine (10.2 mL, 100 mmol) in THF (50 mL) was added benzyl bromide (11.9 mL, 100 mmol). After the reaction was stirred for 2 h, a 10% w/w solution of NaOH in MeOH (125 mL) was added into the reaction vessel over 30 min at 0 °C. The reaction mixture was stirred for another 2 h at ambient temperature. The reaction mixture was then concentrated under reduced pressure. To the residue was added water (30 mL) and the product was extracted with CH_2Cl_2 (15 mL × 4). The combined organic

layers were dried over Na_2SO_4, filtered, and concentrated under reduced pressure. The crude product was purified using flash column chromatography (5% MeOH in CH_2Cl_2) to yield 8.71 g (47%) of *N*-benzyl-4-pyridone as a light yellow solid (mp 115–119 °C). ^{1}H NMR (400 MHz, $CDCl_3$) δ 7.38–7.40 (m, 3H), 7.31 (d, *J* = 8.0 Hz, 2H), 7.18 (d, *J* = 8.0 Hz, 2H), 6.38 (d, *J* = 8.0 Hz, 2H), 4.93 (s, 2H); ^{13}C NMR (100 MHz, $CDCl_3$) δ 178.6, 140.1, 134.7, 129.4, 129.0, 127.4, 118.8, 60.2; FTIR (Film, cm^{-1}) 3049, 2977, 1640, 1567, 1454, 1405, 1179, 851; HRMS (ESI+) *m/z* calculated for $[M+H]^+$ $C_{12}H_{12}NO$: 186.0919, found 186.0906.

Step 2) Preparation of *N*-benzyl-2-(*p*-methoxyphenyl)-2,3-dihydropyridin-4(1*H*)-one

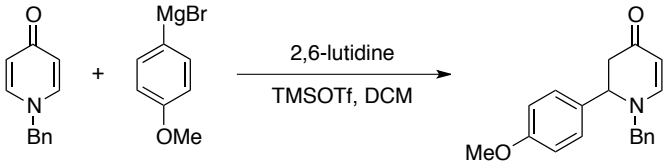

N-Benzyl-4-pyridone (5.0 g, 26.99 mmol) in dry CH_2Cl_2 (50 mL) was treated with TMSOTf (10.5 mL, 53.97 mmol) at room temperature under a N_2 atmosphere. After the reaction was stirred for 1 h, 2,6-lutidine (6.3 mL, 53.97 mmol) was added, followed by slow addition of a 0.5 M solution of *p*-methoxyphenylmagnesium bromide in THF (81.0 mL, 40.49 mmol) with a syringe pump. The reaction was stirred for another 2 h and then quenched with saturated NH_4Cl (15 mL). The mixture was extracted with CH_2Cl_2 (15 mL × 4). The combined organic layers were dried over Na_2SO_4, filtered, and concentrated under reduced pressure. Further purification was carried out by flash column chromatography (3:2 EtOAc/hexanes) to produce 4.0 g (51%) of *N*-benzyl-2-(*para*-methoxyphenyl)-2,3-dihydropyridin-4(1*H*)-one as an orange oil. ^{1}H NMR (400 MHz, $CDCl_3$) δ 7.31–7.37 (m, 3H), 7.27 (d, *J* = 8.0 Hz, 1H), 7.16 (d, *J* = 8.0 Hz, 2H), 7.11 (d, *J* = 8.0 Hz, 2H), 6.87 (d, *J* = 8.0 Hz, 2H), 5.08 (d, *J* = 8.0 Hz, 1H), 4.45 (t, *J* = 8.0 Hz, 1H), 4.31 (d, *J* = 16.0 Hz, 1H), 4.11 (d, *J* = 16.0 Hz, 1H), 3.81 (s, 3H), 2.79 (dd, *J* = 16.0, 8.0 Hz, 1H), 2.68 (dd, *J* = 16.0, 8.0 Hz, 1H); ^{13}C NMR (100 MHz, $CDCl_3$) δ 190.6, 159.5, 154.3, 135.9, 130.5, 128.9, 128.4, 128.2, 127.7, 114.3, 98.5, 60.2, 57.0, 55.3, 43.7;

FTIR (Film, cm^{-1}) 3031, 2931, 2837, 1637, 1590, 1512, 1251, 1174, 1032, 834; HRMS (ESI+) *m/z* calculated for $[M+H]^+$ $C_{19}H_{20}NO_2$: 294.1494, found 294.1476.

8.2.2 Synthesis of *N*-benzyl-2-isopropyl-2,3-dihydropyridin-4(1*H*)-one

Step 1) Preparation of *N*-benzyl-4-pyridone (the same as in Section 8.2.1)

Step 2) Preparation of *N*-benzyl-2-isopropyl-2,3-dihydropyridin-4(1*H*)-one

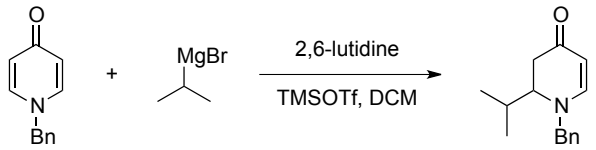

N-Benzyl-4-pyridone (3.0 g, 16.20 mmol) in dry CH_2Cl_2 (30 mL) was treated with TMSOTf (6.3 mL, 32.39 mmol) at room temperature under a N_2 atmosphere. After the reaction was stirred for 1 h, 2,6-lutidine (3.8 mL, 32.39 mmol) was added, followed by slow addition of a 2.0 M solution of isopropylmagnesium bromide in THF (12.2 mL, 24.29 mmol) with a syringe pump. The reaction was stirred for another 2 h and then quenched with saturated NH_4Cl (15 mL). The mixture was extracted with CH_2Cl_2 (15 mL × 4). The combined organic layers were dried over Na_2SO_4, filtered, and concentrated under reduced pressure. Further purification was carried out by flash column chromatography (3:1 EtOAc/hexanes) to produce 2.1 g (57%) of *N*-benzyl-2-isopropyl-2,3-dihydropyridin-4(1*H*)-one as an orange oil. ^{1}H NMR (400 MHz, $CDCl_3$) δ 7.41–7.30 (m, 3H), 7.29–7.24 (m, 2H), 7.12 (d, *J* = 7.4 Hz, 1H), 4.91 (d, *J* = 7.4 Hz, 1H), 4.47 (d, *J* = 15.4 Hz, 1H), 4.39 (d, *J* = 15.4 Hz, 1H), 3.22 (td, *J* = 6.9, 4.0 Hz, 1H), 2.60 (dd, *J* = 16.7, 7.5 Hz, 1H), 2.39 (dd, *J* = 16.7, 3.8 Hz, 1H), 2.28 (dq, *J* = 13.4, 6.7 Hz, 1H), 0.95 (d, *J* = 6.8 Hz, 6H); ^{13}C NMR (100 MHz, $CDCl_3$) δ 191.3, 153.7, 137.0, 129.2, 128.4, 127.4, 97.5, 61.4, 58.8, 36.5, 29.1, 19.8, 18.1; FTIR (Film, cm^{-1}) 3054, 2984, 2876, 1635, 1591, 1496, 1455, 1441, 1421, 1387, 1357, 1344, 1204, 1166, 1094, 1077, 1029, 1014, 1002, 955, 896; HRMS (ESI+) *m/z* calculated for $[M+Na]^+$ $C_{15}H_{19}NONa$: 252.1359, found 252.1354.

8.2.3 Synthesis of other cyclic enaminones

Other cyclic enaminones were prepared according to the reported procedures (Scheme 8-1).[24, 50, 51, 79-81, 544-546]

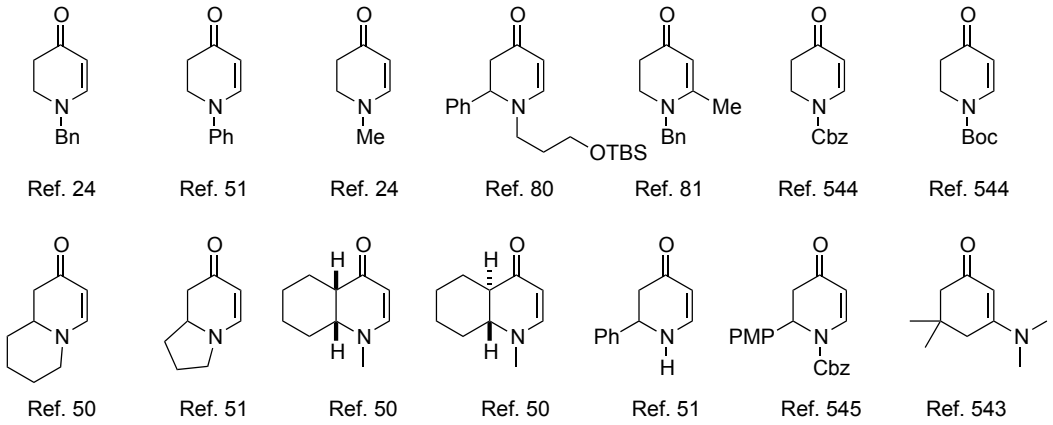

Scheme 8-1. References for enaminone preparation.

8.2.4 Synthesis of uracils

Uracil and 1,3-dimethyluracil are commercially available. Other uracil derivatives were prepared according to the corresponding procedures (Scheme 8-2).[416-423, 425]

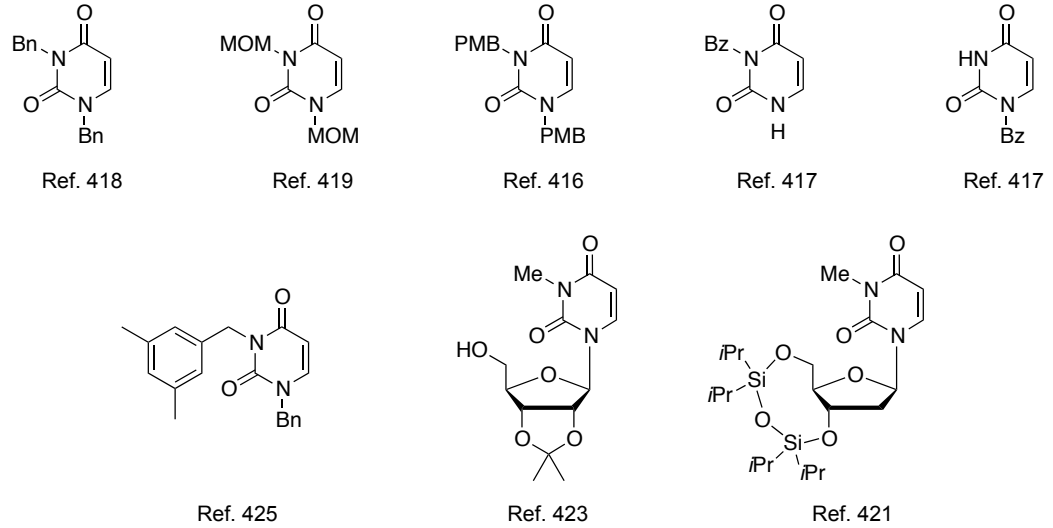

Scheme 8-2. References for uracil preparation.

8.3 Chapter 3

8.3.1 General procedure for the direct C–H arylation of cyclic enaminones

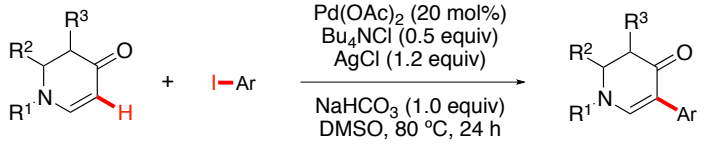

In a clear 1-dram vial, cyclic enaminone (0.1 mmol), aryl iodide (0.3 mmol, 3.0 equiv), $Pd(OAc)_2$ (4.5 mg, 0.02 mmol, 20 mol %), Bu_4NCl (13.9 mg, 0.05 mmol, 0.5 equiv), $NaHCO_3$ (8.4 mg, 0.1 mmol, 1.0 equiv), and AgCl (17.2 mg, 0.12 mmol, 1.2 equiv) were mixed in DMSO (0.5 mL). The reaction vessel was then capped and stirred at 80 °C for 24 h, and then cooled to room temperature. The mixture was filtered through a pad of Celite (washed with EtOAc). The filtrate was concentrated under reduced pressure and purified by flash column chromatography.

8.3.2 Compound characterization

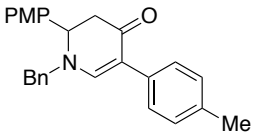

1-Benzyl-2-(4-methoxyphenyl)-5-(*p*-tolyl)-2,3-dihydropyridin-4(1*H*)-one (3.8). Prepared by the general procedure described above and purified by flash column chromatography (30% EtOAc in hexanes) on silica gel to provide 27.3 mg (72%) as an orange wax. Spectroscopic data are consistent with those from our previous report.[81]

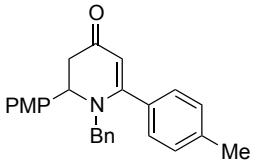

1-Benzyl-2-(4-methoxyphenyl)-6-(*p*-tolyl)-2,3-dihydropyridin-4(1*H*)-one (3.9). A side product (2–18%) during the optimization study and purified by flash column chromatography (25% EtOAc in hexanes) on silica gel as a yellow wax. ^{1}H NMR (400

MHz, $CDCl_3$) δ 7.40–7.20 (m, 9H overlapping with $CHCl_3$), 7.15 (d, *J* = 6.8 Hz, 2H), 6.89 (d, *J* = 8.7 Hz, 2H), 5.17 (s, 1H), 4.76 (d, *J* = 15.7 Hz, 1H), 4.61 (dd, *J* = 7.3, 4.0 Hz, 1H), 3.99 (d, *J* = 15.7 Hz, 1H), 3.81 (s, 3H), 2.97 (dd, *J* = 16.5, 7.4 Hz, 1H), 2.61 (dd, *J* = 16.7, 3.9 Hz, 1H), 2.38 (s, 3H); ^{13}C NMR (100 MHz, $CDCl_3$) δ 190.1, 164.9, 159.4, 140.0, 137.8, 133.6, 131.3, 129.6, 129.0, 128.0, 128.0, 127.8, 127.2, 114.4, 102.8, 59.4, 55.5, 53.9, 42.6, 21.5; FTIR (NaCl, cm^{-1}) 3054, 2987, 1639, 1598, 1513, 1442, 1179, 1032, 896; HRMS (ESI+) *m/z* calculated for $[M+H]^+$ $C_{26}H_{26}NO_2$: 384.1963, found 384.1969.

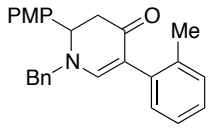

1-Benzyl-2-(4-methoxyphenyl)-5-(*o*-tolyl)-2,3-dihydropyridin-4(1*H*)-one (3.10). Prepared by the general procedure described above and purified by flash column chromatography (25% EtOAc in hexanes) on silica gel to provide 16.9 mg (43%) as a yellow solid (mp 139–142 °C). ^{1}H NMR (400 MHz, $CDCl_3$) δ 7.32–7.22 (m, 4H overlapping with $CHCl_3$), 7.18–7.03 (m, 8H), 6.83 (d, *J* = 8.6 Hz, 2H), 4.48 (t, *J* = 7.6 Hz, 1H), 4.27 (d, *J* = 15.1 Hz, 1H), 4.10 (d, *J* = 15.1 Hz, 1H), 3.75 (s, 3H), 2.85 (dd, *J* = 16.3, 6.7 Hz, 1H), 2.76 (dd, *J* = 16.3, 8.7 Hz, 1H), 2.16 (s, 3H); ^{13}C NMR (100 MHz, $CDCl_3$) δ 187.7, 159.7, 154.0, 138.2, 136.2, 136.0, 130.6, 130.2, 129.1, 128.6, 128.5, 128.3, 127.9, 127.2, 125.8, 114.5, 112.6, 60.7, 57.3, 55.5, 44.4, 20.7; FTIR (NaCl, cm^{-1}) 3054, 2987, 1638, 1596, 1551, 1422, 1157, 1029, 896; HRMS (ESI+) *m/z* calculated for $[M+Na]^+$ $C_{26}H_{25}NO_2Na$: 406.1783, found 406.1779.

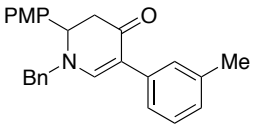

1-Benzyl-2-(4-methoxyphenyl)-5-(*m*-tolyl)-2,3-dihydropyridin-4(1*H*)-one (3.11). Prepared by the general procedure described above and purified by flash column chromatography (30% EtOAc in hexanes) on silica gel to provide 27.2 mg (72%) as a

yellow wax. ^{1}H NMR (400 MHz, $CDCl_3$) δ 7.53 (s, 1H), 7.34 (td, *J* = 18.5, 15.9, 9.5 Hz, 4H), 7.25–7.14 (m, 6H), 7.07–6.99 (m, 1H), 6.89 (d, *J* = 8.5 Hz, 2H), 4.52 (t, *J* = 7.5 Hz, 1H), 4.41 (d, *J* = 15.1 Hz, 1H), 4.21 (d, *J* = 15.1 Hz, 1H), 3.82 (s, 3H), 2.95 (dd, *J* = 16.2, 6.8 Hz, 1H), 2.82 (dd, *J* = 16.2, 8.3 Hz, 1H), 2.37 (s, 3H); ^{13}C NMR (100 MHz, $CDCl_3$) δ 188.0, 159.7, 153.3, 137.8, 136.1, 130.6, 129.1, 128.6, 128.6, 128.5, 128.3, 128.3, 127.8, 126.7, 124.8, 114.5, 111.4, 60.4, 57.5, 55.5, 44.6, 21.7; FTIR (NaCl, cm^{-1}) 3054, 2987, 1639, 1598, 1513, 1422, 1179, 1035, 896; HRMS (ESI+) *m/z* calculated for $[M+Na]^+$ $C_{26}H_{25}NO_2Na$: 406.1783, found 406.1779.

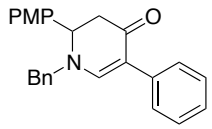

1-Benzyl-2-(4-methoxyphenyl)-5-phenyl-2,3-dihydropyridin-4(1*H*)-one (3.12). Prepared by the general procedure described above and purified by flash column chromatography (30% EtOAc in hexanes) on silica gel to provide 24.8 mg (68%) as a yellow oil. Spectroscopic data are consistent with those from our previous report.[81]

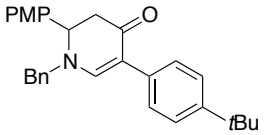

1-Benzyl-5-(4-(*tert*-butyl)phenyl)-2-(4-methoxyphenyl)-2,3-dihydropyridin-4(1*H*)-one (3.13). Prepared by the general procedure described above and purified by flash column chromatography (25% EtOAc in hexanes) on silica gel to provide 27.9 mg (66%) as a yellow wax. ^{1}H NMR (400 MHz, $CDCl_3$) δ 7.53 (s, 1H), 7.43–7.29 (m, 7H), 7.24–7.14 (m, 4H), 6.88 (d, *J* = 8.7 Hz, 2H), 4.52 (t, *J* = 7.5 Hz, 1H), 4.40 (d, *J* = 15.1 Hz, 1H), 4.20 (d, *J* = 15.1 Hz, 1H), 3.82 (s, 3H), 2.96 (dd, *J* = 16.2, 6.8 Hz, 1H), 2.83 (dd, *J* = 16.2, 8.4 Hz, 1H), 1.33 (s, 9H); ^{13}C NMR (100 MHz, $CDCl_3$) δ 188.1, 159.7, 153.1, 148.7, 136.1, 133.2, 130.7, 129.1, 128.5, 128.3, 127.9, 127.4, 125.3, 114.5, 111.3, 60.5, 57.5, 55.5, 44.6, 34.5, 31.5; FTIR (NaCl, cm^{-1}) 3054, 2986, 1637, 1598, 1513, 1422, 1376,

1358, 1306, 1179, 1130, 1034, 896, 837; HRMS (ESI+) *m/z* calculated for $[M+Na]^+$ $C_{29}H_{31}NO_2Na$: 448.2252, found 448.2259.

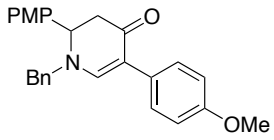

1-Benzyl-2,5-bis(4-methoxyphenyl)-2,3-dihydropyridin-4(1*H*)-one (3.14). Prepared by the general procedure described above and purified by flash column chromatography (50% EtOAc in hexanes) on silica gel to provide 29.2 mg (74%) as a yellow oil. Spectroscopic data are consistent with those from our previous report.[81]

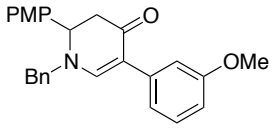

1-Benzyl-5-(3-methoxyphenyl)-2-(4-methoxyphenyl)-2,3-dihydropyridin-4(1*H*)-one (3.15). Prepared by the general procedure described above and purified by flash column chromatography (35% EtOAc in hexanes) on silica gel to provide 31.2 mg (79%) as a red oil. Spectroscopic data are consistent with those from our previous report.[81]

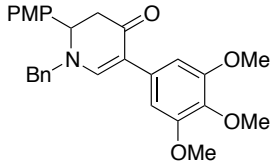

1-Benzyl-2-(4-methoxyphenyl)-5-(3,4,5-trimethoxyphenyl)-2,3-dihydropyridin-4(1*H*)-one (3.16). Prepared by the general procedure described above and purified by flash column chromatography (50% EtOAc in hexanes) on silica gel to provide 36.5 mg (80%) as a yellow solid (mp 125–128 °C). ^{1}H NMR (400 MHz, $CDCl_3$) δ 7.51 (s, 1H), 7.39–7.31 (m, 3H), 7.23–7.14 (m, 4H), 6.89 (d, *J* = 8.6 Hz, 2H), 6.67 (s, 2H), 4.52 (t, *J* = 7.5 Hz, 1H), 4.42 (d, *J* = 15.1 Hz, 1H), 4.22 (d, *J* = 15.1 Hz, 1H), 3.87 (s, 6H), 3.83 (s, 3H), 3.81 (s, 3H), 2.95 (dd, *J* = 16.2, 6.8 Hz, 1H), 2.81 (dd, *J* = 16.2, 8.2 Hz, 1H); ^{13}C NMR (100 MHz, $CDCl_3$) δ 188.0, 159.8, 153.1, 136.5, 136.0, 131.9, 130.5, 129.1, 128.5,

128.5, 128.4, 127.9, 114.6, 111.0, 105.2, 61.0, 60.4, 57.5, 56.3, 55.5, 44.6; FTIR (NaCl, cm^{-1}) 3054, 2987, 2840, 1639, 1598, 1583, 1512, 1422, 1357, 1327, 1129, 1034, 1005, 896; HRMS (ESI+) *m/z* calculated for $[M+H]^+$ $C_{28}H_{30}NO_5$: 460.2118, found 460.2126.

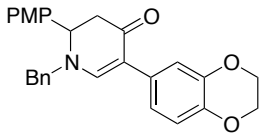

1-Benzyl-5-(2,3-dihydrobenzo[*b*][1,4]dioxin-6-yl)-2-(4-methoxyphenyl)-2,3-dihydropyridin-4(1*H*)-one (3.17). Prepared by the general procedure described above and purified by flash column chromatography (40% EtOAc in hexanes) on silica gel to provide 35.4 mg (83%) as an orange wax. ^{1}H NMR (400 MHz, $CDCl_3$) δ 7.46 (s, 1H), 7.39–7.30 (m, 3H), 7.20–7.14 (m, 4H), 6.98–6.81 (m, 5H), 4.50 (dd, *J* = 8.4, 6.8 Hz, 1H), 4.37 (d, *J* = 15.1 Hz, 1H), 4.24 (s, 4H), 4.17 (d, *J* = 15.1 Hz, 1H), 3.81 (s, 3H), 2.92 (dd, *J* = 16.2, 6.7 Hz, 1H), 2.80 (dd, *J* = 16.2, 8.6 Hz, 1H); ^{13}C NMR (100 MHz, $CDCl_3$) δ 188.1, 159.7, 152.9, 143.3, 142.0, 136.1, 130.6, 129.7, 129.1, 128.5, 128.3, 127.8, 121.1, 117.0, 116.7, 114.5, 111.0, 108.8, 64.5, 60.5, 57.4, 55.5, 44.6; FTIR (NaCl, cm^{-1}) 3155, 2935, 1635, 1597, 1583, 1511, 1459, 1442, 1377, 1357, 1315, 1298, 1282, 1250, 1178, 1127, 1071, 1036, 834; HRMS (ESI+) *m/z* calculated for $[M+Na]^+$ $C_{27}H_{25}NO_4Na$: 450.1681, found 450.1684.

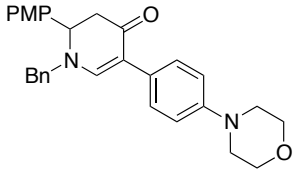

1-Benzyl-2-(4-methoxyphenyl)-5-(4-morpholinophenyl)-2,3-dihydropyridin-4(1*H*)-one (3.18). Prepared by the general procedure described above and purified by flash column chromatography (70% EtOAc in hexanes) on silica gel to provide 33.9 mg (75%) as a yellow oil. ^{1}H NMR (400 MHz, $CDCl_3$) δ 7.47 (s, 1H), 7.38–7.30 (m, 5H), 7.23–7.12 (m, 4H), 6.92–6.86 (m, 4H), 4.51 (t, *J* = 7.6 Hz, 1H), 4.38 (d, *J* = 15.1 Hz, 1H), 4.18 (d, *J* = 15.1 Hz, 1H), 3.86 (t, *J* = 4.6 Hz, 4H), 3.81 (s, 3H), 3.14 (t, *J* = 4.0 Hz, 4H), 2.93 (dd, *J*

= 16.3, 6.6 Hz, 1H), 2.82 (dd, *J* = 16.2, 8.7 Hz, 1H); ^{13}C NMR (100 MHz, $CDCl_3$) δ 188.3, 159.7, 152.7, 149.6, 136.2, 130.7, 129.1, 128.6, 128.6, 128.3, 127.8, 116.0, 114.5, 114.5, 111.3, 67.1, 60.6, 57.4, 55.4, 49.8, 44.7; FTIR (NaCl, cm^{-1}) 3155, 2967, 2901, 2839, 1794, 1634, 1595, 1514, 1452, 1380, 1307, 1231, 1177, 1121, 1035, 907; HRMS (ESI+) *m/z* calculated for $[M+H]^+$ $C_{29}H_{31}N_2O_3$: 455.2329, found 455.2324.

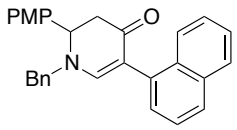

1-Benzyl-2-(4-methoxyphenyl)-5-(naphthalen-1-yl)-2,3-dihydropyridin-4(1*H*)-one (3.19). Prepared by the general procedure described above and purified by flash column chromatography (40% EtOAc in hexanes) on silica gel to provide 33.3 mg (80%) as a red wax. ^{1}H NMR (400 MHz, $CDCl_3$) δ 7.89–7.75 (m, 3H), 7.50–7.28 (m, 10H), 7.19 (d, *J* = 6.5 Hz, 2H), 6.95 (d, *J* = 8.5 Hz, 2H), 4.66 (t, *J* = 7.7 Hz, 1H), 4.38 (d, *J* = 15.1 Hz, 1H), 4.23 (d, *J* = 15.1 Hz, 1H), 3.86 (s, 3H), 3.06 (dd, *J* = 16.3, 6.5 Hz, 1H), 2.97 (dd, *J* = 16.2, 8.6 Hz, 1H); ^{13}C NMR (100 MHz, $CDCl_3$) δ 188.3, 159.8, 154.8, 136.1, 134.3, 134.0, 133.2, 130.5, 129.1, 128.6, 128.6, 128.4, 128.0, 128.0, 127.9, 127.7, 126.3, 125.7, 125.7, 114.6, 111.1, 60.7, 57.4, 55.6, 44.5; FTIR (NaCl, cm^{-1}) 3155, 3035, 2936, 2840, 1794, 1637, 1599, 1513, 1464, 1442, 1388, 1376, 1359, 1306, 1253, 1178, 1137, 1096, 1035, 834, 796; HRMS (ESI+) *m/z* calculated for $[M+Na]^+$ $C_{29}H_{25}NO_2Na$: 442.1783, found 442.1783.

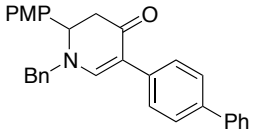

5-([1,1'-Biphenyl]-4-yl)-1-benzyl-2-(4-methoxyphenyl)-2,3-dihydropyridin-4(1*H*)-one (3.20). Prepared by the general procedure described above and purified by flash column chromatography (30% EtOAc in hexanes) on silica gel to provide 32.2 mg (73%) as a yellow wax. ^{1}H NMR (400 MHz, $CDCl_3$) δ 7.68–7.51 (m, 7H), 7.46–7.31 (m, 6H), 7.23–7.18 (m, 4H), 6.90 (d, *J* = 8.6 Hz, 2H), 4.55 (t, *J* = 7.5 Hz, 1H), 4.44 (d, *J* = 15.1

Hz, 1H), 4.23 (d, J = 15.1 Hz, 1H), 3.82 (s, 3H), 2.99 (dd, J = 16.2, 6.8 Hz, 1H), 2.86 (dd, J = 16.2, 8.2 Hz, 1H); ^{13}C NMR (100 MHz, $CDCl_3$) δ 188.0, 159.8, 153.1, 141.3, 138.6, 136.0, 135.3, 130.5, 129.1, 128.8, 128.5, 128.5, 128.4, 128.0, 127.9, 127.1, 127.1, 114.6, 110.9, 60.5, 57.6, 55.5, 44.6; FTIR (NaCl, cm^{-1}) 3054, 2087, 1638, 1597, 1513, 1488, 1421, 1357, 1179, 1126, 1035, 896; HRMS (ESI+) *m/z* calculated for $[M+Na]^+$ $C_{31}H_{27}NO_2Na$: 468.1939, found 468.1937.

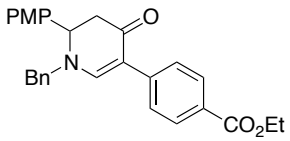

1-Benzyl-5-(4-(ethoxycarbonyl)phenyl)-2-(4-methoxyphenyl)-2,3-dihydropyridin-4(1*H*)-one (3.21). Prepared by the general procedure described above and purified by flash column chromatography (30% EtOAc in hexanes) on silica gel to provide 21.9 mg (50%) as a yellow wax. ^{1}H NMR (400 MHz, $CDCl_3$) δ 7.99 (d, J = 8.4 Hz, 2H), 7.64 (s, 1H), 7.55 (d, J = 8.4 Hz, 2H), 7.42–7.32 (m, 3H), 7.22–7.14 (m, 4H), 6.88 (d, J = 8.6 Hz, 2H), 4.55 (t, J = 7.3 Hz, 1H), 4.46 (d, J = 15.1 Hz, 1H), 4.36 (q, J = 7.1 Hz, 2H), 4.25 (d, J = 15.1 Hz, 1H), 3.81 (s, 3H), 2.98 (dd, J = 16.2, 6.9 Hz, 1H), 2.82 (dd, J = 16.2, 7.8 Hz, 1H), 1.39 (t, J = 7.1 Hz, 3H); ^{13}C NMR (100 MHz, $CDCl_3$) δ ^{13}C 187.7, 166.9, 159.9, 153.5, 141.1, 135.7, 130.2, 129.7, 129.2, 128.6, 128.4, 127.89, 127.4, 126.9, 114.6, 110.0, 60.8, 60.3, 57.8, 55.4, 44.5, 14.5; FTIR (NaCl, cm^{-1}) 3054, 2987, 1707, 1642, 1597, 1513, 1422, 1368, 1180, 1127, 1107, 1034, 896; HRMS (ESI+) *m/z* calculated for $[M+Na]^+$ $C_{28}H_{27}NO_4Na$: 464.1838, found 464.1832.

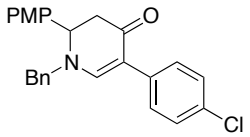

1-Benzyl-5-(4-chlorophenyl)-2-(4-methoxyphenyl)-2,3-dihydropyridin-4(1*H*)-one (3.22). Prepared by the general procedure described above and purified by flash column chromatography (25% EtOAc in hexanes) on silica gel to provide 20.3 mg (51%) as a yellow wax. Spectroscopic data are consistent with those from our previous report.[81]

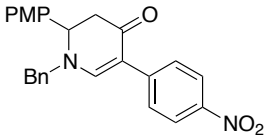

1-Benzyl-2-(4-methoxyphenyl)-5-(4-nitrophenyl)-2,3-dihydropyridin-4(1*H*)-one (3.23). Prepared by the general procedure described above and purified by flash column chromatography (30% EtOAc in hexanes) on silica gel to provide 13.0 mg (32%) as a bright yellow solid (mp 98–100 °C). Spectroscopic data are consistent with those from our previous report.[81]

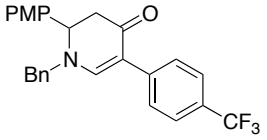

1-Benzyl-2-(4-methoxyphenyl)-5-(4-(trifluoromethyl)phenyl)-2,3-dihydropyridin-4(1*H*)-one (3.24). Prepared by the general procedure described above and purified by flash column chromatography (25% EtOAc in hexanes) on silica gel to provide 12.8 mg (30%) as a yellow wax. Spectroscopic data are consistent with those from our previous report.[81]

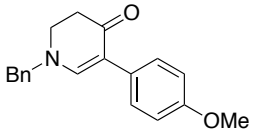

1-Benzyl-5-(4-methoxyphenyl)-2,3-dihydropyridin-4(1*H*)-one (3.26). Prepared by the general procedure described above and purified by flash column chromatography (70% EtOAc in hexanes) on silica gel to provide 22.6 mg (78%) as a yellow oil. Spectroscopic data are consistent with those from our previous report.[81]

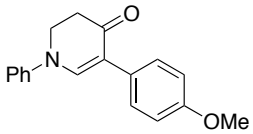

5-(4-Methoxyphenyl)-1-phenyl-2,3-dihydropyridin-4(1*H*)-one (3.27). Prepared by the general procedure described above and purified by flash column chromatography (50%

EtOAc in hexanes) on silica gel to provide 14.1 mg (50%) as an orange solid (mp 129–132 °C). Spectroscopic data are consistent with those from our previous report.[81]

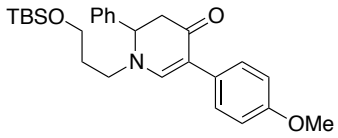

1-(3-((*tert*-Butyldimethylsilyl)oxy)propyl)-5-(4-methoxyphenyl)-2-phenyl-2,3-dihydropyridin-4(1*H*)-one (3.28). Prepared by the general procedure described above and purified by flash column chromatography (30% EtOAc in hexanes) on silica gel to provide 20.3 mg (45%) as a colorless oil. ^{1}H NMR (400 MHz, $CDCl_3$) δ 7.40 (s, 1H), 7.39–7.28 (m, 7H), 6.87 (d, J = 8.7 Hz, 2H), 4.67 (t, J = 7.4 Hz, 1H), 3.80 (s, 3H), 3.64 (t, J = 5.6 Hz, 2H), 3.37 (dt, J = 14.6, 7.4 Hz, 1H), 3.23 (dt, J = 13.6, 6.4 Hz, 1H), 3.01 (dd, J = 16.2, 6.7 Hz, 1H), 2.82 (dd, J = 16.2, 8.0 Hz, 1H), 1.72 (p, J = 6.3 Hz, 2H), 0.85 (s, 9H), 0.01 (s, 3H), -0.01 (s, 3H); ^{13}C NMR (100 MHz, $CDCl_3$) δ 187.6, 157.9, 153.3, 138.9, 129.2, 128.9, 128.9, 128.4, 127.0, 113.8, 110.8, 61.4, 59.4, 55.5, 50.5, 44.6, 31.7, 26.0, 18.3, -5.3; FTIR (NaCl, cm^{-1}) 3054, 2987, 2930, 2857, 1635, 1596, 1512, 1422, 1178, 1156, 1101, 1036, 896, 836; HRMS (ESI+) *m/z* calculated for $[M+Na]^+$ $C_{27}H_{37}NO_3SiNa$: 474.2440, found 474.2440.

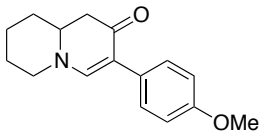

3-(4-Methoxyphenyl)-7,8,9,9a-tetrahydro-1*H*-quinolizin-2(6*H*)-one (3.29). Prepared by the general procedure described above and purified by flash column chromatography (50% EtOAc in hexanes) on silica gel to provide 16.0 mg (63%) as a yellow oil. Spectroscopic data are consistent with those from our previous report.[81]

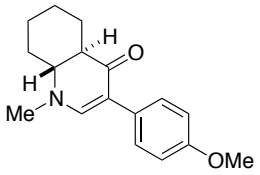

(4a*R*,8a*R*)-3-(4-Methoxyphenyl)-1-methyl-4a,5,6,7,8,8a-hexahydroquinolin-4(1*H*)-one (3.30). Prepared by the general procedure described above and purified by flash column chromatography (30% EtOAc in hexanes) on silica gel to provide 12.9 mg (48%) as a yellow wax. Spectroscopic data are consistent with those from our previous report.[81]

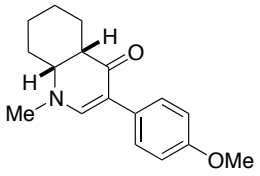

(4a*S*,8a*R*)-3-(4-Methoxyphenyl)-1-methyl-4a,5,6,7,8,8a-hexahydroquinolin-4(1*H*)-one (3.31). Prepared by the general procedure described above and purified by flash column chromatography (50% EtOAc in hexanes) on silica gel to provide 16.3 mg (60%) as a yellow wax. Spectroscopic data are consistent with those from our previous report.[81]

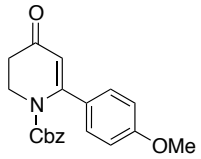

1-(Benzoxycarbonyl)-6-(4-methoxyphenyl)-2,3-dihydropyridin-4(1*H*)-one (3.37). Prepared by the general procedure described above and purified by flash column chromatography (30% EtOAc in hexanes) on silica gel to provide 20.3 mg (60%) as a yellow wax. ^{1}H NMR (400 MHz, $CDCl_3$) δ 7.35–7.18 (m, 5H), 6.92 (d, J = 6.7 Hz, 2H), 6.84 (d, J = 8.7 Hz, 2H), 5.71 (s, 1H), 5.00 (s, 2H), 4.28 (t, J = 6.4 Hz, 2H), 3.84 (s, 3H), 2.62 (t, J = 6.4 Hz, 2H); ^{13}C NMR (100 MHz, $CDCl_3$) δ 195.1, 161.6, 157.2, 154.1, 134.9, 129.2, 128.4, 128.2, 128.2, 128.1, 114.1, 113.4, 68.7, 55.6, 47.1, 38.4; FTIR (NaCl, cm^{-1}) 3155, 2983, 1794, 1714, 1659, 1607, 1589, 1568, 1511, 1464, 1384, 1341, 1318, 1256, 1242, 1219, 1176, 1144, 1097, 1033, 989, 834; HRMS (ESI+) *m/z* calculated for $[M+Na]^+$ $C_{20}H_{19}NO_4Na$: 360.1212, found 360.1207.

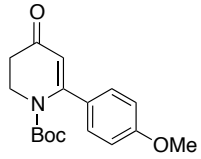

1-(*tert*-Butoxycarbonyl)-6-(4-methoxyphenyl)-2,3-dihydropyridin-4(1*H*)-one (3.39). Prepared by the general procedure described above and purified by flash column chromatography (25% EtOAc in hexanes) on silica gel to provide 9.4 mg (31%) as a yellow oil. ^{1}H NMR (400 MHz, $CDCl_3$) δ 7.33 (d, J = 8.7 Hz, 2H), 6.91 (d, J = 8.7 Hz, 2H), 5.63 (s, 1H), 4.20 (t, J = 6.4 Hz, 2H), 3.85 (s, 3H), 2.60 (t, J = 6.4 Hz, 2H), 1.15 (s, 9H); ^{13}C NMR (100 MHz, $CDCl_3$) δ 195.3, 161.3, 157.7, 152.7, 130.1, 128.1, 113.7, 112.6, 82.4, 55.5, 46.4, 38.2, 27.6; FTIR (NaCl, cm^{-1}) 3155, 2983, 1793, 1706, 1654, 1607, 1587, 1567, 1510, 1465, 1386, 1350, 1354, 1226, 1177, 1146, 1097, 988, 830; HRMS (ESI+) *m/z* calculated for $[M+Na]^+$ $C_{17}H_{21}NO_4Na$: 326.1368, found 326.1364.

8.4 Chapter 4

8.4.1 General procedure for the dehydrogenative alkenylation of cyclic enaminones

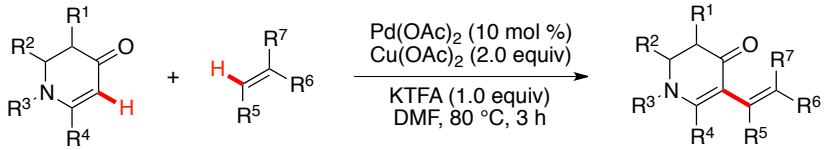

Cyclic enaminone (0.40 mmol) was mixed with $Pd(OAc)_2$ (9.0 mg, 0.04 mmol), $Cu(OAc)_2$ (145.3 mg, 0.80 mmol), and KTFA (60.8 mg, 0.40 mmol). To the mixture was added alkene (0.80 mmol), followed by DMF (2 mL). The reaction vessel was purged with N_2 and then sealed. After being stirred for 5 min, the reaction was heated at 80 °C for 3 h. The reaction was diluted with EtOAc (4 mL), neutralized with excess K_2CO_3 (1 g), and stirred for another 5 min. The mixture was filtered through Celite, and the filter cake was washed with EtOAc (25 mL). The filtrate was then concentrated under reduced pressure and purified by flash chromatography on silica gel.

8.4.2 Compound characterization

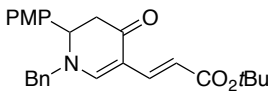

(*E*)-1-Benzyl-5-(2-(*t*-butoxycarbonyl)vinyl)-2-(4-methoxyphenyl)-2,3-dihydropyridin-4(1*H*)-one (4.3). Prepared by the general procedure described above and 140 mg (81%) was isolated as a light yellow solid (mp 64–68 °C). ^{1}H NMR (400 MHz, $CDCl_3$) δ 7.52 (s, 1H), 7.42–7.34 (m, 3H), 7.09–7.15 (m, 5H), 6.86 (d, *J* = 8.8 Hz, 2H), 6.60 (d, *J* = 15.6 Hz, 1H), 4.50 (t, *J* = 6.8 Hz, 1H), 4.43 (d, *J* = 14.9 Hz, 1H), 4.25 (d, *J* = 14.9 Hz, 1H), 3.81 (s, 3H), 2.92 (dd, *J* = 16.3, 7.2 Hz, 1H), 2.71 (dd, *J* = 16.3, 6.4 Hz, 1H), 1.48 (s, 9H); ^{13}C NMR (100 MHz, $CDCl_3$) δ 188.1, 168.7, 160.0, 156.6, 138.8, 135.0, 129.8, 129.4, 128.9, 128.3, 128.0, 114.7, 114.1, 106.5, 79.4, 60.1, 58.2, 55.5, 44.2, 28.5; FTIR (Film, cm^{-1}) 3066, 2972, 2854, 1690, 1656, 1595, 1511, 1428, 1316, 1254, 1145, 1111, 1032, 790; HRMS (ESI+) *m/z* calculated for $[M+H]^+$ $C_{26}H_{30}NO_4$: 420.2175, found 420.2191.

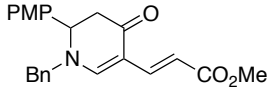

(*E*)-1-Benzyl-5-(2-(methoxycarbonyl)vinyl)-2-(4-methoxyphenyl)-2,3-dihydropyridin-4(1*H*)-one (4.4). Prepared by the general procedure described above and 61.6 mg (82%) was isolated as a light yellow solid (mp 50–55 °C). ^{1}H NMR (400 MHz, $CDCl_3$) δ 7.56 (s, 1H), 7.46–7.33 (m, 3H), 7.21 (d, *J* = 15.6 Hz, 1H), 7.14 (dd, *J* = 7.2, 2.2 Hz, 2H), 7.11 (d, *J* = 8.7 Hz, 2H), 6.87 (d, *J* = 8.7 Hz, 2H), 6.70 (d, *J* = 15.6 Hz, 1H), 4.52 (t, *J* = 6.8 Hz, 1H), 4.44 (d, *J* = 14.9 Hz, 1H), 4.27 (d, *J* = 14.9 Hz, 1H), 3.81 (s, 3H), 3.73 (s, 3H), 2.93 (dd, *J* = 16.4, 7.3 Hz, 1H), 2.72 (dd, *J* = 16.4, 6.4 Hz, 1H); ^{13}C NMR (100 MHz, $CDCl_3$) δ 188.0, 169.7, 160.1, 157.0, 140.3, 134.8, 129.7, 129.4, 128.9, 128.3, 128.0, 114.8, 111.5, 106.4, 60.1, 58.2, 55.5, 51.3, 44.2; FTIR (film, cm^{-1}) 3055, 2987, 2951, 1696, 1657, 1595, 1513, 1438, 1392, 1317, 1165, 1092, 1034, 989, 896, 835; HRMS (ESI+) *m/z* calculated for $[M+H]^+$ $C_{23}H_{24}NO_4$: 378.1705, found 378.1711.

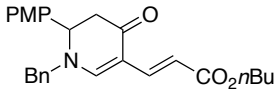

(*E*)-1-Benzyl-5-(2-(*n*-butoxycarbonyl)vinyl)-2-(4-methoxyphenyl)-2,3-dihydropyridin-4(1*H*)-one (4.5). Prepared by the general procedure described above and 72.7 mg (87%) was isolated as a light yellow solid (mp 102–104 °C). ^{1}H NMR (400 MHz, $CDCl_3$) δ 7.56 (s, 1H), 7.42–7.34 (m, 3H), 7.20 (d, *J* = 15.6 Hz, 1H), 7.14 (dd, *J* = 7.2, 2.1 Hz, 2H), 7.11 (d, *J* = 8.7 Hz, 2H), 6.87 (d, *J* = 8.7 Hz, 2H), 6.69 (d, *J* = 15.6 Hz, 1H), 4.51 (t, *J* = 6.8 Hz, 1H), 4.44 (d, *J* = 14.9 Hz, 1H), 4.26 (d, *J* = 14.9 Hz, 1H), 4.14 (t, *J* = 6.7 Hz, 2H), 3.81 (s, 3H), 2.93 (dd, *J* = 16.3, 7.3 Hz, 1H), 2.71 (dd, *J* = 16.4, 6.3 Hz, 1H), 1.69–1.60 (m, 2H), 1.41 (dq, *J* = 14.6, 7.4 Hz, 2H), 0.93 (t, *J* = 7.4 Hz, 3H); ^{13}C NMR (100 MHz, $CDCl_3$) δ 188.1, 169.4, 160.0, 156.9, 139.9, 134.9, 129.7, 129.4, 128.9, 128.3, 128.0, 114.8, 112.1, 106.5, 63.8, 60.1, 58.2, 55.5, 44.2, 31.1, 19.4, 13.9; FTIR (film, cm^{-1}) 3054, 2963, 2986, 1692, 1655, 1595, 1513, 1441, 1422, 1316, 1165, 1090, 1033, 989, 896, 834; HRMS (ESI+) *m/z* calculated for $[M+H]^+$ $C_{26}H_{30}NO_4$: 420.2175, found 420.2170.

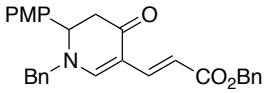

(*E*)-5-(2-(Benzoxycarbonyl)vinyl)-1-benzyl-2-(4-methoxyphenyl)-2,3-dihydropyridin-4(1*H*)-one (4.6). Prepared by the general procedure described above and 82.2 mg (91%) was isolated as a light yellow solid (mp 49–53 °C). ^{1}H NMR (400 MHz, $CDCl_3$) δ 7.55 (s, 1H), 7.43–7.28 (m, 8H), 7.27–7.21 (m, 2H), 7.11 (d, *J* = 8.7 Hz, 2H), 6.87 (d, *J* = 8.7 Hz, 2H), 6.76 (d, *J* = 15.6 Hz, 1H), 5.20 (s, 2H), 4.51 (t, *J* = 6.8 Hz, 1H), 4.44 (d, *J* = 14.9 Hz, 1H), 4.26 (d, *J* = 14.9 Hz, 1H), 3.81 (s, 3H), 2.93 (dd, *J* = 16.4, 7.3 Hz, 1H), 2.71 (dd, *J* = 16.4, 6.3 Hz, 1H); ^{13}C NMR (100 MHz, $CDCl_3$) δ 188.0, 169.1, 160.0, 157.0, 140.6, 137.0, 134.8, 129.7, 129.4, 128.9, 128.6, 128.3, 128.2, 128.0, 128.0, 114.8, 111.6, 106.4, 65.7, 60.1, 58.3, 55.5, 44.2; FTIR (film, cm^{-1}) 3054, 2986, 1696, 1655, 1594, 1513, 1441, 1392, 1316, 1179, 1156, 1090, 1029, 989, 896; HRMS (ESI+) *m/z* calculated for $[M+H]^+$ $C_{29}H_{28}NO_4$: 454.2018, found 454.2007.

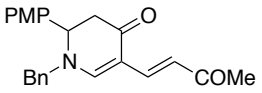

(*E*)-1-Benzyl-2-(4-methoxyphenyl)-5-(3-oxobut-1-enyl)-2,3-dihydropyridin-4(1*H*)-one (4.7). Prepared by the general procedure described above and 61.0 mg (85%) was isolated as a light yellow solid (mp 48–52 °C). ^{1}H NMR (400 MHz, $CDCl_3$) δ 7.66 (s, 1H), 7.44–7.35 (m, 3H), 7.23 (d, J = 15.8 Hz, 1H), 7.15 (dd, J = 7.0, 2.3 Hz, 2H), 7.12 (d, J = 8.7 Hz, 2H), 6.89 (dd, J = 12.2, 9.6 Hz, 3H), 4.57–4.51 (m, 1H), 4.47 (d, J = 14.9 Hz, 1H), 4.29 (d, J = 14.9 Hz, 1H), 3.81 (s, 3H), 2.95 (dd, J = 16.4, 7.4 Hz, 1H), 2.72 (dd, J = 16.4, 6.0 Hz, 1H), 2.26 (s, 3H); ^{13}C NMR (100 MHz, $CDCl_3$) δ 199.3, 188.0, 160.1, 156.7, 138.6, 134.7, 129.5, 129.4, 129.0, 128.2, 128.0, 120.5, 114.8, 106.1, 60.1, 58.5, 55.5, 44.0, 28.3; FTIR (film, cm^{-1}) 3054, 2987, 1655, 1593, 1579, 1513, 1422, 1356, 1179, 1033, 896; HRMS (ESI+) *m/z* calculated for $[M+H]^+$ $C_{23}H_{24}NO_3$: 362.1756, found 362.1754.

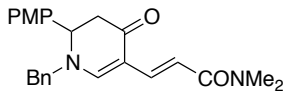

(*E*)-1-Benzyl-5-(2-(dimethylcarbamoyl)vinyl)-2-(4-methoxyphenyl)-2,3-dihydropyridin-4(1*H*)-one (4.8). Prepared by the general procedure described above and 73.9 mg (95%) was isolated as a yellow solid (mp 50–54 °C). ^{1}H NMR (400 MHz, $CDCl_3$) δ 7.51 (s, 1H), 7.41 (d, J = 14.8 Hz, 1H), 7.38–7.32 (m, 3H), 7.20–7.09 (m, 4H), 7.07 (d, J = 14.8 Hz, 1H), 6.87 (d, J = 8.7 Hz, 2H), 4.49 (t, J = 7.0 Hz, 1H), 4.43 (d, J = 14.9 Hz, 1H), 4.23 (d, J = 14.9 Hz, 1H), 3.80 (s, 3H), 3.11 (s, 3H), 3.02 (s, 3H), 2.93 (dd, J = 16.3, 7.2 Hz, 1H), 2.71 (dd, J = 16.3, 6.7 Hz, 1H); ^{13}C NMR (100 MHz, $CDCl_3$) δ 188.6, 169.0, 160.0, 158.0, 138.0, 135.0, 129.9, 129.3, 128.8, 128.3, 128.0, 114.7, 112.4, 107.0, 60.0, 58.1, 55.5, 44.6, 29.4; FTIR (film, cm^{-1}) 3054, 2985, 1707, 1655, 1600, 1513, 1442, 1395, 1357, 1179, 1089, 1034, 988, 896; HRMS (ESI+) *m/z* calculated for $[M+H]^+$ $C_{24}H_{27}N_2O_3$: 391.2022, found 391.2013.

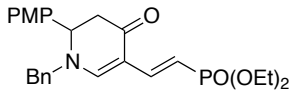

(*E*)-1-Benzyl-5-(2-(diethoxyphosphinyl)vinyl)-2-(4-methoxyphenyl)-2,3-dihydropyridin-4(1*H*)-one (4.9). Prepared by the general procedure described above and 61.7 mg (68%) was isolated as a yellow oil. ^{1}H NMR (400 MHz, $CDCl_3$) δ 7.49 (s, 1H), 7.44–7.32 (m, 3H), 7.12 (dd, *J* = 9.2, 6.1 Hz, 4H), 7.01–6.84 (m, 3H), 6.54 (dd, *J* = 21.9, 17.1 Hz, 1H), 4.50 (t, *J* = 6.9 Hz, 1H), 4.41 (d, *J* = 14.9 Hz, 1H), 4.24 (d, *J* = 14.9 Hz, 1H), 4.16–3.97 (m, 4H), 3.81 (s, 3H), 2.91 (dd, *J* = 16.3, 7.3 Hz, 1H), 2.70 (dd, *J* = 16.4, 6.5 Hz, 1H), 1.32 (td, *J* = 7.1, 1.5 Hz, 6H); ^{13}C NMR (100 MHz, $CDCl_3$) δ 188.2, 160.0, 157.2, 144.6 (d, *J* = 7.9 Hz), 134.8, 129.7, 129.4, 128.9, 128.3, 128.1, 114.8, 107.0 (d, *J* = 27.4 Hz), 106.0 (d, *J* = 139.7 Hz), 61.5 (d, *J* = 5.2 Hz), 60.1, 58.1, 55.5, 44.3, 16.6 (d, *J* = 5.7 Hz); FTIR (film, cm^{-1}) 3054, 2987, 1654, 1600, 1422, 1393, 1030, 961, 896; HRMS (ESI+) *m/z* calculated for $[M+H]^+$ $C_{25}H_{31}NO_5P$: 456.1940, found 456.1940.

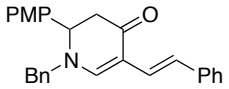

(*E*)-1-Benzyl-2-(4-methoxyphenyl)-5-styryl-2,3-dihydropyridin-4(1*H*)-one (4.10). Prepared by the general procedure described above and 52.4 mg (66%) was isolated as a yellow solid (mp 53–57 °C). ^{1}H NMR (400 MHz, $CDCl_3$) δ 7.57 (s, 1H), 7.38 (dt, *J* = 13.9, 6.9 Hz, 5H), 7.29 (d, *J* = 7.5 Hz, 2H), 7.23–7.11 (m, 5H), 7.08 (d, *J* = 16.3 Hz, 1H), 6.87 (d, *J* = 8.7 Hz, 2H), 6.82 (d, *J* = 16.3 Hz, 1H), 4.55–4.39 (m, 2H), 4.23 (d, *J* = 15.1 Hz, 1H), 3.81 (s, 3H), 2.92 (dd, *J* = 16.3, 7.0 Hz, 1H), 2.75 (dd, *J* = 16.3, 7.5 Hz, 1H); ^{13}C NMR (100 MHz, $CDCl_3$) δ 188.5, 159.8, 152.8, 139.1, 135.9, 130.3, 129.2, 128.6, 128.5, 128.5, 127.8, 126.3, 125.8, 123.2, 122.8, 114.6, 108.5, 60.0, 57.9, 55.5, 44.4; FTIR (film, cm^{-1}) 3054, 2987, 1646, 1592, 1513, 1422, 1179, 969; HRMS (ESI+) *m/z* calculated for $[M+H]^+$ $C_{27}H_{26}NO_2$: 396.1964, found 396.1970.

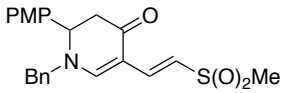

(*E*)-1-Benzyl-2-(4-methoxyphenyl)-5-(2-(methylsulfonyl)vinyl)-2,3-dihydropyridin-4(1*H*)-one (4.11). Prepared by the general procedure described above and 44.7 mg (56%) was isolated as a light yellow oil. ^{1}H NMR (400 MHz, $CDCl_3$) δ 7.62 (s, 1H), 7.46–7.33 (m, 4H), 7.20–7.12 (m, 2H), 7.10 (d, J = 8.8 Hz, 2H), 6.96 (d, J = 14.7 Hz, 1H), 6.87 (d, J = 8.8 Hz, 2H), 4.59–4.45 (m, 2H), 4.28 (d, J = 14.8 Hz, 1H), 3.79 (s, 3H), 3.01–2.90 (m, 4H), 2.69 (dd, J = 16.4, 5.6 Hz, 1H); ^{13}C NMR (100 MHz, $CDCl_3$) δ 187.9, 160.1, 158.4, 138.8, 134.4, 129.5, 129.2, 129.1, 128.2, 128.1, 119.7, 114.9, 104.2, 60.0, 58.4, 55.5, 44.0, 43.9; FTIR (film, cm^{-1}) 3055, 2987, 1656, 1602, 1513, 1442, 1301, 1176, 1124, 1033, 962, 909; HRMS (ESI+) *m/z* calculated for $[M+H]^+$ $C_{22}H_{24}NO_4S$: 398.1426, found 398.1430.

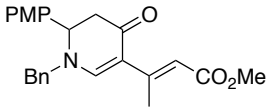

(*E*)-1-Benzyl-5-(2-(methoxycarbonyl)1-methyl-vinyl)-2-(4-methoxyphenyl)-2,3-dihydropyridin-4(1*H*)-one (4.14). Prepared by the general procedure described above and 32.8 mg (42%) was isolated as a waxy solid. ^{1}H NMR (400 MHz, $CDCl_3$) δ 7.59 (s, 1H), 7.44–7.29 (m, 3H), 7.18–7.05 (m, 4H), 6.86 (d, J = 8.8 Hz, 2H), 6.45 (d, J = 1.2 Hz, 1H), 4.44 (m, 2H), 4.23 (d, J = 15.1 Hz, 1H), 3.80 (s, 4H), 3.67 (s, 3H), 2.89 (dd, J = 16.0, 7.1 Hz, 1H), 2.69 (dd, J = 16.0, 7.0 Hz, 1H), 2.40 (d, J = 1.2 Hz, 3H); ^{13}C NMR (100 MHz, $CDCl_3$) δ 187.9, 168.5, 159.9, 153.5, 151.7, 135.5, 130.0, 129.3, 128.7, 128.3, 127.8 114.7, 113.3, 111.7, 59.8, 58.1, 55.5, 50.9, 44.8, 17.4; FTIR (film, cm^{-1}) 3055, 2987, 1648, 1579, 1513, 1422, 1170, 1034, 896; HRMS (ESI+) *m/z* calculated for $[M+H]^+$ $C_{24}H_{26}NO_4$: 392.1862, found 392.1865.

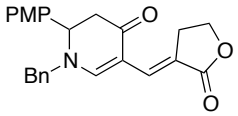

(*E*)-1-Benzyl-2-(4-methoxyphenyl)-5-((2-oxodihydrofuran-3(2*H*)-ylidene)methyl)-2,3-dihydropyridin-4(1*H*)-one (4.15a). Prepared by the general procedure described above and 18.4 mg (24%) was isolated as a light yellow solid (mp 57–63 °C). ^{1}H NMR (400 MHz, $CDCl_3$) δ 7.63 (s, 1H), 7.45–7.32 (m, 4H), 7.20–7.07 (m, 4H), 6.88 (d, J = 8.7 Hz, 2H), 4.58 (t, J = 6.8 Hz, 1H), 4.46 (d, J = 14.7 Hz, 1H), 4.34–4.24 (m, 3H), 3.80 (s, 3H), 2.93 (m, 3H), 2.73 (dd, J = 16.3, 6.4 Hz, 1H); ^{13}C NMR (100 MHz, $CDCl_3$) δ 187.5, 173.7, 160.0, 155.7, 134.7, 131.2, 129.6, 129.4, 128.9, 128.3, 128.2, 114.8, 114.3, 106.8, 65.2, 60.4, 58.3, 55.5, 43.7, 28.2; FTIR (film, cm^{-1}) 3055, 2987, 1738, 1658, 1594, 1581, 1513, 1422, 1194, 1033, 896; HRMS (ESI+) *m/z* calculated for $[M+H]^+$ $C_{24}H_{24}NO_4$: 390.1705, found 390.1693.

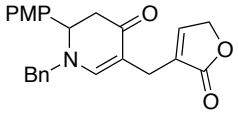

1-Benzyl-2-(4-methoxyphenyl)-5-((2-oxo-2,5-dihydrofuran-3-yl)methyl)-2,3-dihydropyridin-4(1*H*)-one (4.15b). Prepared by the general procedure described above and 46.1 mg (59%) was isolated as a light yellow solid (mp 59–66 °C). ^{1}H NMR (400 MHz, $CDCl_3$) δ 7.50 (s, 1H), 7.37–7.27 (m, 3H), 7.18 (s, 1H), 7.10 (ddd, J = 9.4, 4.9, 2.4 Hz, 4H), 6.89–6.81 (m, 2H), 4.71 (d, J = 1.5 Hz, 2H), 4.43–4.30 (m, 2H), 4.08 (d, J = 15.1 Hz, 1H), 3.79 (s, 3H), 3.16 (dd, J = 15.0, 1.2 Hz, 1H), 3.09 (dd, J = 15.0, 1.1 Hz, 1H), 2.73 (dd, J = 16.5, 6.7 Hz, 1H), 2.63 (dd, J = 16.5, 8.8 Hz, 1H); ^{13}C NMR (100 MHz, $CDCl_3$) δ 189.0, 174.8, 159.6, 154.5, 145.6, 136.0, 132.6 130.2, 128.9, 128.4, 128.2, 127.9, 114.4, 105.3, 70.2, 60.3, 57.3, 55.4, 44.1, 23.8; FTIR (film, cm^{-1}) 3054, 2987, 1753, 1602, 1512, 1422, 1195, 1063, 896; HRMS (ESI+) *m/z* calculated for $[M+H]^+$ $C_{24}H_{24}NO_4$: 390.1705, found 390.1706.

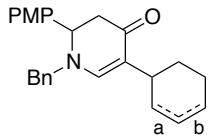

1-Benzyl-5-(2-cyclohexene)-2-(4-methoxyphenyl)-2,3-dihydropyridin-4(1*H*)-one (4.16a) and 1-benzyl-5-(3-cyclohexene)-2-(4-methoxyphenyl)-2,3-dihydropyridin-4(1*H*)-one (4.16b). Prepared by the general procedure described above and 36.3 mg (49%) were isolated as a light yellow oil. Two constitutional isomers were inseparable. The ratio was determined by ^{1}H NMR. ^{1}H NMR (400 MHz, $CDCl_3$) δ 7.36–7.28 (m, 6H, **4.16a**, **4.16b**), 7.17–7.01 (m, 10H, **4.16a**, **4.16b**), 6.90–6.82 (m, 4H, **4.16a**, **4.16b**), 5.92–5.76 (m, 2H, **4.16a**, **4.16b**), 5.58–5.50 (m, 2H, **4.16a**, **4.16b**), 4.41–4.22 (m, 4H, **4.16a**, **4.16b**), 4.14–4.02 (m, 2H, **4.16a**, **4.16b**), 3.81 (m, 6H, **4.16a**, **4.16b**), 3.51 (br, 2H, **4.16a**), 2.77 (dd, *J* = 16.3, 6.7 Hz, 1H, **4.16a**), 2.73–2.60 (m, 3H, **4.16a**, **4.16b**), 2.03–1.95 (m, 4H, **4.16a**, **4.16b**), 1.92–1.83 (m, 2H, **4.16a**, **4.16b**), 1.68–1.50 (m, 4H, **4.16a**, **4.16b**), 1.50–1.35 (m, 2H, **4.16b**); ^{13}C NMR (100 MHz, $CDCl_3$) δ 189.4 (**4.16b**), 189.1 (**4.16a**), 159.6 (**4.16b**), 159.5 (**4.16a**), 153.5 (**4.16b**), 153.2 (**4.16a**), 136.6 (**4.16a**), 136.5 (**4.16b**), 131.0 (**4.16a**), 130.0 (**4.16b**), 129.9 (**4.16a**), 129.1 (**4.16a**), 128.9 (**4.16b**), 128.9 (**4.16b**), 128.8 (**4.16a**), 128.7 (**4.16a**), 128.5 (**4.16b**), 128.0 (**4.16a**), 128.0 (**4.16b**), 127.7 (**4.16b**), 114.4 (**4.16b**), 114.3 (**4.16a**), 114.2 (**4.16b**), 113.8 (**4.16a**), 60.7 (**4.16b**), 60.2 (**4.16a**), 57.3 (**4.16a**), 57.0 (**4.16b**), 55.4 (**4.16a, 4.16b**), 44.7 (**4.16b**), 44.3 (**4.16a**), 31.6 (**4.16a**), 31.5 (**4.16b**), 30.0 (**4.16b**), 29.7 (**4.16a**), 25.3 (**4.16a**), 25.3 (**4.16b**), 20.1 (**4.16a**), 20.1 (**4.16b**); FTIR (film, cm^{-1}) 3016, 2927, 1636, 1598, 1512, 1443, 1380, 1360, 1298, 1178, 1032, 834; HRMS (ESI+) *m/z* calculated for $[M+H]^+$ $C_{25}H_{28}NO_2$: 374.2120, found 374.2125.

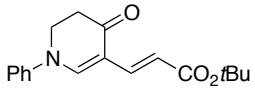

(*E*)-5-(2-(*tert*-Butoxycarbonyl)vinyl)-1-phenyl-2,3-dihydropyridin-4(1*H*)-one (4.17). Prepared by the general procedure described above and 45.1 mg (76%) was isolated as a light yellow solid (mp 150–152 °C). ^{1}H NMR (400 MHz, $CDCl_3$) δ 7.69 (s, 1H), 7.43 (dd, *J* = 8.4, 7.6 Hz, 2H), 7.26–7.12 (m, 4H), 6.60 (d, *J* = 15.7 Hz, 1H), 4.10–4.02 (m,

2H), 2.78–2.70 (m, 2H), 1.49 (s, 9H); ^{13}C NMR (100 MHz, $CDCl_3$) δ 189.3, 168.1, 152.0, 144.7, 138.4, 130.1, 125.9, 119.2, 115.9, 109.5, 79.6, 47.8, 36.5, 28.4; FTIR (film, cm^{-1}) 3155, 2982, 1794, 1691, 1578, 1493, 1390, 1316, 1281, 1153, 1110, 986; HRMS (ESI+) *m/z* calculated for $[M+Na]^+$ $C_{18}H_{21}NO_3Na$: 322.1419, found 322.1425.

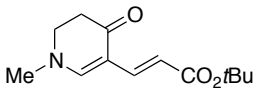

(*E*)-5-(2-(*tert*-Butoxycarbonyl)vinyl)-1-methyl-2,3-dihydropyridin-4(1*H*)-one (4.18). Prepared by the general procedure described above and 40.0 mg (84%) was isolated as a light yellow solid (mp 128–134 °C). ^{1}H NMR (400 MHz, $CDCl_3$) δ 7.25 (s, 1H), 7.08 (d, *J* = 15.6 Hz, 1H), 6.51 (d, *J* = 15.6 Hz, 1H), 3.51 (t, *J* = 7.8 Hz, 2H), 3.18 (s, 3H), 2.62–2.53 (m, 2H), 1.47 (s, 9H); ^{13}C NMR (100 MHz, $CDCl_3$) δ 188.4, 168.7, 157.2, 138.9, 113.4, 106.1, 79.3, 48.6, 44.0, 35.9, 28.5; FTIR (film, cm^{-1}) 3155, 2982, 1794, 1689, 1651, 1604, 1473, 1392, 1317, 1152, 1101, 986; HRMS (ESI+) *m/z* calculated for $[M+H]^+$ $C_{13}H_{20}NO_3$: 238.1443, found 238.1436.

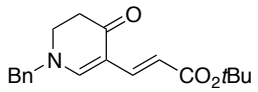

(*E*)-1-Benzyl-5-(2-(*tert*-butoxycarbonyl)vinyl)-2,3-dihydropyridin-4(1*H*)-one (4.19). Prepared by the general procedure described above and 43.1 mg (92%) was isolated as a light yellow oil. ^{1}H NMR (400 MHz, $CDCl_3$) δ 7.47–7.35 (m, 4H), 7.26–7.23 (m, 2H), 7.11 (d, *J* = 15.6 Hz, 1H), 6.56 (d, *J* = 15.6 Hz, 1H), 4.48 (s, 2H), 3.45 (t, *J* = 7.6 Hz, 2H), 2.54 (t, *J* = 7.9 Hz, 2H), 1.48 (s, 9H); ^{13}C NMR (100 MHz, $CDCl_3$) δ 188.7, 168.6, 156.5, 139.0, 134.6, 129.4, 129.0, 127.9, 114.0, 106.5, 79.4, 60.8, 46.5, 36.1, 28.5; FTIR (film, cm^{-1}) 3055, 2987, 1689, 1597, 1422, 1150, 896; HRMS (ESI+) *m/z* calculated for $[M+H]^+$ $C_{19}H_{24}NO_3$: 314.1756, found 314.1742.

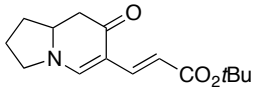

(*E*)-6-(2-(*tert*-Butoxycarbonyl)vinyl)-2,3,8,8a-tetrahydroindolizin-7(1*H*)-one (4.20). Prepared by the general procedure described above and 38.3 mg (73%) was isolated as a light yellow solid (mp 122–126 °C). ^{1}H NMR (400 MHz, $CDCl_3$) δ 7.51 (s, 1H), 7.17 (d, *J* = 15.6 Hz, 1H), 6.44 (d, *J* = 15.6 Hz, 1H), 3.78 (ddd, *J* = 21.0, 10.5, 5.4 Hz, 1H), 3.72–3.54 (m, 2H), 2.57 (dd, *J* = 15.9, 4.7 Hz, 1H), 2.46–2.28 (m, 2H), 2.16 (dt, *J* = 14.0, 7.1 Hz, 1H), 2.05–1.90 (m, 1H), 1.79–1.66 (m, 1H), 1.47 (s, 9H); ^{13}C NMR (100 MHz, $CDCl_3$) δ 189.3, 168.7, 152.4, 139.1, 112.4, 105.8, 79.2, 58.0, 50.5, 42.1, 32.9, 28.5, 24.4; FTIR (film, cm^{-1}) 3155, 2981, 1794, 1687, 1652, 1590.0, 1476, 1430, 1369, 1319, 1249, 1150, 1097, 990; HRMS (ESI+) *m/z* calculated for $[M+H]^+$ $C_{15}H_{22}NO_3$: 264.1600, found 264.1602.

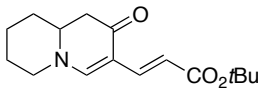

(*E*)-3-(2-(*tert*-Butoxycarbonyl)vinyl)-7,8,9,9a-tetrahydro-1*H*-quinolizin-2(6*H*)-one (4.21). Prepared by the general procedure described above and 47.1 mg (86%) was isolated as a light yellow solid (mp 122–124 °C). ^{1}H NMR (400 MHz, $CDCl_3$) δ 7.16 (s, 1H), 7.05 (d, *J* = 15.6 Hz, 1H), 6.57 (d, *J* = 15.6 Hz, 1H), 3.57–3.49 (m, 1H), 3.49–3.39 (m, 1H), 3.18 (td, *J* = 12.9, 2.9 Hz, 1H), 2.62 (dd, *J* = 16.4, 5.8 Hz, 1H), 2.43 (dd, *J* = 16.4, 11.7 Hz, 1H), 1.94–1.86 (m, 1H), 1.86–1.76 (m, 2H), 1.68–1.42 (m, 12H); ^{13}C NMR (100 MHz, $CDCl_3$) δ 189.3, 168.6, 157.0, 138.9, 114.1, 106.7, 79.3, 56.9, 54.0, 43.6, 31.8, 28.5, 25.9, 23.2; FTIR (film, cm^{-1}) 3155, 2981, 1793, 1688, 1654, 1593, 1450, 1392, 1321, 1246, 1155, 1107, 987; HRMS (ESI+) *m/z* calculated for $[M+H]^+$ $C_{26}H_{24}NO_3$: 278.1756, found 278.1759.

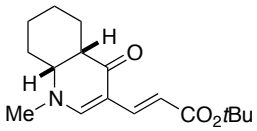

(*E*)-(*cis*)-3-(2-(*tert*-Butoxycarbonyl)vinyl)-1-methyl-4a,5,6,7,8,8a-hexahydroquinolin-4(1*H*)-one (4.22). Prepared by the general procedure described above and 45.1 mg (77%) was isolated as a light yellow solid (mp 182–184 °C). ^{1}H NMR (400 MHz, $CDCl_3$) δ 7.15 (s, 1H), 7.09 (d, *J* = 15.6 Hz, 1H), 6.53 (d, *J* = 15.6 Hz, 1H), 3.44 (dd, *J* = 14.1, 6.2 Hz, 1H), 3.16 (s, 3H), 2.84–2.73 (m, 1H), 2.40 (d, *J* = 11.0 Hz, 1H), 1.78–1.65 (m, 3H), 1.46 (s, 9H), 1.43–1.21 (m, 4H); ^{13}C NMR (100 MHz, $CDCl_3$) δ 190.5, 168.8, 155.5, 139.3, 112.6, 105.0, 79.1, 60.8, 45.0, 41.7, 28.5, 24.5, 24.0, 23.6, 22.2; FTIR (film, cm^{-1}) 3155, 2939, 1794, 1687, 1653, 1597, 1478, 1384, 1329, 1254, 1156, 1144, 1095, 993; HRMS (ESI+) *m/z* calculated for $[M+H]^+$ $C_{17}H_{26}NO_3$: 292.1913, found 292.1920.

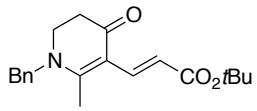

(*E*)-1-Benzyl-5-(2-(*tert*-butoxycarbonyl)vinyl)-6-methyl-2,3-dihydropyridin-4(1*H*)-one (4.23). Prepared by the general procedure described above and 14.2 mg (22%) was isolated as a light yellow solid (mp 118–120 °C). ^{1}H NMR (400 MHz, $CDCl_3$) δ 7.50 (d, *J* = 15.4 Hz, 1H), 7.37 (m, 3H), 7.18 (d, *J* = 7.0 Hz, 2H), 6.84 (d, *J* = 15.4 Hz, 1H), 4.69 (s, 2H), 3.64–3.53 (m, 2H), 2.59–2.49 (m, 2H), 2.33 (s, 3H), 1.49 (s, 9H); ^{13}C NMR (100 MHz, $CDCl_3$) δ 189.2, 169.4, 164.6, 137.6, 135.7, 129.5, 128.4, 126.3, 116.1, 107.3, 79.3, 56.4, 49.3, 36.5, 28.5, 17.4; FTIR (film, cm^{-1}) 3155, 2981, 1794, 1686, 1642, 1590, 1535, 1471, 1388, 1305, 1154, 1096, 985; HRMS (ESI+) *m/z* calculated for $[M+H]^+$ $C_{20}H_{26}NO_3$: 328.1913, found 328.1923.

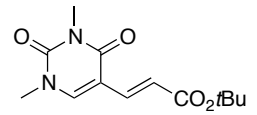

(*E*)-1,3-Dimethyl-5-(2'-*t*-butoxycarbonylvinyl)uracil (4.24). Prepared by the general procedure described above and purified by flash chromatography (30–40% EtOAc in

hexanes) on silica gel to provide 35.1 mg (33%) as an off-white solid (mp 140–142 °C). ^{1}H NMR (400 MHz, $CDCl_3$) δ 7.37 (s, 1H), 7.19 (d, *J* = 15.8 Hz, 1H), 6.89 (d, *J* = 16.6 Hz, 1H), 3.47 (s, 3H), 3.38 (s, 3H), 1.49 (s, 9H); ^{13}C NMR (100 MHz, $CDCl_3$) δ 166.9, 161.5, 150.9, 144.2, 135.1, 121.4, 109.3, 80.5, 37.6, 28.3, 28.3; FTIR (NaCl, cm^{-1}) 3155, 2953, 1710, 1665, 1629, 1457, 1437, 1370, 1301, 1263, 1194, 1172, 1091, 984, 907; HRMS (ESI+) *m/z* calculated for $[M+Na]^+$ $C_{13}H_{18}N_2O_4Na$: 289.1159, found 289.1158.

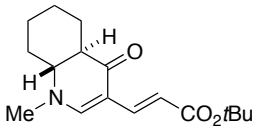

(*E*)-(*trans*)-3-(2-(*tert*-Butoxycarbonyl)vinyl)-1-methyl-4a,5,6,7,8,8a-hexahydroquinolin-4(1*H*)-one (4.25). Prepared by the general procedure described above and 43.5 mg (75%) was isolated as a light yellow solid (mp 146–148 °C). ^{1}H NMR (400 MHz, $CDCl_3$) δ 7.27 (s, 1H), 7.09 (d, *J* = 15.6 Hz, 1H), 6.55 (d, *J* = 15.6 Hz, 1H), 3.20–3.05 (m, 4H), 2.44 (ddd, *J* = 11.1, 5.6, 2.7 Hz, 1H), 2.29–2.20 (m, 1H), 2.14 (ddd, *J* = 14.8, 11.4, 3.7 Hz, 1H), 1.94–1.79 (m, 2H), 1.50–1.36 (m, 10H), 1.35–1.04 (m, 3H); ^{13}C NMR (100 MHz, $CDCl_3$) δ 191.2, 168.7, 157.6, 139.2, 113.5, 106.2, 79.2, 61.3, 48.7, 40.1, 30.2, 28.5, 24.8, 24.7, 24.5; FTIR (film, cm^{-1}) 3155, 2939, 1794, 1687, 1602, 1474, 1392, 1297, 1154, 1136, 1095, 987; HRMS (ESI+) *m/z* calculated for $[M+H]^+$ $C_{17}H_{26}NO_3$: 292.1913, found 292.1913.

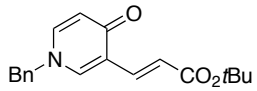

(*E*)-1-Benzyl-3-(2-(*tert*-butoxycarbonyl)vinyl)pyridin-4(1*H*)-one (4.26). Prepared by the general procedure described above and 4.4 mg (7%) was isolated as a waxy solid. ^{1}H NMR (400 MHz, $CDCl_3$) δ 7.50 (d, *J* = 2.4 Hz, 1H), 7.45–7.37 (m, 3H), 7.33–7.23 (m, 2H), 7.22–7.14 (m, 3H), 6.45 (d, *J* = 7.5 Hz, 1H), 4.97 (s, 2H), 1.49 (s, 9H); ^{13}C NMR (100 MHz, $CDCl_3$) δ 177.2, 167.5, 141.8, 138.4, 137.2, 134.4, 129.7, 129.4, 127.6, 124.2, 122.8, 120.2, 80.3, 60.7, 28.3; FTIR (film, cm^{-1}) 3155, 2982, 1794, 1697, 1643, 1578,

1482, 1382, 1317, 1163, 1096, 987; HRMS (ESI+) *m/z* calculated for $[M+H]^+$ $C_{19}H_{22}NO_3$: 312.1600, found 312.1588.

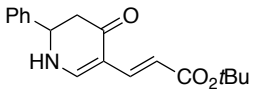

(*E*)-2-Phenyl-5-(2-(*tert*-butoxycarbonyl)vinyl)-2,3-dihydropyridin-4(1*H*)-one (4.27). Prepared by the general procedure described above and 3.5 mg (6%) was isolated as a light yellow solid (mp 193–196 °C). ^{1}H NMR (400 MHz, $CDCl_3$) δ 7.52 (d, *J* = 6.9 Hz, 1H), 7.46–7.34 (m, 5H), 7.14 (d, *J* = 15.7 Hz, 1H), 6.62 (d, *J* = 15.7 Hz, 1H), 5.52 (dd, *J* = 21.3, 9.5 Hz, 1H), 4.83 (dd, *J* = 13.7, 5.1 Hz, 1H), 2.85 (dd, *J* = 16.2, 13.8 Hz, 1H), 2.69 (dd, *J* = 16.2, 5.0 Hz, 1H), 1.49 (s, 9H); ^{13}C NMR (100 MHz, $CDCl_3$) δ 189.4, 153.4, 138.5, 129.5, 129.1, 126.6, 118.8, 115.3, 110.3, 107.8, 79.6, 58.2, 44.9, 28.5; FTIR (film, cm^{-1}) 3426, 3155, 2983, 1794, 1710, 1595, 1471, 1382, 1224, 1152, 1095, 988; HRMS (ESI+) *m/z* calculated for $[M+H]^+$ $C_{18}H_{22}NO_3$: 300.1600, found 300.1593.

8.5 Chapter 5

8.5.1 General procedure for the dehydrogenative alkenylation of uracils

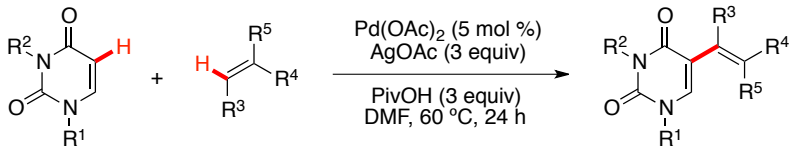

Uracil (0.1 mmol) was mixed in a clear 1-dram vial with $Pd(OAc)_2$ (0.005 mmol), AgOAc (0.3 mmol), and PivOH (0.3 mmol). To the mixture was added alkene (0.2 mmol), followed by DMF (0.5 mL). The reaction vessel was then capped. After being stirred for 2 min, the reaction was heated at 60 °C for 24 h in dark. The reaction was then cooled, diluted with EtOAc (1 mL), and pressure-filtered over Celite. The filter cake was washed with EtOAc (20 mL). The filtrate was then concentrated under reduced pressure and purified by flash chromatography on silica gel.

8.5.2 Compound characterization

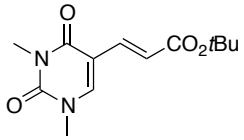

(*E*)-1,3-Dimethyl-5-(2'-*t*-butoxycarbonylvinyl)uracil (5.5). Prepared by the general procedure described above and purified by flash chromatography (30–40% EtOAc in hexanes) on silica gel to provide 24.3 mg (92%) as an off-white solid (mp 140–142 °C). ^{1}H NMR (400 MHz, $CDCl_3$) δ 7.37 (s, 1H), 7.19 (d, J = 15.8 Hz, 1H), 6.89 (d, J = 16.6 Hz, 1H), 3.47 (s, 3H), 3.38 (s, 3H), 1.49 (s, 9H); ^{13}C NMR (100 MHz, $CDCl_3$) δ 166.9, 161.5, 150.9, 144.2, 135.1, 121.4, 109.3, 80.5, 37.6, 28.3, 28.3; FTIR (NaCl, cm^{-1}) 3155, 2953, 1710, 1665, 1629, 1457, 1437, 1370, 1301, 1263, 1194, 1172, 1091, 984, 907; HRMS (ESI+) *m/z* calculated for $[M+Na]^+$ $C_{13}H_{18}N_2O_4Na$: 289.1159, found 289.1158.

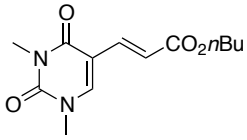

(*E*)-1,3-Dimethyl-5-(2'-*n*-butoxycarbonylvinyl)uracil (5.6). Prepared by the general procedure described above and purified by flash chromatography (40% EtOAc in hexanes) on silica gel to provide 24.1 mg (91%) as a colorless solid (mp 138–140 °C). ^{1}H NMR (400 MHz, $CDCl_3$) δ 7.41 (s, 1H), 7.28 (d, J = 16.3 Hz, 1H), 6.99 (d, J = 15.8 Hz, 1H), 4.16 (t, J = 6.6 Hz, 2H), 3.47 (s, 3H), 3.38 (s, 3H), 1.65 (m, 2H), 1.41 (m, 2H), 0.94 (t, J = 7.4 Hz, 3H); ^{13}C NMR (100 MHz, $CDCl_3$) δ 167.8, 161.4, 150.8, 144.8, 136.3, 119.3, 109.0, 64.4, 37.6, 30.9, 28.3, 19.3, 13.8; FTIR (NaCl, cm^{-1}) 3055, 2987, 2963, 1708, 1665, 1628, 1454, 1422, 1355, 1299, 1173, 1090, 1063, 985, 867; HRMS (ESI+) *m/z* calculated for $[M+Na]^+$ $C_{13}H_{18}N_2O_4Na$: 289.1159, found 289.1159.

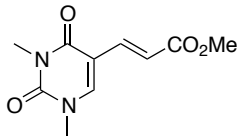

(*E*)-5-(2'-Methoxycarbonylvinyl)-1,3-dimethyluracil (5.7). Prepared by the general procedure described above and purified by flash chromatography (50% EtOAc in hexanes) on silica gel to provide 21.0 mg (94%) as a colorless solid (mp 163–165 °C). ^{1}H NMR (400 MHz, $CDCl_3$) δ 7.41 (s, 1H), 7.30 (d, J = 15.8 Hz, 1H), 7.00 (d, J = 15.8 Hz, 1H), 3.77 (s, 3H), 3.48 (s, 3H), 3.39 (s, 3H); ^{13}C NMR (100 MHz, $CDCl_3$) δ 168.2, 161.4, 150.8, 144.9, 136.6, 118.9, 109.0, 51.8, 37.7, 28.3; FTIR (NaCl, cm^{-1}) 3124, 2953, 1710, 1666, 1630, 1456, 1437, 1369, 1301, 1262, 1172, 1091, 984, 908; HRMS (ESI+) *m/z* calculated for $[M+Na]^+$ $C_{10}H_{12}N_2O_4Na$: 247.0689, found 247.0695.

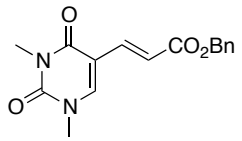

(*E*)-5-(2'-Benzoxycarbonylvinyl)-1,3-dimethyluracil (5.8). Prepared by the general procedure described above and purified by flash chromatography (50% EtOAc in hexanes) on silica gel to provide 15.7 mg (52%) as a colorless solid (mp 180–182 °C). ^{1}H NMR (400 MHz, $CDCl_3$) δ 7.42—7.30 (m, 7H), 7.06 (d, J = 15.7 Hz, 1H), 5.22 (s, 2H), 3.47 (s, 3H), 3.38 (s, 3H); ^{13}C NMR (100 MHz, $CDCl_3$) δ 167.5, 161.4, 150.8, 145.0, 136.9, 136.3, 128.7, 128.3, 128.2, 119.0, 109.0, 66.4, 37.7, 28.3; FTIR (NaCl, cm^{-1}) 3167, 2956, 1710, 1666, 1629, 1456, 1380, 1299, 1166, 1093, 985, 907; HRMS (ESI+) *m/z* calculated for $[M+Na]^+$ $C_{16}H_{16}N_2O_4Na$: 323.1002, found 323.1003.

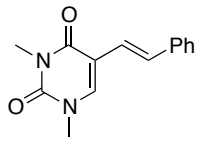

(*E*)-1,3-Dimethyl-5-styryluracil (5.9). Prepared by the general procedure described above and purified by flash chromatography (40% EtOAc in hexanes) on silica gel to provide 24.0 mg (98%) as a light yellow solid (mp 139–141 °C). ^{1}H NMR (400 MHz,

$CDCl_3$) δ 7.45 (d, *J* = 7.6 Hz, 2H), 7.38 (d, *J* = 16.4 Hz, 1H), 7.28 (m, 4H), 6.84 (d, *J* = 16.3 Hz, 1H), 3.46 (s, 3H), 3.41 (s, 3H); ^{13}C NMR (100 MHz, $CDCl_3$) δ 162.4, 151.2, 139.4, 137.5, 129.5, 128.8, 127.8, 126.5, 120.1, 111.6, 37.4, 28.3; FTIR (NaCl, cm^{-1}) 3055, 2987, 1702, 1659, 1459, 1369, 1087, 968; HRMS (ESI+) *m/z* calculated for $[M+Na]^+$ $C_{14}H_{14}N_2O_2Na$: 265.0947, found 265.0943.

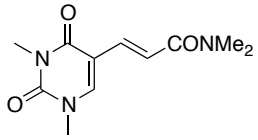

(*E*)-1,3-Dimethyl-5-(2'-dimethylcarbamoylvinyl)uracil (5.10). Prepared by the general procedure described above and purified by flash chromatography (100% acetone) on silica gel to provide 23.5 mg (100%) as a light yellow solid (mp 208–210 °C). ^{1}H NMR (400 MHz, $CDCl_3$) δ 7.58 (d, *J* = 15.0 Hz, 1H), 7.13 (s, 1H), 7.07 (d, *J* = 15.0 Hz, 1H), 3.33 (s, 3H), 3.25 (s, 3H), 3.01 (s, 3H), 2.90 (s, 3H); ^{13}C NMR (100 MHz, $CDCl_3$) δ 167.3, 161.9, 150.8, 145.3, 134.3, 118.8, 109.5, 37.5, 36.0, 28.2; FTIR (NaCl, cm^{-1}) 3155, 2929, 1709, 1663, 1599, 1454, 1398, 1354, 1146, 1090, 980, 908; HRMS (ESI+) *m/z* calculated for $[M+Na]^+$ $C_{11}H_{15}N_3O_3Na$: 260.1006, found 260.1011.

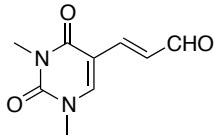

(*E*)-5-(2'-Formylvinyl)-1,3-dimethyluracil (5.11/5.11'). Prepared by the general procedure described above and purified by flash chromatography (100% EtOAc) on silica gel to provide 15.3 mg (79%) as a colorless solid (mp 175–177 °C). ^{1}H NMR (400 MHz, $CDCl_3$) δ 9.59 (d, *J* = 7.6 Hz, 1H), 7.57 (s, 1H), 7.23 (d, *J* = 15.9 Hz, 1H), 7.02 (dd, *J* = 15.9, 7.6 Hz, 1H), 3.52 (s, 3H), 3.41 (s, 3H); ^{13}C NMR (100 MHz, $CDCl_3$) δ 193.9, 161.1, 150.8, 144.6, 144.2, 128.5, 108.8, 37.9, 28.4; FTIR (NaCl, cm^{-1}) 3155, 2949, 2847, 1716, 1665, 1630, 1455, 1372, 1127, 1092, 908; HRMS (ESI+) *m/z* calculated for $[M+Na]^+$ $C_9H_{10}N_2O_3Na$: 217.0584, found 217.0580.

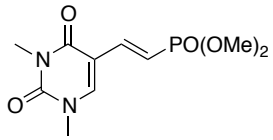

(*E*)-5-(2'-Dimethoxyphosphinylvinyl)-1,3-dimethyluracil (5.12). Prepared by the general procedure described above and purified by flash chromatography (100% acetone) on silica gel to provide 23.0 mg (84%) as a yellow solid (mp 155–157 °C). ^{1}H NMR (400 MHz, $CDCl_3$) δ 7.42 (s, 1H), 7.10 (dd, *J* = 24.1, 17.3 Hz, 1H), 6.91 (dd, *J* = 17.3, 20.1 Hz, 1H), 3.73 (d, *J* = 11.1 Hz, 6H), 3.47 (s, 3H), 3.36 (s, 3H); ^{13}C NMR (100 MHz, $CDCl_3$) δ 161.6, 150.7, 145.6, 141.7 (d, *J* = 7.1 Hz), 113.6 (d, *J* = 185.8 Hz), 109.0 (d, *J* = 23.2 Hz), 52.6 (d, *J* = 13.9 Hz), 37.7, 28.2; FTIR (NaCl, cm^{-1}) 3055, 2987, 2954, 1711, 1664, 1454, 1422, 1356, 1266, 1196, 1057, 1034, 989, 863, 838; HRMS (ESI+) *m/z* calculated for $[M+Na]^+$ $C_{10}H_{15}N_2O_5PNa$: 297.0611, found 297.0607.

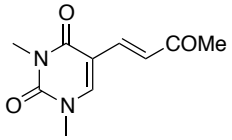

(*E*)-1,3-Dimethyl-5-(3'-oxobut-1'-enyl)uracil (5.13). Prepared by the general procedure described above and purified by flash chromatography (100% EtOAc) on silica gel to provide 15.8 mg (75%) as an off-white solid (mp 164–166 °C). ^{1}H NMR (400 MHz, $CDCl_3$) δ 7.48 (s, 1H), 7.22 (s, 2H), 3.49 (s, 3H), 3.39 (s, 3H), 2.31 (s, 3H); ^{13}C NMR (100 MHz, $CDCl_3$) δ 198.6, 161.6, 150.8, 145.0, 134.7, 126.7, 109.0, 37.8, 28.9, 28.3; FTIR (NaCl, cm^{-1}) 3155, 2980, 2938, 2834, 1727, 1703, 1676, 1634, 1456, 1393, 1368, 1318, 1288, 1155, 1100, 1057, 983, 908, 870; HRMS (ESI+) *m/z* calculated for $[M+Na]^+$ $C_{10}H_{12}N_2O_3Na$: 231.0740, found 231.0742.

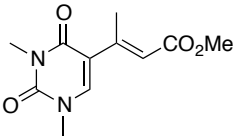

(*E*)-5-(2'-Methoxycarbonyl-1'-methylvinyl)-1,3-dimethyluracil (5.14). Prepared by the general procedure described above and purified by flash chromatography (40%

EtOAc in hexanes) on silica gel to provide 13.9 mg (59%) as a colorless solid (mp 108–110 °C). ^{1}H NMR (400 MHz, $CDCl_3$) δ 7.28 (s, 1H), 6.39 (s, 1H), 3.72 (s, 3H), 3.45 (s, 3H), 3.36 (s, 3H), 2.43 (s, 3H); ^{13}C NMR (100 MHz, $CDCl_3$) δ 167.2, 161.5, 151.2, 148.5, 141.1, 118.8, 115.5, 51.4, 37.5, 28.3, 17.7; FTIR (NaCl, cm^{-1}) 3208, 2951, 1702, 1655, 1450, 1363, 1341, 1291, 1214, 1175, 1040; HRMS (ESI+) *m/z* calculated for $[M+Na]^+$ $C_{11}H_{14}N_2O_4Na$: 261.0846, found 261.0852.

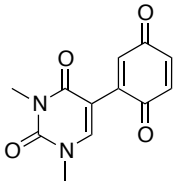

1,3-Dimethyl-5-*p*-quinonyluracil (5.15). Prepared by the general procedure described above and purified by flash chromatography (50% EtOAc in hexanes) on silica gel to provide 13.7 mg (56%) as an orange solid (mp 159–161 °C). ^{1}H NMR (400 MHz, $CDCl_3$) δ 7.84 (s, 1H), 7.46 (d, J = 2.1 Hz, 1H), 6.83–6.76 (m, 2H), 3.51 (s, 3H), 3.40 (s, 3H); ^{13}C NMR (100 MHz, $CDCl_3$) δ 187.4, 186.7, 161.4, 150.7, 146.2, 137.0, 136.9, 136.6, 134.1, 104.3, 38.0, 28.6; FTIR (NaCl, cm^{-1}) 3055, 2087, 1710, 1655, 1422, 1357, 1109, 996; HRMS (ESI+) *m/z* calculated for $[M+Na]^+$ $C_{12}H_{10}N_2O_4Na$: 269.0533, found 269.0536.

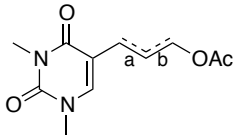

(*E*)-5-(3'-Acetoxyprop-1'-enyl)-1,3-dimethyluracil (5.16a) and **(*E*)-5-(3'-Acetoxyprop-2'-enyl)-1,3-dimethyluracil (5.16b).** Prepared by the general procedure described above and purified by flash chromatography (60% EtOAc in hexanes) on silica gel to provide 12.5 mg (53%) of an inseparable mixture as a colorless solid (mp 108–110 °C). ^{1}H NMR (400 MHz, $CDCl_3$) δ 7.27 (s, 1H, **5.16b**), 7.22 (s, 1H, **5.16a**), 6.58 (dt, J = 15.8, 6.3 Hz, 1H, **5.16a**), 6.43 (d, J = 12.2 Hz, 1H, **5.16b**), 6.35 (d, J = 15.9 Hz, 1H, **5.16a**), 5.83 (dt, J = 7.0, 11.6 Hz, 1H, **5.16b**), 4.70 (d, J = 7.0 Hz, 2H, **5.16b**), 4.65 (d, J =

6.3 Hz, 2H, **5.16a**), 3.44 (s, 3H, **5.16b**), 3.43 (s, 3H, **5.16a**), 3.37 (s, 3H, **5.16a**), 3.37 (s, 3H, **5.16b**), 2.08 (s, 3H, **5.16b**), 2.07 (s, 3H, **5.16a**); ^{13}C NMR (100 MHz, $CDCl_3$) δ 170.9 (**5.16a**), 162.2 (**5.16a**), 151.2 (**5.16a**), 140.3 (**5.16a**), 125.3 (**5.16a**), 124.6 (**5.16a**), 110.4 (**5.16a**), 65.3 (**5.16a**), 37.3 (**5.16a**), 28.2 (**5.16a**), 21.1 (**5.16a**); FTIR (NaCl, cm^{-1}) 3055, 2087, 1735, 1707, 1655, 1458, 1421, 1369, 1089, 1025, 970; HRMS (ESI+) *m/z* calculated for $[M+Na]^+$ $C_{11}H_{14}N_2O_4Na$: 261.0846, found 261.0848.

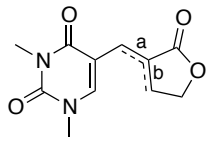

(*E*)-1,3-Dimethyl-5-((2-oxodihydrofuran-3(2*H*)-ylidene)methyl)uracil (5.17a) and **1,3-Dimethyl-5-((2-oxo-2,5-dihydrofuran-3-yl)methyl)uracil (5.17b).** Prepared by the general procedure described above and purified by flash chromatography (60% acetone in hexanes) on silica gel to provide 22.4 mg (96%) of an inseparable mixture as a yellow solid (mp 130–132 °C). ^{1}H NMR (400 MHz, $CDCl_3$) δ 7.44 (t, *J* = 2.9 Hz, 1H, **5.17a**), 7.42 (s, 1H, **5.17a**), 7.36 (s, 1H, **5.17b**), 7.31 (s, 1H, **5.17b**), 4.76 (d, *J* = 1.4 Hz, 2H, **5.17b**), 4.40 (t, *J* = 7.2 Hz, 2H, **5.17a**), 3.49 (s, 3H, **5.17a**), 3.38 (s, 3H, **5.17a**), 3.38 (s, 3H, **5.17b**), 3.33 (s, 3H, **5.17b**), 3.31 (s, 2H, **5.17b**), 3.13 (td, *J* = 7.1, 2.7 Hz, 2H, **5.17a**); ^{13}C NMR (100 MHz, $CDCl_3$) δ 174.3 (**5.17b**), 171.9 (**5.17a**), 163.4 (**5.17b**), 161.4 (**5.17a**), 151.7 (**5.17b**), 150.9 (**5.17a**), 147.2 (**5.17b**), 143.8 (**5.17a**), 141.6 (**5.17b**), 130.5 (**5.17b**), 127.9 (**5.17a**), 123.3 (**5.17a**), 109.6 (**5.17a**), 108.8 (**5.17b**), 70.3 (**5.17b**), 65.3 (**5.17a**), 37.9 (**5.17a**), 37.1 (**5.17b**), 28.5 (**5.17a**), 28.2 (**5.17a**), 28.1 (**5.17b**), 23.5 (**5.17b**); FTIR (NaCl, cm^{-1}) 3224, 2930, 1752, 1702, 1664, 1459, 1375, 1343, 1205, 1171, 1081, 1052, 907, 833, 312; HRMS (ESI+) *m/z* calculated for $[M+Na]^+$ $C_{11}H_{12}N_2O_4Na$: 259.0689, found 259.0686.

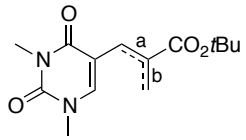

(*E*)-1,3-Dimethyl-5-(2'-*t*-butoxycarbonylpropenyl)uracil (5.18a) and **1,3-Dimethyl-5-(2'-*t*-butoxycarbonylallyl)uracil (5.18b).** Prepared by the general procedure described above and purified by flash chromatography (50% EtOAc in hexanes) on silica gel to provide 13.2 mg (47%) of an inseparable mixture as colorless crystals (mp 93–95 °C). ^{1}H NMR (400 MHz, $CDCl_3$) δ 7.41 (s, 1H, **5.18a**), 7.28 (s, 1H, **5.18a**), 7.10 (s, 1H, **5.18b**), 6.15 (s, 1H, **5.18b**), 5.69 (s, 1H, **5.18b**), 3.46 (s, 3H, **5.18a**), 3.38 (s, 3H, **5.18a**), 3.37 (s, 3H, **5.18b**), 3.35 (s, 3H, **5.18b**), 3.29 (s, 2H, **5.18b**), 1.98 (s, 3H, **5.18a**), 1.51 (s, 9H, **5.18a**), 1.47 (s, 9H, **5.18b**); ^{13}C NMR (100 MHz, $CDCl_3$) δ 167.1 (**5.18a**), 166.1 (**5.18b**), 163.5 (**5.18b**), 162.5 (**5.18a**), 151.9 (**5.18b**), 151.2 (**5.18a**), 142.2 (**5.18a**), 140.8 (**5.18b**), 138.6 (**5.18b**), 130.3 (**5.18a**), 128.6 (**5.18a**), 126.7 (**5.18b**), 111.0 (**5.18b**), 110.1 (**5.18a**), 81.1 (**5.18b**), 81.0 (**5.18a**), 37.6 (**5.18a**), 37.0 (**5.18a**, **5.18b**), 29.6 (**5.18a**, **5.18b**), 28.2 (**5.18a**, **5.18b**), 14.9 (**5.18a**); FTIR (NaCl, cm^{-1}) 3055, 2086, 1702, 1660, 1457, 1422, 1369, 1341, 1143, 1085, 1049, 954, 849; HRMS (ESI+) *m/z* calculated for $[M+Na]^+$ $C_{14}H_{20}N_2O_4Na$: 303.1315, found 303.1316.

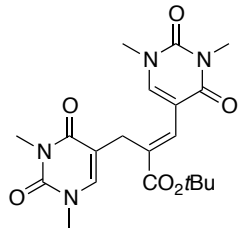

(*E*)-1,3-Dimethyl-5-(3'-(1,3-dimethyluracil-5-yl)-2'-*t*-butoxycarbonylallyl)uracil (5.18c). Prepared by the general procedure described above and purified by flash chromatography (100% EtOAc) on silica gel to provide 6.6 mg (24%) as a colorless wax. ^{1}H NMR (400 MHz, $CDCl_3$) δ 8.56 (s, 1H), 7.50 (s, 1H), 7.37 (s, 1H), 3.50 (s, 3H), 3.44 (s, 2H), 3.38 (s, 6H), 3.36 (s, 3H), 1.50 (s, 9H); ^{13}C NMR (100 MHz, $CDCl_3$) δ 167.4, 164.3, 162.8, 151.6, 151.4, 144.3, 143.1, 131.1, 130.7, 109.6, 108.5, 81.6, 37.6, 37.2, 37.2, 28.3, 25.4; FTIR (NaCl, cm^{-1}) 3054, 2987, 1702, 1659, 1552, 1422, 1370, 1344,

1157, 1102; HRMS (ESI+) *m/z* calculated for $[M+Na]^+$ $C_{20}H_{26}N_4O_6Na$: 441.1745, found 441.1751.

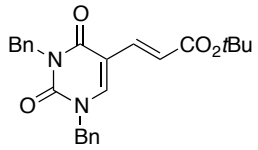

(*E*)-1,3-Dibenzyl-5-(2'-*t*-butoxycarbonylvinyl)uracil (5.19). Prepared by the general procedure described above and purified by flash chromatography (20% EtOAc in hexanes) on silica gel to provide 38.4 mg (94%) as a colorless oil. ^{1}H NMR (400 MHz, $CDCl_3$) δ 7.49 (d, *J* = 6.7 Hz, 2H), 7.42–7.26 (m, 9H), 7.12 (d, *J* = 15.8 Hz, 1H), 6.88 (d, *J* = 15.7 Hz, 1H), 5.18 (s, 2H), 4.97 (s, 2H), 1.47 (s, 9H); ^{13}C NMR (100 MHz, $CDCl_3$) δ 166.9, 161.1, 150.8, 143.3, 136.6, 135.2, 134.7, 129.4, 129.3, 129.0, 128.6, 128.4, 127.9, 121.6, 109.9, 80.5, 52.8, 45.0, 28.3; FTIR (NaCl, cm^{-1}) 3055, 2983, 2933, 1708, 1664, 1629, 1496, 1452, 1384, 1368, 1317, 1155, 1080, 1030, 984, 910; HRMS (ESI+) *m/z* calculated for $[M+Na]^+$ $C_{25}H_{26}N_2O_4Na$: 441.1785, found 441.1790.

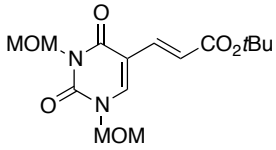

(*E*)-1,3-Bis(methoxymethyl)-5-(2'-*t*-butoxycarbonylvinyl)uracil (5.20). Prepared by the general procedure described above and purified by flash chromatography (50% EtOAc in hexanes) on silica gel to provide 21.7 mg (68%) as a colorless oil. ^{1}H NMR (400 MHz, $CDCl_3$) δ 7.51 (s, 1H), 7.21 (d, *J* = 15.8 Hz, 1H), 6.88 (d, *J* = 15.8 Hz, 1H), 5.42 (s, 2H), 5.18 (s, 2H), 3.45 (s, 3H), 3.41 (s, 3H), 1.49 (s, 9H); ^{13}C NMR (100 MHz, $CDCl_3$) δ 166.6, 161.1, 150.9, 142.7, 134.7, 122.4, 110.4, 80.6, 79.3, 72.5, 58.2, 57.5, 28.3; FTIR (NaCl, cm^{-1}) 3155, 2980, 2938, 1724, 1676, 1634, 1456, 1368, 1318, 1288, 1155, 1100, 984, 908; HRMS (ESI+) *m/z* calculated for $[M+Na]^+$ $C_{15}H_{21}N_2O_6Na$: 349.1370, found 349.1367.

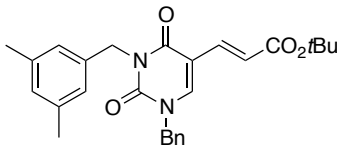

(*E*)-1-Benzyl-3-(3',5'-dimethylbenzyl)-5-(2'-*t*-butoxycarbonylvinyl)uracil (5.21). Prepared by the general procedure described above and purified by flash chromatography (20% EtOAc in hexanes) on silica gel to provide 33.3 mg (76%) as a colorless oil. ^{1}H NMR (400 MHz, $CDCl_3$) δ 7.40–7.27 (m, 6H), 7.13 (d, *J* = 15.8 Hz, 1H), 7.06 (s, 2H), 6.90–6.87 (m, 2H), 5.11 (s, 2H), 4.98 (s, 2H), 2.28 (s, 6H), 1.48 (s, 9H); ^{13}C NMR (100 MHz, $CDCl_3$) δ 166.9, 161.0, 150.8, 143.3, 138.1, 136.4, 135.3, 134.8, 129.5, 129.4, 129.0, 128.3, 126.7, 121.5, 109.9, 80.5, 52.8, 44.9, 28.3, 21.4; FTIR (NaCl, cm^{-1}) 3156, 2079, 2948, 2869, 1704, 1660, 1466, 1368, 1329, 1297, 1153, 1116, 1041, 993, 908; HRMS (ESI+) *m/z* calculated for $[M+Na]^+$ $C_{27}H_{30}N_2O_4Na$: 469.2098, found 469.2097.

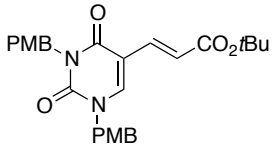

(*E*)-1,3-Bis(*p*-methoxybenzyl)-5-(2'-*t*-butoxycarbonylvinyl)uracil (5.22). Prepared by the general procedure described above and purified by flash chromatography (50% EtOAc in hexanes) on silica gel to provide 46.1 mg (96%) as a colorless oil. ^{1}H NMR (400 MHz, $CDCl_3$) δ 7.46 (d, *J* = 8.6 Hz, 2H), 7.28 (s, 1H), 7.22 (d, *J* = 8.6 Hz, 2H), 7.10 (d, *J* = 15.8 Hz, 1H), 6.92–6.80 (m, 5H), 5.10 (s, 2H), 4.88 (s, 2H), 3.81 (s, 3H), 3.77 (s, 3H), 1.47 (s, 9H); ^{13}C NMR (100 MHz, $CDCl_3$) δ 166.9, 161.0, 160.1, 159.3, 150.8, 143.1, 135.4, 130.9, 130.1, 128.9, 126.5, 121.3, 114.8, 113.8, 109.7, 80.4, 55.4, 52.3, 44.4, 28.3; FTIR (NaCl, cm^{-1}) 3055, 2987, 2839, 1706, 1663, 1628, 1623, 1514, 1456, 1422, 1368, 1178, 1155, 1034, 985, 896; HRMS (ESI+) *m/z* calculated for $[M+Na]^+$ $C_{27}H_{30}N_2O_6Na$: 501.1996, found 501.1995.

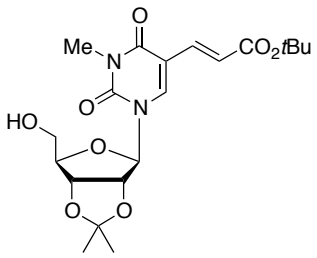

(*E*)-2′,3′-*O*-Isopropylidene-3-methyl-5-(2'-*t*-butoxycarbonylvinyl)uridine (5.23). Prepared by the general procedure described above and purified by flash chromatography (35% EtOAc in hexanes) on silica gel to provide 27.1 mg (66%) as a colorless wax. ^{1}H NMR (400 MHz, $CDCl_3$) δ 7.83 (s, 1H), 7.19 (d, J = 15.8 Hz, 1H), 6.81 (d, J = 15.8 Hz, 1H), 5.76 (d, J = 1.4 Hz, 1H), 4.96–4.89 (m, 2H), 4.42–4.34 (m, 1H), 3.96 (dd, J = 11.8, 2.3 Hz, 1H), 3.83 (dd, J = 11.8, 2.9 Hz, 1H), 3.34 (s, 3H), 2.95 (br, 1H), 1.58 (s, 3H), 1.48 (s, 9H), 1.35 (s, 3H); ^{13}C NMR (100 MHz, $CDCl_3$) δ 167.1, 161.1, 150.1, 141.2, 135.4, 121.3, 114.4, 109.2, 96.0, 87.2, 84.9, 80.7, 62.8, 28.3, 28.1, 27.3, 25.4; FTIR (NaCl, cm^{-1}) 3468, 3055, 2987, 1710, 1667, 1627, 1466, 1422, 1369, 1265, 1155, 1112, 1084, 987, 855; HRMS (ESI+) *m/z* calculated for $[M+Na]^+$ $C_{20}H_{28}N_2O_8Na$: 447.1738, found 447.1737.

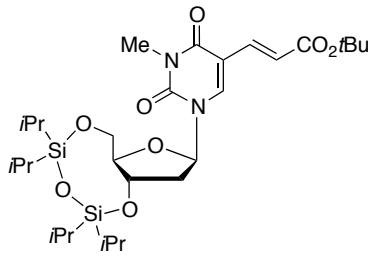

(*E*)-2'-Deoxy-3′,5′-*O*-(1',1',3',3'-tetraisopropyldisiloxy)-3-methyl-5-(2'-*t*-butoxycarbonylvinyl)uridine (5.24). Prepared by the general procedure described above and purified by flash chromatography (10–20% EtOAc in hexanes) on silica gel to provide 44.6 mg (75%) as a colorless oil. ^{1}H NMR (400 MHz, $CDCl_3$) δ 7.94 (s, 1H), 7.26 (d, J = 15.8 Hz, 1H), 6.84 (d, J = 15.9 Hz, 1H), 6.02 (d, J = 6.6 Hz, 1H), 4.44 (q, J = 8.0 Hz, 1H), 4.16 (d, J = 13.1 Hz, 1H), 4.03 (dd, J = 13.2, 2.5 Hz, 1H), 3.81 (d, J = 8.2 Hz, 1H), 3.35 (s, 3H), 2.54 (ddd, J = 13.4, 10.2, 7.2 Hz, 1H), 2.29 (dd, J = 13.4, 7.2 Hz, 1H), 1.48 (s, 9H), 1.11–0.98 (m, 28H); ^{13}C NMR (100 MHz, $CDCl_3$) δ 166.7, 161.2,

149.9, 138.6, 135.7, 121.1, 108.8, 85.5, 80.2, 67.1, 60.1, 40.2, 28.3, 27.9, 17.5, 17.1, 13.6, 13.1, 12.8, 12.6; FTIR (NaCl, cm^{-1}) 3156, 2079, 2948, 2869, 1704, 1660, 1466, 1368, 1320, 1297, 1153, 1116, 1041, 993, 908, 885; HRMS (ESI+) *m/z* calculated for $[M+Na]^+$ $C_{29}H_{50}N_2O_8Si_2Na$: 633.3003, found 633.2995.

8.6 Chapter 6

8.6.1 General procedure for the aerobic alkenylation of cyclic enaminones

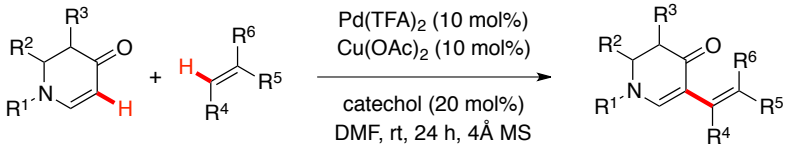

In a 2-dram vial, cyclic enaminone (0.10 mmol) was mixed with $Pd(TFA)_2$ (3.3 mg, 0.01 mmol), $Cu(OAc)_2$ (1.8 mg, 0.01 mmol), catechol (2.2 mg, 0.02 mmol), and 4Å molecular sieves (*ca.* 30 mg). To the mixture was added alkene (0.40 mmol), followed by DMF (0.5 mL). The vial was purged with O_2 and then sealed with an O_2 balloon attached. After stirring at room temperature for 24 h, the reaction was diluted with acetone (2 mL). The mixture was filtered through Celite, and the filter cake was washed with acetone (20 mL). The filtrate was then concentrated under reduced pressure and purified by flash chromatography on silica gel.

8.6.2 General procedure for the synthesis of chalcones via the tandem reaction

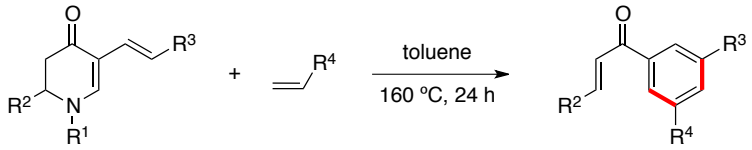

In a 2-dram vial, alkenylated cyclic enaminone (0.07 mmol) was mixed with alkene (0.56 mmol) and toluene (1 mL). The vial was then sealed and stirred at 160 °C. After 24 h, the reaction mixture was cooled, concentrated under reduced pressure, and then purified by flash chromatography on silica gel.

8.6.3 Compound characterization

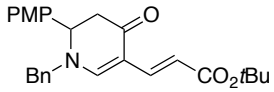

(*E*)-1-Benzyl-5-(2-(*t*-butoxycarbonyl)vinyl)-2-(4-methoxyphenyl)-2,3-dihydropyridin-4(1*H*)-one (6.3). Prepared by the general procedure described above and 35.1 mg (89%) was isolated as a light yellow solid (mp 64–68 °C). Spectroscopic data are consistent with those from compound **4.3**.

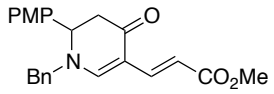

(*E*)-1-Benzyl-5-(2-(methoxycarbonyl)vinyl)-2-(4-methoxyphenyl)-2,3-dihydropyridin-4(1*H*)-one (6.4). Prepared by the general procedure described above and 28.0 mg (78%) was isolated as a light yellow solid (mp 52–55 °C). Spectroscopic data are consistent with those from compound **4.4**.

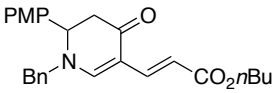

(*E*)-1-Benzyl-5-(2-(*n*-butoxycarbonyl)vinyl)-2-(4-methoxyphenyl)-2,3-dihydropyridin-4(1*H*)-one (6.5). Prepared by the general procedure described above and 34.2 mg (85%) was isolated as a light yellow solid (mp 102–104 °C). Spectroscopic data are consistent with those from compound **4.5**.

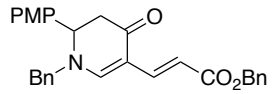

(*E*)-5-(2-(Benzoxycarbonyl)vinyl)-1-benzyl-2-(4-methoxyphenyl)-2,3-dihydropyridin-4(1*H*)-one (6.6). Prepared by the general procedure described above and 37.4 mg (87%) was isolated as a light yellow solid (mp 49–52 °C). Spectroscopic data are consistent with those from compound **4.6**.

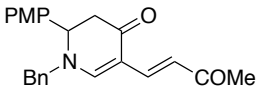

(*E*)-1-Benzyl-2-(4-methoxyphenyl)-5-(3-oxobut-1-enyl)-2,3-dihydropyridin-4(1*H*)-one (6.7). Prepared by the general procedure described above and 23.7 mg (69%) was isolated as a light yellow solid (mp 49–52 °C). Spectroscopic data are consistent with those from compound **4.7**.

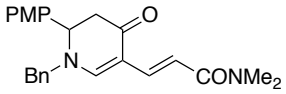

(*E*)-1-Benzyl-5-(2-(dimethylcarbamoyl)vinyl)-2-(4-methoxyphenyl)-2,3-dihydropyridin-4(1*H*)-one (6.8). Prepared by the general procedure described above and 29.4 mg (80%) was isolated as a yellow solid (mp 51–53 °C). Spectroscopic data are consistent with those from compound **4.8**.

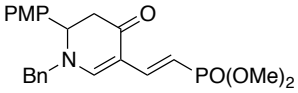

(*E*)-1-Benzyl-5-(2-(diethoxyphosphinyl)vinyl)-2-(4-methoxyphenyl)-2,3-dihydropyridin-4(1*H*)-one (6.9). Prepared by the general procedure described above and 27.4 mg (68%) was isolated as a yellow wax. ^{1}H NMR (400 MHz, $CDCl_3$) δ 7.50 (s, 1H), 7.42–7.34 (m, 3H), 7.18–7.07 (m, 4H), 6.95 (dd, *J* = 24.7, 17.1 Hz, 1H), 6.87 (d, *J* = 8.5 Hz, 2H), 6.52 (dd, *J* = 22.2, 17.0 Hz, 1H), 4.51 (t, *J* = 6.8 Hz, 1H), 4.42 (d, *J* = 14.9 Hz, 1H), 4.25 (d, *J* = 14.9 Hz, 1H), 3.81 (s, 3H), 3.72 (d, *J* = 3.3 Hz, 3H), 3.69 (d, *J* = 3.2 Hz, 3H), 2.92 (dd, *J* = 16.4, 7.3 Hz, 1H), 2.70 (dd, *J* = 16.3, 6.4 Hz, 1H); ^{13}C NMR (100 MHz, $CDCl_3$) δ 188.2, 160.0, 157.3, 145.4 (d, *J* = 8.0 Hz), 134.7, 129.6, 129.4, 128.9, 128.3, 128.0, 114.8, 106.7 (d, *J* = 22.0 Hz) , 104.5 (d, *J* = 189.5 Hz), 60.1, 58.2, 55.5, 52.3 (d, *J* = 5.3 Hz), 52.3 (d, *J* = 5.3 Hz), 44.3; FTIR (NaCl, cm^{-1}) 3156, 2953, 2930, 2851, 1654, 1600, 1513, 1457, 1442, 1392, 1358, 1298, 1194, 1179, 1059, 1035, 991, 868, 832; HRMS (ESI+) *m/z* calculated for $[M+Na]^+$ $C_{23}H_{26}NO_5PNa$: 450.1441, found 450.1447.

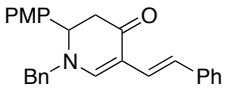

(*E*)-1-Benzyl-2-(4-methoxyphenyl)-5-styryl-2,3-dihydropyridin-4(1*H*)-one (6.10). Prepared by the general procedure described above and 17.0 mg (46%) was isolated as a yellow solid (mp 54–56 °C). Spectroscopic data are consistent with those from compound **4.10**.

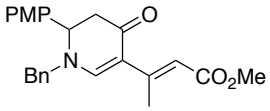

(*E*)-1-Benzyl-5-(2-(methoxycarbonyl)-1-methyl-vinyl)-2-(4-methoxyphenyl)-2,3-dihydropyridin-4(1*H*)-one (6.11). Prepared by the general procedure described above and 7.0 mg (19%) was isolated as a waxy solid. Spectroscopic data are consistent with those from compound **4.14**.

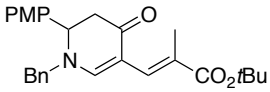

(*E*)-1-Benzyl-5-(2-(*tert*-butoxycarbonyl)propenyl)-2-(4-methoxyphenyl)-2,3-dihydropyridin-4(1*H*)-one (6.12). Prepared by the general procedure described above and 12.2 mg (37%) was isolated as a waxy solid. ^{1}H NMR (400 MHz, $CDCl_3$) δ 7.58 (s, 1H), 7.50 (d, J = 0.9 Hz, 1H), 7.39–7.33 (m, 3H), 7.22–7.12 (m, 4H), 6.88 (d, J = 8.6 Hz, 2H), 4.54 (t, J = 7.0 Hz, 1H), 4.41 (d, J = 14.9 Hz, 1H), 4.26 (d, J = 14.9 Hz, 1H), 3.81 (s, 3H), 2.92 (dd, J = 16.4, 7.1 Hz, 1H), 2.73 (dd, J = 16.5, 6.9 Hz, 1H), 1.90 (d, J = 1.2 Hz, 3H), 1.50 (s, 9H); ^{13}C NMR (100 MHz, $CDCl_3$) δ 188.5, 168.4, 159.9, 154.5, 135.4, 131.9, 130.0, 129.3, 128.7, 128.4, 128.0, 123.0, 114.7, 107.3, 80.0, 60.1, 58.1, 55.5, 43.5, 28.4, 15.2; FTIR (NaCl, cm^{-1}) 3035, 2981, 1640, 1594, 1513, 1466, 1442, 1391, 1368, 1299, 1176, 1121, 1035, 833; HRMS (ESI+) *m/z* calculated for $[M+Na]^+$ $C_{27}H_{31}NO_4Na$: 456.2145, found 456.2144.

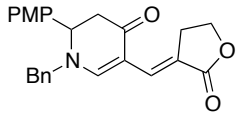

(*E*)-1-Benzyl-2-(4-methoxyphenyl)-5-((2-oxodihydrofuran-3(2*H*)-ylidene)methyl)-2,3-dihydropyridin-4(1*H*)-one (6.13). Prepared by the general procedure described above and 21.2 mg (57%) was isolated as a light yellow solid (mp 59–62 °C). Spectroscopic data are consistent with those from compound **4.15a**.

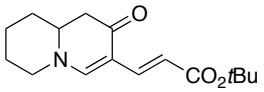

(*E*)-3-(2-(*tert*-Butoxycarbonyl)vinyl)-7,8,9,9a-tetrahydro-1*H*-quinolizin-2(6*H*)-one (6.14). Prepared by the general procedure described above and 15.5 mg (59%) was isolated as a light yellow solid (mp 122–124 °C). Spectroscopic data are consistent with those from compound **4.21**.

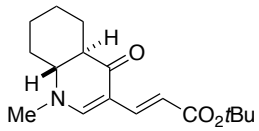

(*E*)-(*trans*)-3-(2-(*tert*-Butoxycarbonyl)vinyl)-1-methyl-4a,5,6,7,8,8a-hexahydroquinolin-4(1*H*)-one (6.15). Prepared by the general procedure described above and 16.4 mg (59%) was isolated as a light yellow solid (mp 146–148 °C). Spectroscopic data are consistent with those from compound **4.25**.

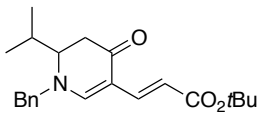

(*E*)-1-Benzyl-5-(2-(*tert*-butoxycarbonyl)vinyl)-2-isopropyl-2,3-dihydropyridin-4(1*H*)-one (6.16). Prepared by the general procedure described above and 27.0 mg (83%) was isolated as a yellow wax. ^{1}H NMR (400 MHz, $CDCl_3$) δ 7.43–7.35 (m, 4H), 7.25 (d, *J* = 7.0 Hz, 2H), 7.08 (d, *J* = 15.6 Hz, 1H), 6.50 (d, *J* = 15.6 Hz, 1H), 4.58 (d, *J* = 15.0 Hz, 1H), 4.48 (d, *J* = 15.1 Hz, 1H), 3.32–3.22 (m, 1H), 2.63 (dd, *J* = 16.6, 7.6 Hz, 1H),

2.47 (dd, J = 16.6, 2.3 Hz, 1H), 2.22 (dq, J = 13.4, 6.7 Hz, 1H), 1.46 (s, 9H), 0.98 (d, J = 6.8 Hz, 3H), 0.92 (d, J = 6.8 Hz, 3H); ^{13}C NMR (100 MHz, $CDCl_3$) δ 188.7, 168.6, 155.9, 138.9, 135.6, 129.4, 128.9, 127.6, 113.1, 105.9, 79.2, 61.8, 59.8, 37.5, 29.7, 28.4, 19.8, 18.1; FTIR (NaCl, cm^{-1}) 3052, 2975, 2932, 1685, 1654, 1594, 1496, 1455, 1439, 1391, 1367, 1319, 1271, 1241, 1151, 1093, 990, 859; HRMS (ESI+) *m/z* calculated for $[M+Na]^+$ $C_{22}H_{29}NO_3Na$: 378.2040, found 378.2038.

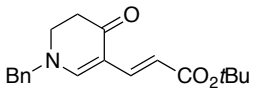

(*E*)-1-Benzyl-5-(2-(*tert*-butoxycarbonyl)vinyl)-2,3-dihydropyridin-4(1*H*)-one (6.17). Prepared by the general procedure described above and 17.7 mg (59%) was isolated as a light yellow oil. Spectroscopic data are consistent with those from compound **4.19**.

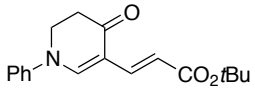

(*E*)-5-(2-(*tert*-Butoxycarbonyl)vinyl)-1-phenyl-2,3-dihydropyridin-4(1*H*)-one (6.18). Prepared by the general procedure described above and 9.0 mg (32%) was isolated as a light yellow solid (mp 150–152 °C). Spectroscopic data are consistent with those from compound **4.17**.

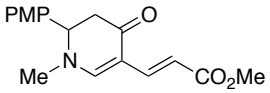

(*E*)-5-(2-(Methoxycarbonyl)vinyl)-2-(4-methoxyphenyl)-1-methyl-2,3-dihydropyridin-4(1*H*)-one (6.33). Prepared by the general procedure described above in **8.2.1** and **8.4.1** as a starting material for the Diels-Alder tandem reaction and isolated as a light yellow solid (mp 123–125 °C). ^{1}H NMR (400 MHz, $CDCl_3$) δ 7.48 (s, 1H), 7.32 (d, J = 16.1 Hz, 1H), 7.25 (d, J = 8.7 Hz, 2H), 6.96 (d, J = 7.4 Hz, 2H), 6.74 (d, J = 13.9 Hz, 1H), 4.60 (t, J = 6.8 Hz, 1H), 3.88 (s, 3H), 3.80 (s, 3H), 3.13–3.00 (m, 4H), 2.81 (dd, J = 16.5, 7.1 Hz, 1H); ^{13}C NMR (100 MHz, $CDCl_3$) δ 187.9, 169.7, 160.0, 157.8, 140.3, 129.6, 128.2, 114.8, 110.9, 106.0, 62.7, 55.5, 51.3, 44.1, 42.4; FTIR (NaCl, cm^{-1}) 3055,

2987, 1654, 1607, 1514, 1422, 1317, 1171, 1099, 1034, 989, 896; HRMS (ESI+) *m/z* calculated for $[M+Na]^+$ $C_{17}H_{19}NO_4Na$: 324.1206, found 324.1210.

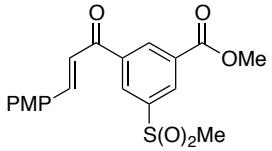

(*E*)-Methyl 3-(3-(4-Methoxyphenyl)acryloyl)-5-(methylsulfonyl)benzoate (6.36). (In a compound name all new words are caps.) Prepared by the general procedure described above and 15.0 mg (82%) was isolated as a yellow solid (mp 185–187 °C). ^{1}H NMR (400 MHz, $CDCl_3$) δ 8.89 (s, 1H), 8.77 (s, 1H), 8.72 (s, 1H), 7.89 (d, *J* = 15.4 Hz, 1H), 7.65 (d, *J* = 7.8 Hz, 2H), 7.42 (d, *J* = 15.5 Hz, 1H), 6.96 (d, *J* = 7.8 Hz, 2H), 4.02 (s, 3H), 3.88 (s, 3H), 3.15 (s, 3H); ^{13}C NMR (100 MHz, $CDCl_3$) δ 187.6, 164.9, 162.5, 147.3, 142.2, 140.4, 134.0, 132.5, 131.8, 131.1, 131.0, 127.1, 118.1, 114.7, 55.6, 53.1, 44.5; FTIR (NaCl, cm^{-1}) 3055, 2987, 1732, 1665, 1592, 1571, 1513, 1422, 1325, 1308, 1212, 1174, 1149, 1060, 1030, 984, 961, 896, 828; HRMS (ESI+) *m/z* calculated for $[M+Na]^+$ $C_{19}H_{18}O_6SNa$: 397.0716, found 397.0716.

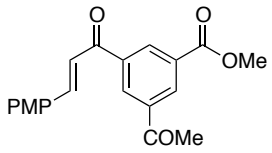

(*E*)-Methyl 3-Acetyl-5-(3-(4-methoxyphenyl)acryloyl)benzoate (6.39). Prepared by the general procedure described above and 17.5 mg (66%) was isolated as a yellow solid (mp 72–74 °C). ^{1}H NMR (400 MHz, $CDCl_3$) δ 8.83 (s, 1H), 8.78 (s, 1H), 8.75 (s, 1H), 7.86 (d, *J* = 15.5 Hz, 1H), 7.65 (d, *J* = 7.7 Hz, 1H), 7.46 (d, *J* = 15.4 Hz, 1H), 6.96 (d, *J* = 7.8 Hz, 2H), 4.00 (s, 3H), 3.87 (s, 3H), 2.72 (s, 3H); ^{13}C NMR (100 MHz, $CDCl_3$) δ 196.8, 188.7, 165.9, 162.3, 146.4, 139.5, 137.9, 133.4, 132.9, 132.0, 131.5, 130.8, 127.3, 118.7, 114.7, 55.6, 52.8, 27.1; FTIR (NaCl, cm^{-1}) 3055, 2987, 1728, 1693, 1664, 1599, 1572, 1513, 1422, 1361, 1195, 1173, 1031, 985, 829; HRMS (ESI+) *m/z* calculated for $[M+Na]^+$ $C_{20}H_{18}O_5Na$: 361.1046, found 361.1044.

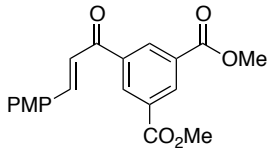

(*E*)-Dimethyl 5-(3-(4-Methoxyphenyl)acryloyl)isophthalate (6.40). Prepared by the general procedure described above and 20.3 mg (73%) was isolated as a yellow solid (mp 111–113 °C). ^{1}H NMR (400 MHz, $CDCl_3$) δ 8.88 (s, 1H), 8.84 (s, 2H), 7.88 (d, *J* = 15.4 Hz, 1H), 7.66 (d, *J* = 7.6 Hz, 2H), 7.46 (d, *J* = 15.3 Hz, 1H), 6.97 (d, *J* = 8.7 Hz, 2H), 4.01 (s, 6H), 3.89 (s, 3H); ^{13}C NMR (100 MHz, $CDCl_3$) δ 188.6, 165.8, 162.3, 146.3, 139.4, 134.2, 133.4, 131.4, 130.8, 127.4, 118.8, 114.7, 55.6, 52.8; FTIR (NaCl, cm^{-1}) 3055, 2987, 2956, 1730, 1664, 1601, 1572, 1513, 1422, 1208, 1173, 1032, 1002, 896, 830; HRMS (ESI+) *m/z* calculated for $[M+Na]^+$ $C_{20}H_{18}O_6Na$: 377.0996, found 377.1005.

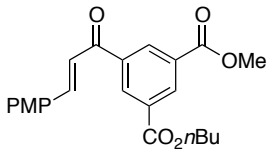

(*E*)-1-Butyl 3-Methyl 5-(3-(4-Methoxyphenyl)acryloyl)isophthalate (6.41). Prepared by the general procedure described above and 23.2 mg (75%) was isolated as a yellow wax. ^{1}H NMR (400 MHz, $CDCl_3$) δ 8.85 (s, 1H), 8.82 (s, 2H), 7.86 (d, *J* = 15.3 Hz, 1H), 7.64 (d, *J* = 8.1 Hz, 2H), 7.45 (d, *J* = 15.3 Hz, 1H), 6.96 (d, *J* = 8.2 Hz, 2H), 4.40 (t, *J* = 7.2 Hz, 2H), 4.00 (s, 3H), 3.87 (s, 3H), 1.81 (m, 2H), 1.50 (h, *J* = 7.4, 6.9 Hz, 2H), 1.00 (t, *J* = 8.1 Hz, 3H); ^{13}C NMR (100 MHz, $CDCl_3$) δ 188.7, 165.8, 165.4, 162.2, 146.3, 139.3, 134.1, 133.4, 133.3, 131.8, 131.3, 130.7, 127.4, 118.8, 114.7, 65.8, 55.6, 52.8, 30.9, 19.4, 13.9; FTIR (NaCl, cm^{-1}) 3053, 2962, 2936, 1725, 1664, 1601, 1572, 1513, 1464, 1443, 1424, 1386, 1288, 1204, 1173, 1109, 1065, 1032, 986, 828; HRMS (ESI+) *m/z* calculated for $[2M+Na]^+$ $C_{46}H_{48}O_{12}Na$: 815.3038, found 815.3044.

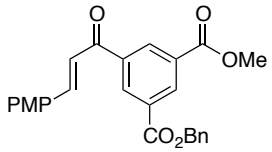

(*E*)-1-Benzyl 3-Methyl 5-(3-(4-Methoxyphenyl)acryloyl)isophthalate (6.42). Prepared by the general procedure described above and 24.0 mg (86%) was isolated as a yellow wax. ^{1}H NMR (400 MHz, $CDCl_3$) δ 8.88 (s, 1H), 8.85 (s, 1H), 8.82 (s, 1H), 7.85 (d, *J* = 15.5 Hz, 1H), 7.64 (d, *J* = 7.8 Hz, 2H), 7.50–7.37 (m, 6H), 6.96 (d, *J* = 7.8 Hz, 2H), 5.44 (s, 2H), 3.99 (s, 3H), 3.87 (s, 3H); ^{13}C NMR (100 MHz, $CDCl_3$) δ 188.6, 165.8, 165.2, 162.2, 146.3, 139.4, 135.7, 134.2, 133.6, 133.5, 131.5, 131.4, 130.8, 128.8, 128.7, 128.6, 127.4, 118.8, 114.7, 67.6, 55.6, 52.8; FTIR (NaCl, cm^{-1}) 3055, 2987, 1728, 1664, 1601, 1588, 1572, 1513, 1422, 1201, 1173, 1030, 986, 896, 829; HRMS (ESI+) *m/z* calculated for $[M+Na]^+$ $C_{26}H_{22}O_6Na$: 453.1309, found 453.1314.

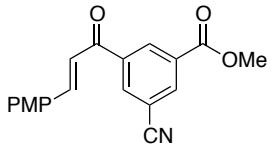

(*E*)-Methyl 3-Cyano-5-(3-(4-methoxyphenyl)acryloyl)benzoate (6.43). Prepared by the general procedure described above and 16.6 mg (80%) was isolated as a light yellow solid (mp 257–259 °C). ^{1}H NMR (400 MHz, $CDCl_3$) δ 8.82 (s, 1H), 8.49 (s, 1H), 8.45 (s, 1H), 7.87 (d, *J* = 15.4 Hz, 1H), 7.65 (d, *J* = 7.2 Hz, 2H), 7.38 (d, *J* = 15.4 Hz, 1H), 6.97 (d, *J* = 6.8 Hz, 2H), 4.01 (s, 3H), 3.88 (s, 3H); ^{13}C NMR (100 MHz, $CDCl_3$) δ 187.3, 164.7, 162.5, 147.3, 140.0, 136.3, 135.8, 133.0, 132.1, 130.9, 127.1, 117.9, 117.4, 114.8, 113.8, 55.6, 53.2; FTIR (NaCl, cm^{-1}) 3156, 2957, 2932, 2254, 1794, 1731, 1662, 1600, 1571, 1513, 1465, 1444, 1382, 1307, 1287, 1225, 1173, 1096, 1034, 987, 827; HRMS (ESI+) *m/z* calculated for $[M+Na]^+$ $C_{19}H_{15}NO_4Na$: 344.0893, found 344.0891.

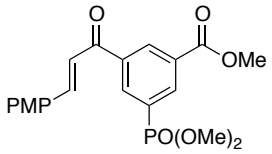

(*E*)-Methyl 3-(Dimethoxyphosphoryl)-5-(3-(4-methoxyphenyl)acryloyl)benzoate (6.44). Prepared by the general procedure described above and 6.0 mg (23%) was isolated as a yellow wax. ^{1}H NMR (400 MHz, $CDCl_3$) δ 8.83 (s, 1H), 8.64 (d, *J* = 12.1 Hz, 1H), 8.60 (d, *J* = 12.1 Hz, 1H), 7.87 (d, *J* = 15.6 Hz, 1H), 7.65 (d, *J* = 8.6 Hz, 2H), 7.44 (d, *J* = 15.5 Hz, 1H), 6.96 (d, *J* = 8.6 Hz, 2H), 3.99 (s, 3H), 3.88 (s, 3H), 3.83 (d, *J* = 11.1 Hz, 6H); ^{13}C NMR (100 MHz, $CDCl_3$) δ 188.5, 165.7, 162.3, 146.6, 139.4 (d, *J* = 13.9 Hz), 136.4 (d, *J* = 10.9 Hz), 135.7 (d, *J* = 11.0 Hz), 133.2 (d, *J* = 3.0 Hz), 131.4 (d, *J* = 15.2 Hz), 130.9, 129.1 (d, *J* = 191.5 Hz), 127.3, 118.6, 114.7, 55.6, 53.2 (d, *J* = 5.8 Hz), 52.9; FTIR (NaCl, cm^{-1}) 3055, 2987, 1738, 1638, 1512, 1422, 1174, 1033, 896; HRMS (ESI+) *m/z* calculated for $[M+Na]^+$ $C_{20}H_{21}O_7PNa$: 427.0917, found 427.0929.

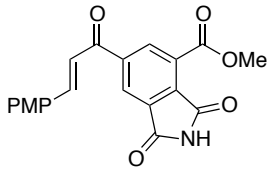

(*E*)-4-Methoxycarbonyl-6-(3-(4-methoxyphenyl)acryloyl)isoindoline-1,3-dione (6.45). Prepared by the general procedure described above and 4.4 mg (16%) was isolated as a bright yellow solid (mp 165–167 °C). ^{1}H NMR (400 MHz, $CDCl_3$) δ 8.61 (s, 1H), 8.56 (s, 1H), 7.89 (d, *J* = 15.5 Hz, 2H), 7.65 (d, *J* = 8.7 Hz, 2H), 7.40 (d, *J* = 15.5 Hz, 1H), 6.97 (d, *J* = 8.7 Hz, 2H), 4.05 (s, 3H), 3.88 (s, 3H); ^{13}C NMR (100 MHz, $CDCl_3$) δ 187.5, 165.9, 165.0, 164.5, 162.7, 147.7, 144.0, 134.7, 134.4, 132.7, 131.0, 130.8, 127.0, 125.4, 118.1, 114.8, 55.7, 53.4; FTIR (NaCl, cm^{-1}) 3413, 3055, 2987, 1783, 1744, 1638, 1513, 1421, 1173, 896; HRMS (ESI+) *m/z* calculated for $[M+Na]^+$ $C_{20}H_{15}NO_6Na$: 388.0792, found 388.0791.

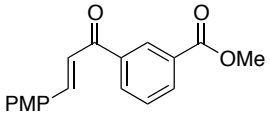

(*E*)-Methyl 3-(3-(4-Methoxyphenyl)acryloyl)benzoate (6.46). Prepared by the general procedure described above and 7.6 mg (33%) was isolated as an off-white solid (mp 93–95 °C). ^{1}H NMR (400 MHz, $CDCl_3$) δ 8.65 (s, 1H), 8.29–8.14 (m, 2H), 7.83 (d, *J* = 15.5 Hz, 1H), 7.61 (dd, *J* = 20.1, 8.0 Hz, 3H), 7.44 (d, *J* = 15.5 Hz, 1H), 6.95 (d, *J* = 8.0 Hz, 2H), 3.97 (s, 3H), 3.87 (s, 3H); ^{13}C NMR (100 MHz, $CDCl_3$) δ 189.5, 166.4, 161.9, 145.5, 138.8, 133.4, 132.7, 130.6, 130.4, 129.4, 128.9, 127.4, 119.2, 114.5, 55.4, 52.4; FTIR (NaCl, cm^{-1}) 3155, 2984, 2955, 2929, 1793, 1722, 1660, 1595, 1572, 1512, 1466, 1382, 1305, 1291, 1208, 1173, 1096, 1034, 830; HRMS (ESI+) *m/z* calculated for $[M+Na]^+$ $C_{18}H_{16}O_4Na$: 319.0941, found 319.0946.

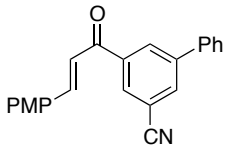

(*E*)-3-Cyano-5-(3-(4-methoxyphenyl)acryloyl)-1,1'-biphenyl (6.47). Prepared by the general procedure described above and 10.5 mg (46%) was isolated as a yellow solid (mp 61–63°C). ^{1}H NMR (400 MHz, $CDCl_3$) δ 8.42 (s, 1H), 8.24 (s, 1H), 8.06 (s, 1H), 7.88 (d, *J* = 15.5 Hz, 1H), 7.70–7.62 (m, 4H), 7.51 (m, 3H), 7.40 (d, *J* = 15.7 Hz, 1H), 6.98 (d, *J* = 7.8 Hz, 2H), 3.89 (s, 3H); ^{13}C NMR (100 MHz, $CDCl_3$) δ 188.4, 162.4, 146.7, 143.3, 140.1, 138.3, 134.0, 131.2, 130.8, 130.5, 129.4, 129.0, 127.3, 127.2, 118.6, 118.3, 114.7, 113.6, 55.6; FTIR (NaCl, cm^{-1}) 3155, 2929, 2254, 1794, 1710, 1663, 1597, 1571, 1513, 1465, 1382, 1342, 1308, 1288, 1206, 1173, 1095, 1049, 1032, 985, 827; HRMS (ESI+) *m/z* calculated for $[M+Na]^+$ $C_{23}H_{17}NO_2Na$: 362.1151, found 362.1153.

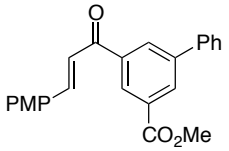

(*E*)-3-Methoxycarbonyl-5-(3-(4-methoxyphenyl)acryloyl)-1,1'-biphenyl (6.48). Prepared by the general procedure described above and 13.0 mg (52%) was isolated as a

yellow solid (mp 124–126 °C). ^{1}H NMR (400 MHz, $CDCl_3$) δ 8.61 (s, 1H), 8.48 (s, 1H), 8.42 (s, 1H), 7.86 (d, *J* = 15.5 Hz, 1H), 7.73–7.62 (m, 4H), 7.52–7.40 (m, 4H), 6.96 (d, *J* = 8.0 Hz, 2H), 4.00 (s, 3H), 3.87 (s, 3H); ^{13}C NMR (100 MHz, $CDCl_3$) δ 189.7, 166.6, 162.1, 145.8, 142.3, 139.5, 139.4, 132.1, 131.3, 131.3, 130.6, 129.2, 128.4, 128.2, 127.6, 127.4, 119.4, 114.6, 55.6, 52.6; FTIR (NaCl, cm^{-1}) 3055, 2987, 1723, 1662, 1599, 1572, 1513, 1438, 1422, 1349, 1197, 1173, 1048, 1031, 983, 896, 828; HRMS (ESI+) *m/z* calculated for $[M+Na]^+$ $C_{24}H_{20}O_4Na$: 395.1254, found 395.1254.

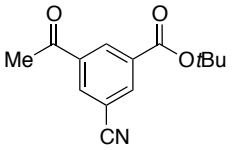

***tert*-Butyl 3-Acetyl-5-cyanobenzoate (6.49).** Prepared by the general procedure described above and 8.1 mg (48%) was isolated as a colorless oil. ^{1}H NMR (400 MHz, $CDCl_3$) δ 8.71 (s, 1H), 8.42 (s, 1H), 8.37 (s, 1H), 2.67 (s, 3H), 1.63 (s, 9H); ^{13}C NMR (100 MHz, $CDCl_3$) δ 195.3, 163.0, 138.2, 136.8, 135.1, 134.1, 133.0, 117.4, 113.7, 83.4, 28.2, 26.8; FTIR (NaCl, cm^{-1}) 3055, 2986, 2931, 2238, 1721, 1698, 1639, 1552, 1422, 1371, 1330, 1158, 1129, 978, 896, 844; HRMS (ESI+) *m/z* calculated for $[M+Na]^+$ $C_{14}H_{15}NO_3Na$: 268.0944, found 268.0943.

8.7 Chapter 7

8.7.1 Procedure for direct C–H trifluoromethylation of cyclic enaminones

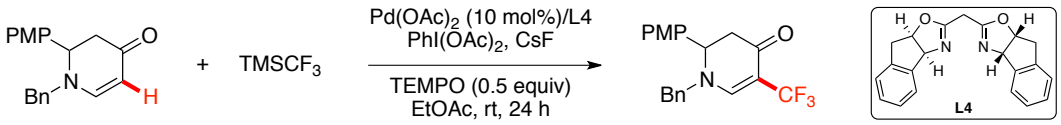

In a 2-dram vial, cyclic enaminone (29.3 mg, 0.1 mmol), $Pd(OAc)_2$ (2.3 mg, 0.01 mmol), $PhI(OAc)_2$ (64.4 mg, 0.2 mmol), ligand L4 (5.0 mg, 0.015 mmol), and TEMPO (7.8 mg, 0.05 mmol) were added. The vial was transferred to a glove box to add CsF (60.8 mg, 0.4 mmol). Sequentially, $TMSCF_3$ (59 μL, 0.4 mmol) and anhydrous EtOAc (1 mL) were added. After stirring at room temperature for 24 h, the reaction was diluted with EtOAc

(2 mL) and filtered through Celite. The filter cake was then washed with EtOAc (20 mL). The filtrate was concentrated under reduced pressure and purified by flash chromatography on silica gel.

8.7.2 Compound characterization

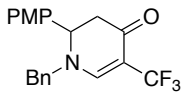

(*E*)-1-Benzyl-2-(4-methoxyphenyl)-5-trifluoromethyl-2,3-dihydropyridin-4(1*H*)-one (7.4). Prepared by the general procedure described above and 24.3 mg (70%) was isolated as a yellow wax. ^{1}H NMR (400 MHz, $CDCl_3$) δ 7.73 (s, 1H), 7.38 (d, J = 4.5 Hz, 3H), 7.17–7.07 (m, 4H), 6.89 (d, J = 8.1 Hz, 2H), 4.51 (t, J = 6.2 Hz, 1H), 4.44 (d, J = 15.0 Hz, 1H), 4.26 (d, J = 14.9 Hz, 1H), 3.81 (s, 3H), 2.89 (dd, J = 16.6, 7.0 Hz, 1H), 2.69 (dd, J = 16.5, 5.8 Hz, 1H); ^{13}C NMR (100 MHz, $CDCl_3$) δ 185.4, 160.1, 152.6, 134.7, 129.4, 129.3, 128.9, 128.3, 127.9, 114.8, 59.8, 58.2, 55.5, 43.4; ^{19}F NMR (376 MHz,) δ -60.87; FTIR (NaCl, cm^{-1}) 3055, 2987, 1660, 1622, 1514, 1441, 1422, 1396, 1357, 1181, 1125, 1034, 1017, 972, 935, 896; HRMS (ESI+) *m/z* calculated for $[M+Na]^+$ $C_{20}H_{18}F_3NO_2Na$: 384.1182, found 384.1178.

Chapter 9 Bibliography

[1] Hijicek, I. Trends in total synthesis of alkaloids. *Chem. Listy* **2005**, *99*, 298.

[2] Alcaide, B.; Almendros, P. Beta-lactams as versatile synthetic intermediates for the preparation of heterocycles of biological interest. *Curr. Med. Chem.* **2004**, *11*, 1921.

[3] Lopez, M. D.; Cobo, J.; Nogueras, M. Building bicyclic polyhydroxylated alkaloids: An overview from 1995 to the present. *Curr. Org. Chem.* **2008**, *12*, 718.

[4] Yoda, H. Recent advances in the synthesis of naturally occurring polyhydroxylated alkaloids. *Curr. Org. Chem.* **2002**, *6*, 223.

[5] Bur, S. K.; Padwa, A., The synthesis of heterocycles using cascade chemistry. In *Advances in Heterocyclic Chemistry, Vol 94*, Elsevier Academic Press Inc: San Diego, **2007**; Vol. 94, pp 1.

[6] Wolfe, J. P.; Thomas, J. S. Recent developments in palladium-catalyzed heterocycle synthesis and functionalization. *Curr. Org. Chem.* **2005**, *9*, 625.

[7] Tietze, L. F.; Kettschau, G., Hetero Diels-Alder reactions in organic chemistry. In *Stereoselective Heterocyclic Synthesis I*, Springer-Verlag Berlin: Berlin 33, **1997**; Vol. 189, pp 1.

[8] Padwa, A.; Bur, S. K. The domino way to heterocycles. *Tetrahedron* **2007**, *63*, 5341.

[9] Weinreb, S. M.; Levin, J. I. Synthesis of nitrogen-containing heterocycles by the imino Diels-Alder reaction. *Heterocycles* **1979**, *12*, 949.

[10] Arisawa, M.; Terada, Y.; Theeraladanon, C.; Takahashi, K.; Nakagawa, M.; Nishida, A. Development of novel reactions using ruthenium carbene catalyst and its application to novel methods for preparing nitrogen-containing heterocycles. *J. Organomet. Chem.* **2005**, *690*, 5398.

[11] Fujii, T. Highlights from 43 years of chemistry of naturally occurring nitrogen-containing heterocycles .2. Syntheses and reactions of purines and of their nucleosides. *J. Pharm. Soc. Jpn.* **1996**, *116*, 355.

[12] Lewis, J. C.; Bergman, R. G.; Ellman, J. A. Direct functionalization of nitrogen heterocycles via Rh-catalyzed C-H bond activation. *Acc. Chem. Res.* **2008**, *41*, 1013.

[13] Arisawa, M.; Nishida, A.; Nakagawa, M. Preparation of nitrogen-containing heterocycles using ring-closing metathesis (RCM) and its application to natural product synthesis. *J. Organomet. Chem.* **2006**, *691*, 5109.

[14] Michael, J. P.; de Koning, C. B.; Gravestock, D.; Hosken, G. D.; Howard, A. S.; Jungmann, C. M.; Krause, R. W. M.; Parsons, A. S.; Pelly, S. C.; Stanbury, T. V. Enaminones: versatile intermediates for natural product synthesis. *Pure Appl. Chem.* **1999**, *71*, 979.

[15] Edafiogho, I. O.; Kombian, S. B.; Ananthalakshmi, K. V. V.; Salama, N. N.; Eddington, N. D.; Wilson, T. L.; Alexander, M. S.; Jackson, P. L.; Hanson, C. D.;

Scott, K. R. Enaminones: Exploring additional therapeutic activities. *J. Pharm. Sci.* **2007**, *96*, 2509.
[16] Salama, N. N.; Eddington, N. D.; Payne, D.; Wilson, T. L.; Scott, K. R. Multidrug resistance and anticonvulsants: New studies with some enaminones. *Curr. Med. Chem.* **2004**, *11*, 2093.
[17] Negri, G.; Kascheres, C.; Kascheres, A. J. Recent development in preparation reactivity and biological activity of enaminoketones and enaminothiones and their utilization to prepare heterocyclic compounds. *J. Heterocycl. Chem.* **2004**, *41*, 461.
[18] Elassar, A. Z. A.; El-Khair, A. A. Recent developments in the chemistry of enaminones. *Tetrahedron* **2003**, *59*, 8463.
[19] Edafiogho, I. O.; Moore, J. A.; Farrar, V. A.; Nicholson, J. M.; Scott, K. R. Synthesis, reactions, and preliminary evaluations of enaminone esters. *J. Pharm. Sci.* **1994**, *83*, 79.
[20] Comins, D. L.; Hong, H. The addition of metallo-enolates to chiral 1-acylpyridinium salts - An asymmetric-synthesis of (-)-Sedamine. *J. Org. Chem.* **1993**, *58*, 5035.
[21] Comins, D. L.; Hong, H. Asymmetric-synthesis of (-)-Porantheridine. *J. Am. Chem. Soc.* **1993**, *115*, 8851.
[22] Comins, D. L.; Dehghani, A. A short, asymmetric-synthesis of (-)-Pumiliotoxin-C. *J. Chem. Soc., Chem. Commun.* **1993**, 1838.
[23] Comins, D. L.; Hong, H. Chiral dihydropyridones as synthetic intermediates - Asymmetric-synthesis of (+)-Elaeokanine-A and (+)-Elaeokanine-C. *J. Am. Chem. Soc.* **1991**, *113*, 6672.
[24] Guerry, P.; Neier, R. Reduktion von 4-Pyridinonen. *Synthesis* **1984**, *1984*, 485.
[25] Follmann, M.; Kunz, H. Desymmetrization Reactions on 4-Pyridone Using Carbohydrate Templates. *Synlett* **1998**, *1998*, 989.
[26] Nicolaou, K. C.; Montagnon, T.; Baran, P. S. Modulation of the Reactivity Profile of IBX by Ligand Complexation: Ambient Temperature Dehydrogenation of Aldehydes and Ketones to α,β-Unsaturated Carbonyl Compounds. *Angew. Chem. Int. Ed.* **2002**, *41*, 993.
[27] Ishii, Y.; Chatani, N.; Kakiuchi, F.; Murai, S. Rhodium-Catalyzed Reaction of N-Acylpiperazines with CO and Ethylene. Carbonylation at a C-H Bond Directed by an Amido Group. *Tetrahedron Lett.* **1997**, *38*, 7565.
[28] Flick, A. C.; Padwa, A. A new route to heterocyclic compounds by the mercuric acetate oxidation of N-alkyl substituted 4-piperidones. *Tetrahedron Lett.* **2008**, *49*, 5739.
[29] Diao, T.; Stahl, S. S. Synthesis of Cyclic Enones via Direct Palladium-Catalyzed Aerobic Dehydrogenation of Ketones. *J. Am. Chem. Soc.* **2011**, *133*, 14566.
[30] Tubéry, F.; Grierson, D. S.; Husson, H.-P. Simple 4-acetoxy-5,6-dihydropyridinium salts: New synthons for the preparation of functionalized piperidine systems. *Tetrahedron Lett.* **1987**, *28*, 6457.

[31] Comins, D. L.; Joseph, S. P.; Goehring, R. R. Asymmetric-synthesis of 2-alkyl(aryl)-2,3-dihydro-4-pyridones by addition of Grignard-reagents to chiral 1-acyl-4-methoxypyridinium salts. *J. Am. Chem. Soc.* **1994**, *116*, 4719.
[32] Kuethe, J. T.; Comins, D. L. Addition of metallo enolates to chiral 1-acylpyridinium salts: Total synthesis of (+)-cannabisativine. *Org. Lett.* **2000**, *2*, 855.
[33] Loncaric, C.; Manabe, K.; Kobayashi, S. AgOTf-catalyzed aza-Diels-Alder reactions of Danishefsky's diene with imines in water. *Adv. Synth. Catal.* **2003**, *345*, 475.
[34] Cheng, K.; Zeng, B. Q.; Yu, Z. P.; Gao, B.; Feng, X. M. A mild and efficient synthesis of 2,5-disubstituted 2,3-dihydro-4-pyridones catalyzed by Yb(OTf)(3). *Synlett* **2005**, 1018.
[35] Akiyama, T.; Takaya, J.; Kagoshima, H. Bronsted acid-catalyzed aza Diels-Alder reaction of Danishefsky's diene with aldimine generated in situ from aldehyde and amine in aqueous media. *Tetrahedron Lett.* **1999**, *40*, 7831.
[36] Yuan, Y.; Li, X.; Ding, K. L. Acid-free aza Diels-Alder reaction of Danishefsky's diene with imines. *Org. Lett.* **2002**, *4*, 3309.
[37] Akiyama, T.; Matsuda, K.; Fuchibe, K. Montmorillonite K10-catalyzed aza Diels-Alder reaction of Danishefsky's diene with aldimines, generated in situ from aliphatic aldehydes and amine, in aqueous media. *Synlett* **2002**, 1898.
[38] Zulfiqar, F.; Kitazume, T. One-pot aza-Diels-Alder reactions in ionic liquids. *Green Chem.* **2000**, *2*, 137.
[39] Wang, Y. H.; Wilson, S. R. Solid phase synthesis of 2,3-dihydro-4-pyridones: Reaction of Danishefsky's diene with polymer-bound imines. *Tetrahedron Lett.* **1997**, *38*, 4021.
[40] Guo, H. C.; Wang, Z.; Ding, K. L. PEG-polymer-supported liquid-phase combinatorial synthesis of structurally diverse 2,3-dihydro-4-pyridones. *Synthesis* **2005**, 1061.
[41] Creswell, M. W.; Bolton, G. L.; Hodges, J. C.; Meppen, M. Combinatorial synthesis of dihydropyridone libraries and their derivatives. *Tetrahedron* **1998**, *54*, 3983.
[42] Yu, R. T.; Lee, E. E.; Malik, G.; Rovis, T. Total Synthesis of Indolizidine Alkaloid (-)-209D: Overriding Substrate Bias in the Asymmetric Rhodium-Catalyzed 2+2+2 Cycloaddition. *Angew. Chem. Int. Ed.* **2009**, *48*, 2379.
[43] Friedman, R. K.; Rovis, T. Predictable and Regioselective Insertion of Internal Unsymmetrical Alkynes in Rhodium-Catalyzed Cycloadditions with Alkenyl Isocyanates. *J. Am. Chem. Soc.* **2009**, *131*, 10775.
[44] Lee, E. E.; Rovis, T. Enantioselective synthesis of indolizidines bearing quaternary substituted stereocenters via rhodium-catalyzed 2+2+2 cycloaddition of alkenyl isocyanates and terminal alkynes. *Org. Lett.* **2008**, *10*, 1231.
[45] Yu, R. T.; Rovis, T. Rhodium-catalyzed 2+2+2 cycloaddition of alkenyl isocyanates and alkynes. *J. Am. Chem. Soc.* **2006**, *128*, 2782.

[46] Yu, R. T.; Rovis, T. Enantioselective rhodium-catalyzed 2+2+2 cycloaddition of alkenyl isocyanates and terminal alkynes: Application to the total synthesis of (+)-lasubine II. *J. Am. Chem. Soc.* **2006**, *128*, 12370.

[47] Renault, O.; Guillon, J.; Dallemagne, P.; Rault, S. Efficient synthesis of 2-aryl-6-methyl-2,3-dihydro-1H-pyridin-4-ones. *Tetrahedron Lett.* **2000**, *41*, 681.

[48] Svetlik, J.; Kettmann, V.; Zaleska, B. A new convenient synthesis of functionalized 2,3-dihydro-4-pyridones. *Tetrahedron Lett.* **2005**, *46*, 5511.

[49] Dong, D. W.; Bi, X. H.; Liu, Q.; Cong, F. D. [5C+1N] Annulation: a novel synthetic strategy for functionalized 2,3-dihydro-4-pyridones. *Chem. Commun.* **2005**, 3580.

[50] Turunen, B. J.; Georg, G. I. Amino acid-derived enaminones: A study in ring formation providing valuable asymmetric synthons. *J. Am. Chem. Soc.* **2006**, *128*, 8702.

[51] Niphakis, M. J.; Turunen, B. J.; Georg, G. I. Synthesis of 6- and 7-membered cyclic enaminones: scope and mechanism. *J. Org. Chem.* **2010**, *75*, 6793.

[52] Seki, H.; Georg, G. I. Synthesis of amino acid derived enaminones via Wolff rearrangement using vinylogous amides as carbon nucleophiles. *J. Am. Chem. Soc.* **2010**, *132*, 15512.

[53] Lue, P.; Greenhill, J. V., Enaminones in heterocyclic synthesis. In *Advances in Heterocyclic Chemistry, Vol. 67*, Academic Press Inc: San Diego, **1997**; Vol. 67, pp 207.

[54] Kuethe, J. T.; Wong, A.; Davies, I. W.; Reider, P. J. Aza-Diels-Alder/intramolecular Heck cyclization approach to the tetrahydro-beta-carboline skeleton of the ajmaline/sarpagine alkaloids. *Tetrahedron Lett.* **2002**, *43*, 3871.

[55] Chemler, S. Phenanthroindolizidines and Phenanthroquinolizidines: Promising Alkaloids for Anti-Cancer Therapy. *Curr. Bioact. Compd.* **2009**, *5*, 2.

[56] Yang, C.-W.; Chen, W.-L.; Wu, P.-L.; Tseng, H.-Y.; Lee, S.-J. Anti-inflammatory mechanisms of phenanthroindolizidine alkaloids. *Mol. Pharmacol.* **2006**, *69*, 749.

[57] Yang, C. W.; Lee, Y. Z.; Kang, I. J.; Barnard, D. L.; Jan, J. T.; Lin, D.; Huang, C. W.; Yeh, T. K.; Chao, Y. S.; Lee, S. J. Identification of phenanthroindolizines and phenanthroquinolizidines as novel potent anti-coronaviral agents for porcine enteropathogenic coronavirus transmissible gastroenteritis virus and human severe acute respiratory syndrome coronavirus. *Antivir. Res.* **2010**, *88*, 160.

[58] Yang, C. W.; Chuang, T. H.; Wu, P. L.; Huang, W. H.; Lee, S. J. Anti-inflammatory effects of 7-methoxycryptopleurine and structure-activity relations of phenanthroindolizidines and phenanthroquinolizidines. *Biochem. Biophys. Res. Commun.* **2007**, *354*, 942.

[59] Niphakis, M. J.; Georg, G. I. Total syntheses of arylindolizidine alkaloids (+)-ipalbidine and (+)-antofine. *J. Org. Chem.* **2010**, *75*, 6019.

[60] Niphakis, M. J.; Georg, G. I. Synthesis of tylocrebrine and related phenanthroindolizidines by VOF3-mediated oxidative aryl-alkene coupling. *Org. Lett.* **2011**, *13*, 196.

[61] Tsukanov, S. V.; Comins, D. L. Concise total synthesis of the frog alkaloid (-)-205B. *Angew. Chem. Int. Ed.* **2011**, *50*, 8626.

[62] Wolfe, B.; Libby, A.; Al-Awar, R.; Foti, C.; Comins, D. Asymmetric synthesis of all the known phlegmarine alkaloids. *J. Org. Chem.* **2010**, *75*, 8564.
[63] Wilson, M.; Padwa, A. A stereoselective approach to the azaspiro[5.5]undecane ring system using a conjugate addition/dipolar cycloaddition cascade: application to the total synthesis of (+/-)-2,7,8-epi-perhydrohistrionicotoxin. *J. Org. Chem.* **2008**, *73*, 9601.
[64] Pizzuti, M.; Minnaard, A.; Feringa, B. Catalytic asymmetric synthesis of the alkaloid (+)-myrtine. *Org. Biomol. Chem.* **2008**, *6*, 3464.
[65] Leighty, M. W.; Georg, G. I. Total Syntheses and Cytotoxicity of (R)- and (S)-Boehmeriasin A. *ACS Med. Chem. Lett.* **2011**, *2*, 313.
[66] Seki, H. Cyclic Enaminones: Methodology Development, Total Synthesis, and Library Construction. Ph.D. Dissertation. University of Minnesota-Twin Cities, Minneapolis, MN, **2012**.
[67] Joseph, S.; Comins, D. L. Synthetic applications of chiral 2,3-dihydro-4-pyridones. *Curr. Opin. Drug Disc.* **2002**, *5*, 870.
[68] Comins, D. L.; Joseph, S. P.; Hong, H.; Alawar, R. S.; Foti, C. J.; Zhang, Y. M.; Chen, X. H.; LaMunyon, D. H.; GuerraWeltzien, M. Asymmetric synthesis and synthetic utility of 2,3-dihydro-4-pyridones. *Pure Appl. Chem.* **1997**, *69*, 477.
[69] Kirschbaum, S.; Waldmann, H. Three-step access to the tricyclic benzo[a]quinolizine ring system. *J. Org. Chem.* **1998**, *63*, 4936.
[70] Waldmann, H.; Braun, M.; Weymann, M.; Gewehr, M. Asymmetric-Synthesis of Indolo[2,3-a]Quinolizidin-2-Ones - Congeners to Yohimbine-Type Alkaloids. *Tetrahedron* **1993**, *49*, 397.
[71] Kitazume, T.; Murata, K.; Okabe, A.; Takahashi, Y.; Yamazaki, T. A Highly Stereocontrolled Synthetic Approach to 1,6-Dideoxy-6,6-Difluoroazasugar Derivatives. *Tetrahedron-Asymmetry* **1994**, *5*, 1029.
[72] Waldmann, H.; Braun, M. Asymmetric Tandem Mannich-Michael Reactions of Amino-Acid Ester Imines with Danishefsky Diene. *J. Org. Chem.* **1992**, *57*, 4444.
[73] Young, D. W.; Comins, D. L. Tandem directed lithiations of N-boc-1,2-dihydropyridines toward highly functionalized 2,3-dihydro-4-pyridones. *Org. Lett.* **2005**, *7*, 5661.
[74] Sahn, J. J.; Comins, D. L. [2 + 2] Photochemical cycloaddition/ring opening of 6-alkenyl-2,3-dihydro-4-pyridones. *J. Org. Chem.* **2010**, *75*, 6728.
[75] Sahn, J. J.; Bharathi, P.; Comins, D. L. Studies toward the synthesis of spirolucidine. Preparation of ABC and EF ring fragments. *Tetrahedron Lett.* **2012**, *53*, 1347.
[76] Comins, D. L.; Joseph, S. P.; Chen, X. Regiospecific substitution of N-acyl-2,3-dihydro-4-pyridones at C-5 via halogenation and cross-coupling. *Tetrahedron Lett.* **1995**, *36*, 9141.
[77] Kranke, B.; Kunz, H. Stereoselective syntheses of piperidinones and their modification by organometallic coupling reactions. *Org. Biomol. Chem.* **2007**, *5*, 349.

[78] Wang, X.; Turunen, B. J.; Leighty, M. W.; Georg, G. I. Microwave-assisted Suzuki-Miyaura couplings on alpha-iodoenaminones. *Tetrahedron Lett.* **2007**, *48*, 8811.
[79] Ge, H.; Niphakis, M. J.; Georg, G. I. Palladium(II)-catalyzed direct arylation of enaminones using organotrifluoroborates. *J. Am. Chem. Soc.* **2008**, *130*, 3708.
[80] Bi, L.; Georg, G. I. Direct Hiyama cross-coupling of enaminones with triethoxy(aryl)silanes and dimethylphenylsilanol. *Org. Lett.* **2011**, *13*, 5413.
[81] Kim, Y. W.; Niphakis, M. J.; Georg, G. I. Copper-assisted palladium(II)-catalyzed direct arylation of cyclic enaminones with arylboronic acids. *J. Org. Chem.* **2012**, *77*, 9496.
[82] Doucet, H.; Hierso, J. C. Palladium coupling catalysts for pharmaceutical applications. *Curr. Opin. Drug Disc.* **2007**, *10*, 672.
[83] Kakiuchi, F.; Chatani, N. Catalytic methods for C-H bond functionalization: Application in organic synthesis. *Adv. Synth. Catal.* **2003**, *345*, 1077.
[84] Labinger, J. A.; Bercaw, J. E. Understanding and exploiting C-H bond activation. *Nature* **2002**, *417*, 507.
[85] Shilov, A. E.; Shul'pin, G. B. Activation of C-H bonds by metal complexes. *Chem. Rev.* **1997**, *97*, 2879.
[86] Arndtsen, B. A.; Bergman, R. G.; Mobley, T. A.; Peterson, T. H. Selective intermolecular carbon-hydrogen bond activation by synthetic metal complexes in homogeneous solution. *Acc. Chem. Res.* **1995**, *28*, 154.
[87] Godula, K.; Sames, D. C-H bond functionalization in complex organic synthesis. *Science* **2006**, *312*, 67.
[88] Wencel-Delord, J.; Dröge, T.; Liu, F.; Glorius, F. Towards mild metal-catalyzed C-H bond activation. *Chem. Soc. Rev.* **2011**, *40*, 4740.
[89] Ackermann, L. Carboxylate-Assisted Transition-Metal-Catalyzed C-H Bond Functionalizations: Mechanism and Scope. *Chem. Rev.* **2011**, *111*, 1315.
[90] Scheuermann, C. J. Beyond Traditional Cross Couplings: The Scope of the Cross Dehydrogenative Coupling Reaction. *Chem.-Asian J.* **2010**, *5*, 436.
[91] Lyons, T. W.; Sanford, M. S. Palladium-catalyzed ligand-directed C-H functionalization reactions. *Chem. Rev.* **2010**, *110*, 1147.
[92] Li, C.-J. Cross-dehydrogenative coupling (CDC): exploring C-C bond formations beyond functional group transformations. *Acc. Chem. Res.* **2009**, *42*, 335.
[93] Kakiuchi, F.; Kochi, T. Transition-Metal-Catalyzed Carbon-Carbon Bond Formation via Carbon-Hydrogen Bond Cleavage. *Synthesis* **2008**, 3013.
[94] Crabtree, R. H. The organometallic chemistry of alkanes. *Chem. Rev.* **1985**, *85*, 245.
[95] Dyker, G. Transition Metal Catalyzed Coupling Reactions under C−H Activation. *Angew. Chem. Int. Ed.* **1999**, *38*, 1698.
[96] Crabtree, R. H. Alkane C-H activation and functionalization with homogeneous transition metal catalysts: a century of progress-a new millennium in prospect. *J. Chem. Soc., Dalton Trans.* **2001**, 2437.
[97] Bergman, R. G. Organometallic chemistry: C-H activation. *Nature* **2007**, *446*, 391.

[98] Hartwig, J. F. Carbon-heteroatom bond formation catalysed by organometallic complexes. *Nature* **2008**, *455*, 314.
[99] Bruckl, T.; Baxter, R. D.; Ishihara, Y.; Baran, P. S. Innate and guided C-H functionalization logic. *Acc. Chem. Res.* **2012**, *45*, 826.
[100] Alberico, D.; Scott, M. E.; Lautens, M. Aryl-aryl bond formation by transition-metal-catalyzed direct arylation. *Chem. Rev.* **2007**, *107*, 174.
[101] Neufeldt, S. R.; Sanford, M. S. Controlling site selectivity in palladium-catalyzed C-H bond functionalization. *Acc. Chem. Res.* **2012**, *45*, 936.
[102] Yang, F.; Wu, Y. J.; Zhu, Z. W.; Zhang, J. L.; Li, Y. N. Direct ortho-arylation of 2-arylbenzoxazoles via C-H activation. *Tetrahedron* **2008**, *64*, 6782.
[103] Kalyani, D.; Sanford, M. S. Regioselectivity in palladium-catalyzed C-H activation/oxygenation reactions. *Org. Lett.* **2005**, *7*, 4149.
[104] Shabashov, D.; Daugulis, O. Palladium-catalyzed anilide ortho-arylation and subsequent one-pot cyclization to phenanthridines. *J. Org. Chem.* **2007**, *72*, 7720.
[105] Wang, G. W.; Yuan, T. T.; Wu, X. L. Direct ortho-acetoxylation of anilides via palladium-catalyzed sp(2) C-H bond oxidative activation. *J. Org. Chem.* **2008**, *73*, 4717.
[106] Ji, Y. N.; Brueckl, T.; Baxter, R. D.; Fujiwara, Y.; Seiple, I. B.; Su, S.; Blackmond, D. G.; Baran, P. S. Innate C-H trifluoromethylation of heterocycles. *Proc. Natl. Acad. Sci. U. S. A.* **2011**, *108*, 14411.
[107] Fujiwara, Y.; Dixon, J.; O'Hara, F.; Funder, E.; Dixon, D.; Rodriguez, R.; Baxter, R.; Herlé, B.; Sach, N.; Collins, M.; Ishihara, Y.; Baran, P. Practical and innate carbon-hydrogen functionalization of heterocycles. *Nature* **2012**, *492*, 95.
[108] You, S. L.; Xia, J. B., Palladium-Catalyzed Aryl-Aryl Bond Formation Through Double C-H Activation. In *C-H Activation*, Yu, J. Q.; Shi, Z., Eds.**2010**; Vol. 292, pp 165.
[109] Daugulis, O., Palladium and copper catalysis in regioselective, intermolecular coupling of C-H and C-Hal bonds. In *C-H Activation*, Yu, J. Q.; Shi, Z., Eds.**2010**; Vol. 292, pp 57.
[110] Chen, X.; Engle, K. M.; Wang, D. H.; Yu, J. Q. Palladium(II)-Catalyzed C-H Activation/C-C Cross-Coupling Reactions: Versatility and Practicality. *Angew. Chem. Int. Ed.* **2009**, *48*, 5094.
[111] Li, B. J.; Yang, S. D.; Shi, Z. J. Recent advances in direct arylation via palladium-catalyzed aromatic C-H activation. *Synlett* **2008**, 949.
[112] Beccalli, E.; Broggini, G.; Martinelli, M.; Sottocornola, S. C-C, C-O, C-N bond formation on sp2 carbon by Pd(II)-catalyzed reactions involving oxidant agents. *Chem. Rev.* **2007**, *107*, 5318.
[113] Catellani, M.; Chiusoli, G. P. Palladacycle formation by electrophilic aromatic substitution, as monitored by 1H NMR spectroscopy. *J. Organomet. Chem.* **1992**, *425*, 151.
[114] Hennessy, E. J.; Buchwald, S. L. Synthesis of Substituted Oxindoles from α-Chloroacetanilides via Palladium-Catalyzed C−H Functionalization. *J. Am. Chem. Soc.* **2003**, *125*, 12084.

[115] Glover, B.; Harvey, K. A.; Liu, B.; Sharp, M. J.; Tymoschenko, M. F. Regioselective Palladium-Catalyzed Arylation of 3-Carboalkoxy Furan and Thiophene. *Org. Lett.* **2003**, *5*, 301.
[116] Park, C.-H.; Ryabova, V.; Seregin, I. V.; Sromek, A. W.; Gevorgyan, V. Palladium-catalyzed arylation and heteroarylation of indolizines. *Org. Lett.* **2004**, *6*, 1159.
[117] Lane, B. S.; Brown, M. A.; Sames, D. Direct Palladium-Catalyzed C-2 and C-3 Arylation of Indoles: A Mechanistic Rationale for Regioselectivity. *J. Am. Chem. Soc.* **2005**, *127*, 8050.
[118] Zollinger, H., Hydrogen Isotope Effects in Aromatic Substitution Reactions. In *Adv. Phys. Org. Chem.*, Gold, V., Ed. Academic Press**1964**; Vol. Volume 2, pp 163.
[119] Mota, A. J.; Dedieu, A.; Bour, C.; Suffert, J. Cyclocarbopalladation Involving an Unusual 1,5-Palladium Vinyl to Aryl Shift as Termination Step: Theoretical Study of the Mechanism. *J. Am. Chem. Soc.* **2005**, *127*, 7171.
[120] Davies, D. L.; Donald, S. M. A.; Macgregor, S. A. Computational Study of the Mechanism of Cyclometalation by Palladium Acetate. *J. Am. Chem. Soc.* **2005**, *127*, 13754.
[121] Hughes, C. C.; Trauner, D. Concise Total Synthesis of (−)-Frondosin B Using a Novel Palladium-Catalyzed Cyclization. *Angew. Chem. Int. Ed.* **2002**, *41*, 1569.
[122] Toyota, M.; Ilangovan, A.; Okamoto, R.; Masaki, T.; Arakawa, M.; Ihara, M. Simple Construction of Bicyclo[4.3.0]nonane, Bicyclo[3.3.0]octane, and Related Benzo Derivatives by Palladium-Catalyzed Cycloalkenylation. *Org. Lett.* **2002**, *4*, 4293.
[123] Capito, E.; Brown, J. M.; Ricci, A. Directed palladation: fine tuning permits the catalytic 2-alkenylation of indoles. *Chem. Commun.* **2005**, 1854.
[124] Lafrance, M.; Fagnou, K. Palladium-catalyzed benzene arylation: incorporation of catalytic pivalic acid as a proton shuttle and a key element in catalyst design. *J. Am. Chem. Soc.* **2006**, *128*, 16496.
[125] Stuart, D. R.; Fagnou, K. The catalytic cross-coupling of unactivated arenes. *Science* **2007**, *316*, 1172.
[126] Gorelsky, S. I.; Lapointe, D.; Fagnou, K. Analysis of the concerted metalation-deprotonation mechanism in palladium-catalyzed direct arylation across a broad range of aromatic substrates. *J. Am. Chem. Soc.* **2008**, *130*, 10848.
[127] Liegault, B.; Lapointe, D.; Caron, L.; Vlassova, A.; Fagnou, K. Establishment of Broadly Applicable Reaction Conditions for the Palladium-Catalyzed Direct Arylation of Heteroatom-Containing Aromatic Compounds. *J. Org. Chem.* **2009**, *74*, 1826.
[128] Lapointe, D.; Fagnou, K. Overview of the Mechanistic Work on the Concerted Metallation-Deprotonation Pathway. *Chem. Lett.* **2010**, *39*, 1119.
[129] Gorelsky, S. I.; Lapointe, D.; Fagnou, K. Analysis of the palladium-catalyzed (aromatic)C-H bond metalation-deprotonation mechanism spanning the entire spectrum of arenes. *J. Org. Chem.* **2012**, *77*, 658.

[130] Guchhait, S. K.; Kandekar, S.; Kashyap, M.; Taxak, N.; Bharatam, P. V. C-H Bond Functionalization Under Metalation-Deprotonation Process: Regioselective Direct Arylation of 3-Aminoimidazo 1,2-a pyrazine. *J. Org. Chem.* **2012**, *77*, 8321.
[131] Seregin, I.; Gevorgyan, V. Direct transition metal-catalyzed functionalization of heteroaromatic compounds. *Chem. Soc. Rev.* **2007**, *36*, 1173.
[132] Ackermann, L.; Vicente, R.; Kapdi, A. Transition-metal-catalyzed direct arylation of (hetero)arenes by C-H bond cleavage. *Angew. Chem. Int. Ed.* **2009**, *48*, 9792.
[133] Liu, C.; Zhang, H.; Shi, W.; Lei, A. Bond formations between two nucleophiles: transition metal catalyzed oxidative cross-coupling reactions. *Chem. Rev.* **2011**, *111*, 1780.
[134] Sun, C.-L.; Li, B.-J.; Shi, Z.-J. Pd-catalyzed oxidative coupling with organometallic reagents via C-H activation. *Chem. Commun.* **2010**, *46*, 677.
[135] Ashenhurst, J. Intermolecular oxidative cross-coupling of arenes. *Chem. Soc. Rev.* **2010**, *39*, 540.
[136] Shang, X.; Liu, Z.-Q. Transition metal-catalyzed C(vinyl)-C(vinyl) bond formation via double C(vinyl)-H bond activation. *Chem. Soc. Rev.* **2013**, *42*, 3253.
[137] Yeung, C. S.; Dong, V. M. Catalytic dehydrogenative cross-coupling: forming carbon-carbon bonds by oxidizing two carbon-hydrogen bonds. *Chem. Rev.* **2011**, *111*, 1215.
[138] Le Bras, J.; Muzart, J. Intermolecular dehydrogenative Heck reactions. *Chem. Rev.* **2011**, *111*, 1170.
[139] Cho, S.; Kim, J.; Kwak, J.; Chang, S. Recent advances in the transition metal-catalyzed twofold oxidative C-H bond activation strategy for C-C and C-N bond formation. *Chem. Soc. Rev.* **2011**, *40*, 5068.
[140] Bakherad, M. Recent progress and current applications of Sonogashira coupling reaction in water. *Appl. Organomet. Chem.* **2013**, *27*, 125.
[141] Chinchilla, R.; Najera, C. Recent advances in Sonogashira reactions. *Chem. Soc. Rev.* **2011**, *40*, 5084.
[142] Chinchilla, R.; Najera, C. The sonogashira reaction: A booming methodology in synthetic organic chemistry. *Chem. Rev.* **2007**, *107*, 874.
[143] Dudnik, A.; Gevorgyan, V. Formal inverse Sonogashira reaction: direct alkynylation of arenes and heterocycles with alkynyl halides. *Angew. Chem. Int. Ed.* **2010**, *49*, 2096.
[144] Kalinin, V.; Pashchenko, D.; She, F. Palladium-catalysed Synthesis of 4-Heteroaryl and 4-Alkynyl-substituted Sydnones. 5-Oxido-3-phenyl-1,2,3-oxadiazol-3-ium-4-ylzinc Chloride. *Mendeleev Commun.* **1992**, *2*, 60.
[145] Seregin, I.; Ryabova, V.; Gevorgyan, V. Direct palladium-catalyzed alkynylation of N-fused heterocycles. *J. Am. Chem. Soc.* **2007**, *129*, 7742.
[146] Gu, Y.; Wang, X.-M. Direct palladium-catalyzed C-3 alkynylation of indoles. *Tetrahedron Lett.* **2009**, *50*, 763.
[147] Tobisu, M.; Ano, Y.; Chatani, N. Palladium-catalyzed direct alkynylation of C-H bonds in benzenes. *Org. Lett.* **2009**, *11*, 3250.

[148] Zhao, Y.; He, G.; Nack, W.; Chen, G. Palladium-catalyzed alkenylation and alkynylation of ortho-C(sp2)-H bonds of benzylamine picolinamides. *Org. Lett.* **2012**, *14*, 2948.
[149] Mizoroki, T.; Mori, K.; Ozaki, A. Arylation of Olefin with Aryl Iodide Catalyzed by Palladium. *Bull. Chem. Soc. Jpn.* **1971**, *44*, 581.
[150] Mc Cartney, D.; Guiry, P. J. The asymmetric Heck and related reactions. *Chem. Soc. Rev.* **2011**, *40*, 5122.
[151] Karimi, B.; Behzadnia, H.; Elhamifar, D.; Akhavan, P. F.; Esfahani, F. K.; Zamani, A. Transition-Metal-Catalyzed Oxidative Heck Reactions. *Synthesis* **2010**, 1399.
[152] Bellina, F.; Chiappe, C. The Heck Reaction in Ionic Liquids: Progress and Challenges. *Molecules* **2010**, *15*, 2211.
[153] Knowles, J. P.; Whiting, A. The Heck-Mizoroki cross-coupling reaction: a mechanistic perspective. *Org. Biomol. Chem.* **2007**, *5*, 31.
[154] Zaitsev, V.; Daugulis, O. Catalytic coupling of haloolefins with anilides. *J. Am. Chem. Soc.* **2005**, *127*, 4156.
[155] Gottumukkala, A. L.; Derridj, F.; Djebbar, S.; Doucet, H. Alkenyl bromides: useful coupling partners for the palladium-catalysed coupling with heteroaromatics via a C–H bond activation. *Tetrahedron Lett.* **2008**, *49*, 2926.
[156] Besselièvre, F. o.; Piguel, S.; Mahuteau-Betzer, F.; Grierson, D. S. Stereoselective Direct Copper-Catalyzed Alkenylation of Oxazoles with Bromoalkenes. *Org. Lett.* **2008**, *10*, 4029.
[157] Verrier, C.; Hoarau, C.; Marsais, F. Direct palladium-catalyzed alkenylation, benzylation and alkylation of ethyl oxazole-4-carboxylate with alkenyl-, benzyl- and alkyl halides. *Org. Biomol. Chem.* **2009**, *7*, 647.
[158] Mousseau, J. J.; Fortier, A. l.; Charette, A. B. Synthesis of 2-Substituted Pyrazolo[1,5-a]pyridines through Cascade Direct Alkenylation/Cyclization Reactions. *Org. Lett.* **2010**, *12*, 516.
[159] Geary, L. M.; Hultin, P. G. Modular Construction of 2-Substituted Benzo[b]furans from 1,2-Dichlorovinyl Ethers. *Org. Lett.* **2009**, *11*, 5478.
[160] Koubachi, J.; Kazzouli, S. E.; Berteina-Raboin, S.; Mouaddib, A.; Guillaumet, G. New and Efficient Palladium(0)-Mediated Microwave-Assisted Direct C3 Alkenylation of Imidazo[1,2- a]pyridines. *Synthesis* **2008**, 2537.
[161] Yamaguchi, J.; Yamaguchi, A. D.; Itami, K. C-H bond functionalization: emerging synthetic tools for natural products and pharmaceuticals. *Angew. Chem. Int. Ed.* **2012**, *51*, 8960.
[162] Chiusoli, G. P.; Catellani, M.; Costa, M.; Motti, E.; Della Ca, N.; Maestri, G. Catalytic C-C coupling through C-H arylation of arenes or heteroarenes. *Coord. Chem. Rev.* **2010**, *254*, 456.
[163] Suzuki, A. Recent developments of biaryl synthesis via cross-coupling reactions of areneboronic acid derivatives. *J. Syn. Org. Chem. Jpn.* **2005**, *63*, 312.
[164] Ames, D. E.; Bull, D. Some reactions of 3-halogenocinnolines catalysed by palladium compounds. *Tetrahedron* **1982**, *38*, 383.

[165] Nakamura, N.; Tajima, Y.; Sakai, K. Direct phenylation of isoxazole ring using palladium catalysts - synthesis of 4-phenylmuscimol. *Heterocycles* **1982**, *19*, 152.
[166] Satoh, T.; Kawamura, Y.; Miura, M.; Nomura, M. Palladium-catalyzed regioselective mono- and diarylation reactions of 2-phenylphenols and naphthols with aryl halides. *Angew. Chem. Int. Ed.* **1997**, *36*, 1740.
[167] de Mendoza, P.; Echavarren, A. M., Mechanistic Aspects of Transition Metal Catalyzed Direct Arylation Reactions. In *Modern Arylation Methods*, 1st ed.; Ackermann, L., Ed. Wiley-VCH: Weinheim, **2009**; pp 363.
[168] García-Cuadrado, D.; de Mendoza, P.; Braga, A.; Maseras, F.; Echavarren, A. Proton-abstraction mechanism in the palladium-catalyzed intramolecular arylation: substituent effects. *J. Am. Chem. Soc.* **2007**, *129*, 6880.
[169] Pascual, S.; de Mendoza, P.; Braga, A. A. C.; Maseras, F.; Echavarren, A. M. Bidentate phosphines as ligands in the palladium-catalyzed intramolecular arylation: the intermolecular base-assisted proton abstraction mechanism. *Tetrahedron* **2008**, *64*, 6021.
[170] García-Cuadrado, D.; Braga, A.; Maseras, F.; Echavarren, A. Proton abstraction mechanism for the palladium-catalyzed intramolecular arylation. *J. Am. Chem. Soc.* **2006**, *128*, 1066.
[171] Campeau, L.-C.; Rousseaux, S.; Fagnou, K. A solution to the 2-pyridyl organometallic cross-coupling problem: regioselective catalytic direct arylation of pyridine N-oxides. *J. Am. Chem. Soc.* **2005**, *127*, 18020.
[172] Kametani, Y.; Satoh, T.; Miura, M.; Nomura, M. Regioselective arylation of benzanilides with aryl triflates or bromides under palladium catalysis. *Tetrahedron Lett.* **2000**, *41*, 2655.
[173] Satoh, T.; Kametani, Y.; Terao, Y.; Miura, M.; Nomura, M. Palladium-catalyzed multiple arylation of phenyl ketones with aryl bromides. *Tetrahedron Lett.* **1999**, *40*, 5345.
[174] Daugulis, O.; Zaitsev, V. Anilide ortho-arylation by using C-H activation methodology. *Angew. Chem. Int. Ed.* **2005**, *44*, 4046.
[175] Shabashov, D.; Daugulis, O. Ortho-arylation of benzamides. *Org. Lett.* **2006**, *8*, 4947.
[176] Lazareva, A.; Daugulis, O. Direct palladium-catalyzed ortho-arylation of benzylamines. *Org. Lett.* **2006**, *8*, 5211.
[177] Shabashov, D.; Daugulis, O. Catalytic coupling of C-H and C-I bonds using pyridine as a directing group. *Org. Lett.* **2005**, *7*, 3657.
[178] Humphrey, G.; Kuethe, J. Practical methodologies for the synthesis of indoles. *Chem. Rev.* **2006**, *106*, 2875.
[179] Horton, D.; Bourne, G.; Smythe, M. The combinatorial synthesis of bicyclic privileged structures or privileged substructures. *Chem. Rev.* **2003**, *103*, 893.
[180] Joucla, L.; Djakovitch, L. Transition Metal-Catalysed, Direct and Site-Selective N1-, C2- or C3-Arylation of the Indole Nucleus: 20 Years of Improvements. *Adv. Synth. Catal.* **2009**, *351*, 673.
[181] Wang, X.; Gribkov, D.; Sames, D. Phosphine-free palladium-catalyzed C-H bond arylation of free (N-H)-indoles and pyrroles. *J. Org. Chem.* **2007**, *72*, 1476.

[182] Zhang, Z.; Hu, Z.; Yu, Z.; Lei, P.; Chi, H.; Wang, Y.; He, R. Direct palladium-catalyzed C-3 arylation of indoles. *Tetrahedron Lett.* **2007**, *48*, 2415.
[183] Bellina, F.; Benelli, F.; Rossi, R. Direct palladium-catalyzed C-3 arylation of free (NH)-indoles with aryl bromides under ligandless conditions. *J. Org. Chem.* **2008**, *73*, 5529.
[184] Okazawa, T.; Satoh, T.; Miura, M.; Nomura, M. Palladium-catalyzed multiple arylation of thiophenes. *J. Am. Chem. Soc.* **2002**, *124*, 5286.
[185] Chuprakov, S.; Chernyak, N.; Dudnik, A.; Gevorgyan, V. Direct Pd-catalyzed arylation of 1,2,3-triazoles. *Org. Lett.* **2007**, *9*, 2333.
[186] Cerna, I.; Pohl, R.; Hocek, M. The first direct C-H arylation of purine nucleosides. *Chem. Commun.* **2007**, 4729.
[187] Catellani, M.; Motti, E.; Della Ca, N. Catalytic sequential reactions involving palladacycle-directed aryl coupling steps. *Acc. Chem. Res.* **2008**, *41*, 1512.
[188] Lautens, M.; Alberico, D.; Bressy, C.; Fang, Y.-Q.; Mariampillai, B.; Wilhelm, T. Palladium-catalyzed ring-forming reactions: Methods and applications. *Pure Appl. Chem.* **2006**, *78*, 351.
[189] Laleu, B.; Lautens, M. Synthesis of annulated 2H-indazoles and 1,2,3- and 1,2,4-triazoles via a one-pot palladium-catalyzed alkylation/direct arylation reaction. *J. Org. Chem.* **2008**, *73*, 9164.
[190] Mariampillai, B.; Alliot, J.; Li, M.; Lautens, M. A convergent synthesis of polysubstituted aromatic nitriles via palladium-catalyzed C-H functionalization. *J. Am. Chem. Soc.* **2007**, *129*, 15372.
[191] Ohta, A.; Akita, Y.; Inoue, A.; Yamamoto, K.; Kurihara, T.; Shimizu, M. Palladium-catalyzed Coupling Reaction of Chloropyrazines with Indole. *Heterocycles* **1985**, *23*, 2327.
[192] Ohta, A.; Aoyagi, Y.; Inoue, A.; Koizumi, I.; Hashimoto, R.; Tokunaga, K.; Gohma, K.; Komatsu, J.; Sekine, K.; Miyafuji, A.; Kunoh, J.; Honma, R.; Akita, Y. Palladium-catalyzed Cross-coupling Ractions of Chloropyrazines with Aromatic Heterocycles. *Heterocycles* **1992**, *33*, 257.
[193] Campeau, L.-C.; Parisien, M.; Jean, A.; Fagnou, K. Catalytic direct arylation with aryl chlorides, bromides, and iodides: intramolecular studies leading to new intermolecular reactions. *J. Am. Chem. Soc.* **2006**, *128*, 581.
[194] Chiong, H. A.; Pham, Q.-N.; Daugulis, O. Two methods for direct ortho-arylation of benzoic acids. *J. Am. Chem. Soc.* **2007**, *129*, 9879.
[195] Chiong, H.; Daugulis, O. Palladium-catalyzed arylation of electron-rich heterocycles with aryl chlorides. *Org. Lett.* **2007**, *9*, 1449.
[196] Nadres, E. T.; Lazareva, A.; Daugulis, O. Palladium-Catalyzed Indole, Pyrrole, and Furan Arylation by Aryl Chlorides. *J. Org. Chem.* **2010**, *76*, 471.
[197] Ackermann, L.; Vicente, R.; Born, R. Palladium-Catalyzed Direct Arylations of 1,2,3-Triazoles with Aryl Chlorides using Conventional Heating. *Adv. Synth. Catal.* **2008**, *350*, 741.
[198] Leclerc, J.-P.; Fagnou, K. Palladium-catalyzed cross-coupling reactions of diazine N-oxides with aryl chlorides, bromides, and iodides. *Angew. Chem. Int. Ed.* **2006**, *45*, 7781.

[199] Lafrance, M.; Rowley, C.; Woo, T.; Fagnou, K. Catalytic intermolecular direct arylation of perfluorobenzenes. *J. Am. Chem. Soc.* **2006**, *128*, 8754.
[200] Lafrance, M.; Shore, D.; Fagnou, K. Mild and general conditions for the cross-coupling of aryl halides with pentafluorobenzene and other perfluoroaromatics. *Org. Lett.* **2006**, *8*, 5097.
[201] Vachhani, D. D.; Sharma, A.; Van der Eycken, E. Pd/Cu-Catalyzed C-H Arylation of 1,3,4-Thiadiazoles with (Hetero)aryl Iodides, Bromides, and Triflates. *J. Org. Chem.* **2012**, *77*, 8768.
[202] Schipper, D. J.; El-Salfiti, M.; Whipp, C. J.; Fagnou, K. Direct arylation of azine N-oxides with aryl triflates. *Tetrahedron* **2009**, *65*, 4977.
[203] Roger, J.; Doucet, H. Aryl triflates: useful coupling partners for the direct arylation of heteroaryl derivatives via Pd-catalyzed C-H activation-functionalization. *Org. Biomol. Chem.* **2008**, *6*, 169.
[204] Dai, F. L.; Gui, Q. W.; Liu, J. D.; Yang, Z. Y.; Chen, X.; Guo, R. Q.; Tan, Z. Pd-catalyzed C3-selective arylation of pyridines with phenyl tosylates. *Chem. Commun.* **2013**, *49*, 4634.
[205] Lee, D. S.; Choy, P. Y.; So, C. M.; Wang, J.; Lau, C. P.; Kwong, F. Y. Palladium-catalyzed direct arylation of polyfluoroarenes with aryl tosylates and mesylates. *RSC Adv.* **2012**, *2*, 9179.
[206] So, C. M.; Lau, C. P.; Kwong, F. Y. Palladium-Catalyzed Direct Arylation of Heteroarenes with Aryl Mesylates. *Chem.-Eur. J.* **2011**, *17*, 761.
[207] Fan, S. L.; Yang, J.; Zhang, X. G. Pd-Catalyzed Direct Cross-Coupling of Electron-Deficient Polyfluoroarenes with Heteroaromatic Tosylates. *Org. Lett.* **2011**, *13*, 4374.
[208] Ackermann, L.; Fenner, S. Direct arylations of electron-deficient (hetero)arenes with aryl or alkenyl tosylates and mesylates. *Chem. Commun.* **2011**, *47*, 430.
[209] Ackermann, L.; Althammer, A.; Fenner, S. Palladium-Catalyzed Direct Arylations of Heteroarenes with Tosylates and Mesylates. *Angew. Chem. Int. Ed.* **2009**, *48*, 201.
[210] Ackermann, L.; Althammer, A.; Born, R. Catalytic arylation reactions by C-H bond activation with aryl tosylates. *Angew. Chem. Int. Ed.* **2006**, *45*, 2619.
[211] Nervig, C. S.; Waller, P. J.; Kalyani, D. Palladium-Catalyzed Intramolecular C-H Arylation of Arenes Using Tosylates and Mesylates as Electrophiles. *Org. Lett.* **2012**, *14*, 4838.
[212] Cárdenas, D. J. Advances in Functional-Group-Tolerant Metal-Catalyzed Alkyl–Alkyl Cross-Coupling Reactions. *Angew. Chem. Int. Ed.* **2003**, *42*, 384.
[213] Frisch, A. C.; Beller, M. Catalysts for Cross-Coupling Reactions with Non-activated Alkyl Halides. *Angew. Chem. Int. Ed.* **2005**, *44*, 674.
[214] Terao, J.; Kambe, N. Cross-Coupling Reaction of Alkyl Halides with Grignard Reagents Catalyzed by Ni, Pd, or Cu Complexes with π-Carbon Ligand(s). *Acc. Chem. Res.* **2008**, *41*, 1545.
[215] Rudolph, A.; Lautens, M. Secondary Alkyl Halides in Transition-Metal-Catalyzed Cross-Coupling Reactions. *Angew. Chem. Int. Ed.* **2009**, *48*, 2656.

[216] Hofmann, N.; Ackermann, L. meta-Selective C-H Bond Alkylation with Secondary Alkyl Halides. *J. Am. Chem. Soc.* **2013**, *135*, 5877.
[217] Zhao, Y. S.; Chen, G. Palladium-Catalyzed Alkylation of ortho-C(sp(2))-H Bonds of Benzylamide Substrates with Alkyl Halides. *Org. Lett.* **2011**, *13*, 4850.
[218] Ackermann, L. Metal-catalyzed direct alkylations of (hetero)arenes via C-H bond cleavages with unactivated alkyl halides. *Chem. Commun.* **2010**, *46*, 4866.
[219] Zhang, Y. H.; Shi, B. F.; Yu, J. Q. Palladium(II)-Catalyzed ortho Alkylation of Benzoic Acids with Alkyl Halides. *Angew. Chem. Int. Ed.* **2009**, *48*, 6097.
[220] Lapointe, D.; Fagnou, K. Palladium-catalyzed benzylation of heterocyclic aromatic compounds. *Org. Lett.* **2009**, *11*, 4160.
[221] Ackermann, L.; Barfüsser, S.; Pospech, J. Palladium-catalyzed direct arylations, alkenylations, and benzylations through C-H bond cleavages with sulfamates or phosphates as electrophiles. *Org. Lett.* **2010**, *12*, 724.
[222] Mukai, T.; Hirano, K.; Satoh, T.; Miura, M. Palladium-catalyzed direct benzylation of azoles with benzyl carbonates. *Org. Lett.* **2010**, *12*, 1360.
[223] Tremont, S. J. Ortho-alkylation of acetanilides using alkyl halides and palladium acetate. *J. Am. Chem. Soc.* **1984**, *106*, 5759.
[224] Shabashov, D.; Daugulis, O. Auxiliary-assisted palladium-catalyzed arylation and alkylation of sp2 and sp3 carbon-hydrogen bonds. *J. Am. Chem. Soc.* **2010**, *132*, 3965.
[225] Yue, W.; Li, Y.; Jiang, W.; Zhen, Y.; Wang, Z. Direct meta-selective alkylation of perylene bisimides via palladium-catalyzed C-H functionalization. *Org. Lett.* **2009**, *11*, 5430.
[226] Xiao, B.; Liu, Z.-J.; Liu, L.; Fu, Y. Palladium-catalyzed C-H activation/cross-coupling of pyridine N-oxides with nonactivated secondary alkyl bromides. *J. Am. Chem. Soc.* **2013**, *135*, 616.
[227] Han, F. S. Transition-metal-catalyzed Suzuki-Miyaura cross-coupling reactions: a remarkable advance from palladium to nickel catalysts. *Chem. Soc. Rev.* **2013**, *42*, 5270.
[228] Polshettiwar, V.; Decottignies, A.; Len, C.; Fihri, A. Suzuki-Miyaura Cross-Coupling Reactions in Aqueous Media: Green and Sustainable Syntheses of Biaryls. *Chemsuschem* **2010**, *3*, 502.
[229] Bai, L.; Wang, J. X. Environmentally friendly Suzuki aryl-aryl cross-coupling reaction. *Curr. Org. Chem.* **2005**, *9*, 535.
[230] Suzuki, A. Organoborane coupling reactions (Suzuki coupling). *Proc. Jpn. Acad. Ser. B-Phys. Biol. Sci.* **2004**, *80*, 359.
[231] Bellina, F.; Carpita, A.; Rossi, R. Palladium catalysts for the Suzuki cross-coupling reaction: An overview of recent advances. *Synthesis* **2004**, 2419.
[232] Kotha, S.; Lahiri, K.; Kashinath, D. Recent applications of the Suzuki-Miyaura cross-coupling reaction in organic synthesis. *Tetrahedron* **2002**, *58*, 9633.
[233] Pan, F.; Wang, H.; Shen, P. X.; Zhao, J.; Shi, Z. J. Cross coupling of thioethers with aryl boroxines to construct biaryls via Rh catalyzed C-S activation. *Chem. Sci.* **2013**, *4*, 1573.

[234] Liang, A.; Li, X. J.; Liu, D. F.; Li, J. Y.; Zou, D. P.; Wu, Y. J.; Wu, Y. S. The palladium-catalyzed cross-coupling reactions of trifluoroethyl iodide with aryl and heteroaryl boronic acid esters. *Chem. Commun.* **2012**, *48*, 8273.

[235] Glasspoole, B. W.; Ghozati, K.; Moir, J. W.; Crudden, C. M. Suzuki-Miyaura cross-couplings of secondary allylic boronic esters. *Chem. Commun.* **2012**, *48*, 1230.

[236] Xu, L.; Li, B. J.; Wu, Z. H.; Lu, X. Y.; Guan, B. T.; Wang, B. Q.; Zhao, K. Q.; Shi, Z. J. Nickel-Catalyzed Efficient and Practical Suzuki-Miyaura Coupling of Alkenyl and Aryl Carbamates with Aryl Boroxines. *Org. Lett.* **2010**, *12*, 884.

[237] Yang, D. X.; Colletti, S. L.; Wu, K.; Song, M. Y.; Li, G. Y.; Shen, H. C. Palladium-Catalyzed Suzuki-Miyaura Coupling of Pyridyl-2-boronic Esters with Aryl Halides Using Highly Active and Air-Stable Phosphine Chloride and Oxide Ligands. *Org. Lett.* **2009**, *11*, 381.

[238] Molander, G. A.; Ellis, N. Organotrifluoroborates: Protected boronic acids that expand the versatility of the Suzuki coupling reaction. *Acc. Chem. Res.* **2007**, *40*, 275.

[239] Chen, X.; Goodhue, C. E.; Yu, J.-Q. Palladium-Catalyzed Alkylation of sp2 and sp3 C−H Bonds with Methylboroxine and Alkylboronic Acids: Two Distinct C−H Activation Pathways. *J. Am. Chem. Soc.* **2006**, *128*, 12634.

[240] Giri, R.; Maugel, N.; Li, J.-J.; Wang, D.-H.; Breazzano, S. P.; Saunders, L. B.; Yu, J.-Q. Palladium-Catalyzed Methylation and Arylation of sp2 and sp3 C−H Bonds in Simple Carboxylic Acids. *J. Am. Chem. Soc.* **2007**, *129*, 3510.

[241] Wang, D.-H.; Mei, T.-S.; Yu, J.-Q. Versatile Pd(II)-catalyzed C-H activation/aryl-aryl coupling of benzoic and phenyl acetic acids. *J. Am. Chem. Soc.* **2008**, *130*, 17676.

[242] Wan, X.; Ma, Z.; Li, B.; Zhang, K.; Cao, S.; Zhang, S.; Shi, Z. Highly selective C-H functionalization/halogenation of acetanilide. *J. Am. Chem. Soc.* **2006**, *128*, 7416.

[243] Sun, C.-L.; Liu, N.; Li, B.-J.; Yu, D.-G.; Wang, Y.; Shi, Z.-J. Pd-catalyzed C-H functionalizations of O-methyl oximes with arylboronic acids. *Org. Lett.* **2010**, *12*, 184.

[244] Chu, J.-H.; Chen, C.-C.; Wu, M.-J. Palladium-Catalyzed Arylation and Alkylation of 3,5-Diphenylisoxazole with Boronic Acids via C−H Activation. *Organometallics* **2008**, *27*, 5173.

[245] Romero-Revilla, J. A.; García-Rubia, A.; Goméz Arrayás, R.; Fernández-Ibáñez, M. Á.; Carretero, J. C. Palladium-Catalyzed Coupling of Arene C–H Bonds with Methyl- and Arylboron Reagents Assisted by the Removable 2-Pyridylsulfinyl Group. *J. Org. Chem.* **2011**, *76*, 9525.

[246] Neufeldt, S. R.; Seigerman, C. K.; Sanford, M. S. Mild Palladium-Catalyzed C–H Alkylation Using Potassium Alkyltrifluoroborates in Combination with MnF3. *Org. Lett.* **2013**, *15*, 2302.

[247] Yang, S.-D.; Sun, C.-L.; Fang, Z.; Li, B.-J.; Li, Y.-Z.; Shi, Z.-J. Palladium-catalyzed direct arylation of (hetero)arenes with aryl boronic acids. *Angew. Chem. Int. Ed.* **2008**, *47*, 1473.

[248] Zhao, J.; Zhang, Y.; Cheng, K. Palladium-catalyzed direct C-2 arylation of indoles with potassium aryltrifluoroborate salts. *J. Org. Chem.* **2008**, *73*, 7428.
[249] Fugami, K.; Kosugi, M. Organotin compounds. *Top. Curr. Chem.* **2002**, *219*, 87.
[250] Duncton, M. A. J.; Pattenden, G. The intramolecular Stille reaction. *J. Chem. Soc., Perkin Trans. 1* **1999**, 1235.
[251] Mitchell, T. N. Palladium-catalyzed reactions of organotin compounds. *Synthesis* **1992**, 803.
[252] Ehrlich, M.; Carell, T. Total Syntheses and Biological Evaluation of 3-O-Methylfunicone and Its Derivatives Prepared by TMPZnCl center dot LiCl-Mediated Halogenation and Carbonylative Stille Cross-Coupling. *Eur. J. Org. Chem.* **2013**, 77.
[253] Chang, J. H.; Kang, H. U.; Jung, I. H.; Cho, C. G. Total Synthesis of (+/-)-Galanthamine via a C3-Selective Stille Coupling and IMDA Cycloaddition Cascade of 3,5-Dibromo-2-pyrone. *Org. Lett.* **2010**, *12*, 2016.
[254] Tam, N. T.; Cho, C. G. Total synthesis of (+/-)-crinine via the regioselective stille coupling and Diels-Alder reaction of 3,5-dibromo-2-pyrone. *Org. Lett.* **2008**, *10*, 601.
[255] Chen, X.; Li, J.-J.; Hao, X.-S.; Goodhue, C.; Yu, J.-Q. Palladium-catalyzed alkylation of aryl C-H bonds with sp3 organotin reagents using benzoquinone as a crucial promoter. *J. Am. Chem. Soc.* **2006**, *128*, 78.
[256] Kawai, H.; Kobayashi, Y.; Oi, S.; Inoue, Y. Direct C-H bond arylation of arenes with aryltin reagents catalysed by palladium complexes. *Chem. Commun.* **2008**, 1464.
[257] Xue, D.; Li, J.; Liu, Y. X.; Han, W. Y.; Zhang, Z. T.; Wang, C.; Xiao, J. L. Room-Temperature Stille Coupling of Tetraarylstannanes via Palladium-Catalyzed C-H Activation. *Synlett* **2012**, 1941.
[258] Sore, H. F.; Galloway, W.; Spring, D. R. Palladium-catalysed cross-coupling of organosilicon reagents. *Chem. Soc. Rev.* **2012**, *41*, 1845.
[259] Hiyama, T. Transition Metal-catalyzed Reactions of Organosilicon Reagents Through Intramolecular Activation. *J. Syn. Org. Chem. Jpn.* **2010**, *68*, 729.
[260] Hiyama, T.; Shirakawa, E. Organosilicon compounds. *Top. Curr. Chem.* **2002**, *219*, 61.
[261] Denmark, S. E.; Sweis, R. F. Cross-coupling reactions of organosilicon compounds: New concepts and recent advances. *Chem. Pharm. Bull.* **2002**, *50*, 1531.
[262] Mohapatra, D. K.; Das, P. P.; Pattanayak, M. R.; Gayatri, G.; Sastry, G. N.; Yadav, J. S. Protecting-Group Directed Stereoselective Intramolecular Nozaki-Hiyama-Kishi Reaction: A Concise and Efficient Total Synthesis of Amphidinolactone A. *Eur. J. Org. Chem.* **2010**, 4775.
[263] LeClair, C. A.; Boxer, M. B.; Thomas, C. J.; Maloney, D. J. Total synthesis of LL-Z1640-2 utilizing a late-stage intramolecular Nozaki-Hiyama-Kishi reaction. *Tetrahedron Lett.* **2010**, *51*, 6852.

[264] Inoue, M.; Nakada, M. Structure elucidation and enantioselective total synthesis of the potent HMG-CoA reductase inhibitor FR901512 via catalytic asymmetric Nozaki-Hiyama reactions. *J. Am. Chem. Soc.* **2007**, *129*, 4164.
[265] Sabino, A. A.; Pilli, R. A. Total synthesis of (+)-herbarumin I via intermolecular Nozaki-Hiyama-Kishi reaction. *Tetrahedron Lett.* **2002**, *43*, 2819.
[266] Yang, S.; Li, B.; Wan, X.; Shi, Z. Ortho arylation of acetanilides via Pd(II)-catalyzed C-H functionalization. *J. Am. Chem. Soc.* **2007**, *129*, 6066.
[267] Zhou, H.; Xu, Y.-H.; Chung, W.-J.; Loh, T.-P. Palladium-catalyzed direct arylation of cyclic enamides with aryl silanes by sp(2) C-H activation. *Angew. Chem. Int. Ed.* **2009**, *48*, 5355.
[268] Liang, Z.; Yao, B.; Zhang, Y. Pd(OAc)2-catalyzed regioselective arylation of indoles with arylsiloxane in acidic medium. *Org. Lett.* **2010**, *12*, 3185.
[269] Fuchita, Y.; Utsunomiya, Y.; Yasutake, M. Synthesis and reactivity of arylgold(III) complexes from aromatic hydrocarbons via C–H bond activation. *J. Chem. Soc., Dalton Trans.* **2001**, 2330.
[270] de Haro, T.; Nevado, C. Gold-catalyzed ethynylation of arenes. *J. Am. Chem. Soc.* **2010**, *132*, 1512.
[271] Wei, Y.; Zhao, H.; Kan, J.; Su, W.; Hong, M. Copper-catalyzed direct alkynylation of electron-deficient polyfluoroarenes with terminal alkynes using O2 as an oxidant. *J. Am. Chem. Soc.* **2010**, *132*, 2522.
[272] Chinchilla, R.; Nájera, C. Chemicals from Alkynes with Palladium Catalysts. *Chem. Rev.* **2013**, ASAP.
[273] Yang, L.; Zhao, L.; Li, C.-J. Palladium-catalyzed direct oxidative Heck-Cassar-Sonogashira type alkynylation of indoles with alkynes under oxygen. *Chem. Commun.* **2010**, *46*, 4184.
[274] Kim, S.; Yoon, J.; Chang, S. Palladium-catalyzed oxidative alkynylation of heterocycles with terminal alkynes under air conditions. *Org. Lett.* **2011**, *13*, 1474.
[275] Wu, C.; Li, P.; Fang, Y.; Zhao, J.; Xue, W.; Li, Y.; Larock, R. C.; Shi, F. Pd-catalyzed oxidative coupling of monosubstituted sydnones and terminal alkynes. *Tetrahedron Lett.* **2011**, *52*, 3797.
[276] Shibahara, F.; Dohke, Y.; Murai, T. Palladium-catalyzed C-H bond direct alkynylation of 5-membered heteroarenes: a well-defined synthetic route to azole derivatives containing two different alkynyl groups. *J. Org. Chem.* **2012**, *77*, 5381.
[277] Jie, X.; Shang, Y.; Hu, P.; Su, W. Palladium-Catalyzed Oxidative Cross-Coupling between Heterocycles and Terminal Alkynes with Low Catalyst Loading. *Angew. Chem. Int. Ed.* **2013**, *52*, 3630.
[278] Hadi, V.; Yoo, K. S.; Jeong, M.; Jung, K. W. Expeditious enyne construction from alkynes via oxidative Pd(II)-catalyzed Heck-type coupling. *Tetrahedron Lett.* **2009**, *50*, 2370.
[279] Shao, Y.-L.; Zhang, X.-H.; Han, J.-S.; Zhong, P. Pd(II)-Catalyzed Dehydrogenative Olefination of Terminal Arylalkynes with Allylic Ethers:

General and Selective Access to Linear (Z)-1,3-Enynes. *Org. Lett.* **2012**, *14*, 5242.
[280] Moritanl, I.; Fujiwara, Y. Aromatic substitution of styrene-palladium chloride complex. *Tetrahedron Lett.* **1967**, *8*, 1119.
[281] Fujiwara, Y.; Moritani, I.; Matsuda, M.; Teranishi, S. Aromatic substitution of styrene-palladium chloride complex. II effect of metal acetate. *Tetrahedron Lett.* **1968**, *9*, 633.
[282] van Helden, R.; Verberg, G. The oxidative coupling of aromatic compounds with palladium salts. *Recl. Trav. Chim. Pays-Bas* **1965**, *84*, 1263.
[283] Iataaki, H.; Yoshimoto, H. Palladium-catalyzed syntheses of aromatic coupling compounds. *J. Org. Chem.* **1973**, *38*, 76.
[284] Okamoto, M.; Yamaji, T. A Selective Synthesis of Biphenyl by the Pd(OAc)2/MoO2(acac)2/O2/AcOH Catalyst System. *Chem. Lett.* **2001**, *30*, 212.
[285] Yokota, T.; Sakaguchi, S.; Ishii, Y. Aerobic Oxidation of Benzene to Biphenyl Using a Pd(II)/Molybdovanadophosphoric Acid Catalytic System. *Adv. Synth. Catal.* **2002**, *344*, 849.
[286] Mukhopadhyay, S.; Rothenberg, G.; Gitis, D.; Sasson, Y. Tandem one-Pot palladium-catalyzed reductive and oxidative coupling of benzene and chlorobenzene. *J. Org. Chem.* **2000**, *65*, 3107.
[287] Mukhopadhyay, S.; Rothenberg, G.; Lando, G.; Agbaria, K.; Kazanci, M.; Sasson, Y. Air Oxidation of Benzene to Biphenyl - A Dual Catalytic Approach. *Adv. Synth. Catal.* **2001**, *343*, 455.
[288] Itahara, T.; Hashimoto, M.; Yumisashi, H. Oxidative Dimerization of Thiophenes and Furans bearing Electron-Withdrawing Substituents by Palladium Acetate. *Synthesis* **1984**, *1984*, 255.
[289] Masui, K.; Ikegami, H.; Mori, A. Palladium-catalyzed C-H homocoupling of thiophenes: facile construction of bithiophene structure. *J. Am. Chem. Soc.* **2004**, *126*, 5074.
[290] Liang, Z.; Zhao, J.; Zhang, Y. Palladium-catalyzed regioselective oxidative coupling of indoles and one-pot synthesis of acetoxylated biindolyls. *J. Org. Chem.* **2010**, *75*, 170.
[291] Hull, K.; Lanni, E.; Sanford, M. Highly regioselective catalytic oxidative coupling reactions: synthetic and mechanistic investigations. *J. Am. Chem. Soc.* **2006**, *128*, 14047.
[292] Hull, K. L.; Sanford, M. S. Catalytic and highly regioselective cross-coupling of aromatic C-H substrates. *J. Am. Chem. Soc.* **2007**, *129*, 11904.
[293] Hull, K. L.; Sanford, M. S. Mechanism of benzoquinone-promoted palladium-catalyzed oxidative cross-coupling reactions. *J. Am. Chem. Soc.* **2009**, *131*, 9651.
[294] Li, B.-J.; Tian, S.-L.; Fang, Z.; Shi, Z.-J. Multiple C-H activations to construct biologically active molecules in a process completely free of organohalogen and organometallic components. *Angew. Chem. Int. Ed.* **2008**, *47*, 1115.
[295] Xia, J.-B.; You, S.-L. Carbon−Carbon Bond Formation through Double sp 2 C−H Activations: Synthesis of Ferrocenyl Oxazoline Derivatives. *Organometallics* **2007**, *26*, 4869.

[296] Brasche, G.; García-Fortanet, J.; Buchwald, S. Twofold C-H functionalization: palladium-catalyzed ortho arylation of anilides. *Org. Lett.* **2008**, *10*, 2207.
[297] Zhao, X.; Yeung, C.; Dong, V. Palladium-catalyzed ortho-arylation of O-phenylcarbamates with simple arenes and sodium persulfate. *J. Am. Chem. Soc.* **2010**, *132*, 5837.
[298] Li, R.; Li, J., Li; Lu, W. Intermolecular Cross-Coupling of Simple Arenes via C−H Activation by Tuning Concentrations of Arenes and TFA. *Organometallics* **2006**, *25*, 5973.
[299] Dwight, T.; Rue, N.; Charyk, D.; Josselyn, R.; DeBoef, B. C-C bond formation via double C-H functionalization: aerobic oxidative coupling as a method for synthesizing heterocoupled biaryls. *Org. Lett.* **2007**, *9*, 3137.
[300] Bugaut, X.; Glorius, F. Palladium-Catalyzed Selective Dehydrogenative Cross-Couplings of Heteroarenes. *Angew. Chem. Int. Ed.* **2011**, *50*, 7479.
[301] Xi, P.; Yang, F.; Qin, S.; Zhao, D.; Lan, J.; Gao, G.; Hu, C.; You, J. Palladium(II)-catalyzed oxidative C-H/C-H cross-coupling of heteroarenes. *J. Am. Chem. Soc.* **2010**, *132*, 1822.
[302] He, C.-Y.; Fan, S.; Zhang, X. Pd-catalyzed oxidative cross-coupling of perfluoroarenes with aromatic heterocycles. *J. Am. Chem. Soc.* **2010**, *132*, 12850.
[303] Wei, Y.; Su, W. Pd(OAc)(2)-catalyzed oxidative C-H/C-H cross-coupling of electron-deficient polyfluoroarenes with simple arenes. *J. Am. Chem. Soc.* **2010**, *132*, 16377.
[304] He, C.-Y.; Min, Q.-Q.; Zhang, X. Palladium-Catalyzed Aerobic Dehydrogenative Cross-Coupling of Polyfluoroarenes with Thiophenes: Facile Access to Polyfluoroarene–Thiophene Structure. *Organometallics* **2011**, *31*, 1335.
[305] Chen, F.; Feng, Z.; He, C.-Y.; Wang, H.-Y.; Guo, Y.-l.; Zhang, X. Pd-Catalyzed Dehydrogenative Cross-Coupling of Polyfluoroarenes with Heteroatom-Substituted Enones. *Org. Lett.* **2012**, *14*, 1176.
[306] Fu, X.-P.; Xuan, Q.-Q.; Liu, L.; Wang, D.; Chen, Y.-J.; Li, C.-J. Dual C–H activations of electron-deficient heteroarenes: palladium-catalyzed oxidative cross coupling of thiazoles with azine N-oxides. *Tetrahedron* **2013**, *69*, 4436.
[307] Jia, C.; Piao, D.; Oyamada, J.; Lu, W.; Kitamura, T.; Fujiwara, Y. Efficient activation of aromatic C-H bonds for addition to C-C multiple bonds. *Science* **2000**, *287*, 1992.
[308] Punniyamurthy, T.; Velusamy, S.; Iqbal, J. Recent advances in transition metal catalyzed oxidation of organic substrates with molecular oxygen. *Chem. Rev.* **2005**, *105*, 2329.
[309] Shi, Z.; Zhang, C.; Tang, C.; Jiao, N. Recent advances in transition-metal catalyzed reactions using molecular oxygen as the oxidant. *Chem. Soc. Rev.* **2012**, *41*, 3381.
[310] Fujiwara, Y.; Moritani, I.; Matsuda, M.; Teranishi, S. Aromatic substitution of olefin. IV Reaction with palladium metal and silver acetate. *Tetrahedron Lett.* **1968**, *9*, 3863.

[311] Shue, R. S. Catalytic coupling of aromatics and olefins by homogeneous palladium(II) compounds under oxygen. *J. Chem. Soc. D: Chem. Commun.* **1971**, 1510.
[312] Yokota, T.; Tani, M.; Sakaguchi, S.; Ishii, Y. Direct coupling of benzene with olefin catalyzed by Pd(OAc)(2) combined with heteropolyoxometalate under dioxygen. *J. Am. Chem. Soc.* **2003**, *125*, 1476.
[313] Minami, K.; Kawamura, Y.; Koga, K.; Hosokawa, T. Palladium(II)-catalyzed oxidative transformation of allylic alcohols and vinyl ethers into 2-alkoxytetrahydrofurans: catechol as an activator of catalyst. *Org. Lett.* **2005**, *7*, 5689.
[314] Beck, E.; Grimster, N.; Hatley, R.; Gaunt, M. Mild aerobic oxidative palladium (II) catalyzed C-H bond functionalization: regioselective and switchable C-H alkenylation and annulation of pyrroles. *J. Am. Chem. Soc.* **2006**, *128*, 2528.
[315] Grimster, N.; Gauntlett, C.; Godfrey, C.; Gaunt, M. Palladium-catalyzed intermolecular alkenylation of indoles by solvent-controlled regioselective C-H functionalization. *Angew. Chem. Int. Ed.* **2005**, *44*, 3125.
[316] Boele, M.; van Strijdonck, G.; de Vries, A.; Kamer, P.; de Vries, J.; van Leeuwen, P. Selective Pd-catalyzed oxidative coupling of anilides with olefins through C-H bond activation at room temperature. *J. Am. Chem. Soc.* **2002**, *124*, 1586.
[317] Li, J.-J.; Mei, T.-S.; Yu, J.-Q. Synthesis of indolines and tetrahydroisoquinolines from arylethylamines by Pd(II)-catalyzed C-H activation reactions. *Angew. Chem. Int. Ed.* **2008**, *47*, 6452.
[318] Wang, D.-H.; Engle, K.; Shi, B.-F.; Yu, J.-Q. Ligand-enabled reactivity and selectivity in a synthetically versatile aryl C-H olefination. *Science* **2010**, *327*, 315.
[319] Engle, K.; Wang, D.-H.; Yu, J.-Q. Ligand-accelerated C-H activation reactions: evidence for a switch of mechanism. *J. Am. Chem. Soc.* **2010**, *132*, 14137.
[320] Engle, K. M.; Mei, T.-S.; Wasa, M.; Yu, J.-Q. Weak Coordination as a Powerful Means for Developing Broadly Useful C–H Functionalization Reactions. *Acc. Chem. Res.* **2011**, *45*, 788.
[321] Wu, J.; Cui, X.; Chen, L.; Jiang, G.; Wu, Y. Palladium-Catalyzed Alkenylation of Quinoline-N-oxides via C−H Activation under External-Oxidant-Free Conditions. *J. Am. Chem. Soc.* **2009**, *131*, 13888.
[322] Cho, S.; Hwang, S.; Chang, S. Palladium-catalyzed C-H functionalization of pyridine N-oxides: highly selective alkenylation and direct arylation with unactivated arenes. *J. Am. Chem. Soc.* **2008**, *130*, 9254.
[323] Zhang, X.; Fan, S.; He, C.-Y.; Wan, X.; Min, Q.-Q.; Yang, J.; Jiang, Z.-X. Pd(OAc)2 Catalyzed Olefination of Highly Electron-Deficient Perfluoroarenes. *J. Am. Chem. Soc.* **2010**, *132*, 4506.
[324] Majewski, M.; Gleave, D. M. Diastereoselective aldol reactions of cyclohexanone lithium enolate. *Tetrahedron Lett.* **1989**, *30*, 5681.
[325] Maryanoff, B. E.; Reitz, A. B. The Wittig olefination reaction and modifications involving phosphoryl-stabilized carbanions. Stereochemistry, mechanism, and selected synthetic aspects. *Chem. Rev.* **1989**, *89*, 863.

[326] Cabri, W.; Candiani, I. Recent Developments and New Perspectives in the Heck Reaction. *Acc. Chem. Res.* **1995**, *28*, 2.
[327] da Silva, M. J.; Gusevskaya, E. V. Palladium-catalyzed oxidation of monoterpenes: novel tandem oxidative coupling–oxidation of camphene by dioxygen. *J. Mol. Catal. A-Chem.* **2001**, *176*, 23.
[328] Hatamoto, Y.; Sakaguchi, S.; Ishii, Y. Oxidative cross-coupling of acrylates with vinyl carboxylates catalyzed by a Pd(OAc)2/HPMoV/O2 system. *Org. Lett.* **2004**, *6*, 4623.
[329] Xu, Y.-H.; Lu, J.; Loh, T.-P. Direct cross-coupling reaction of simple alkenes with acrylates catalyzed by palladium catalyst. *J. Am. Chem. Soc.* **2009**, *131*, 1372.
[330] Yu, H.; Jin, W.; Sun, C.; Chen, J.; Du, W.; He, S.; Yu, Z. Palladium-catalyzed cross-coupling of internal alkenes with terminal alkenes to functionalized 1,3-butadienes using C-H bond activation: efficient synthesis of bicyclic pyridones. *Angew. Chem. Int. Ed.* **2010**, *49*, 5792.
[331] Zhang, Y.; Cui, Z.; Li, Z.; Liu, Z.-Q. Pd(II)-catalyzed dehydrogenative olefination of vinylic C-H bonds with allylic esters: general and selective access to linear 1,3-butadienes. *Org. Lett.* **2012**, *14*, 1838.
[332] Bai, Y.; Zeng, J.; Cai, S.; Liu, X.-W. Palladium-catalyzed direct cross-coupling reaction of glycals with activated alkenes. *Org. Lett.* **2011**, *13*, 4394.
[333] Gigant, N.; Gillaizeau, I. Palladium(II)-catalyzed direct alkenylation of nonaromatic enamides. *Org. Lett.* **2012**, *14*, 3304.
[334] Xu, Y.-H.; Chok, Y. K.; Loh, T.-P. Synthesis and characterization of a cyclic vinylpalladium(ii) complex: vinylpalladium species as the possible intermediate in the catalytic direct olefination reaction of enamide. *Chem. Sci.* **2011**, *2*, 1822.
[335] Yoo, W. J.; Li, C. J., Cross-Dehydrogenative Coupling Reactions of sp(3)-Hybridized C-H Bonds. In *C-H Activation*, Yu, J. Q.; Shi, Z., Eds.**2010**; Vol. 292, pp 281.
[336] Li, Z.; Li, C.-J. CuBr-catalyzed direct indolation of tetrahydroisoquinolines via cross-dehydrogenative coupling between sp3 C-H and sp2 C-H bonds. *J. Am. Chem. Soc.* **2005**, *127*, 6968.
[337] Mo, H.; Bao, W. Efficient Palladium-Catalyzed Oxidative Indolation of Allylic Compounds with DDQ via sp 3 C–H Bond Activation and Carbon-Carbon Bond Formation Under Mild Conditions. *Adv. Synth. Catal.* **2009**, *351*, 2845.
[338] Deng, G.; Zhao, L.; Li, C.-J. Ruthenium-catalyzed oxidative cross-coupling of chelating arenes and cycloalkanes. *Angew. Chem. Int. Ed.* **2008**, *47*, 6278.
[339] Wang, X.; Widenhoefer, R. Palladium(II)- and platinum(II)-catalyzed addition of stabilized carbon nucleophiles to ethylene and propylene. *Chem. Commun.* **2004**, 660.
[340] Wu, Z.; Pi, C.; Cui, X.; Bai, J.; Wu, Y. Direct C-2 Alkylation of Quinoline N-Oxides with Ethers via Palladium-Catalyzed Dehydrogenative Cross-Coupling Reaction. *Adv. Synth. Catal.* **2013**, *355*, 1971.

[341] Yu, Y.-Y.; Niphakis, M. J.; Georg, G. I. Palladium(II)-catalyzed dehydrogenative alkenylation of cyclic enaminones via the Fujiwara-Moritani reaction. *Org. Lett.* **2011**, *13*, 5932.
[342] Furman, B.; Lipner, G. Rhodium-catalyzed intramolecular conjugate addition of vinylstannanes to dihydro-4-pyridones: a simple method for stereoselective construction of 1-azabicyclic alkaloids. *Tetrahedron* **2008**, *64*, 3464.
[343] Kitagawa, H.; Kumura, K.; Atsumi, K. A Novel Synthesis of 2,3-Disubstituted-4-pyridones from 4-Methoxypyridine. *Chem. Lett.* **2006**, *35*, 712.
[344] Knauer, S.; Kunz, H. Palladium-catalysed C–C coupling reactions in the enantioselective synthesis of 2,4-disubstituted 4,5-dehydropiperidines using galactosylamine as a stereodifferentiating auxiliary. *Tetrahedron-Asymmetry* **2005**, *16*, 529.
[345] Davis, F. A.; Xu, H.; Zhang, J. Y. Asymmetric synthesis of ring functionalized trans-2,6-disubstituted piperidines from N-sulfinyl delta-amino beta-keto phosphonates. Total synthesis of (-)-myrtine. *J. Org. Chem.* **2007**, *72*, 2046.
[346] Michael, J. P.; de Koning, C. B.; van der Westhuyzen, C. W. Studies towards the enantioselective synthesis of 5,6,8-trisubstituted amphibian indolizidine alkaloids via enaminone intermediates. *Org. Biomol. Chem.* **2005**, *3*, 836.
[347] Comins, D. L.; Sahn, J. J. A six-step asymmetric synthesis of (+)-hyperaspine. *Org. Lett.* **2005**, *7*, 5227.
[348] Back, T. G.; Hamilton, M. D.; Lim, V. J. J.; Parvez, M. Synthesis of the quinolizidine alkaloids (-)-lasubine II and (+/-)-myrtine by conjugate addition and intramolecular acylation of amino esters with acetylenic sulfones. *J. Org. Chem.* **2005**, *70*, 967.
[349] Niphakis, M. J.; Gay, B. C.; Hong, K. H.; Bleeker, N. P.; Georg, G. I. Synthesis and evaluation of the anti-proliferative and NF-kappa B activities of a library of simplified tylophorine analogs. *Biorg. Med. Chem.* **2012**, *20*, 5893.
[350] Kuhl, N.; Hopkinson, M. N.; Wencel-Delord, J.; Glorius, F. Beyond directing groups: transition-metal-catalyzed C-H activation of simple arenes. *Angew. Chem. Int. Ed.* **2012**, *51*, 10236.
[351] Baudoin, O. Transition metal-catalyzed arylation of unactivated C(sp(3))-H bonds. *Chem. Soc. Rev.* **2011**, *40*, 4902.
[352] Shirakawa, E.; Hayashi, T. Transition-metal-free Coupling Reactions of Aryl Halides. *Chem. Lett.* **2012**, *41*, 130.
[353] Zhao, D. B.; You, J. S.; Hu, C. W. Recent Progress in Coupling of Two Heteroarenes. *Chem.-Eur. J.* **2011**, *17*, 5466.
[354] Roger, J.; Gottumukkala, A. L.; Doucet, H. Palladium-Catalyzed C3 or C4 Direct Arylation of Heteroaromatic Compounds with Aryl Halides by C-H Bond Activation. *Chemcatchem* **2010**, *2*, 20.
[355] Bellina, F.; Rossi, R. Transition Metal-Catalyzed Direct Arylation of Substrates with Activated sp(3)-Hybridized C-H Bonds and Some of Their Synthetic Equivalents with Aryl Halides and Pseudohalides. *Chem. Rev.* **2010**, *110*, 1082.
[356] Daugulis, O.; Do, H. Q.; Shabashov, D. Palladium- and Copper-Catalyzed Arylation of Carbon-Hydrogen Bonds. *Acc. Chem. Res.* **2009**, *42*, 1074.

[357] Beletskaya, I. P.; Cheprakov, A. V. The Heck Reaction as a Sharpening Stone of Palladium Catalysis. *Chem. Rev.* **2000**, *100*, 3009.
[358] Jeffery, T. On the efficiency of tetraalkylammonium salts in Heck type reactions. *Tetrahedron* **1996**, *52*, 10113.
[359] Engle, K. M.; Mei, T. S.; Wasa, M.; Yu, J. Q. Weak Coordination as a Powerful Means for Developing Broadly Useful C-H Functionalization Reactions. *Acc. Chem. Res.* **2012**, *45*, 788.
[360] Albano, V. G.; Di Serio, M.; Monari, M.; Orabona, I.; Panunzi, A.; Ruffo, F. Mechanism of Silver-Promoted Ligand Metathesis in Square-Planar Complexes of d8 Ions. Kinetics of Formation and Molecular Structures of a Trinuclear Intermediate [(Me)(N−N)Pt(μ -Cl)Ag(μ -Cl)Pt(N−N)(Me)]+ and Its Dinuclear Evolution Product [(Me)(N−N)Pt(μ -Cl)Pt(N−N)(Me)]+ (N−N = ArNC(Me)C(Me)NAr, Ar = 2,6-(i-Pr)2C6H3). *Inorg. Chem.* **2002**, *41*, 2672.
[361] Liston, D. J.; Lee, Y. J.; Scheidt, W. R.; Reed, C. A. Observations on silver salt metathesis reactions with very weakly coordinating anions. *J. Am. Chem. Soc.* **1989**, *111*, 6643.
[362] Grove, D. M.; Van Koten, G.; Louwen, J. N.; Noltes, J. G.; Spek, A. L.; Ubbels, H. J. C. Trans-2,6-bis[(dimethylamino)methyl]phenyl-N,N',C complexes of palladium(II) and platinum(II). Crystal structure of [PtI[MeC6H3(CH2NMe2)2-o,o']]BF4: a cyclohexadienyl carbonium ion with a .sigma.-bonded metal substituent. *J. Am. Chem. Soc.* **1982**, *104*, 6609.
[363] Ziadi, A.; Martin, R. Ligand-Accelerated Pd-Catalyzed Ketone γ -Arylation via C – C Cleavage with Aryl Chlorides. *Org. Lett.* **2012**, *14*, 1266.
[364] Roy, D.; Mom, S.; Royer, S.; Lucas, D.; Hierso, J.-C.; Doucet, H. Palladium-Catalyzed Direct Arylation of Heteroaromatics with Activated Aryl Chlorides Using a Sterically Relieved Ferrocenyl-Diphosphane. *ACS Catal.* **2012**, *2*, 1033.
[365] Gao, K.; Lee, P.-S.; Long, C.; Yoshikai, N. Cobalt-Catalyzed Ortho-Arylation of Aromatic Imines with Aryl Chlorides. *Org. Lett.* **2012**, *14*, 4234.
[366] Cao, H.; Lin, Y.; Zhan, H.; Du, Z.; Lin, X.; Liang, Q.-M.; Zhang, H. Highly regioselective C-H bond functionalization: palladium-catalyzed arylation of substituted imidazo[1,2-a]pyridine with aryl chlorides. *RSC Adv.* **2012**, *2*, 5972.
[367] Gorelsky, S. I. Origins of regioselectivity of the palladium-catalyzed (aromatic)CH bond metalation–deprotonation. *Coord. Chem. Rev.* **2013**, *257*, 153.
[368] Fujiwara, Y.; Noritani, I.; Danno, S.; Asano, R.; Teranishi, S. Aromatic substitution of olefins. VI. Arylation of olefins with palladium(II) acetate. *J. Am. Chem. Soc.* **1969**, *91*, 7166.
[369] Liu, W.; Li, Y. H.; Xu, B.; Kuang, C. X. Palladium-Catalyzed Olefination and Arylation of 2-Substituted 1,2,3-Triazole N-Oxides. *Org. Lett.* **2013**, *15*, 2342.
[370] Huang, Q. F.; Song, Q. Q.; Cai, J.; Zhang, X. F.; Lin, S. Palladium(II)/Polyoxometalate-Catalyzed Direct C-3 Alkenylation of Indoles using Dioxygen as the Terminal Oxidant. *Adv. Synth. Catal.* **2013**, *355*, 1512.
[371] Yu, M.; Xie, Y. J.; Xie, C. S.; Zhang, Y. H. Palladium-Catalyzed C-H Alkenylation of Arenes Using Thioethers as Directing Groups. *Org. Lett.* **2012**, *14*, 2164.

[372] Wen, P.; Li, Y. M.; Zhou, K.; Ma, C.; Lan, X. B.; Ma, C. W.; Huang, G. S. Palladium-Catalyzed C-2 Selective C-H Olefination of Pyridines. *Adv. Synth. Catal.* **2012**, *354*, 2135.
[373] Xu, Y.-H.; Wang, W.-J.; Wen, Z.-K.; Hartley, J.; Loh, T.-P. Palladium-catalyzed direct cross-coupling reaction between indenes and electron-deficient alkenes. *Tetrahedron Lett.* **2010**, *51*, 3504.
[374] Yao, Q. W.; Kinney, E. P.; Yang, Z. Ligand-free heck reaction: Pd(OAc)(2) as an active catalyst revisited. *J. Org. Chem.* **2003**, *68*, 7528.
[375] Zhao, F. Y.; Bhanage, B. M.; Shirai, M.; Arai, M. Effect of triphenylphosphine concentration on the kinetics of homogeneous Heck reaction in different solvents. *J. Mol. Catal. A-Chem.* **1999**, *142*, 383.
[376] Cabri, W.; Candiani, I.; Debernardinis, S.; Francalanci, F.; Penco, S.; Santi, R. Heck reaction on anthraquinone derivatives - ligand, solvent, and salt effects. *J. Org. Chem.* **1991**, *56*, 5796.
[377] Miyasaka, M.; Hirano, K.; Satoh, T.; Miura, M. Palladium-Catalyzed Direct Oxidative Alkenylation of Azoles. *J. Org. Chem.* **2010**, *75*, 5421.
[378] García-Rubia, A.; Arrayás, R. G.; Carretero, J. C. Palladium(II)-Catalyzed Regioselective Direct C2 Alkenylation of Indoles and Pyrroles Assisted by the N-(2-Pyridyl)sulfonyl Protecting Group. *Angew. Chem. Int. Ed.* **2009**, *48*, 6511.
[379] Cai, G.; Fu, Y.; Li, Y.; Wan, X.; Shi, Z. Indirect ortho Functionalization of Substituted Toluenes through ortho Olefination of N,N-Dimethylbenzylamines Tuned by the Acidity of Reaction Conditions. *J. Am. Chem. Soc.* **2007**, *129*, 7666.
[380] Ozawa, F.; Kubo, A.; Matsumoto, Y.; Hayashi, T.; Nishioka, E.; Yanagi, K.; Moriguchi, K. Palladium-catalyzed asymmetric arylation of 2,3-dihydrofuran with phenyl triflate. A novel asymmetric catalysis involving a kinetic resolution process. *Organometallics* **1993**, *12*, 4188.
[381] Theocharis, D. A.; Coutsogeorgopoulos, C. Mechanism of action of sparsomycin in protein synthesis. *Biochemistry* **1992**, *31*, 5861.
[382] Gazivoda, T.; Raic-Malic, S.; Marjanovic, M.; Kralj, M.; Pavelic, K.; Balzarini, J.; De Clercq, E.; Mintas, M. The novel C-5 aryl, alkenyl, and alkynyl substituted uracil derivatives of L-ascorbic acid: Synthesis, cytostatic, and antiviral activity evaluations. *Biorg. Med. Chem.* **2007**, *15*, 749.
[383] Kumar, R.; Nath, M.; Tyrrell, D. L. J. Design and synthesis of novel 5-substituted acyclic pyrimidine nucleosides as potent and selective inhibitors of hepatitis B virus. *J. Med. Chem.* **2002**, *45*, 2032.
[384] Choi, Y.; Li, L.; Grill, S.; Gullen, E.; Lee, C. S.; Gumina, G.; Tsujii, E.; Cheng, Y. C.; Chu, C. K. Structure-activity relationships of (E)-5-(2-bromovinyl) uracil and related pyrimidine nucleosides as antiviral agents for herpes viruses. *J. Med. Chem.* **2000**, *43*, 2538.
[385] Choi, Y. S.; Li, L.; Grill, S.; Gullen, E.; Lee, C. S.; Gumina, G.; Cheng, Y. C.; Chu, C. K. Structure-activity relationships of (E)-5-(2-Bromovinyl) uracil and related pyrimidine L-nucleosides as antiviral agents for varicella zoster virus. *Antivir. Res.* **2000**, *46*, A81.

[386] Zierkiewicz, W.; Privalov, T. A Theoretical Study of the Essential Role of DMSO as a Solvent/Ligand in the Pd(OAc)2/DMSO Catalyst System for Aerobic Oxidation. *Organometallics* **2005**, *24*, 6019.
[387] Wicke, L.; Engels, J. W. Postsynthetic on Column RNA Labeling via Stille Coupling. *Bioconjugate Chem.* **2012**, *23*, 627.
[388] Srivatsan, S. G.; Tor, Y. Enzymatic Incorporation of Emissive Pyrimidine Ribonucleotides. *Chem.-Asian J.* **2009**, *4*, 419.
[389] Cahova, H.; Havran, L.; Brazdilova, P.; Pivonkova, H.; Pohl, R.; Fojta, M.; Hocek, M. Aminophenyl- and nitrophenyl-labeled nucleoside triphosphates: Synthesis, enzymatic incorporation, and electrochemical detection. *Angew. Chem. Int. Ed.* **2008**, *47*, 2059.
[390] Srivastav, N. C.; Shakya, N.; Bhavanam, S.; Agrawal, A.; Tse, C.; Desroches, N.; Kunimoto, D. Y.; Kumar, R. Antimycobacterial activities of 5-alkyl (or halo)-3 '-substituted pyrimidine nucleoside analogs. *Bioorg. Med. Chem. Lett.* **2012**, *22*, 1091.
[391] Ivanov, A.; Tunitskaya, V.; Smirnova, O.; Buckheit, R.; Seley-Radtke, K.; Ozerov, A.; Novikov, M. Synthesis and Antiviral Activity of Substituted Uracils. *Antivir. Res.* **2009**, *82*, A58.
[392] Chen, C.; Wu, D. P.; Guo, Z. Q.; Xie, Q.; Reinhart, G. J.; Madan, A.; Wen, J.; Chen, T. K.; Huang, C. Q.; Chen, M.; Chen, Y. S.; Tucci, F. C.; Rowbottom, M.; Pontillo, J.; Zhu, Y. F.; Wade, W.; Saunders, J.; Bozigian, H.; Struthers, R. S. Discovery of Sodium R-(+)-4-{2- 5-(2-Fluoro-3-methoxyphenyl)-3-(2-fluoro-6-trifluoromethyl -benzyl)-4-methyl-2,6-dioxo-3,6-dihydro-2H-pyrimidin-1-yl -1-phenylethyl amino}butyrate (Elagolix), a Potent and Orally Available Nonpeptide Antagonist of the Human Gonadotropin-Releasing Hormone Receptor. *J. Med. Chem.* **2008**, *51*, 7478.
[393] Tsoukala, E.; Agelis, G.; Dolinsek, J.; Botic, T.; Cencic, A.; Komiotis, D. An efficient synthesis of 3-fluoro-5-thio-xylofuranosyl nucleosides of thymine, uracil, and 5-fluorouracil as potential antitumor or/and antiviral agents. *Biorg. Med. Chem.* **2007**, *15*, 3241.
[394] Watson, J. D.; Crick, F. H. C. Molecular Structure of Nucleic Acids: A Structure for Deoxyribose Nucleic Acid. *Nature* **1953**, *171*, 737.
[395] Liskamp, R. M. J.; Colstee, J. H.; Ottenheijm, H. C. J.; Lelieveld, P.; Akkerman, W. Structure-activity relationships of sparsomycin and its analogs: octylsparsomycin: The first analog more active than sparsomycin. *J. Med. Chem.* **1984**, *27*, 301.
[396] Wigerinck, P.; Pannecouque, C.; Snoeck, R.; Claes, P.; Declercq, E.; Herdewijn, P. 5-(5-bromothien-2-yl)-2'-deoxyuridine and 5-(5-chlorothien-2-yl)-2'-deoxyuridine are equipotent to (E)-5-(2-bromovinyl)-2'-deoxyuridine in the inhibition of herpes-simplex virus Type-I replication. *J. Med. Chem.* **1991**, *34*, 2383.
[397] Goodchild, J.; Porter, R. A.; Raper, R. H.; Sim, I. S.; Upton, R. M.; Viney, J.; Wadsworth, H. J. Structural requirements of olefinic 5-substituted deoxyuridines for antiherpes activity. *J. Med. Chem.* **1983**, *26*, 1252.

[398] Moa, M. J. G.; Besada, P.; Teran, C. Palladium-catalyzed approach to 1,2-disubstituted carbocyclic nucleoside analogues of 5-alkynyl and 5-alkenyl uracil. *Synthesis* **2006**, 3973.
[399] Ding, V. L.; Girardet, J. L.; Hong, Z.; Shaw, S. Z.; Yao, N. H. Synthesis of 2'-O-methyl-5-alkynyl and alkenyl substituted uridine derivatives to screen for inhibitors of HCV. *Heterocycles* **2006**, *68*, 521.
[400] Crisp, G. T.; Flynn, B. L. Palladium-catalyzed coupling of uridine triflate with organostannanes. *Tetrahedron Lett.* **1990**, *31*, 1347.
[401] Roh, K. R.; Kim, J. Y.; Kim, Y. H. Palladium catalyzed alkenylation or alkynylation at C-5 of uracil nucleosides using novel phenyliodonium triflate. *Tetrahedron Lett.* **1999**, *40*, 1903.
[402] Cernova, M.; Pohl, R.; Hocek, M. Switching the Regioselectivity of Direct C-H Arylation of 1,3-Dimethyluracil. *Eur. J. Org. Chem.* **2009**, 3698.
[403] Cernova, M.; Cerna, I.; Pohl, R.; Hocek, M. Regioselective Direct C-H Arylations of Protected Uracils. Synthesis of 5-and 6-Aryluracil Bases. *J. Org. Chem.* **2011**, *76*, 5309.
[404] Kim, K. H.; Lee, H. S.; Kim, J. N. Palladium-catalyzed direct 5-arylation of 1,3-dimethyluracil with aryl bromides: an electrophilic metalation-deprotonation with electrophilic arylpalladium intermediate. *Tetrahedron Lett.* **2011**, *52*, 6228.
[405] Lee, H. S.; Kim, S. H.; Kim, J. N. Pd(II)-Catalyzed Acetoxylation of Uracil via Electrophilic Palladation. *Bull. Korean Chem. Soc.* **2010**, *31*, 238.
[406] Kim, K. H.; Lee, H. S.; Kim, S. H.; Kim, J. N. Palladium(II)-catalyzed oxidative homo-coupling of 1,3-dimethyluracil derivatives. *Tetrahedron Lett.* **2012**, *53*, 1323.
[407] Nagib, D. A.; MacMillan, D. W. C. Trifluoromethylation of arenes and heteroarenes by means of photoredox catalysis. *Nature* **2011**, *480*, 224.
[408] Hirota, K.; Isobe, Y.; Kitade, Y.; Maki, Y. A simple synthesis of 5-(1-alkenyl)uracil derivatives by palladium-catalyzed oxidative coupling of uracils with olefins. *Synthesis* **1987**, 495.
[409] Moon, Y.; Hong, S. A facile route to isoflavone quinones via the direct cross-coupling of chromones and quinones. *Chem. Commun.* **2012**, *48*, 7191.
[410] Carrer, A.; Rousselle, P.; Florent, J.-C.; Bertounesque, E. Selective Palladium-Catalyzed Direct Arylation of Furo 3,2-b pyridines. *Adv. Synth. Catal.* **2012**, *354*, 2751.
[411] Kurinovich, M. A.; Lee, J. K. The acidity of uracil and uracil analogs in the gas phase: four surprisingly acidic sites and biological implications. *J. Am. Soc. Mass. Spectrom.* **2002**, *13*, 985.
[412] Colby, D. A.; Tsai, A. S.; Bergman, R. G.; Ellman, J. A. Rhodium Catalyzed Chelation-Assisted C–H Bond Functionalization Reactions. *Acc. Chem. Res.* **2011**, *45*, 814.
[413] Colby, D. A.; Bergman, R. G.; Ellman, J. A. Rhodium-Catalyzed C−C Bond Formation via Heteroatom-Directed C−H Bond Activation. *Chem. Rev.* **2009**, *110*, 624.

[414] Lee, H. S.; Kim, K. H.; Kim, S. H.; Kim, J. N. Palladium-Catalyzed, Chelation-Assisted Stereo- and Regioselective Synthesis of Tetrasubstituted Olefins by Oxidative Heck Arylation. *Adv. Synth. Catal.* **2012**, *354*, 2419.
[415] Pan, D.; Yu, M.; Chen, W.; Jiao, N. Pd-II-Catalyzed Highly Selective Arylation of Allyl Esters via C-H Functionalization of Unreactive Arenes with Retention of the Traditional Leaving Group. *Chem.-Asian J.* **2010**, *5*, 1090.
[416] LaFrate, A. L.; Katzenellenbogen, J. A. Improved chemical syntheses of 5,6-dihydro-5-fluorouracil. *J. Org. Chem.* **2007**, *72*, 8573.
[417] Frieden, M.; Giraud, M.; Reese, C. B.; Song, Q. L. Synthesis of 1- cis-3-(hydroxymethyl)cyclobutyl -uracil, -thymine and -cytosine. *J. Chem. Soc., Perkin Trans. 1* **1998**, 2827.
[418] Ishikawa, I.; Itoh, T.; Takayanagi, H.; Oshima, J.; Kawahara, N.; Mizuno, Y.; Ogura, H. The photocycloaddition reactions of uridine and related-compounds with 2,3-dimethyl-2-butene. *Chem. Pharm. Bull.* **1991**, *39*, 1922.
[419] Su, T. L.; Huang, J. T.; Burchenal, J. H.; Watanabe, K. A.; Fox, J. J. Synthesis and biological-activities of 5-deaza analogs of aminopterin and folic-acid. *J. Med. Chem.* **1986**, *29*, 709.
[420] Kundu, N. G.; Sikdar, S.; Hertzberg, R. P.; Schmitz, S. A.; Khatri, S. G. Studies on uracil derivatives and analogs. 8. A non-catalytic method for the conversion of uracil derivatives into dihydrouracil derivatives. *J. Chem. Soc., Perkin Trans. 1* **1985**, 1295.
[421] Robins, M. J.; Wilson, J. S.; Hansske, F. Nucleic-acid related-compounds. 42. A general procedure for the efficient deoxygenation of secondary alcohols - regiospecific and stereoselective conversion of ribonucleosides to 2'-deoxynucleosides. *J. Am. Chem. Soc.* **1983**, *105*, 4059.
[422] Markiewicz, W. T. Tetraisopropyldisiloxane-1,3-diyl, A Group for Simultaneous Protection of 3'-Hydroxy and 5'-hydroxy Functions of Nucleosides. *J. Chem. Res.-S* **1979**, 24.
[423] Hovinen, J. Selective N3- and 5′ -O-Alkylation of 2′ ,3′ -O-isopropylideneuridine with methyl iodide. *Helv. Chim. Acta* **1997**, *80*, 851.
[424] Maruyama, T.; Kozai, S.; Demizu, Y.; Witvrouw, M.; Pannecouque, C.; Balzarini, J.; Snoecks, R.; Andrei, G.; De Clercq, E. Synthesis and anti-HIV-1 and Anti-RCMV activity of 1-substituted 3-(3,5-dimethylbenzyl)uracil derivatives. *Chem. Pharm. Bull.* **2006**, *54*, 325.
[425] Maruyama, T.; Kozai, S.; Yamasaki, T.; Witvrouw, M.; Pannecouque, C.; Balzarini, J.; Snoeck, R.; Andrei, G.; De Clercq, E. Synthesis and antiviral activity of 1,3-disubstituted uracils against HIV-1 and HCMV. *Antivir. Chem. Chemoth.* **2003**, *14*, 271.
[426] Wang, D.-H.; Hao, X.-S.; Wu, D.-F.; Yu, J.-Q. Palladium-Catalyzed Oxidation of Boc-Protected N-Methylamines with IOAc as the Oxidant: A Boc-Directed sp3 C−H Bond Activation. *Org. Lett.* **2006**, *8*, 3387.
[427] Giri, R.; Yu, J.-Q. Synthesis of 1,2- and 1,3-Dicarboxylic Acids via Pd(II)-Catalyzed Carboxylation of Aryl and Vinyl C−H Bonds. *J. Am. Chem. Soc.* **2008**, *130*, 14082.

[428] Piera, J.; Bäckvall, J.-E. Catalytic oxidation of organic substrates by molecular oxygen and hydrogen peroxide by multistep electron transfer--a biomimetic approach. *Angew. Chem. Int. Ed.* **2008**, *47*, 3506.
[429] Kawamura, Y.; Kawano, Y.; Matsuda, T.; Ishitobi, Y.; Hosokawa, T. Palladium(II)-catalyzed asymmetric coupling of allylic alcohols and vinyl ethers: insight into the palladium and copper bimetallic catalyst. *J. Org. Chem.* **2009**, *74*, 3048.
[430] Gigant, N.; Bäckvall, J.-E. Synthesis of Conjugated Dienes via a Biomimetic Aerobic Oxidative Coupling of Two C(vinyl)–H Bonds. *Chem.-Eur. J.* **2013**, *19*, 10799.
[431] Saha, M.; Carter, R. G. Toward a Unified Approach for the Lycopodines: Synthesis of 10-Hydroxylycopodine, Deacetylpaniculine, and Paniculine. *Org. Lett.* **2013**, *15*, 736.
[432] Sasaki, Y.; Kato, D.; Boger, D. L. Asymmetric Total Synthesis of Vindorosine, Vindoline, and Key Vinblastine Analogues. *J. Am. Chem. Soc.* **2010**, *132*, 13533.
[433] Santarem, M.; Vanucci-Bacque, C.; Lhommet, G. Formal total synthesis of (+)-gephyrotoxin. *J. Org. Chem.* **2008**, *73*, 6466.
[434] Yuan, Z. Q.; Ishikawa, H.; Boger, D. L. Total synthesis of natural (-)- and ent-(+)-4-desacetoxy-6,7-dihydrovindorosine and natural and ent-minovine: Oxadiazole tandem intramolecular Diels-Alder/1,3-dipolar cycloaddition reaction. *Org. Lett.* **2005**, *7*, 741.
[435] Kozmin, S. A.; Iwama, T.; Huang, Y.; Rawal, V. H. An efficient approach to Aspidosperma alkaloids via 4+2 cycloadditions of aminosiloxydienes: Stereocontrolled total synthesis of (+/-)-tabersonine. Gram-scale catalytic asymmetric syntheses of (+)-tabersonine and (+)-16-methoxytabersonine. Asymmetric syntheses of (+)-aspidospermidine and (-)-quebrachamine. *J. Am. Chem. Soc.* **2002**, *124*, 4628.
[436] Danieli, B.; Lesma, G.; Luzzani, M.; Passarella, D.; Silvani, A. Diels-Alder reactions of methyl N-p-methoxybenzensulfonylindole-2-(2-propenoate), a convenient dienophile towards the synthesis of andranginine. *Tetrahedron* **1996**, *52*, 11291.
[437] Nowakowska, Z. A review of anti-infective and anti-inflammatory chalcones. *European Journal of Medicinal Chemistry* **2007**, *42*, 125.
[438] Chetana, B. P.; Mahajan, S. K.; Suvarna, A. K. Chalcone: a versatile molecule. *J Pharm Sci Res* **2009**, *1*, 11.
[439] Dimmock, J. R.; Elias, D. W.; Beazely, M. A.; Kandepu, N. M. Bioactivities of chalcones. *Curr. Med. Chem.* **1999**, *6*, 1125.
[440] Steinhoff, B.; King, A.; Stahl, S. Unexpected roles of molecular sieves in palladium-catalyzed aerobic alcohol oxidation. *J. Org. Chem.* **2006**, *71*, 1861.
[441] Comins, D. L.; Kuethe, J. T.; Miller, T. M.; Fevrier, F. C.; Brooks, C. A. Diels-Alder reactions of N-acyl-2-alkyl(aryl)-5-vinyl-2,3-dihydro-4-pyridones. *J. Org. Chem.* **2005**, *70*, 5221.

[442] Kuethe, J. T.; Brooks, C. A.; Comins, D. L. Diels-Alder reactions of 5-vinyl-1-acyl-2-aryl-2,3-dihydro-4-pyridones: regio- and stereoselective synthesis of octahydroquinolines. *Org. Lett.* **2003**, *5*, 321.
[443] Parkinson, C. j.; Mayer, P. M.; Radom, L. An assessment of theoretical procedures for the calculation of reliable radical stabilization energies [dagger][double dagger]. *J. Chem. Soc., Perk. Trans. 2* **1999**, 2305.
[444] Froese, R. D. J.; Morokuma, K. IMOMO-G2MS Approaches to Accurate Calculations of Bond Dissociation Energies of Large Molecules. *J. Phys. Chem. A* **1999**, *103*, 4580.
[445] García, J. I.; Martínez-Merino, V.; Mayoral, J. A.; Salvatella, L. Density Functional Theory Study of a Lewis Acid Catalyzed Diels−Alder Reaction. The Butadiene + Acrolein Paradigm. *J. Am. Chem. Soc.* **1998**, *120*, 2415.
[446] Simon, L.; Goodman, J. M. How reliable are DFT transition structures? Comparison of GGA, hybrid-meta-GGA and meta-GGA functionals. *Org. Biomol. Chem.* **2011**, *9*, 689.
[447] Kuethe, J. T.; Comins, D. L. Tandem Diels–Alder cyclization/aromatization reactions of 5-vinyl-1-acyl-2-aryl-2,3-dihydro-4-pyridones. *Tetrahedron Lett.* **2003**, *44*, 4179.
[448] Bodwell, G. J.; Pi, Z. Electron deficient dienes I. Normal and inverse electron demand Diels-Alder reaction of the same carbon skeleton. *Tetrahedron Lett.* **1997**, *38*, 309.
[449] Bodwell, G. J.; Pi, Z.; Pottie, I. R. Electron Deficient Dienes. 2. One Step Synthesis of a Coumarin-Fused Electron Deficient Diene and its Inverse Electron Demand Diels-Alder Reactions with Enamines. *Synlett* **1999**, 477.
[450] Bodwell, G. J.; Hawco, K. M.; da Silva, R. P. Electron deficient dienes 3: Rapid access to 2-hydroxybenzophenones via inverse electron demand Diels-Alder-driven domino reactions of a chromone-fused electron deficient diene with enamines. *Synlett* **2003**, 179.
[451] Bodwell, G. J.; Hawco, K. M.; Satou, T. Electron deficient dienes. 4. A synthetic equivalent of 4-methyleneglutaconic acid, its mono and diethyl esters and their use in a concise general synthesis of isophthalic acids and isophthalates. *Synlett* **2003**, 879.
[452] Dang, A.-T.; Miller, D. O.; Dawe, L. N.; Bodwell, G. J. Electron-Deficient Dienes. 5. An Inverse-Electron-Demand Diels−Alder Approach to 2-Substituted 4-Methoxyxanthones and 3,4-Dimethoxyxanthones. *Org. Lett.* **2007**, *10*, 233.
[453] Frisch, M. J.; Trucks, G. W.; Schlegel, H. B.; Scuseria, G. E.; Robb, M. A.; Cheeseman, J. R.; Scalmani, G.; Barone, V.; Mennucci, B.; Petersson, G. A.; Nakatsuji, H.; Caricato, M.; Li, X.; Hratchian, H. P.; Izmaylov, A. F.; Bloino, J.; Zheng, G.; Sonnenberg, J. L.; Hada, M.; Ehara, M.; Toyota, K.; Fukuda, R.; Hasegawa, J.; Ishida, M.; Nakajima, T.; Honda, Y.; Kitao, O.; Nakai, H.; Vreven, T.; Montgomery, J., J. A.; Peralta, J. E.; Ogliaro, F.; Bearpark, M.; Heyd, J. J.; Brothers, E.; Kudin, K. N.; Staroverov, V. N.; Kobayashi, R.; Normand, J.; Raghavachari, K.; Rendell, A.; Burant, J. C.; Iyengar, S. S.; Tomasi, J.; Cossi, M.; Rega, N.; Millam, J. M.; Klene, M.; Knox, J. E.; Cross, J. B.; Bakken, V.; Adamo,

C.; Jaramillo, J.; Gomperts, R.; Stratmann, R. E.; Yazyev, O.; Austin, A. J.; Cammi, R.; Pomelli, C.; Ochterski, J. W.; Martin, R. L.; Morokuma, K.; Zakrzewski, V. G.; Voth, G. A.; Salvador, P.; Dannenberg, J. J.; Dapprich, S.; Daniels, A. D.; Farkas, Ö.; Foresman, J. B.; Ortiz, J. V.; Cioslowski, J.; Fox, D. J. *Gaussian 09*, Revision A.1 Gaussian, Inc.: Wallingford CT, 2009.

[454] Claisen, L.; Claparede, A. Condensationen von ketonen mit aldehyden. *Ber. Dtsch. Chem. Ges.* **1881**, *14*, 2460.

[455] Schmidt, J. G. Ueber die Einwirkung von Aceton auf Furfurol und auf Bittermandelöl bei Gegenwart von Alkalilauge. *Ber. Dtsch. Chem. Ges.* **1881**, *14*, 1459.

[456] Eddarir, S.; Cotelle, N.; Bakkour, Y.; Rolando, C. An efficient synthesis of chalcones based on the Suzuki reaction. *Tetrahedron Lett.* **2003**, *44*, 5359.

[457] Wu, X.-F.; Neumann, H.; Beller, M. Palladium-catalyzed coupling reactions: carbonylative Heck reactions to give chalcones. *Angew. Chem. Int. Ed.* **2010**, *49*, 5284.

[458] Wu, X.-F.; Neumann, H.; Spannenberg, A.; Schulz, T.; Jiao, H.; Beller, M. Development of a general palladium-catalyzed carbonylative Heck reaction of aryl halides. *J. Am. Chem. Soc.* **2010**, *132*, 14596.

[459] Wu, X.-F.; Neumann, H.; Beller, M. Palladium-catalyzed oxidative carbonylative coupling reactions of arylboronic acids with styrenes to chalcones under mild aerobic conditions. *Chemistry, an Asian journal* **2012**, *7*, 282.

[460] Unoh, Y.; Hirano, K.; Satoh, T.; Miura, M. Palladium-catalyzed decarboxylative arylation of benzoylacrylic acids toward the synthesis of chalcones. *J. Org. Chem.* **2013**, *78*, 5096.

[461] Bianco, A.; Cavarischia, C.; Guiso, M. The Heck Coupling Reaction Using Aryl Vinyl Ketones: Synthesis of Flavonoids. *Eur. J. Org. Chem.* **2004**, 2894.

[462] Astruc, D., *Modern Arene Chemistry*. 1st ed.; Wiley-VCH: Weinheim, **2002**.

[463] Ackermann, L., *Modern Arylation Methods*. 1st ed.; Wiley-VCH: Weinheim, **2009**.

[464] Boorman, T.; Larrosa, I. Gold-mediated C-H bond functionalisation. *Chem. Soc. Rev.* **2011**, *40*, 1910.

[465] Colby, D.; Bergman, R.; Ellman, J. Rhodium-catalyzed C-C bond formation via heteroatom-directed C-H bond activation. *Chem. Rev.* **2010**, *110*, 624.

[466] McGlacken, G.; Bateman, L. Recent advances in aryl-aryl bond formation by direct arylation. *Chem. Soc. Rev.* **2009**, *38*, 2447.

[467] Stackhouse, P. J.; Wilson, A.; Lacey, D.; Hird, M. Synthesis and properties of novel columnar liquid crystals based on symmetrical and non-symmetrical 1,3,5-trisubstituted benzene derivatives. *Liq. Cryst.* **2010**, *37*, 1191.

[468] Fitié, C.; Roelofs, W.; Kemerink, M.; Sijbesma, R. Remnant polarization in thin films from a columnar liquid crystal. *J. Am. Chem. Soc.* **2010**, *132*, 6892.

[469] Miller, T. M.; Neenan, T. X. Convergent synthesis of monodisperse dendrimers based upon 1,3,5-trisubstituted benzenes. *Chem. Mater.* **1990**, *2*, 346.

[470] Pang, J.; Tao, Y.; Freiberg, S.; Yang, X.-P.; D'Iorio, M.; Wang, S. Syntheses, structures, and electroluminescence of new blue luminescent star-shaped

compounds based on 1,3,5-triazine and 1,3,5-trisubstituted benzene. *J. Mater. Chem.* **2002**, *12*, 206.

[471] Yamaguchi, Y.; Ochi, T.; Miyamura, S.; Tanaka, T.; Kobayashi, S.; Wakamiya, T.; Matsubara, Y.; Yoshida, Z.-I. Rigid molecular architectures that comprise a 1,3,5-trisubstituted benzene core and three oligoaryleneethynylene arms: light-emitting characteristics and pi conjugation between the arms. *J. Am. Chem. Soc.* **2006**, *128*, 4504.

[472] Isaacs, R.; Newton, C.; Cutrona, K.; Mercer, S.; Payne, L.; Stauffer, K.; Williams, P.; Cook, J.; Krueger, J.; Lewis, S.; Lucas, B.; Lyle, E.; Lynch, J.; McMasters, D.; Naylor-Olsen, A.; Michener, M.; Wallace, A. Design, synthesis and SAR of a series of 1,3,5-trisubstituted benzenes as thrombin inhibitors. *Bioorg. Med. Chem. Lett.* **2011**, *21*, 1536.

[473] Georgsson, J.; Sköld, C.; Plouffe, B.; Lindeberg, G.; Botros, M.; Larhed, M.; Nyberg, F.; Gallo-Payet, N.; Gogoll, A.; Karlén, A.; Hallberg, A. Angiotensin II pseudopeptides containing 1,3,5-trisubstituted benzene scaffolds with high AT2 receptor affinity. *J. Med. Chem.* **2005**, *48*, 6620.

[474] Lindman, S.; Lindeberg, G.; Nyberg, F.; Karlén, A.; Hallberg, A. Comparison of three γ-turn mimetic scaffolds incorporated into angiotensin II. *Biorg. Med. Chem.* **2000**, *8*, 2375.

[475] Liu, B.; Shetty, R. S.; Moffett, K. K.; Kelly, M. J. Efficient synthesis of 1,3,5-trisubstituted benzenes via three Pd-mediated carbon–sulfur, carbon–nitrogen and carbon–carbon bond formation reactions. *Tetrahedron Lett.* **2011**, *52*.

[476] Karpuk, E.; Schollmeyer, D.; Meier, H. Photochemical Generation of Cyclophanes from 1,3,5-Trisubstituted Benzenes with Chalcone Chromophores. *Eur. J. Org. Chem.* **2007**, 1983.

[477] Majchrzak, M. W.; Zobel, J. N.; Obradovich, D. J.; Peterson, G. A. A concise synthesis of symmetric 1,3,5-C3-trisubstituted benzenes. *Org. Prep. Proced. Int.* **1997**, *29*, 361.

[478] Dai, H. X.; Li, G.; Zhang, X. G.; Stepan, A. F.; Yu, J. Q. Pd(II)-Catalyzed ortho- or meta-C-H Olefination of Phenol Derivatives. *J. Am. Chem. Soc.* **2013**, *135*, 7567.

[479] Truong, T.; Daugulis, O. Directed Functionalization of C-H Bonds: Now also meta Selective. *Angew. Chem. Int. Ed.* **2012**, *51*, 11677.

[480] Lee, E. Y.; Park, J. Recyclable Copper Catalyst for meta-Selective C-H Bond Arylation. *Chemcatchem* **2011**, *3*, 1127.

[481] Cornella, J.; Righi, M.; Larrosa, I. Carboxylic Acids as Traceless Directing Groups for Formal meta-Selective Direct Arylation. *Angew. Chem. Int. Ed.* **2011**, *50*, 9429.

[482] Chen, B.; Hou, X. L.; Li, Y. X.; Wu, Y. D. Mechanistic Understanding of the Unexpected Meta Selectivity in Copper-Catalyzed Anilide C-H Bond Arylation. *J. Am. Chem. Soc.* **2011**, *133*, 7668.

[483] Zhou, Y.; Zhao, J.; Liu, L. Meta-Selective Transition-Metal Catalyzed Arene C-H Bond Functionalization. *Angew. Chem. Int. Ed.* **2009**, *48*, 7126.

[484] Phipps, R. J.; Gaunt, M. J. A Meta-Selective Copper-Catalyzed C-H Bond Arylation. *Science* **2009**, *323*, 1593.
[485] Yuan, G.; Zheng, J.; Gao, X.; Li, X.; Huang, L.; Chen, H.; Jiang, H. Copper-catalyzed aerobic oxidation and cleavage/formation of C-S bond: a novel synthesis of aryl methyl sulfones from aryl halides and DMSO. *Chem. Commun.* **2012**, *48*, 7513.
[486] Alonso, D. A.; Fuensanta, M.; Nájera, C.; Varea, M. 3,5-Bis(trifluoromethyl)phenyl Sulfones in the Direct Julia−Kocienski Olefination. *J. Org. Chem.* **2005**, *70*, 6404.
[487] Bardelle, C.; Coleman, T.; Cross, D.; Davenport, S.; Kettle, J. G.; Ko, E. J.; Leach, A. G.; Mortlock, A.; Read, J.; Roberts, N. J.; Robins, P.; Williams, E. J. Inhibitors of the tyrosine kinase EphB4. Part 2: Structure-based discovery and optimisation of 3,5-bis substituted anilinopyrimidines. *Bioorg. Med. Chem. Lett.* **2008**, *18*, 5717.
[488] Pilgram, K.; Korte, F. Über die reaktion von nitroarythiocyanaten mit trialkylphosphiten—I. *Tetrahedron* **1964**, *20*, 177.
[489] Dvorak, C. A.; Liu, C.; Shelton, J.; Kuei, C.; Sutton, S. W.; Lovenberg, T. W.; Carruthers, N. I. Identification of Hydroxybenzoic Acids as Selective Lactate Receptor (GPR81) Agonists with Antilipolytic Effects. *ACS Med. Chem. Lett.* **2012**, *3*, 637.
[490] Liao, T.-B.; Ling, Y.; Chen, Z.-X.; Zhou, Y.-M.; Weng, L.-H. A rutile-type porous zinc(ii)-phosphonocarboxylate framework: local proton transfer and size-selected catalysis. *Chem. Commun.* **2010**, *46*, 1100.
[491] Garczarek, P.; Janczak, J.; Zoń, J. New multifunctional phosphonic acid for metal phosphonate synthesis. *J. Mol. Struct.* **2013**, *1036*, 505.
[492] Grushin, V. V. The Organometallic Fluorine Chemistry of Palladium and Rhodium: Studies toward Aromatic Fluorination. *Acc. Chem. Res.* **2009**, *43*, 160.
[493] Müller, K.; Faeh, C.; Diederich, F. Fluorine in Pharmaceuticals: Looking Beyond Intuition. *Science* **2007**, *317*, 1881.
[494] Purser, S.; Moore, P.; Swallow, S.; Gouverneur, V. Fluorine in medicinal chemistry. *Chem. Soc. Rev.* **2008**, *37*, 320.
[495] Jeschke, P. The unique role of fluorine in the design of active ingredients for modern crop protection. *Chembiochem* **2004**, *5*, 571.
[496] Swarts, F. *Bull. Acad. R. Belg.* **1892**, *24*, 309.
[497] Simons, J. H.; Lewis, C. J. The Preparation of Benzotrifluoride. *J. Am. Chem. Soc.* **1938**, *60*, 492.
[498] Wu, X. F.; Neumann, H.; Beller, M. Recent Developments on the Trifluoromethylation of (Hetero)Arenes. *Chem.-Asian J.* **2012**, *7*, 1744.
[499] Studer, A. A "Renaissance" in Radical Trifluoromethylation. *Angew. Chem. Int. Ed.* **2012**, *51*, 8950.
[500] Qing, F. L. Recent Advances of Trifluoromethylation. *Chinese J. Org. Chem.* **2012**, *32*, 815.
[501] Lu, C. P.; Shen, Q. L.; Liu, D. Transition Metal-Catalyzed Arene Trifluoromethylation. *Chinese J. Org. Chem.* **2012**, *32*, 1380.

[502] Garcia-Monforte, M. A.; Martinez-Salvador, S.; Menjon, B. The Trifluoromethyl Group in Transition Metal Chemistry. *Eur. J. Inorg. Chem.* **2012**, 4945.
[503] Tomashenko, O. A.; Grushin, V. V. Aromatic Trifluoromethylation with Metal Complexes. *Chem. Rev.* **2011**, *111*, 4475.
[504] Furuya, T.; Kamlet, A. S.; Ritter, T. Catalysis for fluorination and trifluoromethylation. *Nature* **2011**, *473*, 470.
[505] Liu, H.; Gu, Z. H.; Jiang, X. F. Direct Trifluoromethylation of the CH Bond. *Adv. Synth. Catal.* **2013**, *355*, 617.
[506] Kamei, T. Metal-Catalyzed/Mediated Aromatic C-H Bond Trifluoromethylation. *J. Syn. Org. Chem. Jpn.* **2012**, *70*, 756.
[507] Pan, F.; Shi, Z. Transition Metal-Catalyzed C—H Trifluoromethylation. *Acta Chim. Sinica* **2012**, *70*, 1679.
[508] Besset, T.; Schneider, C.; Cahard, D. Tamed arene and heteroarene trifluoromethylation. *Angew. Chem. Int. Ed.* **2012**, *51*, 5048.
[509] Ma, J.-A.; Cahard, D. Strategies for nucleophilic, electrophilic, and radical trifluoromethylations. *J. Fluorine Chem.* **2007**, *128*, 975.
[510] Wang, X.; Truesdale, L.; Yu, J.-Q. Pd(II)-catalyzed ortho-trifluoromethylation of arenes using TFA as a promoter. *J. Am. Chem. Soc.* **2010**, *132*, 3648.
[511] Zhang, X.-G.; Dai, H.-X.; Wasa, M.; Yu, J.-Q. Pd(II)-catalyzed ortho trifluoromethylation of arenes and insights into the coordination mode of acidic amide directing groups. *J. Am. Chem. Soc.* **2012**, *134*, 11948.
[512] Zhang, L.-S.; Chen, K.; Chen, G.; Li, B.-J.; Luo, S.; Guo, Q.-Y.; Wei, J.-B.; Shi, Z.-J. Palladium-catalyzed trifluoromethylation of aromatic C-H bond directed by an acetamino group. *Org. Lett.* **2013**, *15*, 10.
[513] Ye, Y.; Ball, N.; Kampf, J.; Sanford, M. Oxidation of a cyclometalated Pd(II) dimer with "CF3+": formation and reactivity of a catalytically competent monomeric Pd(IV) aquo complex. *J. Am. Chem. Soc.* **2010**, *132*, 14682.
[514] Wiehn, M.; Vinogradova, E.; Togni, A. Electrophilic trifluoromethylation of arenes and N-heteroarenes using hypervalent iodine reagents. *J. Fluorine Chem.* **2010**, *131*, 951.
[515] Shimizu, R.; Egami, H.; Nagi, T.; Chae, J.; Hamashima, Y.; Sodeoka, M. Direct C2-trifluoromethylation of indole derivatives catalyzed by copper acetate. *Tetrahedron Lett.* **2010**, *51*, 5947.
[516] Egami, H.; Shimizu, R.; Kawamura, S.; Sodeoka, M. Alkene Trifluoromethylation Coupled with C-C Bond Formation: Construction of Trifluoromethylated Carbocycles and Heterocycles. *Angew. Chem. Int. Ed.* **2013**, *52*, 4000.
[517] Feng, C.; Loh, T.-P. Copper-catalyzed olefinic trifluoromethylation of enamides at room temperature. *Chem. Sci.* **2012**, *3*, 3458.
[518] Mu, X.; Chen, S.; Zhen, X.; Liu, G. Palladium-catalyzed oxidative trifluoromethylation of indoles at room temperature. *Chem. Eur. J.* **2011**, *17*, 6039.

[519] Mu, X.; Wu, T.; Wang, H.-y.; Guo, Y.-l.; Liu, G. Palladium-catalyzed oxidative aryltrifluoromethylation of activated alkenes at room temperature. *J. Am. Chem. Soc.* **2012**, *134*, 878.
[520] Chu, L.; Qing, F.-L. Copper-catalyzed direct C-H oxidative trifluoromethylation of heteroarenes. *J. Am. Chem. Soc.* **2012**, *134*, 1298.
[521] Kino, T.; Nagase, Y.; Ohtsuka, Y.; Yamamoto, K.; Uraguchi, D.; Tokuhisa, K.; Yamakawa, T. Trifluoromethylation of various aromatic compounds by CF3I in the presence of Fe(II) compound, H2O2 and dimethylsulfoxide. *J. Fluorine Chem.* **2010**, *131*, 98.
[522] Ye, Y.; Lee, S.; Sanford, M. Silver-mediated trifluoromethylation of arenes using TMSCF3. *Org. Lett.* **2011**, *13*, 5464.
[523] Hafner, A.; Bräse, S. Ortho-trifluoromethylation of functionalized aromatic triazenes. *Angew. Chem. Int. Ed.* **2012**, *51*, 3713.
[524] Parsons, A.; Buchwald, S. Organic chemistry: A radical approach to diversity. *Nature* **2011**, *480*, 184.
[525] Iqbal, N.; Choi, S.; Ko, E.; Cho, E. J. Trifluoromethylation of heterocycles via visible light photoredox catalysis. *Tetrahedron Lett.* **2012**, *53*, 2005.
[526] Chu, L.; Qing, F.-L. Copper-mediated aerobic oxidative trifluoromethylation of terminal alkynes with Me3SiCF3. *J. Am. Chem. Soc.* **2010**, *132*, 7262.
[527] Jiang, X.; Chu, L.; Qing, F.-L. Copper-catalyzed oxidative trifluoromethylation of terminal alkynes and aryl boronic acids using (trifluoromethyl)trimethylsilane. *J. Org. Chem.* **2012**, *77*, 1251.
[528] Zhang, K.; Qiu, X.-L.; Huang, Y.; Qing, F.-L. An Improved Copper-Mediated Oxidative Trifluoromethylation of Terminal Alkynes. *Eur. J. Org. Chem.* **2012**, 58.
[529] Pan, Y.; Wang, S.; Kee, C. W.; Dubuisson, E.; Yang, Y.; Loh, K. P.; Tan, C.-H. Graphene oxide and Rose Bengal: oxidative C–H functionalisation of tertiary amines using visible light. *Green Chem.* **2011**, *13*, 3341.
[530] Chu, L.; Qing, F.-L. Copper-mediated oxidative trifluoromethylation of boronic acids. *Org. Lett.* **2010**, *12*, 5060.
[531] Mitsudera, H.; Li, C.-J. Copper-catalyzed oxidative trifluoromethylation of benzylic sp3 C–H bond adjacent to nitrogen in amines. *Tetrahedron Lett.* **2011**, *52*, 1898.
[532] Xu, J.; Fu, Y.; Luo, D.-F.; Jiang, Y.-Y.; Xiao, B.; Liu, Z.-J.; Gong, T.-J.; Liu, L. Copper-catalyzed trifluoromethylation of terminal alkenes through allylic C-H bond activation. *J. Am. Chem. Soc.* **2011**, *133*, 15300.
[533] Parsons, A.; Buchwald, S. Copper-catalyzed trifluoromethylation of unactivated olefins. *Angew. Chem. Int. Ed.* **2011**, *50*, 9120.
[534] Wang, X.; Ye, Y.; Zhang, S.; Feng, J.; Xu, Y.; Zhang, Y.; Wang, J. Copper-catalyzed C(sp3)-C(sp3) bond formation using a hypervalent iodine reagent: an efficient allylic trifluoromethylation. *J. Am. Chem. Soc.* **2011**, *133*, 16410.
[535] Chu, L.; Qing, F.-L. Copper-catalyzed oxidative trifluoromethylation of terminal alkenes using nucleophilic CF3SiMe3: efficient C(sp3)-CF3 bond formation. *Org. Lett.* **2012**, *14*, 2106.

[536] Nagib, D. A.; Scott, M. E.; MacMillan, D. W. C. Enantioselective alpha-trifluoromethylation of aldehydes via photoredox organocatalysis. *J. Am. Chem. Soc.* **2009**, *131*, 10875.
[537] Allen, A. E.; MacMillan, D. W. C. The productive merger of iodonium salts and organocatalysis: a non-photolytic approach to the enantioselective alpha-trifluoromethylation of aldehydes. *J. Am. Chem. Soc.* **2010**, *132*, 4986.
[538] Pham, P. V.; Nagib, D. A.; MacMillan, D. W. C. Photoredox catalysis: a mild, operationally simple approach to the synthesis of α-trifluoromethyl carbonyl compounds. *Angew. Chem. Int. Ed.* **2011**, *50*, 6119.
[539] Wu, X.; Chu, L.; Qing, F.-L. PhI(OAc)2-mediated oxidative trifluoromethylation of arenes with CF3SiMe3 under metal-free conditions. *Tetrahedron Lett.* **2013**, *54*, 249.
[540] Kita, Y.; Tohma, H.; Hatanaka, K.; Takada, T.; Fujita, S.; Mitoh, S.; Sakurai, H.; Oka, S. Hypervalent Iodine-Induced Nucleophilic Substitution of para-Substituted Phenol Ethers. Generation of Cation Radicals as Reactive Intermediates. *J. Am. Chem. Soc.* **1994**, *116*, 3684.
[541] Dohi, T.; Ito, M.; Morimoto, K.; Iwata, M.; Kita, Y. Oxidative cross-coupling of arenes induced by single-electron transfer leading to biaryls by use of organoiodine(III) oxidants. *Angew. Chem. Int. Ed.* **2008**, *47*, 1301.
[542] Cho, S.; Yoon, J.; Chang, S. Intramolecular oxidative C-N bond formation for the synthesis of carbazoles: comparison of reactivity between the copper-catalyzed and metal-free conditions. *J. Am. Chem. Soc.* **2011**, *133*, 5996.
[543] Kantak, A.; Potavathri, S.; Barham, R.; Romano, K.; DeBoef, B. Metal-free intermolecular oxidative C-N bond formation via tandem C-H and N-H bond functionalization. *J. Am. Chem. Soc.* **2011**, *133*, 19960.
[544] Kowalski, C. J.; Fields, K. W. Enone mesylates. Precursors to .beta.-substituted cyclohexenones. *J. Org. Chem.* **1981**, *46*, 197.
[545] Sebesta, R.; Pizzuti, M. G.; Boersma, A. J.; Minnaard, A. J.; Feringa, B. L. Catalytic enantioselective conjugate addition of dialkylzinc reagents to N-substituted-2,3-dehydro-4-piperidones. *Chem. Commun.* **2005**, 1711.
[546] Comins, D. L.; Brown, J. D. Additiom of Grignard reagents to 1-acyl-4-methoxypyridinum salts. An approach to the synthesis of quinolizidinones. *Tetrahedron Lett.* **1986**, *27*, 4549.

Appendix—List of Publications

I. Palladium(II)-catalyzed dehydrogenative alkenylation of cyclic enaminones via the Fujiwara-Moritani reaction

Yi-Yun Yu, Micah J. Niphakis and Gunda I. Georg

Organic Letters **2011**, *13*, 5932–5935

II. Dehydrogenative alkenylation of uracils via palladium-catalyzed regioselective C–H activation

Yi-Yun Yu and Gunda I. Georg

Chemical Communications **2013**, *49*, 3694–3696

III. Palladium-catalyzed direct C–H arylation of cyclic enaminones with aryl iodides

Yi-Yun Yu, Lei Bi and Gunda I. Georg

The Journal of Organic Chemistry **2013**, *78*, 6163–6169

IV. Biomimetic aerobic C–H alkenylation of cyclic enaminones at room temperature: Development toward the synthesis of unexpected 1,3,5-trisubstituted benzenes

Yi-Yun Yu and Gunda I. Georg

Advanced Synthesis & Catalysis **2013**, *manuscript in preparation*

Notice:

The published papers **I–III** are adapted in Chapters 3–5 with kind permission from the American Chemical Society and the Royal Society of Chemistry respectively.